

Ahsan Ali

# GIS and BIM Integration Model Workflow Towards Digital Twin to Assess Flood Impacts on Buildings

# **GIS and BIM Integration Model Workflow Towards Digital Twin to Assess Flood Impacts on Buildings**

Dem Fachbereich Bauingenieurwesen  
der Rheinland-Pfälzischen Technischen Universität Kaiserslautern Landau  
zur Erlangung des akademischen Grades

**Doktor-Ingenieur (Dr.-Ing.)**

genehmigte

**Dissertation**

von Herrn

**Ahsan Ali, M.Sc.**

aus Naseerabad, Pakistan

Tag der mündlichen Prüfung: Donnerstag, 13. Juli 2023

Dekan:	Prof. Dr.-Ing. Karsten Körkemeyer
Vorsitzender der Promotionkommission:	Prof. Dr.-Ing. Wolfgang Kurz
Erstgutachter:	Prof. Dr. Robert Jüpner
Zweitgutachter:	Prof. Dr.-Ing. Stephan Theobald
Drittgutachter:	Prof. Dr. Jens Brauneck



# **GIS and BIM Integration Model Workflow Towards Digital Twin to Assess Flood Impacts on Buildings**

To the Department of Civil Engineering  
at the Rhineland-Palatinate Technical University Kaiserslautern Landau,  
for the attainment of the academic degree

**Doctor of Engineering (Dr.-Ing.)**  
accepted

**Dissertation**

by Mr.

**Ahsan Ali, M.Sc.**

from Naseerabad, Pakistan

Oral Examination Date: Thursday, July 13, 2023

Dean:	Prof. Dr.-Ing. Karsten Körkemeyer
Chairman of the Doctoral Committee:	Prof. Dr.-Ing. Wolfgang Kurz
First Supervisor:	Prof. Dr. Robert Jüpner
Second Supervisor:	Prof. Dr.-Ing. Stephan Theobald
Third Supervisor:	Prof. Dr. Jens Brauneck





Berichte des Fachgebietes Wasserbau und Wasserwirtschaft der  
Rheinland-Pfälzischen Technischen Universität Kaiserslautern-Landau

Bericht 24 (2024)

**Ahsan Ali**

**GIS and BIM Integration Model Workflow  
Towards Digital Twin to Assess Flood Impacts  
on Buildings**

D 386 (Diss. Rheinland-Pfälzische Technische Universität Kaiserslautern-Landau)

Shaker Verlag  
Düren 2024

**Bibliographic information published by the Deutsche Nationalbibliothek**

The Deutsche Nationalbibliothek lists this publication in the Deutsche Nationalbibliografie; detailed bibliographic data are available in the internet at <http://dnb.d-nb.de>.

Zugl.: Kaiserslautern-Landau, RPTU, Diss., 2024

**Impressum**

Reihe der Berichte des Fachgebietes Wasserbau und Wasserwirtschaft der Technischen Universität Kaiserslautern

**Herausgeber der Schriftenreihe:** Prof. Dr. Robert Jüpner  
Fachgebiet Wasserbau und Wasserwirtschaft  
Technische Universität Kaiserslautern  
Paul-Ehrlich-Straße 14  
67663 Kaiserslautern

**Herausgeber Bericht 24:** Prof. Dr. Robert Jüpner

**Redaktion:** Fachgebiet Wasserbau und Wasserwirtschaft  
der Technischen Universität Kaiserslautern

Kaiserslautern, im

Copyright Shaker Verlag 2024

All rights reserved. No part of this publication may be reproduced, stored in a retrieval system, or transmitted, in any form or by any means, electronic, mechanical, photocopying, recording or otherwise, without the prior permission of the publishers.

Printed in Germany.

ISBN 978-3-8440-9487-9

ISSN 1433-4860

Shaker Verlag GmbH • Am Langen Graben 15a • 52353 Düren

Phone: 0049/2421/99011-0 • Telefax: 0049/2421/99011-9

Internet: [www.shaker.de](http://www.shaker.de) • e-mail: [info@shaker.de](mailto:info@shaker.de)

## **Acknowledgements**

As I reflect on the completion of this thesis, I am reminded of the many people who have played a significant role in my journey. I am deeply grateful to each one of them for their unwavering support, guidance, and encouragement throughout my PhD.

I would like to express my sincere appreciation to my supervisors and mentors, Prof. Dr. Robert Jüpner and Prof. Dr. Jens Brauneck, for their invaluable guidance, expertise, and unwavering support. I am also grateful to Prof. Dr. Stephan Theobald for his valuable input and support in my research.

I would like to acknowledge the financial support and resources provided by DAAD - The German Academic Exchange Service which enabled me to conduct this research. I also extend my sincere thanks to the HEC- Higher Education Commission Pakistan for their support. I would like to express my special gratitude to the University of Applied Sciences Frankfurt and its staff and postgraduate students for assisting in data collection support.

Finally, I extend my heartfelt appreciation to my family for their unconditional love, support, and encouragement throughout my journey. Most importantly to my beloved wife emerging scientist Maria Riffat for her love, support, encouragement, and guidance throughout my PhD journey. I am also grateful to CEO Steffen van Wasen and other colleagues from Fischer Engineering Office for their moral support to conduct my research.

Thank you all for your kindness, generosity, and support.

## **Affidavit**

I hereby declare that the following work, namely my doctoral thesis, has been produced solely by myself and without any unlawful support from external parties. I attest that all sources utilized in the creation of this dissertation have been appropriately identified and acknowledged. This work has not been previously submitted to any examination board, in its current or comparable form. All figures included in this work are accompanied by proper citations, with those lacking explicit sources having been generated by the author himself.

Dated: 31.03.2024

---

Ahsan Ali

## Abstract

Floods are a highly destructive natural hazard that results in severe social and economic impacts. Traditional hazard-based approaches to flood management necessitate urgent improvements. A paradigm shift has been observed toward adopting a flood risk management (FRM) framework. This framework entails a multi-tier risk analysis approach to identify and mitigate flood-related hazards in an integrated manner. By reducing the hazard levels and potential damages, FRM treats these risks at various levels. In FRM, the development of flood-resilient buildings and infrastructures constitutes a crucial measure. However, current building resilience strategies lack the incorporation of distinctive building characteristics and their unique behaviours in risk evaluation.

The need for new approaches and technological tools is imperative for the accurate evaluation of flood risk and the development of resilient buildings and infrastructures. The fast-paced changes in today's world require the incorporation of innovative technologies in the FRM domain to achieve flood-resilient buildings. However, the integration of new technologies, especially big data, presents new challenges for FRM. To overcome these challenges, the potential of emerging technologies in the FRM domain was investigated, revealing that their integration could enhance FRM. The integration of Geographic Information Systems (GIS) and Building Information Modelling (BIM) has been identified as a promising approach to improve FRM by merging hydrodynamic flood and building information into a single geospatial environment. This study investigates how the integration of GIS and BIM can improve flood risk management by creating a 3D digital twin for flood-resilient buildings, and to assess its potential for supporting flood impact assessment on buildings.

In this multidisciplinary study, a novel, multiphase model workflow has been developed to create a 3D digital twin environment in order to enhance FRM for flood-resilient buildings. The digital twin enables an automatic 3D assessment and calculation of flood-induced impacts on a building and its individual components. To validate the functionality of the developed model workflow, a prototype case was implemented to assess the feasibility of its different phases. The prototype case highlighted limitations in the developed model workflow, and the lessons learned from this exercise were used to improve the methodology. The revised methodology was then tested with real-world data in a subsequent case study, resulting in improved accuracy and effectiveness. Leveraging the 3D digital twin framework, numerous geospatial analyses were partially automated within the digital twin environment to evaluate the impact of flooding on diverse building components. The developed system enables thorough evaluation, computation, and identification of flooded building components, as well as the partially automated calculation of flood-induced actions, pressures, and forces on both structural and non-structural building components. The computed pressures and forces from various flood actions can be transferred to various material and structural analysis software for further analysis of building and component stability.

Furthermore, the developed 3D digital twin enables more comprehensive data visualization, enhancing users' ability to perceive the interrelationships between building and flooding information. This facilitates the identification of potential risks and enables more effective communication with stakeholders involved in building design and flood management. By leveraging the same information system, better communication, effective planning, and improved outcomes can be achieved.

**Keywords:** Resilient Building, Hydrodynamic Flood Simulation, Flood Impacts, GIS, BIM, Digital Twin

## Zusammenfassung

Hochwasser sind eine sehr zerstörerische Naturkatastrophe, die schwerwiegende soziale und wirtschaftliche Auswirkungen hat. Traditionelle ansatzbasierte Methoden für das Hochwassermanagement erfordern dringend Verbesserungen. Es wurde ein Paradigmenwechsel hin zur Übernahme eines Hochwasserrisikomanagement-Richtlinien (HWRM-RL) beobachtet. Diese Richtlinien umfassen einen mehrstufigen Risikoanalyse-Ansatz, um Hochwassergefahren in einer integrierten Weise zu identifizieren und zu mildern. Durch die Reduzierung des Gefährdungsgrads und potenzieller Schäden behandelt FRM diese Risiken auf verschiedenen Ebenen. Im HWRM-Kontext stellt die Entwicklung von hochwasserangepassten Gebäuden und Infrastrukturen eine entscheidende Maßnahme dar. Derzeitige Strategien für die Gebäude Resilienz berücksichtigen jedoch nicht die besonderen Gebäudeeigenschaften und deren einzigartiges Verhalten bei der Risikobewertung.

Die Notwendigkeit neuer Ansätze und technologischer Tools ist für eine genaue Bewertung von Hochwasserrisiken und die Entwicklung hochwasserresistenter Gebäude und Infrastrukturen unerlässlich. Der schnelle Wandel in der heutigen Welt erfordert die Integration innovativer Technologien im FRM-Bereich, um hochwasserresistente Gebäude zu erreichen. Die Integration neuer Technologien, insbesondere Big Data, stellt jedoch neue Herausforderungen für FRM dar. Um diese Herausforderungen zu bewältigen, wurde das Potenzial aufstrebender Technologien im FRM-Bereich untersucht, wobei ihre Integration das FRM verbessern kann. Die Integration von Geografisches Informationssystem (GIS) und Gebäudedatenmodellierung (BIM) wurde als vielversprechender Ansatz zur Verbesserung von FRM identifiziert, indem hydrodynamische Hochwasser- und Gebäudeinformationen in einer einzigen Geodaten Umgebung zusammengeführt werden. In dieser Dissertation wird untersucht, wie die Integration von GIS und BIM das Hochwasserrisikomanagement durch die Erstellung eines 3D Digitale Zwilling für hochwasserresistente Gebäude verbessern kann und ihr Potenzial zur Unterstützung der Bewertung von Hochwasserwirkungen auf Gebäude zu bewerten.

In dieser interdisziplinären Studie wurde ein neuartiger, multiphasiger Modellworkflow entwickelt, um eine 3D Digitale Zwilling Umgebung zu erstellen und damit das FRM für hochwasserresistente Gebäude zu verbessern. Der Digitale Zwilling ermöglicht eine teil-automatische 3D-Bewertung und Berechnung der durch Überschwemmungen verursachten Auswirkungen auf ein Gebäude und dessen Einzelkomponenten. Zur Validierung der Funktionalität des entwickelten Modell-Workflows wurde ein Prototypfall implementiert, um die Machbarkeit seiner verschiedenen Phasen zu bewerten. Der Prototyp zeigte die Grenzen des entwickelten Modells auf, und die dabei gewonnenen Erkenntnisse wurden zur Verbesserung der Methodik genutzt. Die überarbeitete Methodik wurde dann in einer zweiten Fallstudie mit verbesserten Daten getestet, was zu einer höheren Genauigkeit und Wirksamkeit führte. Durch Nutzung des 3D Digitale-Zwilling-Frameworks wurden zahlreiche geospatiale Analysen teil-automatisiert, um die Auswirkungen von Überschwemmungen auf verschiedene Gebäudekomponenten zu bewerten. Das entwickelte System ermöglicht eine gründliche Bewertung, Berechnung und Identifizierung von überschwemmten Gebäudekomponenten, wobei teil-automatisch die durch Hochwasserbedingte Auswirkungen, Drücke und Lasten auf strukturelle und nicht-strukturelle Gebäudekomponenten berechnet werden. Diese berechneten Drücke und Lasten aus verschiedenen Überschwemmungsaktionen können in verschiedene Material- und Statik-Software übertragen werden, um weitere Stabilitätsanalysen von Gebäuden und Komponenten durchzuführen.

Darüber hinaus ermöglicht der entwickelte 3D Digitale Zwilling eine umfassendere Datenvisualisierung, was die Fähigkeit der Benutzer erhöht, die Wechselwirkungen zwischen Gebäude- und Hochwasserinformationen wahrzunehmen. Dies erleichtert die Identifizierung potenzieller Risiken und ermöglicht eine effektivere Kommunikation mit den am Gebäudedesign und der Hochwassermanagement beteiligten Interessengruppen. Durch Nutzung desselben Informationssystems können eine bessere Kommunikation, eine effektive Planung und verbesserte Ergebnisse erzielt werden.

**Stichwörter:** Hochwasserangepasste Gebäude, Hydrodynamische Hochwassersimulation, Hochwasserauswirkungen, GIS, BIM, Digitaler Zwilling.



# Table of Contents

1	Introduction.....	2
1.1	Research Background.....	2
1.2	Problem Statement.....	6
1.3	Research Questions.....	7
1.4	Research Scope.....	7
1.5	Thesis Structure.....	8
2	Principles and Methods of Flood Impact Assessment at Building Scale to Improve Flood Risk Management.....	12
2.1	Flood Risk Management (FRM).....	12
2.2	Flood Impact Assessment.....	13
2.2.1	Aspects of Flood Impact Assessment.....	13
2.2.2	Flood Impact Assessment as Decision Support Tool.....	14
2.2.3	Users of Flood Impact Assessment.....	15
2.3	The Relationship between Flood Impact Assessment and Resilience.....	15
2.4	Importance of Flood Impact Assessment for Buildings.....	16
2.5	Existing Models/Methods for Flood Impact Assessment for Buildings.....	17
2.6	Calculation of Flood Actions for Flood Impact Assessment at Building Scale.....	18
2.6.1	Water Interaction.....	21
2.6.2	Hydrostatic Action.....	21
2.6.3	Hydrodynamic Action.....	22
2.6.4	Accidental Impact Action.....	24
2.6.5	Debris Impact.....	25
2.6.6	Drag Side Effect.....	26
2.7	Spatial Hydrodynamic Flood Simulation Models at Building Levels to Evaluate Flood Impact Assessment.....	27
2.7.1	Spatial Hydrodynamic Flood Simulation Models.....	28
3	Technological Advancements to Improve Flood Risk Management.....	38
3.1	Technological Advancements in FRM.....	38
3.1.1	Digital Twin Technology.....	39
3.1.2	Building Information Modelling (BIM).....	41
3.1.3	Unmanned Aerial Vehicles (UAVs) or Drones.....	44
3.1.4	LiDAR in Flood Risk Management.....	44
3.1.5	Point Clouds in Flood Risk Management.....	45
3.1.6	Geographic Information System (GIS).....	46
3.1.7	3D Flood Modelling.....	47

3.2	Exploring the Potential Benefits of Integrating New Tools for Improving FRM.....	48
3.2.1	Combining GIS and Analytical Tools.....	49
3.2.2	Integrating AR/VR and Digital Twin.....	50
3.2.3	Integrating GIS and BIM for FRM .....	51
3.3	Challenges to Integrate New Tools in Improving FRM.....	52
4	Investigation of Technological Developments of GIS-BIM Integration .....	55
4.1	State of the Art of GIS-BIM Integration.....	56
4.1.1	Application-Level Method .....	58
4.1.2	Process Level (Web Based Integration).....	58
4.1.3	Data Level Methods.....	58
4.2	Benefits of Integrating GIS-BIM.....	59
4.3	GIS-BIM Integration for Disaster Management .....	60
4.4	GIS-BIM Integration for Flood Impact Assessment .....	60
4.5	Barriers to GIS-BIM Integration.....	61
5	Research Design and Methodology.....	64
5.1	Research Design .....	64
5.2	Design of Model Workflow.....	66
5.2.1	Input Data and Pre-processing.....	66
5.2.2	2D Flood Simulations.....	66
5.2.3	3D Flood Model .....	67
5.2.4	GIS-BIM Integration.....	67
5.2.5	3D Flood Impact Assessment .....	68
6	Prototype Testing: Case Study 1 – HafenCity, Hamburg, Germany .....	70
6.1	HafenCity, Hamburg .....	70
6.2	Testing of Model Workflow.....	71
6.3	Data Collection and Pre-processing .....	71
6.3.1	Digital Terrain Model (DTM).....	72
6.3.2	Building Footprints .....	72
6.3.3	Land Use and Land Cover Data.....	74
6.3.4	Water Level Hydrograph .....	74
6.4	Hydrodynamic Flood Simulation .....	75
6.5	2D Flood Impact Assessment for Building Exposure .....	80
6.6	3D Flood Model .....	82
6.6.1	Conversion of 2D Simulated Flood Inundation to 3D Flood.....	82
6.6.2	Conversion of 2D Building Footprints to 3D Building Blocks.....	84
6.6.3	3D Visualization and Application.....	87

6.6.4	Limitation of 3D Flood Model.....	88
6.7	GIS -BIM Integration.....	89
6.7.1	Adjustments to the 3D Flood Model.....	90
6.8	Flood Impact Assessment in 3D .....	99
6.8.1	Lessons Learnt and Limitations of Case Study 1.....	101
7	Case Study 2: Testing and Implementation of Model Workflow .....	105
7.1	UAS Frankfurt am Main.....	105
7.2	Testing of Model Workflow.....	106
7.3	Data Collection and Pre-processing .....	106
7.3.1	Digital Terrain Model.....	107
7.3.2	Preparation of Other Input Data for Hydrodynamic Flood Simulation.....	111
7.4	Hydrodynamic Flood Simulations.....	111
7.5	3D Flood Model .....	113
7.5.1	3D Building Generation .....	113
7.6	GIS-BIM Integration.....	122
7.7	Building Component Vulnerability Scenarios.....	123
7.8	3D Flood Impact Assessment with 3D Digital Twin (3D-FIA).....	123
7.8.1	Floodwater Interaction.....	123
7.8.2	Hydrostatic Pressure .....	138
7.8.3	Hydrodynamic Pressure .....	142
7.8.4	Debris Force.....	146
7.8.5	Impact Force.....	148
7.8.6	Drag Side Effect .....	150
7.9	Outcomes of 3D Flood Impact Assessment.....	152
8	Discussion and Conclusion .....	155
8.1	Addressing the Research Questions.....	155
8.2	Limitations of the Study .....	158
8.3	Future Recommendation .....	158
8.4	Conclusion .....	160
9	References.....	164
10	Appendix.....	ii
11	List of Reports / Liste der Berichte.....	32

## List of Figures

Figure 1: Scales of flood impact assessment adopted from (Messner 2007) .....	3
Figure 2: Research scope.....	8
Figure 3: FRM cycle adopted from (LAWA 2018 ) .....	12
Figure 4: Flood actions acting on a building (Source: FEMA 2021) .....	19
Figure 5: Hydrostatic pressure (left) water level outside of the building component; (right) depth difference between inside and outside of a building component (Source: Amirebrahimi et al. 2016) .....	22
Figure 6: Visualization of hydrodynamic and hydrostatic pressure (left); Magnitude of hydrodynamic force on the building component (right) (Source: Amirebrahimi et al. 2016) .....	23
Figure 7: Visualization of flood induced accidental impact due to debris such as cars or other elements (Source: Mahaffey 2018).....	24
Figure 8: Flood induced frontal side impact due to debris (Source: FEMA 2021) .....	26
Figure 9: Flood induced drag side effect parallel to the flow direction (Source: FEMA 2021) .....	27
Figure 10: Emerging technologies for flood risk management adopted from (Batty and Yang 2022) .	38
Figure 11: City digital twin visualization: (a) bird eye view of part of the city (b) bird eye view of the same city with flooding (c) hydrograph at one of the buildings (d) Human eye view of the flooded buildings, (Source: Ghaith et al. 2022) .....	40
Figure 12: Basic concept of BIM (Source: Autodesk 2018) .....	41
Figure 13: The five LODs of BIM (Source: Autodesk 2017) .....	43
Figure 14: 3D Visualization of damaged walls (left), doors (middle) and flooring (right) (Source: Amirebrahimi et al. 2016) .....	44
Figure 15: Type of LiDAR data collection (Source: Escobar Villanueva et al. 2019).....	45
Figure 16: Laser scanned point cloud building data (a) and developed 3D building model (b).....	46
Figure 17: 3D flood visualization representing buildings affected by flooding (Source: SymGEO) .....	48
Figure 18: Integration opportunities of emerging digital tools in FRM .....	49
Figure 19: Digital twin creation for a city-scale flood imitation framework (Source: Ghaith et al. 2022) .....	49
Figure 20: Integration of BIM models into ArcGIS using IFC-format and FME method (Source: Carstens 2019).....	56
Figure 21: Integration of BIM models by direct read-in Revit model with ArcGIS pro (Source: Carstens 2019).....	57
Figure 22: GIS and BIM Systems interacting in infrastructure lifecycle (Source: Carstens 2019).....	59
Figure 23: GIS-BIM integration benefits for flood risk assessment adopted from (Jacob 2015).....	61
Figure 24: Research methodology with detailed phases .....	64
Figure 25: Model workflow for flood impact assessment in a 3D digital twin environment by integrating BIM and GIS approaches.....	67
Figure 26: Selected case study area of HafenCity, Hamburg, Germany (Source: BKG) .....	71
Figure 27: Digital terrain model (meters) of HafenCity with 1 meter resolution (Source: BKG) .....	73
Figure 28: Building footprints and the water body of HafenCity (Source: Geodatenzentrum) .....	73
Figure 29: Merged DTM in meters with building footprints of HafenCity .....	73
Figure 30: Roughness coefficients of each specific land use of HafenCity.....	74
Figure 31: Water level hydrograph of HafenCity .....	75
Figure 32: Spatial distribution of flood inundation depth after (a) 10 min (b) 20 min (c) 30 min simulation duration .....	76
Figure 33: Comparison of (a) simulated flood inundation depth with the (b) available flooding map of 100 year flood (Source: Geoportal der Bundesanstalt für Gewässerkunde) .....	77
Figure 34: Spatial distribution of inundation depth, velocity and water flow direction.....	78

Figure 35: HafenCity flood inundation depth with and without building footprints .....	79
Figure 36: Processing steps for 2D flood impact assessment .....	80
Figure 37: Flood prone buildings under different flood impacts in HafenCity and targeted building..	81
Figure 38: Location of selected building and its facade image (Source: Google Images) .....	81
Figure 39: Framework to develop 3D flood model based on 2D datasets adopted from (Khayyal et al. 2022).....	82
Figure 40: Steps involved in the conversion of 2D simulated flood inundation depth into 3D flooding adopted from (Javadnejad et al. 2017) .....	83
Figure 41: Triangular irregular networks of flood inundation in 3D space .....	84
Figure 42: Steps for conversion of 2D building footprints to 3D building blocks with procedural modelling.....	86
Figure 43: Visualization of 2D to 3D converted building blocks of HafenCity.....	86
Figure 44: Visualization of buildings, terrain and flooding in 3D (3D flood model) .....	88
Figure 45: Comparison of representation of the building components in (left) CityGML and (right) IFC adopted from (Nagel 2014).....	89
Figure 46: Overview of the GIS BIM integration process adopted from (Schaller et al. 2017).....	90
Figure 47: Processing steps for extraction of required data from the CADMAPPER tool.....	91
Figure 48: Extracted topography of the selected area with CADMAPPER (left-3D) and (right-2D).....	92
Figure 49: Targeted building data extraction with CADMAPPER .....	92
Figure 50: Key steps for 3D modelling with Autodesk Revit adopted from (Rocha et al. 2020).....	93
Figure 51: Generated BIM-IFC based 3D model of the targeted building.....	93
Figure 52: Processing steps for conversion of TIN into a volumetric component (multipatch) .....	94
Figure 53: Modified GIS-BIM integration approach via direct read-in of BIM-Revit model to ArcGIS Pro (Carstens 2019) .....	95
Figure 54: Five step data integration approach for GIS-BIM integration.....	96
Figure 55: 3D BIM-IFC based building inside ArcGIS Pro after integration .....	98
Figure 56: Flood intersected building structural and non-structural components.....	101
Figure 57: Comparison of DTM resolution 100-by-100 cm pixel size (left) 10-by-10 cm pixel size (right) .....	102
Figure 58: Selected case study area University of Applied Sciences (UAS) Frankfurt am Main (Source: BKG).....	106
Figure 59: Processing steps for conversion of LAS data into DTM.....	107
Figure 60: Information regarding elevations of case study area LAS data.....	108
Figure 61: LAS data of study area import in ArcGIS local scene for processing and georeferencing .	109
Figure 62: Generated DTM from LAS data of the study area.....	110
Figure 63: Spatial distribution of inundation depth, flow velocity and water flow direction.....	112
Figure 64: Visualization of buildings, terrain and flooding in 3D (3D flood model) .....	113
Figure 65: Das Rotes Haus UAS Frankfurt am Main .....	114
Figure 66: Processing steps for scan to BIM generation adopted from (Rocha et al. 2020).....	114
Figure 67: Processing steps for point cloud database editing and management adopted from (Intignano et al. 2021) .....	116
Figure 68: Colorization option; (a) elevation, (b) intensity, (c) normal, (d) scan location .....	117
Figure 69: Raw image from laser scan (left) and revealed image after cleaning (right) .....	118
Figure 70: BIM-IFC based 3D model of the selected building – Das Rotes Haus .....	122
Figure 71: 3D BIM-IFC based building inside ArcGIS Pro after integration .....	122
Figure 72: Intersected building components with simulated flooding .....	125
Figure 73: Intersected walls, doors, and windows of the building with simulated flooding .....	125
Figure 74: Flow direction of flooding in the study area with respect to targeted building .....	126

Figure 75: Building under investigation (a) frontal side (upstream side); (b) back side (downstream side); (c) left side (parallel to flow direction); (d) right side (parallel to flow direction).....	127
Figure 76: Visualization of volumetric components with information of all the faces .....	128
Figure 77: 3D visualization of surface areas of flood intersected walls .....	128
Figure 78: Highlighted frontal side (upstream side) flood intersected components (walls, ventilation, and door) .....	129
Figure 79: Comparison of surface area of flood intersected walls (frontal wetted perimeter).....	130
Figure 80: Comparison of outer frontal side non-structural components intersected surface area..	130
Figure 81: Highlighted back side (downstream side) flood intersected components (walls, ventilation, and windows) .....	131
Figure 82: Comparison of surface area of flood intersected walls (backside wetted perimeter) .....	131
Figure 83: Comparison of outer back side non-structural components intersected surface area .....	131
Figure 84: Highlighted left side (Parallel to flow) flood intersected components (walls, ventilation, and windows) .....	132
Figure 85: Comparison of surface area of flood intersected walls (left wetted perimeter) .....	132
Figure 86: Comparison of outer left side non-structural components intersected surface area .....	133
Figure 87: Highlighted right side (Parallel to flow) flood intersected components (walls, door, and window).....	133
Figure 88: Comparison of surface area of flood intersected walls (right wetted perimeter) .....	134
Figure 89: Comparison of outer right side non-structural components intersected surface area .....	134
Figure 90: Left exposed basement wall outer face area in ArcGIS Pro .....	135
Figure 91: Left exposed basement wall outer face area in BIM model in Revit .....	136
Figure 92: Comparison of total surface area (all the faces) and outer face area of flood intersected walls.....	136
Figure 93: Flood submerged height of all the flood intersected walls.....	137
Figure 94: 3D representation of intersected walls, created using information on the hydrostatic pressure resulting from their intersections .....	138
Figure 95: Comparison of hydrostatic pressure on different intersected walls.....	139
Figure 96: Comparison of hydrostatic force magnitude on different intersected walls.....	139
Figure 97: Relationship between surface area and hydrostatic force magnitude .....	140
Figure 98: Comparison of hydrostatic pressure and force with respect to the intersected face area	140
Figure 99: 3D Application of hydrostatic pressure on respective walls inside RFEM due to automation in digital twin .....	141
Figure 100: Comparison of hydrodynamic pressure and force on front and back side intersected walls .....	143
Figure 101: Comparison of hydrodynamic pressure and force with respect to intersected face area .....	143
Figure 102: Comparison of hydrostatic and hydrodynamic force.....	144
Figure 103: 3D representation of intersected walls, created using information on the hydrodynamic force resulting from their intersections .....	145
Figure 104: Application of hydrodynamic pressure on respective walls inside RFEM due to automation in digital twin .....	145
Figure 105: Comparison of debris force acting on different intersected walls.....	146
Figure 106: 3D representation of intersected walls, created using information on the debris force resulted from their intersections. ....	147
Figure 107: Application of debris pressure on respective walls inside RFEM due to automation in digital twin.....	147
Figure 108: Comparison of impact force acting on different intersected walls.....	148

Figure 109: 3D representation of intersected walls, created using information on the impact force resulted from their intersections ..... 149

Figure 110: Application of impact pressure on respective walls inside RFEM due to automation in digital twin..... 149

Figure 111: Comparison of drag force acting on different intersected walls ..... 150

Figure 112: 3D representation of intersected walls, created using information on the drag force resulted from their intersections ..... 151

Figure 113: Application of drag side pressure on respective walls inside RFEM due to automation in digital twin..... 151

Figure 114: 3D visualization of intersected building components and necessary information pop-up window..... 152

Figure 115: Comparison of all the forces computed on intersected walls with respect to their intersected areas..... 153

**List of Tables**

Table 1: Flood actions on buildings compiled from (Thieken 2006; Nadal et al. 2010; Moel et al. 2015; FEMA 2021) ..... 20

Table 2: 1D, 2D and 3D Hydrodynamic flood simulation models solving equations adopted from (Teng et al. 2017)..... 29

Table 3: Emerging technologies and their contribution to FRM ..... 39

Table 4: Collected data types and sources for the case study area ..... 72

Table 5: Flood actions automated into digital twin for 3D flood impact assessment ..... 100

Table 6: Collected data types and sources for the case study area ..... 107

## List of Abbreviations

AEC	Architecture, Engineering and Construction
AR	Augmented Reality
BF	Building Footprints
BIM	Building Information Modelling
CAD	Computer Aided Design
CLC	Corine Landcover
DEM	Digital Elevation Model
DIN	Deutsche Institut für Normung
DSM	Digital Surface Model
DT	Digital Twin
DTM	Digital Terrain Model
DXF	Drawing Exchange Format
FDA	Flood Damage Assessment
FEMA	Federal Emergency Management Agency
FIA	Flood Impact Assessment
FME	Feature Manipulation Engine
FRM	Flood Risk Management
GIS	Geographic Information System
GML	Geography Markup Language
GUI	Graphical User Interface
IFC	Industry Foundation Class
LAS	LiDAR Aerial Survey
LiDAR	Light Detection and Ranging
LOD	Level of Detail
LULC	Land use Land Cover
PPGIS	Public Participation Geographic Information System
prj	Projection File
RVT	REVIT Format File
SKP	Sketchup
TIN	Triangular Irregular Networks
UAVs	Unmanned Aerial Vehicles
VR	Virtual Reality
XLSX	Microsoft Excel Format
XML	Extensible Markup Language
1D	One Dimensional
2D	Two Dimensional
3D	Three Dimensional



## List of Units

Meter (m)

Centimeter (cm)

Millimeter (mm)

Kilometer (km)

Meter square (m<sup>2</sup>)

Centimeter square (cm<sup>2</sup>)

Millimeter square (mm<sup>2</sup>)

Cubic meter (m<sup>3</sup>)

Cubic centimeter (cm<sup>3</sup>)

Cubic millimeter (mm<sup>3</sup>)

Meter per second (m/s)

Kilogram per cubic meter (kg/m<sup>3</sup>)

Newton (N)

Kilonewton (kN)

Kilonewton per meter square (kN/m<sup>2</sup>)

# Chapter 1

---

## Introduction

# 1 Introduction

## 1.1 Research Background

Floods are widely recognized as the most prevalent and economically impactful natural disasters worldwide (Gustafsson et al., 2023; Jha et al. 2012; Nektarios and George 2013). Recent reports indicate that severe flooding has resulted in substantial damage to human lives, livestock, agriculture, and infrastructure across various regions of the world (UNISDR 2015; CRED 2022; UNDRR 2019). In Europe, notably in Germany, flooding has caused severe damage (Fekete and Sandholz 2021). Similarly, in Asia, countries like India, Pakistan, and China have experienced catastrophic floods that have claimed numerous lives and caused extensive damage (Rhee et al. 2020; Smith 2020; Nanditha et al. 2023). Additionally, flooding in several regions of America has led to significant loss of life and damage to infrastructure, agriculture, and animals (Smith 2020). According to the Global Assessment Report on Disaster Risk Reduction (UNDRR 2019) by the United Nations, flooding can have catastrophic consequences on urban settlements. The report highlights the potential risks to personal safety, including the need to evacuate from buildings due to the submergence of dry areas, and the potential for high-velocity floods to sweep individuals away before emergency services can reach them. Moreover, flooding can cause substantial damage to buildings and their components, leading to significant losses for individuals, businesses, insurers, and government funds. Critical infrastructure, such as hospitals, can also be adversely affected, resulting in widespread disruption and business interruptions (Aronsson-Storrier 2021).

The flooding events are predicted to increase in frequency and intensity for future events due to the changing climate. This issue has been highlighted at every governance level from global to national to regional and local scale. It also emerged the need for establishing flood resilience at the community levels and requires the effective management of floods towards mitigating their adverse impacts (Brody et al. 2007; McLachlan et al. 2013; Vaidya et al. 2019). Flood resilient development is now a crucial component of flood risk management, emphasizing the concepts of making space for water and living with floods (Hegger et al. 2016). The development methods and building technologies that are robust to flooding have become more important due to the change in flood risk philosophy and experience of flood events. Three strategies to avoid damage at an individual property level are avoidance, water exclusion, and water entry technologies (DWA 2016). Research on flood resilient materials, repair, and reinstatement processes has gained significant attention, particularly the interest and policy have shifted towards water entry approaches. It is acknowledged that experience prompts resilient responses and reinstatement provides an opportunity to install resilient measures.

The traditional focus on flood control or defence measures, highlighted by Hartmann & Juepner (2014), is limited as it can only safeguard against certain types of flooding (such as coastal or river floods) up to a specific level. As a result, there has been a shift towards the Flood Risk Management (FRM) framework, which is a more comprehensive approach to flood management. This framework includes measures such as structural measures, non-structural measures, and flood preparedness and response. By considering a range of factors beyond just structural measures, FRM offers a more holistic approach to flood management that can lead to overall success. By using a multi-tier analysis of risk, FRM intends to identify and treat risks at different levels in an integrated way by (a) minimizing the hazard levels and (b) reducing the potential damages (Begum et al. 2007; Bubeck et al. 2017). A major advantage of FRM over the hazard-based approach lies in its holistic view of risk and consideration for

flood damages (initiated from flood impacts) as evidence for decision-making. This underlines the significance of the concept of Flood Impact Assessment (FIA) as the key component of the FRM for estimating the possible impacts of flooding on infrastructures, buildings, and people for the crucial decisions in flood risk management (FRM) context (Penning-Rowsell et al. 2005; Meyer et al. 2009b; Hammond et al. 2015; Hartmann and Jüpner 2014).

According to Merz et al. (2007) and Moel et al. (2015), FIA can be conducted in three main scales: micro, meso, and macro, which support various levels of risk assessment in FRM in Figure 1. The macro and meso models are typically designed for large-scale applications and provide less detailed outputs, while the micro-level methods are used for the high-resolution object-oriented analysis of individual elements at risk within a small spatial stretch (Merz et al. 2007; Blaschke 2010; Blanco-Vogt and Schanze 2014).

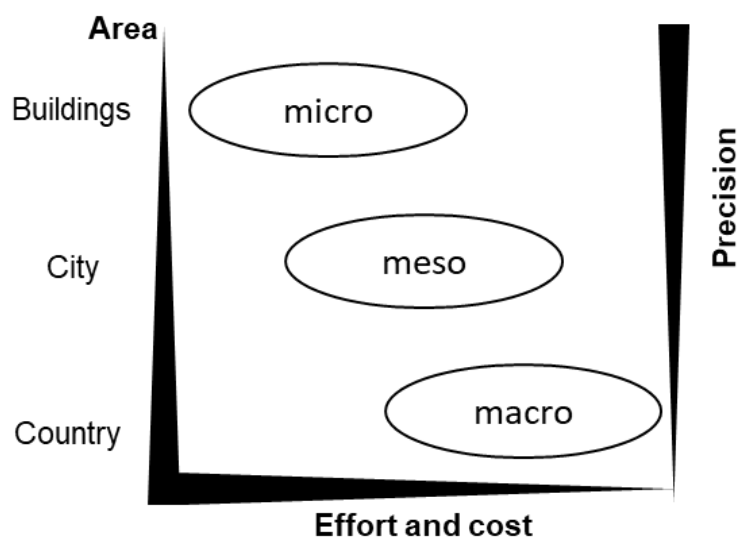


Figure 1: Scales of flood impact assessment adopted from (Messner 2007)

Likewise, according to Messner (2007) and Wang et al. (2021), buildings play a significant role in the economy and contribute greatly to the total community damage caused by floods. Many flood damage assessment (FDA) methods focus mainly on buildings as the representative of the overall flood impact on the community (Terry Cannon and John Twigg 2003; Spekkers et al. 2014; Amirebrahimi et al. 2016). However, recent emphasis has been placed on the safety of people and the performance-based design of buildings against floods at the building level. This requires evidence-based decision support for decision makers to ensure the flood resilience of buildings during their design and planning stages (Dewals et al. 2008; Taggart and van de Lindt 2009). An effective assessment of potential flood impacts at the building level is necessary to understand the behaviour of buildings during floods and identify areas for improvement and retrofitting (CSIRO 2000). Recent advancements in technology have led to an exponential increase in the amount of data that can be collected and analysed, often referred to as "big data". This availability of data brings new opportunities for improving FIA methods by incorporating more detailed and comprehensive data into the models.

One such opportunity is the use of remote sensing techniques to obtain high-resolution data about buildings and their surroundings. Nakazato and Lim (2020) suggest that remote sensing techniques can help to overcome the limitations of traditional data collection methods (such as ground surveys, manual measurements and assessments, and data collection through physical fieldwork) by providing

more detailed information about buildings and their surroundings, particularly in inaccessible or hazardous areas. In addition, the use of machine learning techniques can help to analyse and process large datasets to extract meaningful information about flood impact. Ha et al. (2022) demonstrate the potential of using machine learning techniques such as random forests and support vector machines to predict flood damage to buildings based on various input variables, including building characteristics and flood parameters.

Furthermore, the integration of different data sources such as geographic information systems (GIS), social media, and citizen science can provide a more comprehensive and real-time view of flood impact. Rusca (2018) emphasizes the importance of integrating multiple data sources to improve flood risk communication and decision-making. Overall, the availability of big data presents new opportunities for improving FIA methods by incorporating more detailed and comprehensive data into the models. By doing so, a more accurate understanding of flood impacts on buildings can be obtained and more effective strategies for flood risk management and mitigation can be developed. Literature suggests that performing a comprehensive FIA can facilitate various design alternatives for a building, leading to the adoption of efficient risk reduction measures to mitigate the potential impacts of flooding and reducing the recovery time and resources required following a flood event (Jha et al. 2012). These factors emphasize the significance of assessing the potential flood impacts and implementing measures to improve building resilience to floods at the micro-level and at the early stages of the planning and development process to make informed decisions.

Only micro-level methods amongst numerous FIA models proposed at different scales can allow for the assessment of damages at a building level, as stated by Messner and Meyer (2006) and Apel et al. (2009). However, the current micro-level FIA methods have limitations in considering the distinct behaviour of buildings against floods (Chung et al. 2018; Percival et al. 2019). The generalizations and assumptions about building information inputs, often neglecting the interior of the building, misrepresent the unique characteristics of the building and increase the uncertainty of the outcomes (Thieken 2006; Apel et al. 2009; Tariq Maqsood et al. 2014). Current data input concerns have resulted in the dominance of simpler methods with a higher level of uncertainty, which is directly linked to the model complexity and its predictive capability (Messner 2007; Merz et al. 2010). Additionally, the damage is generally assessed solely against approximated flood parameters, often only the depth of water, despite the lack of a direct relationship between the damage and water depth alone. Therefore, uncertainties and errors increase in the outputs (Smith 1994; Thieken 2006; Apel et al. 2009; Pistrika and Jonkman 2010). Furthermore, damage estimation in the current practice is performed for worst-case scenarios, considering the simultaneous occurrence of maximum flood parameters, which may be rare. Neglecting the spatiotemporal dynamism of the flood parameters, the intermediate flood impacts on a building that may influence its damages are ignored. Moreover, several scientific studies have identified limitations in current FIA methods, as noted in Chung et al. (2018) the need to consider the building's components and geometry, as well as the spatial context, for accurate predictions of flood impact. Maqsood et al. (2014) emphasize the need for high-resolution data, suggesting that advanced techniques such as remote sensing and laser scanning can provide more detailed information. Smith (1994) stresses the importance of considering the location and orientation of openings in buildings. Apel et al. (2009) suggest that advanced modelling techniques such as agent-based modelling and cellular automation can help to capture the unique characteristics of buildings. Merz et al. (2010) note the trade-off between model complexity and predictive capability in FIA, highlighting the importance of incorporating detailed information but also acknowledging the

potential increase in complexity and computational requirements. Taken together, these studies underscore the need to address the limitations of current FIA methods to improve the accuracy of FIA on buildings.

Whereas complex flooding situations can subject buildings to various loads and damage different components through water contact, current FIA/FDA methods singularly concentrate on either water contact damage or estimating damage from flood loads. These methods lack consideration for the combined effects of both phenomena on buildings. Furthermore, the existing FIA/FDA models are developed according to the local conditions and therefore are difficult to transfer to another location or time. The outputs provided by these methods are limited to a single number for the overall building impact assessment or only an indication of whether the building collapses or not for a certain level of water and velocity. Other than these, no further information about the details and the location of damage at the building level is provisioned. Such details are important to reveal the sources of risk for a building for their treatment (Kelman 2003; Mazzorana et al. 2014). Hence, the current FIA/FDA methods generally cannot provide an effective presentation of the details and mode of flood damage to a building and its components. Therefore, crucial information about the underlying factors for the damage cannot be communicated using existing methods which makes it difficult to compute the magnitude of the force of the floodwater on the wetted parameter of the building components. To evaluate the exact impact of the floodwater on building components it requires detailed building components with their semantic properties. This nowadays can be acquired through structured 3D digital models that document building components with their semantic properties. It has now become an urgent necessity, which can be achieved with high levels of automation using 3D surveying technologies. The resulting point clouds can be integrated into Building Information Modelling (BIM) platforms that manage graphic and non-graphic information and component properties data. BIM is a suitable for archiving and organizing information about buildings and integrating geometric information, allowing for in-depth knowledge of the building for optimizing management, maintenance, and analysis processes. BIM adoption is expanding worldwide due to regulatory requirements and improvements in the construction industry. Despite the many benefits of BIM, including support for documentation, energy and structural analysis, and virtual reconstruction, it is rarely used by authorities responsible for flood management, making it a primary research topic.

The use of digital twin technology has also gained importance in FRM due to its potential for improving flood impact assessment. According to Isikdag and Zlatanova (2009), the integration of GIS and BIM can provide a comprehensive workflow for 3D flood impact assessment, with the possibility of developing a digital twin that allows 3D geospatial analysis with 3D flood and building components at a micro-level scale. The advancements in 3D-GIS technology have further enhanced the capabilities of digital twin models in providing accurate and detailed flood analysis and assessment (Dakhil and Alshawi 2014). Therefore, the integration of digital twin technology in FRM can enable better decision-making and improved resilience against flood risks.

The current FIA methods (detailed in Section 2.5) excel in evaluating damage at a larger scale for risk analysis and mapping. However, their limitations prevent effective use at the individual building level for flood-resilient design and planning. This creates a research gap, hindering the shift from traditional code-based approaches to performance-based methods in building engineering. Consequently, many countries prioritize code-conforming methods tailored for wind and earthquakes, neglecting flood hazards.(Taggart and van de Lindt 2009; Christodoulou et al. 2010). Therefore, there is a highlighted need for further research to develop a method capable of incorporating comprehensive input datasets

concerning both the building and flood parameters. This method should consider the building's unique characteristics to conduct a thorough analysis and effectively communicate potential damages. By linking such a method to the early stages of the planning process for a building, FIA can possibly facilitate a flood resilient design of buildings in flood prone areas. This, in addition to the other regional and local flood risk reduction strategies, can improve the overall flood resilience of the community and reduce the cost of damage from such events.

## **1.2 Problem Statement**

Based on recent studies, it has been found that the current FRM approaches for resilient buildings mostly focused on damage assessment and supports broader applications by considering aggregated information as input (Merz et al. 2010; Popat 2017). Nevertheless, these approaches have limitations in evaluating building design or components against floods, as they are unable to conduct a detailed analysis of the potential impact of a specific flood event on a particular building based on its unique geometry and construction. This highlights the need for more advanced methods and workflows that can address these limitations and provide more accurate assessments at the building levels (Merz et al. 2010; Popat 2017). Accordingly, the problem in this research can be formally devised as: Despite the need for implementation of flood impact assessment at a building level during the design and planning phases, it is of utmost importance to mitigate potential risks and safeguard building components. Nevertheless, contemporary building level techniques are insufficient as they fail to provide a streamlined workflow that considers the distinctive features of individual buildings with their components and incorporates hydrodynamic flood simulation in a single model for enhanced risk analysis, visualization, communication, and assessment of flood impacts on a building and its components.

This problem may hinder efficient decision-making at the local level of risk management for buildings and serve as an obstacle to implementing evidence-based solutions that can enhance building resilience to floods for improving FRM.

Advancements in data processing technology and emerging tools have improved efficiency and accuracy, resulting in faster decision-making, innovative solutions, and increased productivity. A comprehensive evaluation of these novel technologies across various domains (Chapter 3) has highlighted the potential benefits of combining various tools to enhance flood risk management. One notable combination is the integration of GIS and BIM to overcome limitations in the FIA process. BIM offers detailed information on all aspects of a building and is currently mandatory for land development processes in many countries ( Ullah et al. 2022; Chen et al. 2023), while GIS and geospatial information can provide geographically extended features such as flood and spatial analysis capabilities for damage assessment. With advances in 3D-GIS technology, it is possible to develop a digital twin that allows for 3D geospatial analysis with 3D flood and building components, even at the micro-level scale. However, there is currently very little theoretical discussion on the potential use of this integrated method and its value for FIA (Angeli et al. 2022 ; Hosseini et al. 2021). Furthermore, limited research or practical evidence exists in the literature that provides a methodology or comprehensive workflow for 3D flood impact analysis using 3D geospatial analysis considering a digital twin environment. This presents an opportunity in the context of FIA to improve FRM. To avoid expensive damage to buildings' structural and non-structural elements, misinterpretation of risks, and potential safety hazards for occupants, it is important to develop customized FIA approaches that account for specific building characteristics such as age, construction materials, and surrounding

topography, as well as a high-resolution 3D visualization. To achieve this, more effective flood impact assessment methods should be given priority, which consider the distinctiveness of individual buildings and account for flood parameters such as depth, velocity, and direction while also improving communication and visualization of flood impacts.

### 1.3 Research Questions

This research mainly focuses to answer the overarching research question that is formulated as follows:

*“How GIS and BIM integration improve flood risk management (FRM) by creating a digital twin for flood resilient buildings, and would it provide support for flood impact analysis on structural and non-structural components of the building?”*

To answer the overarching research question that drives the research, four sub-questions have been developed. They are stated as:

- **Q1:** What are the capacities and limitations of existing 2D and 3D spatial hydrodynamic flood simulation models at building scale?
- **Q2:** What is the state-of-the-art of GIS and BIM technologies, and do they contain integration potential for improving flood risk management at building levels?
- **Q3:** How GIS-BIM integration can be carried out and what practical challenges can emerge during the integration process for flood risk management at building levels?
- **Q4:** How does the integrated GIS-BIM approach support flood impact assessment on structural and non-structural building components?

### 1.4 Research Scope

The research argues that improved FRM requires the integration of two main domains - spatial hydrodynamic flood simulation based on GIS and the development of a digital twin of a building using BIM technology see Figure 2. This research aims to produce a novel workflow for GIS-BIM integration and elaborate on its steps using two case studies. The integration of these domains will allow for a detailed assessment of flood impact on individual building components, leading to improved FRM and a pathway toward resilient building development against flooding.

The first domain of this research involves spatial hydrodynamic flood simulation based on GIS. This involves the use of spatial data to simulate floodwater movement and to assess flood impact. The second domain of this research involves the development of a digital twin of a building using BIM technology. This involves the creation of a virtual model that replicates the physical characteristics of a building.

The integration of GIS and BIM is crucial for improving FRM. This integration will allow for the assessment of flood impacts on individual building components and will facilitate the development of resilient building designs. The workflow for GIS-BIM integration involves several steps, including data acquisition, data integration, model creation, simulation, and visualization. To illustrate the functionalities of the GIS-BIM integration workflow, case studies will be conducted. These case studies will demonstrate how the workflow can be used to assess flood impacts, identify vulnerabilities, and facilitate to develop resilient building designs.



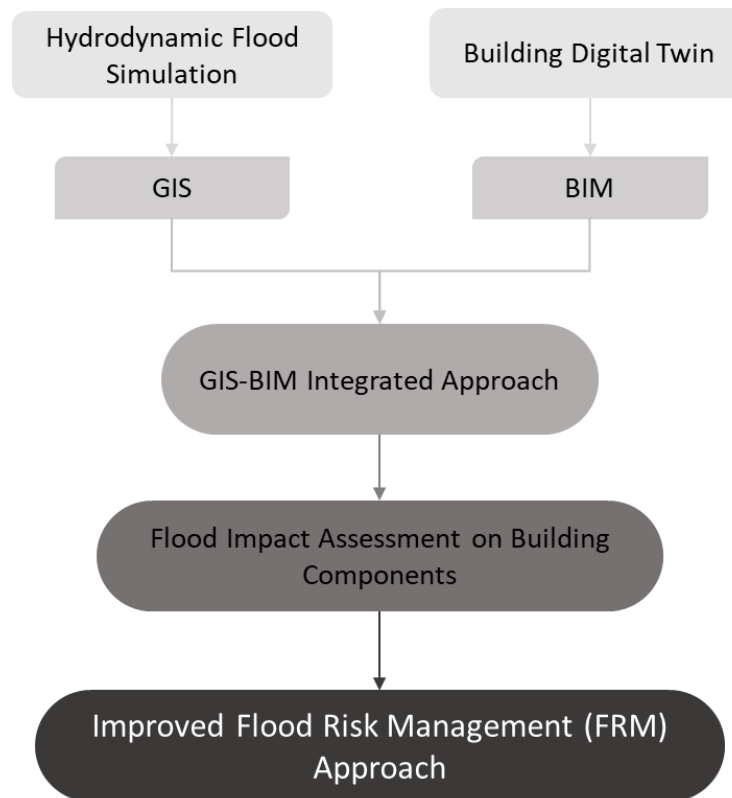


Figure 2: Research scope

## 1.5 Thesis Structure

The dissertation is organized into 10 chapters. A brief explanation of the overall contents and order of each chapter is provided below.

In chapter 2, an overview is given of the literature about FIA at the building scale, as well as the principles and methods involved. The chapter also emphasizes the importance of FIA as a critical component of FRM and explores the various aspects of impact evaluation that are necessary for decision support and building resilience. Additionally, the chapter reviews several applications of FIA to buildings and investigates various flood actions that can occur during a flood event. This review underscores the need for hydrodynamic flood simulation modelling and identifies the most suitable types of models available for FIA purposes. The chapter also discusses the capabilities and limitations of different types of hydrodynamic flood simulation modelling software, including spatial 1D/2D and 3D models, as they pertain to building-level FIA.

Chapter 3 conducts a critical review of the latest technologies that have been presented in the literature to enhance flood risk management holistically. Additionally, the chapter explores how the integration of these emerging technologies could potentially improve flood risk management and simplify the process of flood impact assessment at the building scale. The chapter provides valuable insights into potential combinations of new tools that can enhance flood risk management, including the integration of BIM and GIS. The chapter also discusses the potential applications of BIM and GIS in support of FIA, highlighting how these technologies can address the gaps identified in Chapter 1.

Chapter 4 focuses on exploring the recent advancements in the integration process of GIS and BIM. The chapter highlights the benefits of this integration process for FIA and other disaster management

activities. Moreover, the chapter also investigates the existing barriers in the integration process of GIS and BIM.

In chapter 5, the research methodology used in this study to address the questions posed in Section 1.3 is outlined. The chapter presents the necessary steps involved in the methodology and describes how they are integrated with different aspects of the research. The chapter also provides details on the design of the model workflow and its various components, which are used to answer the research questions in-depth.

Chapter 6 focuses on the testing phase of the developed model and its intermediate steps workflow, which was conducted on a prototype case study. In this chapter, all six phases of the model were tested to effectively address the related research questions. The chapter also outlines the adjustments made to the methodology based on the results of the testing phase. Additionally, the chapter identifies limitations in the overall process and provides lessons for improving the methodology and data inputs. Moreover, this chapter details the implementation of the workflow into a proof-of-concept prototype system. It explains the overall architecture of the prototype system and the technologies adopted in it. The chapter also highlights the data processing and requirements of intermediate steps necessary for integrating the GIS and BIM components.

Chapter 7 presents a real-time case study that demonstrates the improved methodology and lessons learned from the prototype case study. The chapter highlights the improvement in flood risk management by conducting a 3D FIA and provides results based on the assessment and visualization of the impact of flooding and risks to a real building. The chapter further provides details on the results of the flood actions and their visualization in a 3D environment. The chapter concludes with a comprehensive summary of the overall methodology and its effectiveness in assessing and managing flood risk at the building scale. Furthermore, this chapter provides a step-by-step guide on how to use the developed workflow and software tools to conduct a 3D flood impact assessment on a building for different flood actions assessment and calculations. The guide includes details on how to prepare input data, run the workflow, and visualize the results in 3D.

Chapter 8 provides a reflection on the achievements of the research presented in the previous chapters. The chapter summarizes the main findings and contributions of the study and presents concluding remarks based on the outcomes of the research. Additionally, the chapter proposes recommendations for future research directions based on the limitations and potential areas for improvement identified during the study. These recommendations may include further development of the GIS-BIM integration process, improvement of data quality and availability, and refinement of the flood impact assessment methodology. The chapter concludes with a discussion of the potential implications of the study for flood risk management practices and the importance of integrating emerging technologies into the process. Finally, the chapter offers an overview of the overall significance of the study and its potential impact on future research in the field.

Chapter 9 provides an extensive list of literature references that were reviewed and taken into account throughout the research. This chapter includes a comprehensive list of sources that were used to build a theoretical foundation for the research, as well as to inform the methodology and analysis of the results. This helps the readers to find relevant sources related to a particular aspect of the research easily. The sources cited in this research come from a variety of disciplines, including flood risk

management, Hydrodynamic flood simulation, architecture, engineering, urban planning, and environmental science.

Chapter 10 provides additional details in the appendix regarding the methodological process and the python scripting involved in automating different steps of the model workflow. This chapter includes a detailed description of the software tools and frameworks used in the research, along with code snippets and examples to help readers understand the process better. The chapter also includes supplementary material such as data and software used in the research. The supplementary material is intended to provide readers with additional resources to replicate the research or to build upon it further.

## **Chapter 2**

---

# **Principles and Methods of Flood Impact Assessment at Building Scale to Improve Flood Risk Management**

## 2 Principles and Methods of Flood Impact Assessment at Building Scale to Improve Flood Risk Management

### 2.1 Flood Risk Management (FRM)

Flood risk management (FRM) is a comprehensive approach to reducing the impact of floods on people, property, and infrastructure (Jüpner 2018). It involves a combination of measures, including precaution, response, and recovery, to reduce the likelihood and severity of flooding, and to minimize its consequences. One of the key components of flood risk management is flood risk assessment. Flood risk assessment helps to identify areas that are vulnerable to flooding, estimate the potential impact of floods, and prioritize the allocation of resources for risk reduction measures (Jüpner 2019).

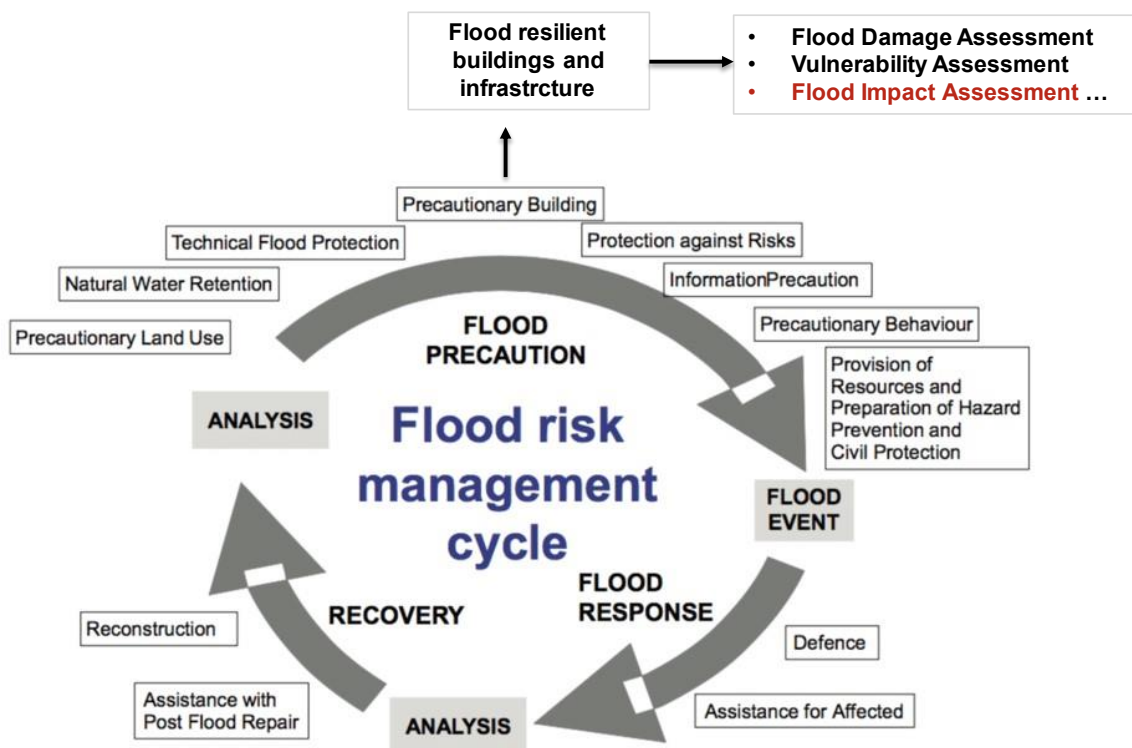


Figure 3: FRM cycle adopted from (LAWA 2018 )

Many approaches are derived in FRM that involves natural, semi-natural, and engineering measures. In addition, the FRM cycle includes precautions, response, and recovery see Figure 3. Precautionary measures include the development of flood warning systems - based on evaluating and analysing the current and future flood forecasts, emergency response plans, and public education programs. Response measures involve the immediate actions taken during a flood event, such as rescue operations and the provision of emergency supplies. Recovery measures involve the restoration of infrastructure and services after a flood event, including repairs, clean up, and the provision of temporary housing. In a nutshell, FRM is a multi-faceted approach to reduce the impact of floods on people, property, and infrastructure (Hartmann and Jüpner 2020).

European union flood Directive (2007/60/EC) is also intricately linked to FRM within the European Union. The directive primarily focuses on establishing a framework for assessing and managing flood risks across EU member states. It outlines key principles and measures aimed at better understanding,

preventing, and mitigating the impacts of floods. The directive emphasizes the importance of comprehensive risk assessment, mapping, and planning to effectively identify vulnerable areas and populations at risk from flooding. It also encourages member states to collaborate and coordinate efforts, recognizing that floods often transcend national borders and require joint strategies for effective management. One of the core aspects of this directive is the requirement for member states to develop flood risk management plans. These plans are expected to integrate various measures such as prevention, protection, preparedness, and communication strategies to minimize the impact of floods on communities and infrastructure.

The FRM emphasizes the importance of a comprehensive approach to managing flood risks, therefore the precautionary phase of the flood risk management cycle leads to the flood resilient buildings and infrastructures, which eventually involves the assessment of potential flood risks, the implementation of measures to prevent or mitigate them, and the monitoring and evaluation of their effectiveness. To achieve flood resilience, it is necessary to conduct a flood impact assessment or flood damage assessment to identify the potential hazards that a flood could pose to the buildings or infrastructure (Kelman et al. 2016; Jüpner et al. 2018). This assessment involves evaluating the risks associated with flooding, such as the potential for structural damage, the risk of water infiltration, and the impact on electrical systems and other critical infrastructure. Vulnerability assessment stands as a crucial aspect within flood risk management, entailing the identification of buildings or infrastructure susceptible to flood damage and gauging their ability to endure such impacts. By pinpointing these vulnerabilities, this assessment aids in recognizing areas needing reinforced resilience against flooding, which may involve initiatives like installing flood barriers, utilizing water-resistant materials, or elevating vital infrastructure elements. Ultimately, flood-resilient buildings and infrastructure form indispensable facets of effective flood risk management strategies. By conducting FIA and vulnerability assessments, stakeholders can identify and address potential flood hazards and implement measures to enhance the resilience of buildings and infrastructure (Kurnio et al. 2021). This proactive approach can help to mitigate the potential damage and losses that can occur in the event of a flood and ensure the safety and sustainability of communities and infrastructure. Hence, this research intends to improve flood impact assessment using novel technologies to improve flood risk management.

## 2.2 Flood Impact Assessment

Flood impact assessment is a process of evaluating the potential impact of flooding on human populations, infrastructure, and the environment. According to the European Union Floods Directive (2007/60/EC), flood impact assessment is defined as "the process of identifying and evaluating the possible adverse consequences of flooding for infrastructure, human health, the environment, cultural heritage, and economic activity" (European Union 2007).

### 2.2.1 Aspects of Flood Impact Assessment

Flood impact assessment involves a comprehensive analysis of the potential impacts of flooding, including the physical, social, and economic impacts on affected populations and infrastructure. The assessment typically includes both direct and indirect impacts, such as damage to infrastructure, loss of life, and economic disruption. Here are some aspects of flood impact assessment:

**Physical Impact Assessment:** This aspect of flood impact assessment involves evaluating the physical damage to buildings, infrastructure, and natural resources. The assessment may include data on the

depth and velocity of floodwaters, the extent of flood inundation, and the damage to roads, bridges, buildings, and other structures (Jongman et al. 2012).

**Social Impact Assessment:** This aspect of flood impact assessment focuses on the social impacts of flooding, including the loss of life, injuries, displacement, and impacts on community well-being. The assessment may also include the potential for social disruption and impacts on vulnerable populations, such as the elderly, children, and low-income households (Karagiorgos et al. 2016).

**Economic Impact Assessment:** This aspect of flood impact assessment involves evaluating the economic consequences of flooding, including the cost of repairing or replacing damaged infrastructure, the loss of income and economic activity, and the long-term impacts on regional or national economies. The assessment may also include estimates of the economic benefits of flood risk management measures (Merz et al. 2007; Johnson and Priest 2008).

**Environmental Impact Assessment:** This aspect of flood impact assessment focuses on the impacts of flooding on natural resources and ecosystems, including the loss of habitat, changes in water quality, and impacts on biodiversity. The assessment may also include the potential for long-term environmental impacts, such as changes in soil quality and erosion.

Flood impact assessment can be a complex and multi-disciplinary process, involving a range of technical, scientific, and social expertise. It is an essential component of flood risk management and can help inform decision-making and resource allocation to reduce the impacts of flooding. This assessment can provide decision-makers with valuable information for developing FRM strategies, such as flood prevention measures, early warning systems, and emergency response plans (Gilbuena et al. 2013).

### **2.2.2 Flood Impact Assessment as Decision Support Tool**

Flood impact assessment serves as a valuable decision-making tool for flood risk management by providing information on the potential impacts of flooding. It can help decision-makers prioritize investments in flood protection and emergency response measures. Jia et al. (2022) used a combination of remote sensing, GIS, and hydrological models to conduct a flood risk assessment in the lower reaches of the Yangtze River in China. The assessment included an evaluation of the potential impacts of flooding on infrastructure, agriculture, and human populations. The authors then used the results of the assessment to inform decision-makers regarding flood risk management measures. The study also found that FIA is a valuable tool for decision-making in FRM by providing detailed information on the potential impacts of flooding. Based on that decision-makers prioritized investments in flood protection measures and emergency response planning. It is highlighted that the use of advanced technologies such as remote sensing and GIS can improve the accuracy and effectiveness of flood impact assessments, allowing decision-makers to make more informed and effective decisions. The process of FIA typically involves several key steps, including hazard identification, exposure assessment, vulnerability assessment, and risk assessment (Merz et al. 2010). These steps involve the collection and analysis of data on flood hazard characteristics, the population and infrastructure at risk, and the vulnerability of these elements to flood damage.

### 2.2.3 Users of Flood Impact Assessment

FIA is utilized by a range of users from diverse backgrounds and professions. Government agencies utilize FIA to make policy decisions regarding flood management, such as determining high-risk areas and implementing mitigation measures. Emergency responders rely on FIA to comprehend the extent and severity of flooding and allocate resources accordingly. Insurance companies utilize FIA to determine risk and set premiums for flood insurance policies. Infrastructure planners utilize FIA to identify suitable locations for essential infrastructure such as hospitals, schools, and transportation systems. Developers and builders use FIA to make decisions about where to construct new structures and how to design buildings and infrastructure to withstand flood events. Environmental organizations use FIA to understand the impact of flooding on ecosystems and inform conservation efforts. Lastly, FIA can inform residents and businesses in flood-prone areas about the risks they face and help them make decisions about how to prepare for and respond to flooding events (Flood Resilience Portal 2021).

### 2.3 The Relationship between Flood Impact Assessment and Resilience

Flood impact assessment and resilience are important for understanding the effects of flooding on communities and for developing strategies to reduce vulnerability to future flood events. It serves a variety of purposes for example local or national governments use them for decision making and risk management so that resources can be allocated to finance structural and non-structural flood mitigation measures. Insurance and reinsurance companies use FIA to understand the value of assets at risk, and to price their policies accordingly (van der Veen 2003; Hammond et al. 2015). Flood impact assessment involves the evaluation of the physical, social, and economic impacts of flooding on communities, including the extent of damage to buildings and infrastructure, the displacement of people and businesses, and the loss of economic activity.

Resilience, on the other hand, refers to the ability of communities to cope with and recover from the impacts of flooding. This includes strategies to reduce vulnerability and increase adaptive capacity, such as improving building codes and infrastructure, developing early warning systems, and promoting social and economic resilience. Recent years have seen increased attention to building resilience against floods, as local governments and national building codes require designers and engineers to design buildings to withstand flood impacts (Tuan Hai and Kim Hoang 2023). This increased focus is partly due to the fact that flood-resilient buildings not only withstand floodwater better, but are also less costly to restore after a flood, and their reinstatement is much quicker (Lamond et al. 2019). Furthermore, adopting proper flood-resilient designs and mitigation measures in FRM at early stages can significantly improve the flood resilience of buildings, thus avoiding costly retrofitting and redesign at later stages (Hartmann et al. 2022).

However, despite the importance of building resilience to floods, building/property-level mitigation measures have received relatively little attention in the past (Keys 2006; Samuels et al. 2006; Golz et al. 2015; Lamond et al. 2019). There is a need for a detailed analysis of the response of homes against floods for a better understanding of their behaviour in such events (Becker et al. 2011). Such detailed studies can allow for the identification of non-conforming developments and potential areas of improvement/retrofitting towards more flood-resilient building designs (CSIRO 2000). This analysis enables engineering designers and owners to use Cost-Benefit Analysis (CBA) to explore different flood



resilience technologies/measures at the property scale (van der Veen 2003; Joseph et al. 2014). Effective flood impact reduction measures for buildings require a thorough assessment of the flood hazard, as stated by the Federal Emergency Management Agency (FEMA 2021). Flood impact assessment plays a crucial role in designing flood-resistant buildings that can withstand flood events and minimize damage, according to a study by Forero-Ortiz et al. (2020). The United Nations Office for Disaster Risk Reduction stresses the importance of flood impact assessment in building resilient communities, stating that flood risk assessment is critical for developing appropriate flood risk reduction measures and protecting the built environment (UNDRR 2019). Furthermore, the American Society of Civil Engineers highlights the significance of flood impact assessment in flood risk management, and engineers play a vital role in conducting flood assessments to evaluate the potential for flood damage and to design and implement mitigation measures to reduce the impact of floods (ASCE 2014).

Researchers like Miller et al. (2010) develop a conceptual framework for assessing resilience in urban areas based on a comprehensive understanding of flood impact assessment. The framework includes four key elements: exposure, sensitivity, adaptive capacity, and coping capacity. The authors argue that a better understanding of these elements can help to inform strategies for building resilience in flood-prone areas. Similarly, Sultana et al. (2020) highlight the importance of resilience in flood management in their study. This study examines the relationship between social capital (i.e., the networks, norms, and trust that facilitate cooperation and coordination among individuals and groups) and resilience to flooding in southwestern Bangladesh. The authors argue that social capital plays a crucial role in promoting resilience to flooding by enabling communities to share resources, coordinate responses, and adapt to changing conditions. These studies demonstrate the importance of considering both flood impact assessment and resilience in developing strategies for managing flood risk and promoting sustainable development in flood-prone areas.

## **2.4 Importance of Flood Impact Assessment for Buildings**

Buildings are crucial for the safety of people Dewals et al. (2008), as demonstrated by the link between flood fatalities and structural failure (Grundy and Thurairaja 2005). Thus, building codes increasingly require designers to consider performance requirements against flood impacts (van der Veen 2003). While flood and response modification measures have a long tradition in flood risk management, building-level mitigation measures have received little attention in the past (Keys 2006; Samuels et al. 2006; Golz et al. 2015; Lamond et al. 2019). Recent studies highlight the need for detailed analysis of building response to floods to improve flood resilience and avoid costly retrofitting and redesign at later stages (Becker et al. 2011; CSIRO 2000). Flood-resilient designs and mitigation measures can significantly improve the resilience of buildings to floods and reduce restoration costs and time (Lamond et al. 2019). The importance of buildings in flood risk management and the need for accurate evaluation of damage to them at different levels and development phases is evident. However, methods for evaluating damage must accommodate the heterogeneity of buildings within land use classes, making micro-scale analysis of individual buildings essential (Amirebrahimi et al. 2016).

In addition to building safety, the economic importance of buildings and their vulnerability to flood damage is highlighted by several studies (Joy 1993; Messner 2007; Dewals et al. 2008). They indicate that over 60% of the total economic damage caused by floods can be attributed to damage to buildings and their contents. Buildings are also considered the most important element in the direct tangible

category of damage and are suggested to be prioritized in any estimation of direct tangible flood damages (Defra and Flood 2003; Messner 2007; Meyer et al. 2009a; Veldhuis 2011). Consequently, flood damage assessments often focus on buildings to represent overall economic damage for cost-benefit analysis purposes (Cannon et al. 1995).

In Germany many pilot studies such as Pforzheim, Munich, and Hamburg along the Reuss, Isar, and Alster rivers respectively, diverse flood impact assessments are carried out. These include hydraulic modelling, risk mapping, vulnerability assessments, cost-benefit analysis, and community engagement. These approaches aim to assess flood risks, predict building impacts, and foster resilient strategies, reflecting Germany's proactive stance in managing flood risks for urban areas (Bühlmann et al 2014; Sera et al 2022).

## 2.5 Existing Models/Methods for Flood Impact Assessment for Buildings

Several methods have been developed for assessing flood impact at the building level, including empirical models, hydrodynamic models, and statistical models (Marvi 2020). The primary focus of this research is to examine the various existing methods employed in hydrodynamic models and engineering analytical models to assess flood impact at building levels. This research only provides a concise overview of the other methods involved.

**Empirical models**, such as the depth-damage function approach, have been widely used to estimate direct tangible damage to buildings caused by floods (Dewan 2013). The building fragility curve approach was proposed by Rehman and Cho (2016) and uses fragility curves to estimate the probability of a building's failure due to flooding. The curves are developed using empirical data and can be used to estimate the potential damage caused by floods.

**Hydrodynamic models**, such as the flood depth-damage curve approach can simulate the interaction between the flood and the built environment and can provide detailed information on the flood impact on buildings (Pistrika et al. 2014). Aerts et al. (2013) use a depth-damage curve approach to assess flood damage to buildings in an urban area in the Netherlands. They collected data on flood depth and building damage from the 1995 and 1998 floods and used this data to develop depth-damage curves for different types of buildings. They then used a GIS-based model to estimate flood damage to buildings in the study area under different flood scenarios. Moel et al. (2014) compare different flood damage models, including depth-damage curves, for assessing flood damage to buildings in the Netherlands. They used flood damage data to calibrate the models and then applied them to estimate flood damage in different flood scenarios. Nguyen et al. (2009) use a depth-damage curve approach to assess flood risk to residential buildings in central Vietnam. The authors collected data on flood depth and building damage from the 2009 floods and used this data to develop depth-damage curves for different types of buildings. They then used a GIS-based model to estimate flood risk to buildings in the study area under different flood scenarios. Flood damage assessment of buildings in Shanghai by (Wu et al. 2019) uses a depth-damage curve approach to assess flood damage to buildings in Shanghai, China. They collected data on flood depth and building damage from the 2013 floods and used this data to develop depth-damage curves for different types of buildings. They then used a GIS-based model to estimate flood damage to buildings in the study area under different flood scenarios.

**Statistical models**, such as the vulnerability-curve approach, use statistical relationships between flood damage and explanatory variables to estimate the damage caused by floods (Liu et al. 2022). These

methods have been applied in various studies to assess flood impact at the building level, and their effectiveness has been evaluated based on their accuracy, simplicity, and data requirements (Papathoma-Köhle et al. 2022). In recent years, new methods have also emerged, such as the agent-based modelling approach, which simulates the behaviour of individuals buildings during a flood event and can provide insights into the social and economic impacts of floods on buildings and their occupants (Taillandier et al. 2021).

**Engineering analytical method**, this approach uses mathematical models and simulations to predict the effects of flood loads on a building. These methods can provide detailed information on the behaviour of the building during flooding, including stress and strain distributions, deformation, and failure modes. Some examples of analytical methods used for flood impact assessment at the building level include finite element analysis (FEA), computational fluid dynamics (CFD), and simplified analytical methods such as the water depth-damage curve approach. One example of the use of FEA for flood impact assessment at a building level is a study by Samali and Kwok (1995) that evaluated the structural response of a typical Chinese style building to flood loads. The study used a finite element model to simulate flood loads and analyse the structural response of the building. The results showed that the building was susceptible to failure under flood loads due to the weak connections between the timber elements.

Another example is a study by Gems et al. (2016) that used CFD simulations to evaluate the hydrodynamic loads on a building during flooding. The study developed a CFD model to simulate the flow of water around a building and analysed the resulting hydrodynamic loads on the building. The study found that the building was subjected to high hydrodynamic loads during flooding, which could cause damage or failure. Another study by Jonkman and Kelman (2005) used a simplified analytical method, the water depth-damage curve approach, to assess the potential damage to buildings from flooding. The study developed a methodology to predict the damage to buildings based on the depth and duration of floodwater exposure. The methodology was validated using data from a flood event in the Netherlands and was found to accurately predict the damage to buildings. Kelman (2003) developed a model to analyse damage profiles at individual component levels of an unreinforced masonry building, while Nadal et al. (2010) introduced vulnerability matrices to estimate the damage to building components. Becker et al. (2011) developed curves for assessing the structural failure of a simple wood-frame house against floods. Ibrahim and Mahmood (2009) and Dai et al. (2015) used Finite Element Method (FEM) for evaluating potential damage to reinforced concrete structures and rural unreinforced masonry houses, respectively. Hailin et al. (2009) proposed a GIS-based platform for analysing damage in a homogeneous environment, and Suppasri et al. (2019) used load-resistance analysis to estimate the possibility of building collapse.

These studies demonstrate the use of various engineering analytical methods for flood impact assessment at the building level, highlighting the importance of considering different approaches to accurately assess the potential risks and vulnerabilities of buildings to flood hazards. Overall, the development of effective methods for flood impact assessment at the building level is critical for improving flood risk management and building resilient communities.

## **2.6 Calculation of Flood Actions for Flood Impact Assessment at Building Scale**

Flood actions refer to the hydrodynamic forces and loads that act on a building during a flood event, such as hydrostatic pressure, water interaction, and debris impact. These flood actions can have

significant effects on the structural integrity of a building, as well as its contents and occupants. Flood actions are a major factor that must be considered during structural assessment or analysis of building damage on a microscale basis (Aribisala et al. 2022).

Calculating flood actions is an important part of flood impact assessment at the building level because it helps determine the potential damage and risk to the building during a flood event. By quantifying the forces and loads that a building is likely to experience, engineers and other experts can assess whether the building is likely to withstand the flood or whether it may suffer damage or even collapse (FEMA 2021). By calculating flood actions, one can better understand the potential impacts of a flood and take measures to mitigate its impacts. An overview of flood actions with respect to their impacts can be seen in Figure 4.

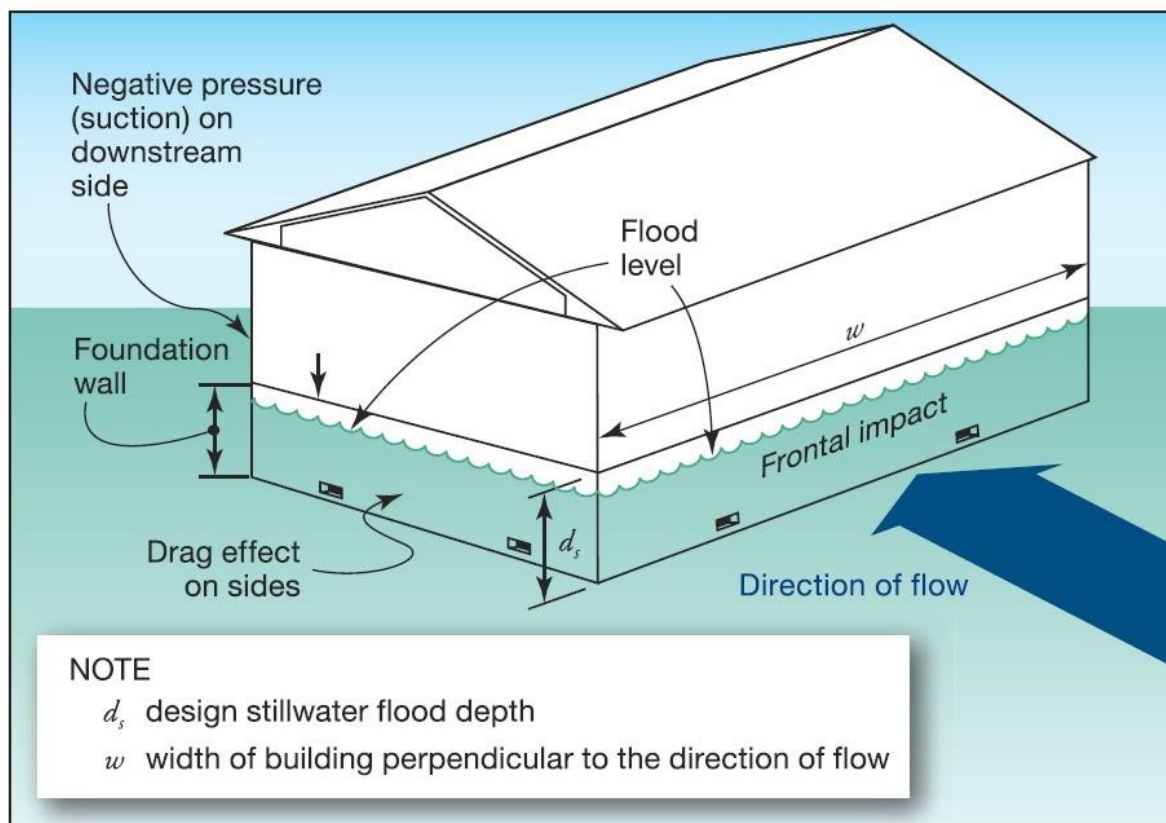


Figure 4: Flood actions acting on a building (Source: FEMA 2021)

This information is crucial for developing effective flood mitigation strategies and for informing building design and construction in flood-prone areas. By understanding the flood actions that a building is likely to face, builders and engineers can take steps to reinforce the structure, improve its resilience, and reduce the risk of damage or collapse during a flood event.

Kelman and Spence (2004) discuss the flood actions applied to buildings in terms of different categories. They include water interaction, hydrostatic and hydrodynamic actions, buoyancy, debris (static and dynamic) action, drag side effect, and impact force action see Table 1. Flood actions may cause the destruction of the foundation or destabilization of the building, failure in its components (e.g. walls and windows), corrosion of walls or foundation materials, and damage to wooden floors or panelling, HVAC systems, wall finishes and so on (Thieken 2006; Nadal et al. 2010; Moel et al. 2015; FEMA 2021).

The primary objective of this study is to compute and evaluate the lateral loads induced by floods and their repercussions on a structure. The following sections justify the necessity of including these loads and furnish a framework and instructions for their computation and evaluation. Subsequently, a brief account of the calculation and evaluation process is provided, followed by an appraisal of the flood effects on the designated edifice and its constituent elements.

Table 1: Flood actions on buildings compiled from (Thieken 2006; Nadal et al. 2010; Moel et al. 2015; FEMA 2021)

<b>Flood Actions</b>	<b>Definition</b>	<b>Significance</b>	<b>Predictability</b>	<b>Flood Parameters</b>
<b>Water Interaction</b>	As the primary source of damage affects those water sensitive components of the building which only contact with water is sufficient for them to be impacted. It involves chemical, nuclear, and biological effects on the building components and their impact.	Highly Relative	Predictable	Above-floor inundation, Building Components (LODs)
<b>Hydrostatic action</b>	Lateral forces imposed on building and its components by the mass of still water and created by the depth-differential on two-sides of a vertical component like wall.	Highly Relative	Predictable	Depth, geometry
<b>Hydro-dynamic action</b>	Lateral forces that are generated by the flowing floodwater. These forces generate five forms of actions which three of them are related to velocity - i.e., lateral pressure, localized changes, and turbulence - and the other two are wave-related (breaking and non-breaking waves). Hydrodynamic forces can push or drag building and its elements depending on the local velocities.	Highly Relative	Predictable	Depth, velocity, geometry
<b>Accidental impact action</b>	Also known as lateral-direction hydrodynamic force, it creates lateral pressure, localized changes in components can punch or drag entire building or its components depending on the mean velocity.	Varies	Difficult	Depth, Velocity, Impact height
<b>Debris action</b>	The forces generated by flood-borne solids (debris) in the water or sediment deposition and aggradations against building components. These include the dynamic (former) and static (latter) debris actions.	Varies	Difficult	Water velocity, Debris velocity, weight, geometry, impact height and duration
<b>Drag side action</b>	These forces can drag building and its elements depending on the local velocities and its geometry.	Varies	Difficult	Depth, Velocity, Geometry
<b>Buoyancy</b>	Also known as upward-direction hydrostatic force, buoyancy is an uplift force as a function of submerged volume of the object which results in a floating of the building or parts of it.	Varies	Difficult	Depth
<b>Erosion</b>	The scouring of the soil away from the side or bed along by moving water.	Varies	Difficult	Depth, flow velocity
<b>Wave</b>	Specific to coastal floods and include forces generated by impacts of waves. Damage to building components is highly variable from non-breaking, breaking and broken waves.	Varies	Difficult	Depth

### 2.6.1 Water Interaction

The impact of floodwater (whether fresh or contaminated) on water-sensitive building elements is known as water interaction or non-physical action (Kelman and Spence 2004). This action is determined by factors such as the water sensitivity of the component material, the duration of water interaction and the exposed area of the component to floodwater. This activity bears significant importance in the evaluation of flood impact and damage estimation. It requires either physical examination or 3D modelling in conjunction with data on the spatial extent of the flood to accurately predict or assess the situation. The following equation formalizes the water interaction in this research.

$$\text{Water interaction for component } (\omega) = f_{\omega}(A, T_c, R(\omega, T_c)) \quad \text{Equation 1}$$

Water interaction can be described as a function of water sensitivity of the component material for a particular water contact duration  $R(\omega, T_c)$ , its exposed area to floodwater  $A$  and the contact duration  $T_c$  and is formalised using the Equation 1.

The determination of the second and third parameters in Equation 1 requires information on the location of components and dynamic simulations of flood and its rate of rise. In contrast, the resistance function for building components is dependent on the duration of flood contact and the material of the component, which has been documented in various literature sources. These sources, including (Proverbs and Soetanto 2004; Garvin et al. 2005; Bowker 2007; Snow and Prasad 2011; Amirebrahimi et al. 2016; FEMA 2021) provide resistance functions for varying durations of flood exposure.

### 2.6.2 Hydrostatic Action

The load imposed on a building component by hydrostatic action is primarily determined by the difference in depth on its sides, as reported in previous studies (Kelman 2003; Amirebrahimi et al. 2016a; FEMA 2021). In addition to lateral hydrostatic pressures arising from water pressure differences, vertical pressures can also be present and generated by buoyancy or the weight of water (Amirebrahimi et al. 2016; FEMA 2021). Buoyancy has been classified as a separate action, but due to the nature of the load, it is sometimes considered a vertical hydrostatic action (Amirebrahimi et al. 2016; FEMA 2021). However, this research only focuses on lateral hydrostatic loads as described earlier. The magnitude of hydrostatic pressure is proportional to the depth of water and forms a triangular distributed load as illustrated in Figure 5. The basic calculation for lateral hydrostatic pressure at a point ( $y$ ) on the  $y$ -axis and outside water depth ( $h$ ) and  $\gamma$  is the density of water ( $\text{KN/m}^3$ ) given by Equation 2, as reported in previous studies (Kelman 2003; Nadal 2007; FEMA 2021).

$$P_s = \text{Hydrostatic pressure} = \gamma \times h \quad \text{Equation 2}$$

$$H_{y\text{static force}} = \frac{1}{2} \times \gamma \times (h - y)^2 \times b \quad \text{Equation 3}$$

As demonstrated in Equation 2, the lateral hydrostatic action is also influenced by the mass density of water. Water quality, the presence of contaminants, or debris may raise the water density of fresh water, resulting in a notable increase in hydrostatic loads (Costa 1988; Kelman 2003). However, in this study, for ease of computation, it is assumed that clear water with a bulk density of  $1000 \text{ kg/m}^3$  is present.

Equation 2 can only calculate the pressure from the water on one side of the component. If inundation depth difference ( $f_{diff}$ ) exists on both sides (e.g., for the window in Figure 5 right), it generates pressure difference ( $\Delta P$ ) between the inside and outside of the building that can cause significant damage to building components. This pressure difference can be calculated using Equation 4 follow:

$$\Delta P = \rho_w g (f_{diff} - y) = \Delta P_{y=0} - \rho_w g y \text{ for } b \leq y \leq f_{diff} \quad \text{Equation 4}$$

$$\Delta P = 0 \text{ for } y > f_{diff} \quad \text{Equation 5}$$

The distributed hydrostatic force can be represented using an equivalent point force in the two-dimensional plain on the relevant building components. This point would be at the height of  $h/3$  from the ground where ( $h$ ) represents the depth of inundation (Amirebrahimi et al. 2016).

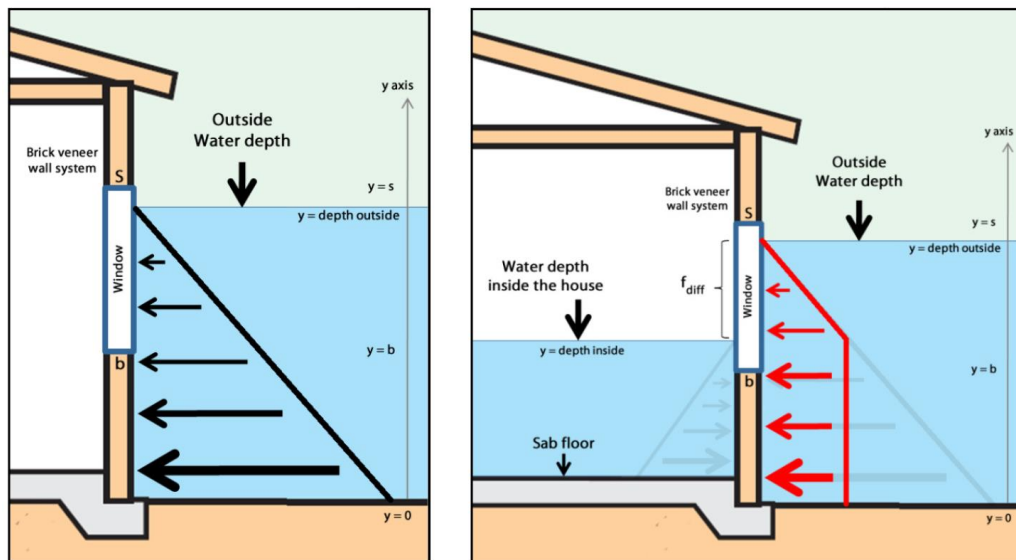


Figure 5: Hydrostatic pressure (left) water level outside of the building component; (right) depth difference between inside and outside of a building component (Source: Amirebrahimi et al. 2016)

### 2.6.3 Hydrodynamic Action

Hydrodynamic flood action is the force exerted by the flow of floodwater on a building or structure (Merz et al. 2010). It is one of the main flood actions that can cause damage to buildings and structures during flood events. The hydrodynamic force is dependent on several factors such as the velocity and depth of the floodwater, the shape and size of the building or structure, and the roughness of the surrounding terrain (Kelman 2003).

The hydrodynamic force generated during flooding affects the front side of the building and varies based on the direction of the flow. This results in a negative suction pressure at the back side of the building, as depicted in Figure 4 (Kabir et al. 2023; FEMA 2021). The calculation of the hydrodynamic force can be complex and requires advanced modelling and simulation tools. Various research studies have been conducted to investigate the effects of hydrodynamic forces on buildings and structures and to develop more accurate methods for calculating the hydrodynamic force (Nistor et al. 2018; Sakuraba et al. 2020).

In recent years, there has been a growing interest in studying the hydrodynamic force and its impact on buildings and structures during flood events. Researchers have been using advanced simulation tools such as computational fluid dynamics (CFD) to better understand the hydrodynamic force and its effects on buildings and structures (Klapp et al. 2020).

The calculation of hydrodynamic flood action using Eurocode EN 1991-1-6-6:2005 equations involve the use of the peak velocity of the floodwater, the duration of the flood event, and the drag coefficient of the building or structure. The Eurocode provides the following equation for calculating the hydrodynamic pressure:

$$P_d = \text{hydrodynamic pressure (KN/m}^2\text{)} = \frac{1}{2} \times k \times \gamma \times v^2 \quad \text{Equation 6}$$

Where,  $\gamma$  is the density of water (KN/m<sup>3</sup>),  $v$  is the peak velocity of the floodwater (m/s) and  $k$  is the drag coefficient which is 1.44 for an object of square or rectangle horizontal cross-section. Hydrodynamic action is predominantly generated from the moving water and is basically a function of water velocity (Kelman 2003; FEMA 2021). In the current practice, the calculation of hydrostatic forces on a building is dependent on a specific velocity threshold (i.e., smaller, or larger than 3 m/s).

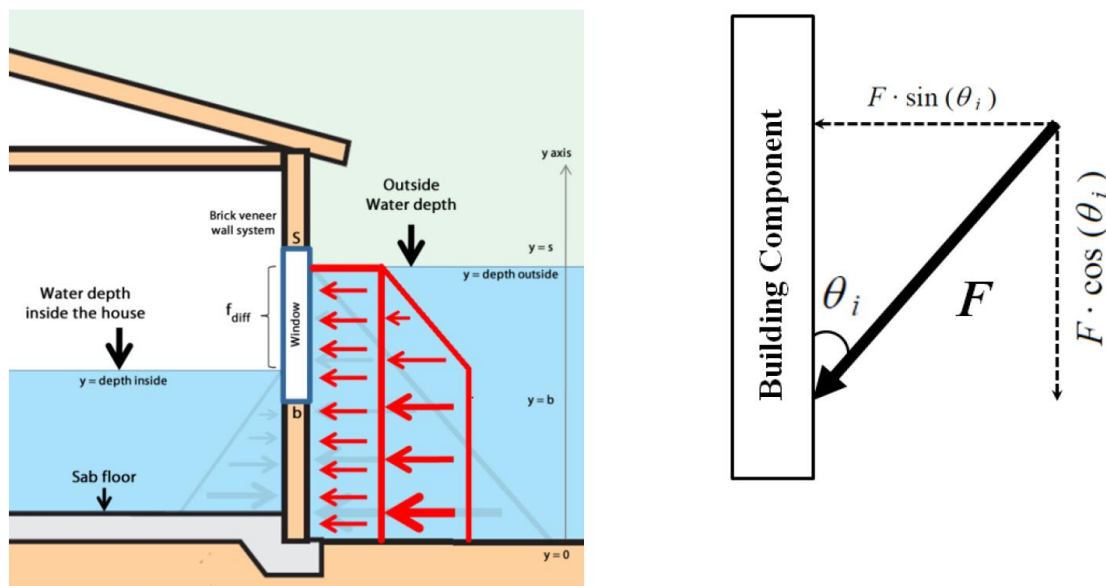


Figure 6: Visualization of hydrodynamic and hydrostatic pressure (left); Magnitude of hydrodynamic force on the building component (right) (Source: Amirebrahimi et al. 2016)

If the velocity exceeds 3 m/s, the hydrodynamic pressure can be calculated directly from the Equation 6 (Becker et al. 2011; FEMA 2021). The equation calculates the magnitude of the velocity vector e.g., force  $F$  in Figure 6. However, depending on the flow direction the magnitude of the load on a building element is mainly from the perpendicular component of the velocity vector which as shown in Figure 6 calculated as  $F = F \times \sin \vartheta_i$ . Where the velocities are less than 3 m/s however, they are suggested to be converted to their equivalent hydrostatic pressure (Amirebrahimi et al. 2016). Similarly in order to obtain hydrodynamic force the following equation can be utilized:

$$F_{\text{Hydrodynamic}} = P_d \times A \quad \text{Equation 7}$$

Where,  $P_d$  is hydrodynamic pressure from Equation 6 and  $A$  is the surface area in m<sup>2</sup>.



### 2.6.4 Accidental Impact Action

Accidental flood action impacts see Figure 7 refer to the force exerted on buildings or structures when impacted by floodwater-borne debris, such as logs, trees, or other floating objects, during a flood event (Nadal et al. 2010). This type of flood action can cause significant damage to buildings and structures and can be difficult to predict due to the variability in the size, shape, and velocity of the debris (Marvi 2020). This action bears significant importance in the evaluation of flood impact assessment for buildings. It requires hydrodynamic flood simulation involving (depth and velocity) as well as proper geometry of the building and clear information of its components (walls, door, window etc.) and materials for estimation of impact force acting on a building. Eurocode 1 (actions on structures) provides guidance for the calculation of accidental impact flood actions on buildings. Where hydrodynamic force was considered with a factor of 1.5 for the initial calculation of impact force. The relevant equation is given in Eurocode 1 (actions on structures) EN 1991-1-7:2006+A1:2014.

The equation to calculate the accidental impact force is:

$$F_{\text{impact}} = 1.5 \times \frac{1}{2} \times k \times \gamma \times v^2 \quad \text{Equation 8}$$

Where:

F is the impact force in (KN),  $\gamma$  is the density of the fluid in ( $\text{kg}/\text{m}^3$ ), V is the velocity of the fluid in (m/s), K is the impact coefficient, which depends on the type of impact and is determined based on the type of structure geometry, the location, and other relevant factors.



Figure 7: Visualization of flood induced accidental impact due to debris such as cars or other elements (Source: Mahaffey 2018)

The Eurocode provides different values of the impact coefficient (k) depending on the type of structure, such as bridges, buildings, and other structures. For buildings, the impact coefficient (k) is typically assumed to be 1.5, as per Eurocode 1. The velocity of the fluid (V) can be obtained from hydrodynamic flood simulation. The density of the fluid ( $\gamma$ ) depends on the type of fluid, which is typically assumed to be clear water with a density of  $1000 \text{ kg}/\text{m}^3$ .

It is important to note that Equation 8 is only applicable for the calculation of flood actions like accidental impact and is not suitable for other types of flood actions. Additionally, it is important to consult the relevant Eurocode guidance and standards and seek professional assistance in the design and construction of buildings to ensure compliance with local regulations and safety requirements.

### 2.6.5 Debris Impact

During a flood, debris carried by the water can impact the building and cause damage. Debris can include large objects such as trees and cars, as well as smaller objects such as rocks and sediment Figure 8. Debris impact flood action refers to the force exerted on buildings or structures when impacted by floodwater-borne debris, such as trees, logs, vehicles, or other objects, during a flood event (Stolle et al. 2019). This type of flood action can cause significant damage to buildings and structures and can be difficult to predict due to the variability in the size, shape, and velocity of the debris (Kelman and Spence 2004; Marvi 2020). Eurocode 1 (EN 1991-1-7:2006+A1:2014) provides an equation for calculating the debris impact flood action on buildings or structures. The equation is expressed as:

$$F_{Debris} = k \times v^2 \times A_{deb} \quad \text{Equation 9}$$

Where:

$F_{Debris}$  is the force of debris in KN,  $k$  is a debris density parameter, in  $\text{Kg/m}^3$ ,  $v$  is the mean velocity of the water averaged over the depth, in m/s (impact velocity of the debris),  $A_{deb}$  is the area of obstruction presented by the trapped debris and falsework, in  $\text{m}^2$

To calculate debris pressure:

$$P_{deb} = \frac{F_{Debris}}{A_{deb}} \quad \text{Equation 10}$$

$P_{deb}$  is the Pressure of debris in  $\text{KN/m}^2$ ,  $F_{Debris}$  is the force of debris in KN,  $A_{deb}$  is the area of obstruction presented by the trapped debris and falsework, in  $\text{m}^2$

Building geometry and material properties are critical factors to consider when evaluating a building's ability to withstand debris impact during a flood event. Studies have shown that the shape and size of a building can significantly affect the impact forces of debris. For instance, a building with a curved shape may experience less impact force than a building with a flat surface, which can create a concentrated impact zone (Vojinovic et al. 2011; Schubert and Sanders 2012). Additionally, the material properties of a building, such as strength and stiffness, can impact its ability to withstand debris impact. For example, a study by Jakob et al. (2012) found that reinforced concrete structures showed better resistance to debris impact than masonry structures.

Therefore, the building geometry and material properties are crucial factors to consider when assessing a building's ability to withstand debris impact during a flood event. Failure to account for these factors may result in underestimating the potential damage caused by debris impact.

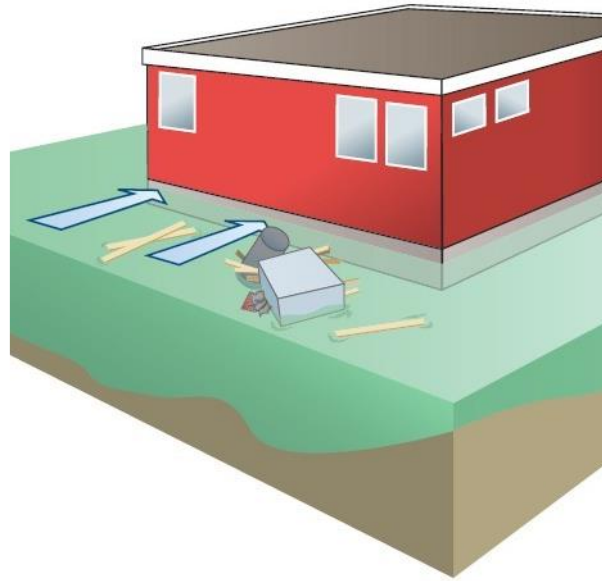


Figure 8: Flood induced frontal side impact due to debris (Source: FEMA 2021)

### 2.6.6 Drag Side Effect

The drag force, also known as the drag side effect of flood action in Figure 9, is the force exerted on a building or structure due to the resistance of floodwater flow around it (Cuomo et al. 2009; Cantelmo and Cuomo 2021). The drag force is one of the three main forces that act on a building or structure during a flood event, the others being the uplift force and the lateral force (FEMA 2009). The drag force is dependent on various factors such as the shape and size of the building or structure, the angle and velocity of the floodwater flow, and the roughness of the building surface depending upon building material properties (Nasim et al. 2019). The calculation of the drag force can be complex and requires advanced modelling and simulation tools (Peiwei Xie and Vincent H Chu 2017; Nasim et al. 2019).

In recent years, there has been a growing interest in studying the drag force and its impact on buildings and structures during flood events. Various research studies have been conducted to investigate the effects of drag force on buildings and structures and to develop more accurate methods for calculating the drag force (Nasim et al. 2019; Cantelmo and Cuomo 2021). Eurocode 1 (EN 1991-1-7:2006+A1:2014) provides guidelines and equations for calculating the drag force on buildings or structures during a flood event.

The equation for calculating the drag force on a rectangular building or structure is expressed as:

$$D_{effect} = C_d \times \frac{1}{2} \times \gamma \times v^2 \times A \quad \text{Equation 11}$$

where:

$D_{effect}$  is the drag force in KN,  $\gamma$  is the density of water ( $\text{kN/m}^3$ ),  $C_d$  is the drag coefficient, which is dependent on the shape of the building or structure and the angle of incidence of the floodwater flow.  $V$  is the flow velocity of the floodwater in (m/s),  $A$  is the projected area of the building or structure perpendicular to the flow direction in  $\text{m}^2$ .

For irregularly shaped buildings or structures, Eurocode 1 recommends using advanced computational fluid dynamics (CFD) models to calculate the drag force.

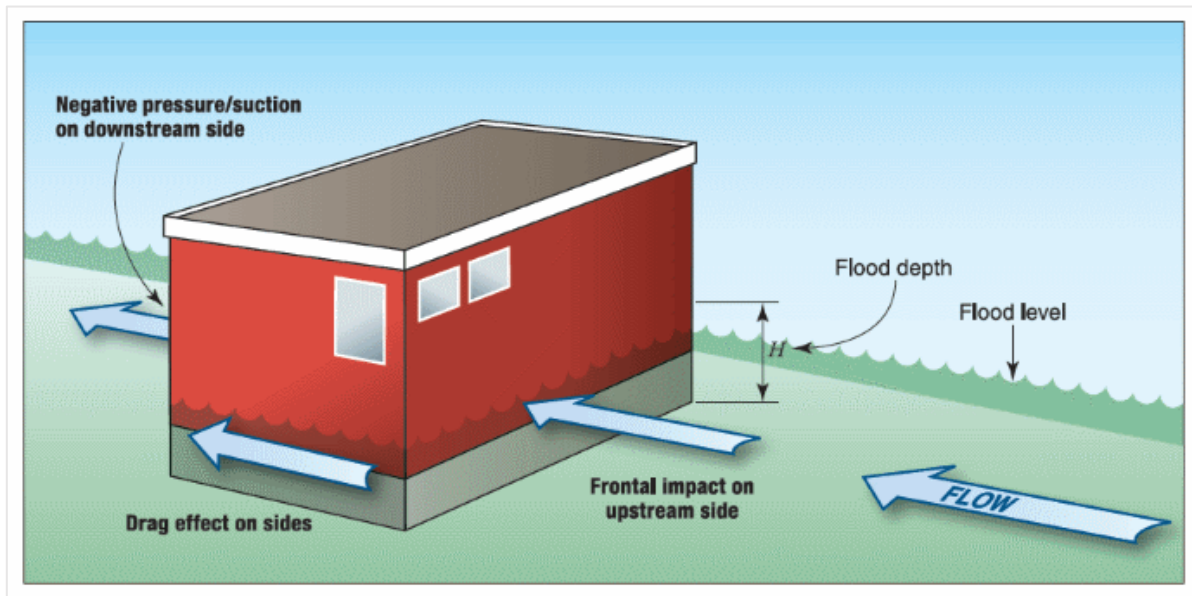


Figure 9: Flood induced drag side effect parallel to the flow direction (Source: FEMA 2021)

The calculation of drag force on buildings or structures during a flood event can be a complex task. According to the United States Army Corps of Engineers (USACE), the calculation of the drag force involves the estimation of the drag coefficient ( $C_d$ ) and the velocity ( $V$ ) of the water flowing around the building or structure (USACE, 2013). The drag coefficient is a function of various parameters, such as the shape and orientation of the building, the roughness of the surface, and the Reynolds number, which depends on the velocity and viscosity of the fluid (Wadell 1934; Tran-Cong et al. 2004). The velocity of the water, on the other hand, depends e.g. on the flow rate and the topography of the surrounding area.

The values of  $C_d$  and  $V$  can vary significantly depending on the specific characteristics of the building or structure and the flood event. For example, a building with a streamlined shape and a smooth surface will have a lower  $C_d$  compared to a building with a complex shape and a rough surface. Similarly, the velocity of the water will be higher in a narrow and steep channel compared to a wide and flat plain. Therefore, it is recommended to consult with experienced engineers and utilize advanced modelling and simulation tools for accurate assessment of the potential impact of drag force on buildings or structures during a flood event. These tools can take into account the specific characteristics of the building or structure, the flood event, and the surrounding area, and provide a more accurate estimation of the drag force. As noted by the USACE (2013) engineering judgment and experience are critical to ensure the accuracy and reliability of the estimates.

## 2.7 Spatial Hydrodynamic Flood Simulation Models at Building Levels to Evaluate Flood Impact Assessment

Spatial hydrodynamic flood simulation models at building levels are important to understand because they can provide valuable insights into the potential impact of floods on buildings. These models simulate the flow of water through an urban environment, taking into account factors such as building location, elevation, and geometry, as well as the characteristics of the floodwater, such as velocity and

depth. By using the outcomes of these models to evaluate flood impact assessments, policymakers and planners can better understand the potential risks and vulnerabilities of urban areas to flooding and develop more effective strategies for mitigating these risks. For example, they can identify areas of the city that are particularly susceptible to flooding, and implement measures such as flood-proofing buildings, improving drainage systems, and developing early warning systems to reduce the impact of future flood events.

Several studies have demonstrated the importance of spatial hydrodynamic flood simulation models at building levels in flood impact assessment. For example, a study by Zhang et al. (2021) used a 2D hydrodynamic model to simulate flooding in a residential area and found that the model provided accurate predictions of flood water levels and velocities, which were important for identifying areas of high risk and developing appropriate flood mitigation measures. A study by Rong et al. (2020) used a 3D hydrodynamic model to simulate flooding in a city and found that the model provided important insights into the potential damage and impact of flooding on individual buildings. The study showed that buildings located in low-lying areas were at a higher risk of flooding and that effective flood mitigation measures could reduce the potential damage and impact of flooding on these buildings.

Similarly, Understanding the capacities and limitations of spatial hydrodynamic flood simulation models at building levels is crucial for flood impact assessment, planning, risk assessment, and resource allocation. Accurate hydrodynamic flood simulation models ensure reliable and trustworthy FIA and identify areas for model improvement ( Sanders 2017; Nkwunonwo et al. 2020). Understanding the capabilities and limitations of hydrodynamic flood simulation models allows for better planning and preparedness for flooding events, as well as identifying areas where additional flood mitigation measures may be necessary (Nkwunonwo et al. 2020). As hydrodynamic flood simulation models can also be used for risk assessment, therefore, understanding their limitations ensures that assessments are neither overly conservative nor optimistic (Vorogushyn et al. 2010). Also, understanding the hydrodynamic flood simulation model can facilitate resource allocation, allowing for more efficient use of emergency response efforts in areas most likely to be impacted by flooding (Sanders 2017). To accurately assess the capacities and limitations of spatial hydrodynamic modelling, it is essential to have a clear understanding of the fundamental concept of hydrodynamic flood simulation and the types of simulation models available. This understanding is necessary as it provides a foundation for evaluating the capabilities and limitations of different simulation models, allowing for the effective utilization and application of such models for flood impact assessments.

Overall, spatial hydrodynamic flood simulation models at building levels are important tools for evaluating FIA and developing effective flood mitigation strategies. By providing accurate predictions of flood water levels and velocities around individual buildings, these models can help identify areas of high risk and develop appropriate flood mitigation measures, ultimately reducing the potential damage and impact of flooding on infrastructures. However, they also have limitations such as high computational requirements and the accuracy of input data. Detailed analysis of the capacities and limitations of reviewed hydrodynamic flood simulation models can be found in the appendix.

### **2.7.1 Spatial Hydrodynamic Flood Simulation Models**

Hydrodynamic models (also referred to hydrodynamic numerical flow calculators) are mathematical models that attempt to replicate fluid motion and typically require solving computationally. These are the fundamental tasks of all planning and optimization work in Hydrodynamic Engineering. These

models simulate water movement by solving equations formulated by applying laws of physics, see Table 2. Depending on their spatial representation of the floodplain flow, the models can be dimensionally grouped into 1D, 2D, 1D-2D coupled and 3D models. A vital factor that must not be overlooked in reviewing flood models from the perspective of dimensionality is the numerical schemes or formulations, which are fundamental in enhancing the scope of flood modelling functionality (Teng et al. 2017). Of course, the lack of an exact solution to the shallow water equations and their simplifications gives rise to numerical formulations, which form important aspects of flood modelling procedure (Brocchini and Dodd 2008). In practical application, these formulations are often evaluated by discretization of a meshed topographic surface. This highlights the importance of quality datasets in modelling urban flooding and the likely implications for areas with data sparse situations. Over the years, various numerical schemes have been formulated to solve a variety of hydrodynamic problems, especially in the computational mathematics and flood modelling literature (Teng et al. 2017; Jodhani et al. 2021).

Table 2: 1D, 2D and 3D Hydrodynamic flood simulation models solving equations adopted from (Teng et al. 2017)

Equations	Dem.	Remarks
<b>Continuity Eq.</b> $\frac{\partial Q}{\partial x} + \frac{\partial A}{\partial t} = 0$ <b>Momentum Eq.</b> $\frac{1}{A} \frac{\partial Q}{\partial t} + \frac{1}{A} \frac{\partial (Q^2)}{\partial x} + g \frac{\partial h}{\partial x} - g(S_0 - S_f) = 0$	1D - Saint-Venant eq.	Here $Q$ is the flow discharge ( $Q = uA$ , where $u$ is the cross-sectional averaged velocity and $A$ is the flow cross-section area), $t$ represents time, $h$ is the water depth, $g$ is the gravitational acceleration, $S_f$ is the friction slope and $S_0$ is the channel bed slope.
<b>Continuity Eq.</b> $\frac{\partial h}{\partial t} + \frac{\partial hu}{\partial x} + \frac{\partial hv}{\partial y} = 0$ <b>Momentum Eq.</b> $\frac{\partial(hu)}{\partial t} + \frac{\partial}{\partial x} \left( hu^2 + \frac{1}{2} gh^2 \right) + \frac{\partial(huv)}{\partial y} = 0$ $\frac{\partial(hu)}{\partial t} + \frac{\partial(huv)}{\partial x} + \frac{\partial}{\partial x} \left( hv^2 + \frac{1}{2} gh^2 \right) = 0$	2D - Navier-Stokes eq.	Where $x$ and $y$ are the two spatial dimensions, and the 2D vector $(u,v)$ is the horizontal velocity averaged across the vertical column. The solution of these equations comprises estimates of $u$ , $v$ , and $h$ over space and time.
<b>Momentum Eq.</b> $\frac{\partial u}{\partial t} + u \cdot \nabla u + \frac{1}{\rho} \nabla p = g + \mu \nabla \cdot \nabla u$ <b>Incompressibility Cond.</b> $\nabla \cdot u = 0$	3D - Navier-Stokes eq.	Here $u$ is the velocity; $\rho$ is the fluid density; $p$ is pressure; $g$ is gravitational acceleration; $\mu$ is kinematic viscosity. Momentum Eq arises from applying Newton's equation $F=ma$ to fluid motion.

### 2.7.1.1 Spatial One-Dimensional Hydrodynamic Flood Models (1D)

One-dimensional (1D) hydrodynamic simulations are widely used to model open-channel flow in rivers and floodplains. This approach simplifies complex natural processes by assuming that the flow is constant in one direction and along the centre line of the channel. The 1D simulation models the

channel and floodplain as a series of cross-sections perpendicular to the flow direction, which makes it computationally efficient and easy to parameterize using traditional field surveying (Mustafa et al. 2017). The 1D model is based on the shallow water equations, which describe the conservation of mass and momentum in a fluid. These equations can be solved numerically using various techniques, such as finite difference, finite element, or spectral methods (Bates and Roo 2000). One common software for 1D hydrodynamic simulations is HEC-RAS, which is a widely used hydrodynamic modelling software developed by the US Army Corps of Engineers (USACE 2013). Other models are provided in the appendix.

One-dimensional models have been applied to various hydrological requirements, such as flood forecasting, river management, and water resources planning. The accuracy of 1D models depends on the complexity of the system being modelled and the availability of accurate input data, such as topography, bathymetry, and boundary conditions (Bates and Roo 2000).

Despite the limitations of 1D models, they remain an important tool for hydrologists and engineers due to their simplicity, computational efficiency, and ability to provide useful insights into the behaviour of open-channel flows. Generally, 1D models solve equations derived by ensuring mass and momentum conservation between two cross sections  $\Delta x$  apart, which yields the well-known one-dimensional Saint-Venant equation Table 2.

### **2.7.1.2 Coupled Model: Spatial One- and Two-Dimensional Hydrodynamic Models (1D-2D Coupling)**

Significantly many flood inundation models adopt an integration of the 1D-2D approach, to exploit the advantages of both modelling schemes. Hence in these models, the 1D model is used to represent the flow in the river reaches, coupled with a 2D scheme that activates when flow out of the riverbank occurs. They are a type of flood simulation software that is used to simulate the behaviour of water flow in rivers, channels, and other waterways. These models use a combination of one-dimensional (1D) and two-dimensional (2D) equations to represent the behaviour of water in different scenarios.

1D/2D Hydrodynamic Models can be used to simulate different types of flooding events, such as river floods, flash floods, and tidal surges. They are used to predict the behaviour of water during floods, including the timing, depth, and extent of flooding, and to assess the impact of different flood mitigation measures. The results from these simulations can be used by flood risk managers and emergency responders to plan for and respond to flooding events (Teng et al. 2017).

### **2.7.1.3 Spatial Two-Dimensional Hydrodynamic Flood Models (2D)**

Two-dimensional flood models are commonly used for flood extent mapping and flood risk estimation studies. These models represent flood flow as a two-dimensional plane and solve the two-dimensional shallow water equation by means of appropriate numerical schemes (Dutta et al. 2007; Teng et al. 2017). The assumption behind these models is that the third-dimension water depth is shallow compared to the other two dimensions (Teng et al. 2017). The two-dimensional shallow water equations can be derived by depth-averaging the Navier-Stokes equations Table 2, which ensure mass and momentum conservation in a plane (Liu et al. 2016).

There are several numerical discretization strategies for 2D models, including finite element, finite difference, and finite volume methods, which can be classified based on their spatial and temporal discretization (Sleigh et al. 1998; Caleffi et al. 2003; MIKE 2012). Spatial representation can use structured mesh (rectangular grids), unstructured mesh (triangular grids), and flexible mesh. The models can also be divided into implicit (the solver cannot proceed to the next time step until the whole domain is solved) and explicit (solving of the current unit independent of solving the rest of the domain for any given time step) models (Guidolin et al. 2016). Several studies have assessed the capability of 2D models for flood modelling. For example, (Néelz and Pender 2009; Néelz and Pender 2010) conducted a comprehensive review of 2D hydrodynamic modelling packages and benchmarked the performance of some commonly used 2D models. Another study reviewed and compared a later set of 2D models (Néelz and Pender 2013).

Recent advances in remote sensing technology, such as airborne LiDAR and Synthetic Aperture Radar (SAR) data, have improved the accuracy and resolution of input data, making two-dimensional models more popular (Wittke et al. 2019). However, high-resolution topographic data are essential for the accurate delineation of urban geometry, such as streets, roads, and buildings, which impose rigorous effects in two-dimensional flood modelling (Bozza et al. 2016; Teng et al. 2017). Spatial 2D flood simulation software uses two-dimensional (2D) equations to simulate the behaviour of water in a geographic information system (GIS) environment. This type of modelling considers the spatial distribution of various parameters such as land use, soil type, topography, and vegetation cover, which can significantly affect the behaviour of water during floods. Spatial 2D flood modelling involves creating a digital elevation model (DEM) of the area of interest, which is then used to develop a mesh of interconnected cells that represent the terrain. The model also considers the hydrodynamic properties of the terrain, such as roughness and permeability. Rainfall data is used to simulate the behaviour of water in the area, including the flow of water overland, in rivers and other waterways, and across structures such as bridges and culverts.

The results of spatial 2D flood modelling can be visualized as flood maps that show the spatial distribution of flood depths and extents. These maps can be used to identify areas that are at risk of flooding, evaluate the effectiveness of flood control measures, and develop emergency response plans. They are widely used in flood risk assessment, floodplain mapping, and flood management planning. They provide a detailed understanding of the spatial distribution of flood risk, which can be used to prioritize investments in flood control measures and to develop effective emergency response plans.

There are several 2D flood simulation models available, each with its own set of features and capabilities (for a complete list see appendix). Some popular 2D flood simulation models include:

- 1) MIKE FLOOD: This is a comprehensive 2D flood simulation model that can simulate both riverine and urban flooding scenarios. It includes a range of tools for creating detailed topographic models, defining rainfall inputs, and analysing flood risk. MIKE FLOOD is widely used for flood risk assessment, floodplain mapping, and emergency response planning.
- 2) HEC-RAS 2D: This is a 2D version of the widely used HEC-RAS hydrodynamic modelling software, which was originally designed for 1D river modelling. HEC-RAS 2D allows for the modelling of overbank flooding and is used in flood risk assessment, dam safety analysis, and river restoration projects.



- 3) TUFLOW: This is a 2D flood simulation model that can simulate both riverine and urban flooding scenarios. It includes a range of tools for creating detailed topographic models, defining rainfall inputs, and analysing flood risk. TUFLOW is widely used in flood risk assessment, floodplain mapping, and emergency response planning.
- 4) LISFLOOD-FP: This is a 2D flood simulation model that is designed to simulate flood inundation in large river basins. It includes a range of tools for creating detailed topographic models, defining rainfall inputs, and analysing flood risk. LISFLOOD-FP is widely used in flood risk assessment, floodplain mapping, and emergency response planning.
- 5) FloodArea: It is based on a simplified hydraulic approach including hydrodynamic calculations for the simulation of small and large areas with a high spatial resolution (< 1 m). Successful applications have been made in large-scale simulations of catchments sized up to 3.000 km<sup>2</sup> in Germany (geomer 2017).

These are just a few examples of the many 2D flood simulation models available. Each model has its own set of strengths and weaknesses see details in appendix, and the choice of model will depend on the specific requirements of the project.

#### **2.7.1.4 Capacities of Spatial 2D Hydrodynamic Flood Simulation Models at Building Scale**

Spatial 2D hydrodynamic models are perhaps the most widely used models in flood extent mapping and flood risk estimation. There has now been much assessment of the capability of the 2D models as they can provide a more accurate representation of the behaviour of water in complex scenarios, such as floodplains and urban environments. These models can simulate a wide range of hydrodynamic phenomena, such as flood wave propagation, flow around structures, and sediment transport while considering the spatial distribution of various parameters that affect the behaviour of water. As mentioned above, these models use a range of inputs, including terrain data, hydrological data, and hydraulic properties of buildings, to predict the water flow and inundation depth in each area. Therefore, their capabilities have been demonstrated in several studies, such as (Yalcin 2019; Arruda Gomes et al. 2021; Zhang et al. 2021a), which used spatial 2D hydrodynamic flood simulation models to predict flood inundation depths and velocities in urban areas.

Moreover, these models can simulate the impact of floodwater on buildings at a detailed level, including the potential for damage due to hydrostatic pressure and buoyancy forces as well as capable of simulating the impact of floodwater on critical infrastructure, such as roads, bridges, and drainage systems. These capabilities have been demonstrated in studies such as (Nadal et al. 2010; Korzani et al. 2018; Liu et al. 2022), where they used spatial 2D hydrodynamic flood simulation models to predict the damage to buildings due to flooding. Similarly, (Hong et al. 2015; Pregnolato et al. 2017; Sohn et al. 2020), has used these models to predict the impact of flood on transportation infrastructure and drainage systems.

In conclusion, spatial 2D hydrodynamic models are powerful tools for predicting flood inundation depths and extents, as well as the impact of floodwater on buildings and critical infrastructure. These models are widely used in flood risk estimation and emergency response planning, as they provide a more accurate representation of the behaviour of water in complex scenarios such as floodplains and urban environments. The capabilities of these models have been demonstrated in several studies,

highlighting their ability to simulate a range of hydrodynamic phenomena and predict the spatial distribution of flood depths and extents. As such, spatial 2D hydrodynamic models are an essential component of flood risk management, enabling decision-makers to identify areas at risk of flooding, evaluate flood control measures, and develop effective emergency response plans.

#### **2.7.1.5 Limitations of Spatial 2D Hydrodynamic Flood Simulation Models at Building Scale**

Even though, spatial 2D Hydrodynamic flood simulation models are the most widely used models for the simulation of dynamic flood inundation depth. But they also have certain limitations linked to data requirements, computational power, forecasting and scenario analysis. These models are unable to capture the vertical component of flooding since these models simulate flooding over a flat area and do not consider the height of floodwater above ground level, which is important when assessing the impact of flooding on multistorey buildings.

According to Apel et al. (2009) and Noh et al. (2018), 2D models do not provide an accurate representation of the flood depth and velocity distribution within and around buildings, and they may underestimate the flood depths and velocities that occur on the ground floor of a building during a flood event. This is because 2D models assume a flat ground surface and a constant water depth across the entire floodplain, which does not accurately represent the complex interactions between floodwaters and buildings. During flooding event the water level on the ground floor of a building can be significantly higher than the water level on the surrounding ground surface due to infiltration or backflow from drainage systems. In addition, the water velocities near the ground floor can be much higher than those on the surrounding ground surface, due to the increased friction and obstruction caused by the building. These effects are not captured by 2D models, leading to an underestimation of the impacts of flooding on buildings. Many 2D models use simplified representations of buildings, which may not accurately represent the actual buildings in the area, leading to inaccuracies in the predicted flood impacts. For example, simplified building representations in 2D flood models can result in significant errors in flood depth estimation (Dottori et al. 2016; Bhola et al. 2020). 2D models require high-quality topographic data, such as Digital Elevation Models (DEMs), which can be costly and time-consuming to obtain. The accuracy of 2D flood models is highly dependent on the quality of the topographic data used as input (Yu and Lane 2006; Gallegos et al. 2009).

While generally less computationally intensive than 3D models, 2D models still require significant computing power and memory to run, especially at city or regional levels. As noted by Bates et al. (2010), 2D flood models can be computationally expensive and may require parallel processing or other techniques to improve their efficiency. Therefore, these models are subject to uncertainty due to the complex nature of flood dynamics, the accuracy of input data, and the assumptions made in the modelling process. According to a review by Beven et al. (2015) and Oddo et al. (2020), the uncertainty associated with 2D flood models can arise from a variety of sources, including model input data, model structure, and boundary conditions. These applications can perform better in data rich countries as compared to developing countries where data availability is not adequate to perfectly run these models.

#### **2.7.1.6 Three-Dimensional Hydrodynamic Flood Models (3D)**

3D hydrodynamic flood simulation models are a more advanced and complex type of software compared to 2D hydrodynamic models. They simulate flood behaviour in three dimensions, including

the depth, width, and height of the water, and consider the impact of structures such as buildings and bridges (Rong et al. 2020).

The 3D flood models solve the full Navier-Stoke equation see Table 2 and consider the flow of flood water as completely three-dimensional (Jiang et al. 2015; Nkwunonwo et al. 2020; Karam et al. 2021). Indeed, to be able to dynamically represent the physics of water flow, especially in urban areas, it is worthwhile to apply the three-dimensional model (D'alpaos and Defina 2007; Nkwunonwo et al. 2020).

For many scales of floodplain flow, complex three-dimensional representation of flow dynamics has tended to be regarded as unnecessary, as a two-dimensional shallow water approximation spiral flow at bends is important during catastrophic floods, such as those occurring due to dam breaks, tsunamis, flash floods or embankment and levee breaches. 3D models were therefore developed to allow the representation of vertical features (Flener et al. 2015; Teng 2020; Tom et al. 2022). Some of these models solve the horizontal flow with 2D shallow water equations and include a quasi-3D extension to model velocity in vertical layers (Jin and Kranenburg 1993; Teng et al. 2017). Other 3D models are derived from the three-dimensional Navier-Stokes equations (Lemarié-Rieusset 2018), which describe the motion of fluid substances and can be seen in Table 2.

Application of 3D models in flood inundation modelling was once considered not viable at the reach-scale (>1 km), being limited by computational feasibility and the problems of accurately representing free surface flows, high-order turbulence and a transient flood shoreline (Teng et al. 2017). This limitation has eased in recent years due to fast development of particle-based models and vast improvements in computing techniques. Particle-based approaches are now favoured owing to several advantages over grid-based approaches, capable of representing small-scale features (of size smaller than a grid cell), have no need for spatial discretization, and have little or no problem with mass preservation or spatial diffusion. Nevertheless, the use of particle-based 3D models in flood modelling that incorporates real topography is quite recent and such studies are rare in the literature in great contrast to 2D models (Hadimlioglu et al. 2020). Here are some examples of 3D hydrodynamic flood simulation software:

- 1) FLOW-3D: This is a commercial software package developed by Flow Science that simulates fluid flow, heat transfer, and solid mechanics. It has been used for simulating river flooding, urban flooding, and dam failures.
- 2) OpenFOAM: This is a free and open-source software package for computational fluid dynamics (CFD) simulations. It can be used for simulating fluid flow and heat transfer in complex geometries and has been used for simulating flood inundation and water flow in rivers.
- 3) XBeach: This is a free and open-source software package developed by Deltares that simulates wave dynamics, sediment transport, and coastal morphology. It can be used for simulating coastal flooding and storm surge events.
- 4) Delft3D: This is a commercial software package developed by Deltares that simulates water flow, sediment transport, and morphology in rivers, estuaries, and coastal zones. It can be used for simulating flood inundation and coastal flooding.
- 5) TELEMAC: This is a free and open-source software package developed by the French government for simulating water flow, sediment transport, and morphology in rivers and estuaries. It can be used for simulating river flooding and dam failures.

Overall, 3D hydrodynamic flood simulation software are more complex and computationally demanding compared to 2D models. They require more detailed data on the topography and structures of the area being modelled, and it may be more difficult to validate and calibrate the model due to its increased complexity. However, they can provide a more accurate representation of the flood behaviour and the impacts of flood risk on structures.

#### **2.7.1.7 Capacities of Spatial 3D Hydrodynamic Flood Simulation Models at Building Scale**

One of the key advantages of spatial 3D hydrodynamic flood simulation models is their ability to provide high-resolution predictions of flood inundation and the associated hazards, including the impact on buildings and other infrastructure. This allows planners and emergency responders to make informed decisions about flood management strategies (Rong et al. 2020; Viccione and Izzo 2022). 3D hydrodynamic flood simulation can help to identify areas that are at high risk of flooding and to understand how floodwater behaves in different environments. This information can be used to improve flood risk management strategies (Wang et al. 2019a).

These models are cost-effective methods of predicting flood behaviour and assessing flood risk, especially when compared to traditional physical models that require significant resources, such as time, money and manpower (Anees et al. 2016). 3D hydrodynamic flood simulation models can be used to simulate floods in different scenarios, such as the effects of climate change on flood risk, or the impacts of different flood management strategies. This flexibility makes it possible to evaluate the effectiveness of different flood management strategies in a virtual environment (Wu et al. 2019). By identifying areas at high risk of flooding, 3D hydrodynamic flood simulation can help to mitigate the risks associated with flooding. This can include the development of flood warning systems, the construction of flood barriers, and the implementation of emergency response plans (Teng et al. 2017; Rong et al. 2020).

At the building scale, these models can be used to predict the flood loads on structures during a flood event because these models also incorporate the vertical component of flooding. Recent studies have shown that spatial 3D hydrodynamic flood simulation models are capable of accurately predicting the flood loads on buildings during flood events (Özgenç Aksoy et al. 2022). For example, a study by Gems et al. (2016) used a 3D hydrodynamic model to simulate the flood inundation of a building and compared the results to physical experiments. They found that the model was able to accurately predict the flood loads on the building, including the pressure distribution and the forces on the walls and roof." Similarly (Robb and Vasquez (2015) and Viccione and Izzo (2022) used a 3D hydrodynamic model to simulate the impact of a flood on a small building with a complex shape. The model was able to accurately predict the inundation depth, the water velocity around the building, and the flood loads on the structure. Altogether, 3D hydrodynamic flood simulation can provide valuable insights into the behaviour of floods in urban environments and help to develop effective flood risk management strategies for buildings. Further research is needed to improve the accuracy and efficiency of these models.

#### **2.7.1.8 Limitation of Spatial 3D Hydrodynamic Flood Simulation Models at Building Scale**

Despite Spatial 3D hydrodynamic flood simulation potential benefits to simulate flood events and assess flood risk at the regional or urban scale. However, when it comes to building-scale simulations, these models have some limitations. Building-scale simulations require accurate and detailed input

data, including topography, building geometry, and material properties, which increases the number of computational cells needed to represent the building and its surroundings accurately. This, in turn, increases the computation time and requires significant computational resources (Zhi et al. 2020).

One of the main limitations of 3D hydrodynamic flood simulation models is their computational complexity, which requires high computational power and time. Due to the high resolution required to simulate the flow dynamics around buildings, the computational time required can be prohibitive, and the models may not be suitable for real-time simulations (Teng et al. 2017; Viccione and Izzo 2022). Another limitation is the requirement for input data, such as topographical information, soil properties, and boundary conditions. Inaccurate or incomplete input data can significantly affect the accuracy of the simulation results. Many models require simplifying assumptions that may not always be valid. For example, some models assume that the flow is steady, which may not be true for highly dynamic and complex flooding scenarios. Others assume that the buildings are stationary, which may not be accurate in cases of buildings with significant deformations or movements during flooding. There is always some degree of uncertainty in the results of flood simulation models due to various sources of uncertainty, such as input data, model simplification, and limitations of the simulation techniques. It is important to quantify and communicate these uncertainties to decision-makers and stakeholders. Finally, validating the results of 3D hydrodynamic flood simulation models is often challenging due to the lack of suitable data for comparison. In some cases, physical experiments may be necessary to validate the simulation results.

## **Chapter 3**

---

# **Technological Advancements to Improve Flood Risk Management**

### 3 Technological Advancements to Improve Flood Risk Management

#### 3.1 Technological Advancements in FRM

Emerging tools are increasingly being used in flood risk management to improve preparedness, response, and recovery efforts. These tools allow stakeholders to better understand and communicate flood risk. They also help to automate many tasks in flood risk management, such as data collection, analysis and mapping allowing for quicker and more efficient response times during floods. Moreover, new tools can enable risk managers to quickly adapt to changing conditions and respond to evolving flood risks, such as through the use of predictive analytics and scenario modelling. By using new technologies to better understand flood risks, communities can take more proactive measures to mitigate risks, such as through the development of floodplain management plans, the use of green infrastructure, and the implementation of flood-resistant building codes. This can ultimately increase the resilience of communities to future flood events.

In addition, emerging technologies can help streamline many tasks involved in flood risk management, such as data collection, analysis, mapping, visualization, and communication. This can lead to more efficient response times during floods and can also free up resources that can be used to enhance other aspects of flood risk management, such as community outreach and education. They can improve communication and collaboration among stakeholders involved in flood risk management. Emergency responders, local officials, and community members can benefit by using advanced tools for data sharing, coordination, visualization, and communication, to work together more effectively and prepare for and respond to flood events.

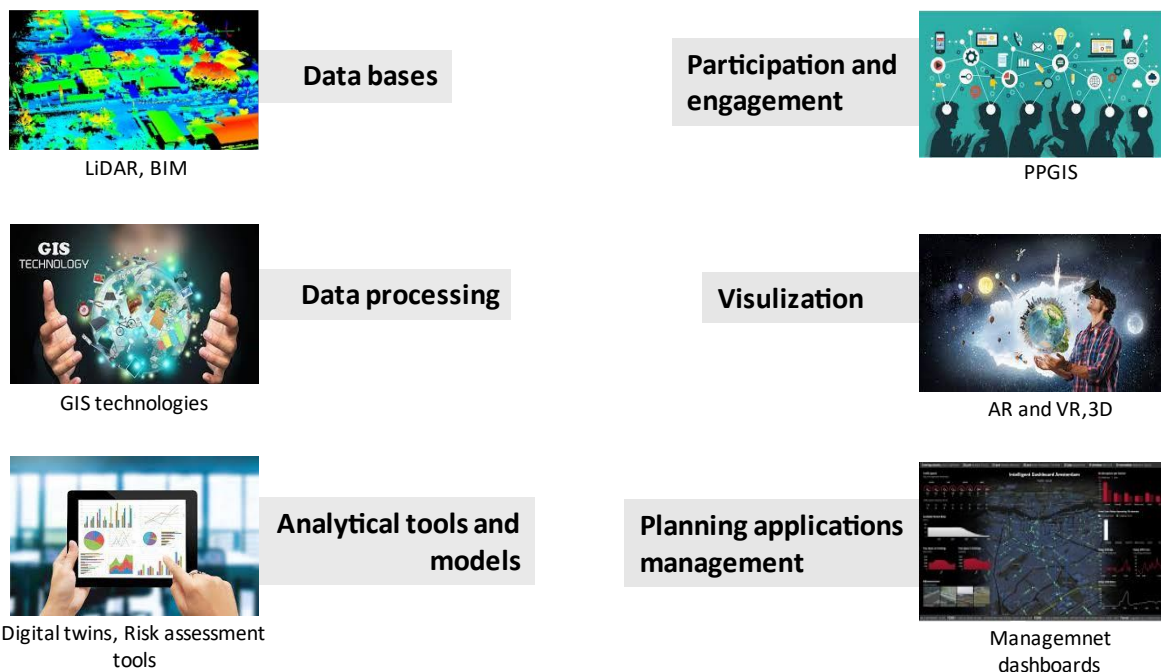


Figure 10: Emerging technologies for flood risk management adopted from (Batty and Yang 2022)

These technologies as shown in Figure 10 can also increase the resilience of communities to flood events by utilizing predictive analytics, scenario modelling, and novel approaches and tools. Communities can take a more proactive approach to flood risk management, implementing measures

such as floodplain management plans, green infrastructure, and flood resilient infrastructure guidelines. There are several tools in flood risk management that have emerged in recent years. To better streamline these emerging technologies, it is important to explicitly understand these technologies in correspondence to the tasks involved in FRM such as data collection from various databases, processing, analysis and mapping, communication, and visualization as well as planning and management. Table 3 shows the emerging technological advancements in correspondence to the tasks involved in improving FRM generally.

Table 3: Emerging technologies and their contribution to FRM

Major Tasks in FRM	Novel Technologies
Data Collection	<ul style="list-style-type: none"> <li>• UAVs – Unarmed Aerial Vehicles or Drones</li> </ul>
Databases	<ul style="list-style-type: none"> <li>• BIM – Building Information Modelling</li> <li>• LiDAR - Light Detection and Ranging</li> <li>• Point Cloud</li> </ul>
Data Processing	<ul style="list-style-type: none"> <li>• GIS – Geographic Information System</li> <li>• BIM – Building Information Modelling</li> <li>• CAD – computer-aided design</li> </ul>
Analytical Approaches and Models	<ul style="list-style-type: none"> <li>• Digital Twin</li> <li>• 3D Flood Modelling</li> <li>• Flood Risk assessment</li> </ul>
Participation and Engagement	<ul style="list-style-type: none"> <li>• PPGIS – Public Participation Geographic Information Systems</li> <li>• Surveys</li> </ul>
Visualization and Communication	<ul style="list-style-type: none"> <li>• AR - Augmented reality</li> <li>• VR - virtual reality</li> <li>• Digital Twin</li> <li>• 3D GIS</li> <li>• BIM</li> </ul>
Planning Application and Management	<ul style="list-style-type: none"> <li>• Digital web applications</li> <li>• Dashboards</li> </ul>

The emerging technologies involved in the process and development of this research are elaborated below in detail.

### 3.1.1 Digital Twin Technology

A digital twin is a virtual representation of a physical system or process that allows real-time monitoring and simulation of its behaviour. Digital twin technology has been gaining popularity in the field of flood risk management due to its ability to provide a virtual replica of physical assets and systems. In the context of flood risk management, digital twins can be used to analyse the impact of flooding on infrastructure, evaluate flood risk scenarios, and develop flood management strategies. Digital twins can be used to simulate the behaviour of a river or a city during a flood event and to test different flood mitigation measures before implementing them in the real world.

Digital twins can provide a powerful tool for flood risk management by integrating data from various sources, such as weather forecasts, river gauges, and urban sensors (White et al. 2021; Ghaith et al. 2022). By combining this data with models of flood behaviour, digital twins can predict the extent and severity of a flood and identify areas of high risk. Furthermore, digital twins can be used to test different flood mitigation measures, such as building flood barriers or improving drainage systems. By



simulating the behaviour of the flood and the effectiveness of these measures, digital twins can help decision-makers to select the most effective and cost-efficient solutions.

ARUP (2019) used the digital twin technology in flood risk management for developing a City Water Resilience Approach (CWRA). The CWRA integrates a range of tools, including a digital twin, to help cities improve their water resilience. The digital twin provides a virtual replica of the city's water infrastructure, which is used to model the impact of floods on the system. This also allowed city officials to develop better flood management strategies, such as the installation of flood barriers or the relocation of critical infrastructure. Similarly, the use of digital twins in the management of the River Thames in the United Kingdom by the Environment Agency of England. They developed a digital twin of the river that integrates data from a range of sources to model the behaviour of the river in real time. It allows them to monitor flood risk and water quality, and to develop and test different flood management strategies. Ghaith et al. (2022) develop a digital twin (Figure 11) under flood hazards through the integration of data acquisition systems, hydrology and hydrodynamic modelling, physical infrastructures and entities, demographic information, and real-time system behaviour.

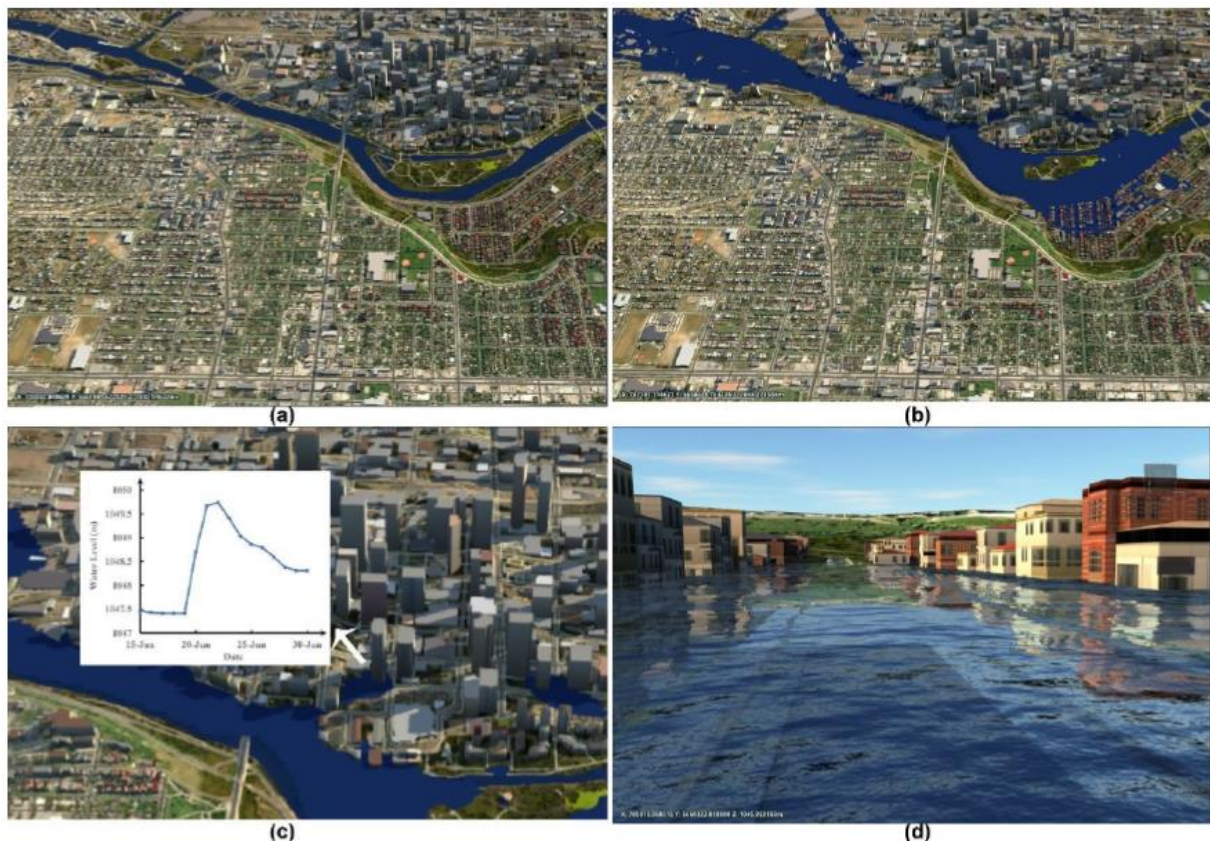


Figure 11: City digital twin visualization: (a) bird eye view of part of the city (b) bird eye view of the same city with flooding (c) hydrograph at one of the buildings (d) Human eye view of the flooded buildings, (Source: Ghaith et al. 2022)

According to Shahat et al. (2021), the accuracy of the digital twin model depends on the quality of input data and the ability of the model to accurately represent the physical system's behaviour. They propose methods to improve data quality and accuracy, such as combining different sources of data and using advanced statistical methods to account for uncertainty. They conclude that digital twins

can be valuable tools for flood risk management, but only if the data used to develop them is of high quality and accurately reflects the physical system's behaviour.

Although digital twin technology has been utilized in several applications, including flood risk management, it is a complex process that necessitates extensive big data to efficiently deliver its advantages. Even though using digital twin technology for flood risk management holds great potential, still its full potential remains undiscovered. Further investigation is necessary to completely uncover the potential of digital twin technology for flood risk management and establish effective approaches/workflow for integrating it into the current flood management.

### 3.1.2 Building Information Modelling (BIM)

Building Information Modelling (BIM) is a process that involves the creation of a 3D digital model of a building, which contains detailed information on its design, construction, and operation. The BIM model contains detailed information on the design, construction, and operation of the building, including its geometry, materials, systems, and components. This information can be used to optimize the design and construction process, as well as to facilitate maintenance and management of the building throughout its lifecycle see Figure 12.

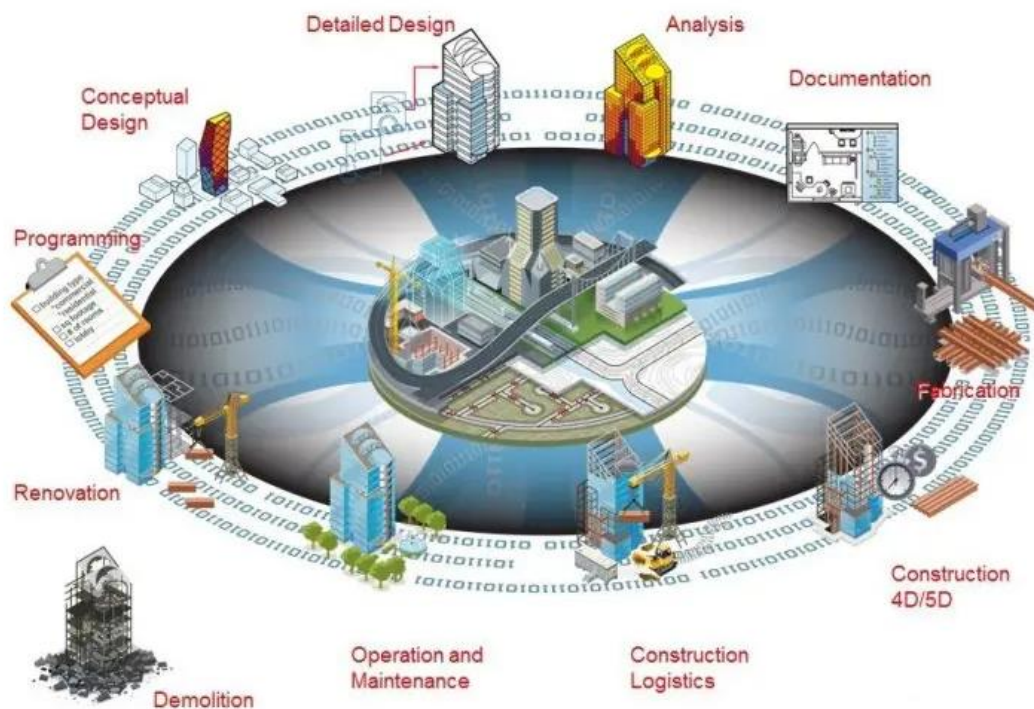


Figure 12: Basic concept of BIM (Source: Autodesk 2018)

BIM also has the potential to be a useful tool in flood risk management by enabling the integration of flood risk information into the building design and construction process. For example, BIM can be used to model the potential impact of flooding on a building, including the extent of flooding, the height of floodwaters, and the potential damage to the building and its systems.

This information can then be used to optimize the building's design and construction to mitigate flood risks, such as by elevating the building, modifying drainage systems, or using flood-resistant materials. Furthermore, BIM can be used to aid in the development of flood evacuation plans by providing accurate 3D models of buildings and infrastructure. These models can be used to simulate flood scenarios and develop effective evacuation plans that ensure the safety of occupants during a flood event. BIM can be used to incorporate flood risk information into building design and construction processes, enabling the identification and mitigation of flood risks at an early stage (Sertyesilisik 2017; Khanmohammadi et al. 2020). The study found that BIM-based flood risk management can reduce flood-related damages and improve the resilience of buildings and infrastructure.

Similarly, a study by Jeong (2020) demonstrated the potential of BIM in flood evacuation planning. The study found that BIM can be used to create accurate 3D models of buildings and infrastructure, which can aid in developing effective flood evacuation plans and improving the safety of occupants. Furthermore, Amirebrahimi et al. (2016) and Xu et al. (2019) highlighted the potential of BIM in flood damage assessment. They found that BIM can be used to create accurate before-and-after flood damage models, which can aid in developing effective post-flood recovery strategies. Eventually, BIM has proven to be a valuable tool in flood risk management, enabling the integration of flood risk information into the building design and construction process, aiding in flood evacuation planning, and improving post-flood recovery efforts. The integration of BIM with other tools and models can aid in developing more effective flood management strategies.

In BIM Level of Detail (LOD) is a standard used in the construction industry to describe the degree of detail or accuracy of BIM models at different stages of the construction process shown in Figure 13. The following are the commonly used BIM LODs:

1. LOD 100: This level represents a conceptual design stage where the model is a basic representation of the building's shape and size. It includes only limited information and is not used for construction purposes.
2. LOD 200: This level represents a schematic design stage where the model includes more detailed information, such as wall thickness and height, floor-to-floor heights, and basic architectural elements.
3. LOD 300: This level represents a detailed design stage where the model includes accurate and comprehensive information, such as mechanical, electrical, and plumbing (MEP) systems, structural details, and dimensions.
4. LOD 400: This level represents a construction stage where the model includes fabrication and assembly information, such as fabrication details, materials, and connections.
5. LOD 500: This level represents an as-built stage where the model includes accurate and comprehensive information about the building's actual components and systems, including maintenance and operation information.

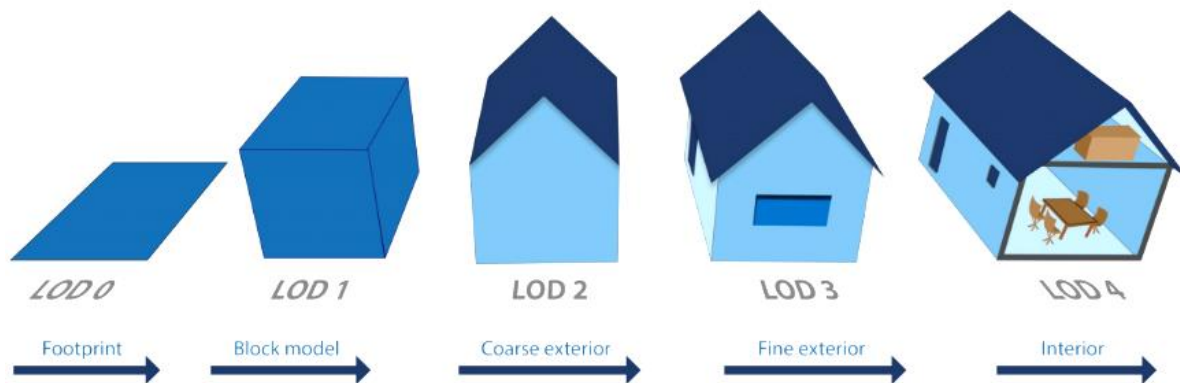


Figure 13: The five LODs of BIM (Source: Autodesk 2017)

BIM Level of Detail (LOD) can be used in flood risk assessment by providing detailed information on the building and its surroundings. The following are some ways in which BIM LODs can help in flood risk assessment:

1. Detailed site analysis: BIM LOD 300 and above can provide detailed information about the site, including topography, soil conditions, and drainage patterns, which can help in understanding the risk of flooding.
2. Accurate flood modelling: BIM LOD 400 and above can provide accurate information about the building's geometry and structural components, which can help in creating accurate flood models to assess flood risk.
3. Identification of flood mitigation measures: BIM LOD 400 and above can provide detailed information about the building's construction materials and components, which can help in identifying potential flood mitigation measures such as flood barriers, waterproofing, and drainage systems.
4. Collaborative approach: BIM LODs can enable collaboration between architects, engineers, and contractors to develop flood-resistant designs and solutions.

Several studies have shown the potential of using BIM LODs in flood risk assessment. For example, Amirebrahimi et al. (2016) and Kim and Park (2016) demonstrated the use of BIM LOD 300 in flood risk assessment and showed that it could help in identifying flood-prone areas and in developing flood-resistant designs. Another study by Patten (2017) showed that BIM LOD 400 and above can be used to create accurate flood models and to identify flood mitigation measures. BIM LODs can help in flood risk assessment by providing detailed information about the building and its surroundings, enabling accurate flood modelling, and identifying potential flood mitigation measures. Amirebrahimi et al. (2016) used a LOD rich BIM model for flood damage assessment shown in Figure 14, where damage to multiple building components can be visualized in 3D.

BIM has been used in various research studies for flood risk management. However, there is still a need to explore the full potential of BIM for this purpose. Despite its potential benefits, such as improved flood response and mitigation strategies, BIM has not been fully utilized in flood risk management. Therefore, further research is needed to fully explore the potential of BIM for flood risk



management and to develop effective strategies to incorporate BIM into existing flood management practices.

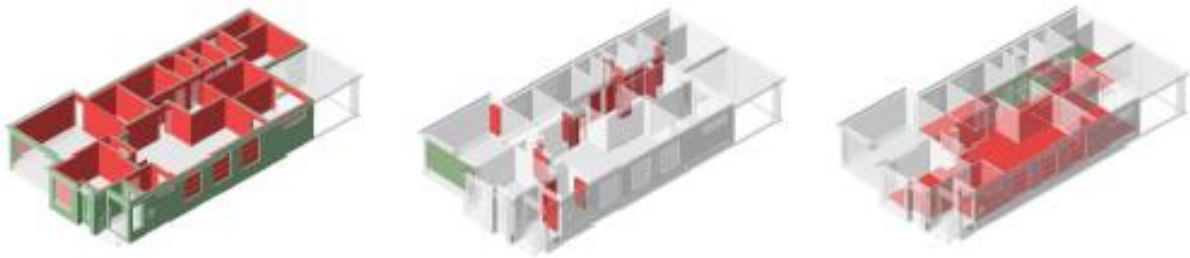


Figure 14: 3D Visualization of damaged walls (left), doors (middle) and flooring (right) (Source: Amirebrahimi et al. 2016)

### 3.1.3 Unmanned Aerial Vehicles (UAVs) or Drones

Unmanned Aerial Vehicles (UAVs) or drones have gained popularity in flood risk management due to their ability to capture high-resolution imagery of flood events and provide real-time monitoring. UAVs can be used for assessing flood damage by providing high-resolution imagery of affected areas (Gebrehiwot et al. 2019). They found that UAVs can provide more detailed and accurate information on flood damage compared to traditional ground-based methods, which can aid in developing effective flood management strategies. Similarly, Abdelkader et al. (2013) demonstrated the potential of UAVs in real-time flood monitoring. This study found that UAVs can provide timely and accurate information on floodwater levels, flow velocity, and sediment transport, which can aid in developing effective flood forecasting and warning systems. Furthermore, a study by Trepekli et al. (2022) highlighted the potential of UAVs in assessing flood risk in urban areas. This study found that UAVs can capture high-resolution imagery of urban areas and provide detailed information on flood risk factors such as building density and drainage systems, which can aid in developing effective flood risk management strategies. In a study conducted by Brauneck et al. (2019) Unarmed Aerial Vehicles (UAVs) were employed to quantify surface flow velocities. Leveraging photogrammetric ranging techniques, the researchers analyzed UAV-captured visual data and established a hydrodynamic model of breach flow. This model was constructed using four distinct digital surface models, encompassing breach widths ranging from 9 to 40 meters. Through meticulous calculations based on these models, the researchers successfully determined the flow rate passing through the breach. Hence, the use of UAVs in flood risk management has proven to be beneficial in assessing flood damage, real-time monitoring, and assessing flood risk in urban areas. The integration of UAVs with other tools and models can aid in developing more effective flood management strategies.

### 3.1.4 LiDAR in Flood Risk Management

LiDAR, or Light Detection and Ranging, is a remote sensing technology that uses laser pulses to create highly detailed and accurate 3D models of the Earth's surface (Awange and Kiema 2019; Novero et al. 2019; Muhadi et al. 2020). LiDAR devices come in various shapes and sizes and are used for different applications. A LiDAR device that is mounted on platforms such as aircraft and helicopters or Drones is known as airborne LiDAR. It is commonly used for creating digital elevation models, mapping land cover, and identifying flood-prone areas. LiDAR devices that collect data from the ground are referred to as ground-based LiDAR that can be categorized into static or mobile laser scanning (Escobar Villanueva et al. 2019). Whereas, static also referred to as terrestrial LiDAR devices are mounted on a

tripod and used for capturing detailed 3D images of buildings, infrastructures, and other objects (Lim et al. 2013). Similarly, mobile LiDAR devices are mounted on vehicles and are used for mapping road networks, utilities, and other infrastructure (Figure 15). LiDAR has become a popular tool in flood risk management due to its ability to provide high-resolution elevation data that can be used to identify flood-prone areas and develop flood management strategies.

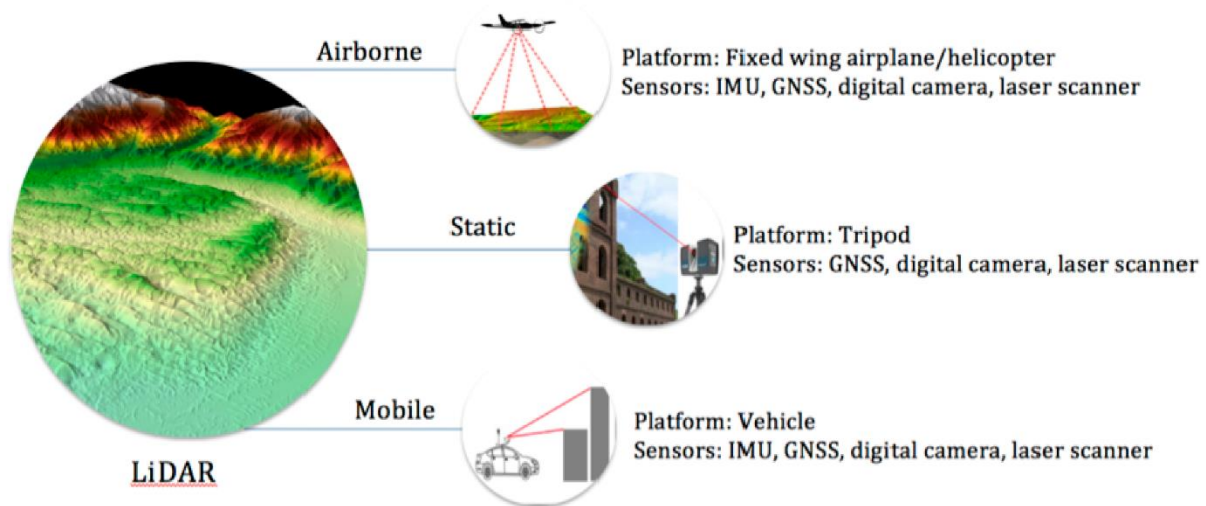


Figure 15: Type of LiDAR data collection (Source: Escobar Villanueva et al. 2019)

LiDAR can be used to create accurate flood inundation maps by combining high-resolution elevation data with hydrodynamic modelling (Bales et al. 2007). They found that LiDAR-based flood modelling can improve the accuracy of flood mapping and enable more effective flood risk management. Similarly, a study by Bodoque et al. (2023) demonstrated the potential of LiDAR in flood hazard assessment. The study found that LiDAR data can provide detailed information on flood hazard factors such as terrain slope, vegetation cover, and land use, which can aid in developing effective flood hazard maps and identifying vulnerable areas. Furthermore, a study by Gracia et al. (2019) highlighted the potential of LiDAR in assessing the impacts of climate change on flood risk. The study found that LiDAR can provide accurate elevation data that can be used to model the impacts of sea-level rise and extreme precipitation events on coastal flooding. LiDAR has proven to be a valuable tool in flood risk management, enabling accurate flood mapping, hazard assessment, and impact assessment. The integration of LiDAR with other tools and models can aid in developing more effective flood management strategies.

### 3.1.5 Point Clouds in Flood Risk Management

Point cloud refers to a collection of data points in a three-dimensional coordinate system that represents the surface of an object, environment, and space. These points are typically obtained through 3D scanning technologies such as laser scanning, photogrammetry, or structured light scanning. Point clouds are often used in fields such as architecture, engineering, and construction to capture the precise measurements and geometry of objects or spaces. The data captured in a point cloud can be used to create detailed 3D models see Figure 16 that can be analysed, modified, and used in various applications. Point clouds are also commonly used in the development of virtual and augmented reality applications, as they can be used to create realistic and immersive environments.

Additionally, point clouds have been utilized in the field of robotics for mapping and localization, as well as in the analysis of flood risk and environmental data. Point clouds are becoming increasingly popular in flood risk management due to their ability to provide detailed and accurate elevation data that can be used to identify flood-prone areas and develop flood management strategies (Miro Govedarica et al. 2018).

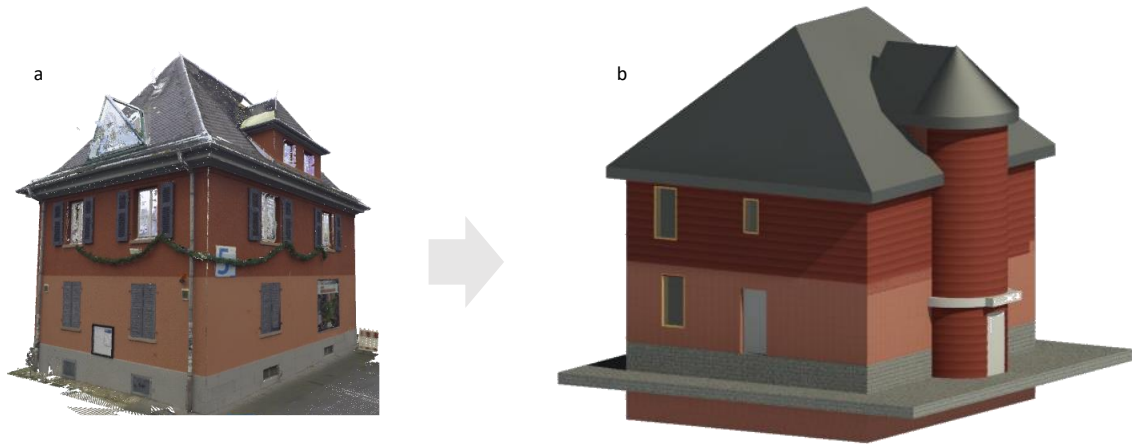


Figure 16: Laser scanned point cloud building data (a) and developed 3D building model (b)

According to Annis et al. (2020), point clouds can be used to create accurate flood inundation maps by combining high-resolution elevation data with hydrodynamic modelling. The study found that point cloud-based flood modelling can improve the accuracy of flood mapping and enable more effective flood risk management. Similarly, a study by Jakovljevic et al. (2019) demonstrated the potential of point clouds in flood hazard assessment. The study found that point cloud data can provide detailed information on flood hazard factors such as terrain slope, vegetation cover, and land use, which can aid in developing effective flood hazard maps and identifying vulnerable areas. Albano (2019) conducted a study that emphasized the usefulness of point clouds in assessing flood damage. Their findings revealed that point cloud data has the potential to generate precise models of flood damage both before and after the event, which can facilitate the creation of effective recovery plans in the aftermath of a flood. Thus, point clouds have proven to be a valuable tool in flood risk management, enabling accurate flood mapping, hazard assessment, and damage assessment.

### 3.1.6 Geographic Information System (GIS)

Geographic Information System (GIS) is a computer-based tool that helps in processing, analysing, managing, and visualizing geographical data via geoprocessing. Geoprocessing in GIS refers to a set of tools and techniques used to manipulate, analyse, and transform spatial data. Geoprocessing tools are used to automate repetitive tasks, perform complex spatial analyses, and produce new datasets from existing data. Geoprocessing tools are typically accessed through a graphical user interface (GUI) or scripting. The tools are organized into toolboxes that are grouped according to function. The tools can perform various tasks such as spatial analysis, data conversion, data management, and visualization.

GIS has been widely used in flood risk management for many years to create flood maps, assess the impact of flood events, and identify areas at risk of flooding (Coppock 1995; Chen et al. 2003). These advancements include the ability to integrate real-time data from various sources, such as weather

sensors and river gauges, into flood models, as well as the ability to use machine learning algorithms to improve flood predictions (Forkuo and Tsawo 2013; Isma'il and Saanyol 2013; Li et al. 2023). GIS technology can be used to analyse satellite imagery and digital elevation models to map flood-prone areas (Abdulrazzaq et al. 2018; Jamali et al. 2018). It is used to model the flow of water during a flood event and predict flood inundation levels. It is also used to assess the impact of flood events on infrastructure and communities. According to Haq et al. (2012), GIS has been used to analyse the damage caused by floods and to prioritize recovery efforts. It is used to develop evacuation plans and identify areas that require additional flood protection measures. Therefore, it is an essential tool for managing flood risk and improving community resilience.

Similarly, 3D GIS is a technology that allows users to create, manage, analyse, and visualize geospatial data in three dimensions. In contrast to traditional GIS, which operates in two dimensions (i.e., latitude and longitude), 3D GIS takes into account elevation and other vertical attributes, enabling users to model and visualize features such as buildings, terrain, and infrastructure in a more accurate and realistic way. In addition to basic visualization and modelling capabilities, 3D GIS also provides powerful analysis tools for performing various geospatial analyses in 3D. These tools can be used to solve a wide range of problems, from analysing the impact of proposed buildings or infrastructure on the surrounding environment to identifying optimal locations for new facilities based on accessibility, visibility, or other criteria. The integration of 3D GIS technology with flood simulation models can improve the accuracy of flood risk assessments by accounting for terrain features such as slopes, valleys, and land use characteristics (Singh and Garg 2016; Bazan-Krzywoszańska et al. 2019). This can aid in identifying vulnerable areas and designing effective flood mitigation measures. Wu et al. (2019) demonstrated that the use of 3D GIS technology can provide a better understanding of the spatial and temporal patterns of floods. The study found that the integration of 3D GIS technology with hydrological models can improve the accuracy of flood forecasting and enable more effective emergency response planning. Furthermore, Ackere et al. (2016) highlighted the potential of 3D GIS technology for flood risk communication and stakeholder engagement and found that the use of 3D visualization tools facilitates easier communication among stakeholders and helps to convey the potential impacts of floods in a more intuitive manner.

### **3.1.7 3D Flood Modelling**

3D modelling is the process of creating a three-dimensional representation of an object or scene using specialized software. It involves creating a digital model that can be manipulated and viewed from different angles and perspectives. 3D models can be used in a variety of fields, including video games, movies, architecture, engineering, and product design. They can be created from scratch using tools like polygon modelling, spline modelling, or NURBS modelling, or by scanning real-world objects using 3D scanning technology (point cloud). Once a 3D model is created, it can be textured, animated, and rendered to produce high-quality images and videos. 3D modelling is an essential part of the modern digital world, and it has revolutionized the way we design and create products, buildings, and even virtual environments. The use of 3D modelling technology for flood risk management has gained popularity due to its ability to provide a more detailed and accurate representation of the terrain, which enables better flood modelling, and visualization capabilities (Figure 17).





Figure 17: 3D flood visualization representing buildings affected by flooding (Source: SymGEO)

According to many studies, 3D modelling can help stakeholders better understand the risks associated with flooding and make informed decisions about mitigation strategies (Hossain, A. K. M. Azad et al. 2012; Kumar et al. 2018; Massaâbi et al. 2018; Douass and Kbir 2019). They also identified that 3D modelling can be used for both urban and rural areas, as well as for simulating various flood scenarios. This allows for a more comprehensive analysis of flood risk, including the identification of potential flood pathways and the assessment of the effectiveness of different flood protection measures. Similarly, Zhi et al. (2020) and Kim and Lee (2021) highlight the potential of 3D modelling to support flood risk management in urban areas. The authors note that 3D modelling can be used to create detailed flood maps that consider the topography and built environment of the area, as well as the potential impact of climate change. Eventually, the use of 3D modelling in flood risk management is a promising approach that has the potential to improve our understanding of flood risk and inform more effective mitigation strategies.

### 3.2 Exploring the Potential Benefits of Integrating New Tools for Improving FRM

Traditional approaches to FRM, such as flood protection infrastructure, are no longer sufficient on their own, and new tools and approaches are needed to improve our ability to predict, prevent, and respond to floods. One promising approach is to integrate new tools for FRM. Integrating these new tools for FRM can have a range of potential benefits. One key benefit is improved flood prediction accuracy. For example, integrating remote sensing data with hydrological models can improve the accuracy of flood forecasts (Khan et al. 2011; Li et al. 2016). Similarly integrating data from different sources, such as hydrological models and decision support systems, can help identify the most effective flood prevention measures (Haberlandt 2010). Therefore, integration of new tools (such as GIS, BIM, LiDAR, point cloud, and 3D modelling etc.) can provide significant benefits for flood risk management. By enabling better visualization, data analysis, and decision-making, these tools can lead to more efficient and cost-effective measures to mitigate flood risks see Figure 18.

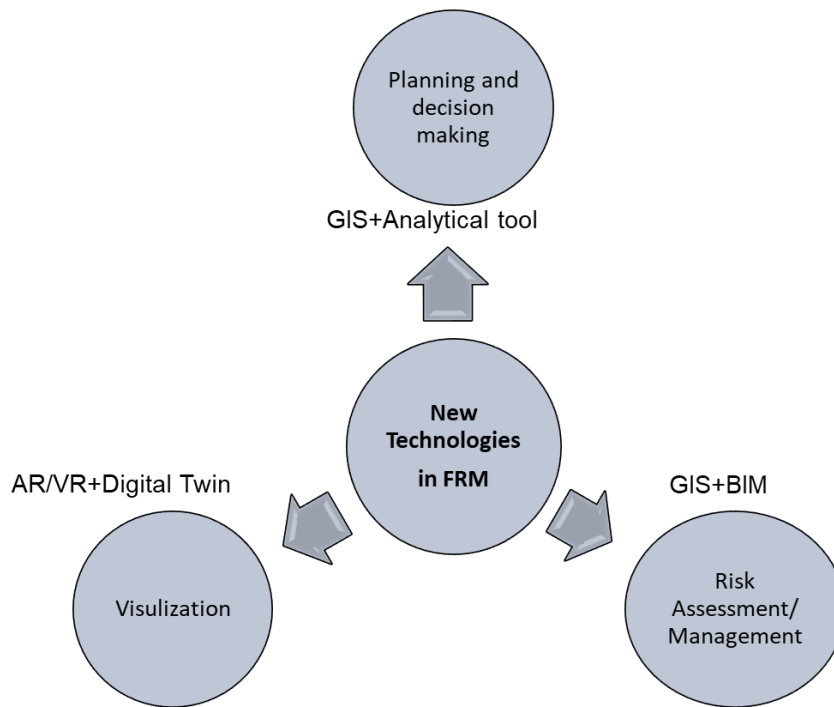


Figure 18: Integration opportunities of emerging digital tools in FRM

### 3.2.1 Combining GIS and Analytical Tools

There is a huge potential to combine GIS with analytical tools such as digital twin or 3D flood models to enhance planning and decision making for flood risk management. Where stakeholders and flood managers as well as people from different walks of life have a better understanding of the risk associated with buildings and infrastructures for planning and decision support.

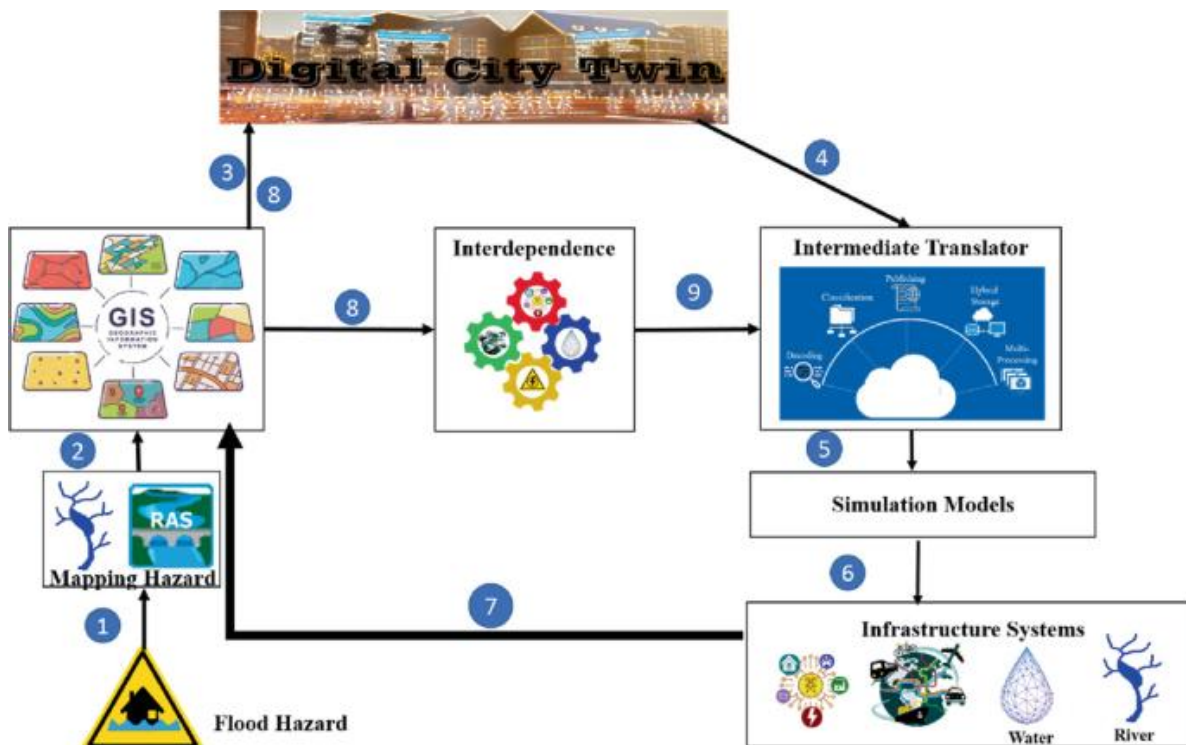


Figure 19: Digital twin creation for a city-scale flood imitation framework (Source: Ghaith et al. 2022)

Ghaith et al. (2022) lays a framework shown in Figure 19 to devise a city digital twin under flood hazards through the integration of analytical data (physical infrastructures and entities, demographic information, and real-time system behaviour) with GIS (hydraulic flood modelling) to provide a continuous imitation of hazards affecting the city infrastructures, identified vulnerable locations across the city under hazardous events, enhanced the city resilience under climate-induced hazards and developed reliable preparedness plans and risk mitigation strategies under climate-related hazards.

The integration of GIS with analytical tools offers numerous advantages for FRM. GIS enables the collection of precise and comprehensive spatial data on areas that are at risk of flooding, and when combined with analytical tools, it can help identify potential flood hazards and vulnerabilities more accurately. Consequently, this integration can enhance the efficiency of allocating resources to address flood risks in the most vulnerable areas, leading to cost savings and more effective flood management. Furthermore, city planners can leverage GIS data and analytical tools to pinpoint areas most susceptible to floods and develop effective mitigation measures to decrease the risk of future floods. The integration of Geographic Information Systems (GIS) with analytical data is a multifaceted process that presents significant challenges due to the voluminous and intricate nature of big data. Further investigation is required to fully elucidate the potential of this integration for effectively managing flood risk.

### **3.2.2 Integrating AR/VR and Digital Twin**

Virtual Reality and Augmented Reality (VR/AR) technology have revolutionized the way we perceive and interact with the digital world. When integrating VR/AR with Digital Twin (DT) technology, it offers a unique opportunity to visualize and communicate complex data in an intuitive and interactive manner. In the context of FRM, the integration of VR/AR and DT technology has the potential to revolutionize the way we assess, plan, and mitigate flood risks (Bakhtiari et al. 2023).

The integration of VR/AR and DT technology in FRM offers several benefits. Such as it allows stakeholders to visualize and interact with flood risk information in a more intuitive and immersive way. For example, using VR/AR, it is possible to create a virtual flood scenario that can be explored from different angles, providing a more comprehensive understanding of the potential impacts of flooding on buildings and infrastructure. This can also help stakeholders to make more informed decisions about mitigation strategies and emergency response plans (Qiu et al. 2019; Dani and Supangkat 2022). This can help to bridge the gap between technical experts and non-technical stakeholders, improving the overall effectiveness of FRM.

Furthermore, the integration can improve flood forecasting and emergency response. By creating a virtual representation of a building or infrastructure using DT technology, it is possible to integrate real-time sensor data into the model to create a real-time simulation of flood events. This can be used to predict the impact of floods on buildings and infrastructure and to develop more effective emergency response plans (Bakhtiari et al. 2023). Despite enormous benefits, there are several challenges to the integration of VR/AR and DT technology in FRM. Firstly, the technology is relatively new and still evolving. Moreover, there may be limitations to its accuracy and reliability. Secondly, the high cost of VR/AR and DT technology can be a barrier to its widespread adoption. Additionally, specialized training and expertise may be required to use the technology effectively. Therefore, further

research is needed to fully evaluate the potential of these technologies for enhancing flood risk management strategies.

### 3.2.3 Integrating GIS and BIM for FRM

The integration of GIS-BIM in flood risk management is a relatively new approach that has not yet been explored to its full potential. However, the existing research shows promising results and highlights the potential of GIS-BIM integration in flood risk assessment, emergency planning, damage assessment, and post-disaster recovery planning. The integration of GIS-BIM can help in the creation of a digital twin of a city or region, which can be used to simulate flood scenarios and plan mitigation strategies. GIS and BIM are two important technologies that can be integrated to improve flood risk management. Geographic systems can provide spatial data and analysis for flood modelling while building information can provide 3D modelling and simulation of buildings and infrastructure.

Therefore, by combining GIS and BIM, it is possible to create a more accurate and comprehensive assessment of the potential impact of floods on buildings and infrastructure. BIM models (digital representations of buildings and infrastructure) can be used to create detailed information that can be combined with GIS data to create flood risk maps that include building-specific information such as the location of critical infrastructure, the height of walls and floors, and the location of electrical and plumbing systems etc. This approach can help decision-makers to better understand the potential impact of floods on buildings and infrastructure and to develop more effective mitigation strategies (Amirebrahimi et al. 2016; Ma and Ren 2017; Lyu et al. 2019). The integration of GIS and BIM has the potential to enhance FRM through improved flood forecasting and early warning systems.

Moreover, the integration of BIM and GIS can improve emergency response and recovery efforts in the event of a flood. BIM models can provide detailed information about building layouts and infrastructure, which can be used by emergency responders to quickly locate critical infrastructure, assess the extent of the damage, and prioritize recovery efforts. For instance, during the 2013 floods in Calgary, Canada, BIM models were utilized to locate the electrical and mechanical rooms in the flooded buildings, assess the extent of the damage, and develop a recovery plan (Moudrak and Feltmate 2019). The integration of GIS and BIM has been found to enhance flood risk management by enabling the generation of more accurate and timely flood warnings, thus allowing decision-makers to take proactive measures to minimize the impacts of floods on buildings and infrastructure. According to researchers, the integration of BIM and GIS facilitates emergency responders to rapidly identify critical infrastructure, evaluate the extent of damage, and prioritize recovery efforts (Messaoudi and Nawari 2020; Mohammadi et al. 2020).

Several studies have explored the use of GIS-BIM integration in flood risk management. For example, a study by Sani and Abdul Rahman (2018) used GIS and BIM to assess the damage caused by floods. The study integrated data from GIS and BIM to create a 3D model of the affected area and to estimate the damage to buildings and infrastructure. They demonstrated the potential of GIS-BIM integration for damage assessment in flood risk management. Similarly many researchers explored the use of GIS-BIM integration for emergency planning in flood risk management (Bi et al. 2013; Boguslawski et al. 2015; Atyabi et al. 2019). They used GIS to map the flood-prone areas and BIM to model the buildings and infrastructure in the affected area. The study evidenced that the integration of GIS and BIM can

be employed to generate realistic simulations of flood scenarios and formulate efficient emergency plans.

Likewise, studies conducted by Amirebrahimi et al. (2016) and Wang et al. (2019a) demonstrated the use of GIS-BIM integration for flood risk management. They aimed to develop a framework for flood risk assessment and emergency planning in urban areas more specifically for buildings. They used GIS to map the spatial distribution of flood risks and BIM to model the buildings. They found that the integration of GIS-BIM can provide a comprehensive understanding of flood risk and helps in the development of effective emergency planning strategies. They also highlighted the potential of GIS-BIM integration for damage assessment and post-disaster recovery planning. Another study by Wang et al. (2019b) explored the use of GIS-BIM integration for flood risk assessment in a rural area. The study developed a flood risk assessment model using GIS to analyse the spatial distribution of flood hazards and BIM to model the rural infrastructure. The study found that the integration of GIS-BIM can provide a more accurate assessment of flood risk compared to traditional methods. The study also highlighted the potential of GIS-BIM integration for cost-effective flood risk management in rural areas. The integration of GIS and BIM is relatively new, but it has been gaining attention in recent years. Further research is required to develop robust frameworks and tools for GIS-BIM integration in flood risk management.

### **3.3 Challenges to Integrate New Tools in Improving FRM**

Integrating new tools for FRM is a complex process which involves various working steps to integrate, thus integration presents several challenges that must be addressed for effective FRM. A major challenge is the interoperability of different data formats and standards used by these tools. For instance, tools like GIS, BIM, LiDAR, point cloud, and 3D models are typically created using different software tools and may use different data formats and standards, making it challenging to integrate data from different sources (Niu et al. 2015; Zhu and Wu 2022). To overcome this challenge, standard data exchange formats such as the Industry Foundation Classes (IFC) and LandXML (see appendix) have been proposed to enable interoperability between different tools (Karan et al. 2016; Shirowzhan et al. 2020; Guyo et al. 2021).

Another challenge is the computational complexity associated with processing and analysing large volumes of data generated by these tools. For example, LiDAR and Point cloud data can generate large datasets that require significant computing resources and expertise to process (Krishnan et al. 2011; Roussel et al. 2020). Additionally, these datasets may be challenging to visualize and interpret, making it difficult to use them in flood management decision-making. To overcome this challenge, several studies have proposed the development of advanced algorithms and visualization techniques to improve the processing and interpretation of these datasets (Shirowzhan and Sepasgozar 2019; Mirzaei et al. 2022). Similarly, the need for specialized knowledge and skills to effectively use these tools in flood risk management is also a challenge. Emerging tools require specialized training and expertise, which may not be readily available to all decision-makers and stakeholders involved in flood risk management (Munawar et al. 2021). To address this challenge, several studies have proposed the development of training programs and educational materials to increase the knowledge and skills of decision-makers and stakeholders in these tools (Wang et al. 2019a; Bakhtiari et al. 2023).

In summary, integrating emerging tools for flood risk management presents several challenges related to interoperability, computational complexity, and specialized knowledge and skills. Addressing these challenges requires the development of standard data exchange formats, advanced algorithms and visualization techniques, and training programs for decision-makers and stakeholders. Despite these challenges, the potential benefits of combining new tools for FRM are significant. By leveraging the latest technology and methods, we can improve our ability to predict, prevent, and respond to flooding events, and ultimately reduce the impacts of floods on society and the environment.

## **Chapter 4**

---

# **Investigation of Technological Developments of GIS-BIM Integration**

## 4 Investigation of Technological Developments of GIS-BIM Integration

Over the past few years, the integration of GIS and BIM has been the focus of research in various fields, including geoinformation, geomatics, construction, architecture, and urban planning. Additionally, organizations such as government-related institutions, national mapping and cadastral agencies, and private companies have also shown interest in this (Noardo et al. 2020).

As explained in Section 3.1, GIS and BIM are two separate but complementary technologies that are increasingly being used in the architecture, engineering, and construction (AEC) industry. GIS as explained in Section 3.1.6 is a software tool that is used for capturing, storing, analysing, and managing spatial or geographical data. While BIM is a software tool that is used for creating and managing digital models of buildings and infrastructure. GIS is primarily used for geographic data management and analysis, including mapping, spatial analysis, and data visualization. It allows users to capture and analyse information related to the physical environment, such as land use, elevation, water bodies, and natural resources. GIS can be used to create maps and other visual representations of geographic data, as well as to analyse patterns and relationships between different types of spatial data. On the other hand, BIM as explained in Section 3.1.2 is primarily used for building design, construction, and management. BIM allows architects, engineers, and construction professionals to create digital models of buildings and infrastructure, which can be used to visualize and simulate different design options, analyse performance, and coordinate construction activities. BIM models contain detailed information about the building's geometry, materials, systems, and components, and can be used to generate construction documents, manage project schedules, and track progress.

Integrating these two technologies can help improve the efficiency of the AEC industry by providing a more comprehensive view of projects that includes both spatial and building information. This integration can help to address some of the challenges faced by the industry, such as improving communication and collaboration among project stakeholders, reducing errors and rework, and enhancing decision-making. For example, GIS data can be used to inform the design and construction of buildings by providing information about the physical environment and infrastructure in the surrounding area. This can include data about land use, zoning, transportation networks, and utility systems, which can be used to inform site selection, building orientation, and design decisions. Similarly, BIM data can be used to inform GIS analyses by providing detailed information about the building's geometry, systems, and components, which can be used to model and analyse how the building interacts with its environment.

The integration of GIS and BIM technologies can help to improve the efficiency and effectiveness of the AEC industry by providing a more comprehensive view of projects that includes both spatial and building information. This integration can help to address some of the challenges faced by the industry, such as improving communication and collaboration among project stakeholders, reducing errors and rework, and enhancing decision-making (Song et al. 2017). The integration of GIS and BIM technologies is still a developing field, but with the continued development of industry standards, software tools, cloud-based platforms, and real-time data integration, the potential for these technologies to improve AEC projects is significant.



#### 4.1 State of the Art of GIS-BIM Integration

One of the key developments in the integration of GIS and BIM technologies is the development of industry standards and guidelines. The Open Geospatial Consortium's CityGML and Building Smart's Industry Foundation Classes (IFC) are examples of such standards that have facilitated interoperability between GIS and BIM software (Gröger and Plümer 2012; Laakso and Kiviniemi 2012). These standards provide a common language for spatial data exchange, making it easier for professionals to integrate GIS and BIM datasets (Laat and van Berlo 2011). Another significant development in GIS-BIM integration is the development of software tools that enable seamless integration between the two technologies. For example, software tools like Esri's ArcGIS Pro and Autodesk's Revit allow for the integration of BIM data into GIS projects and vice versa. This makes it easier for professionals to combine data from different sources and improve the efficiency and accuracy of spatial data management.

Cloud-based platforms, such as Autodesk BIM 360 and Esri ArcGIS Online, are also playing an increasingly important role in the integration of GIS and BIM data. These platforms provide a common platform for data storage and collaboration, making it easier for teams to work together on AEC projects. The integration of real-time data, such as traffic data and weather data, with GIS and BIM models, is another significant development in this field. Real-time data integration can help improve decision-making in AEC projects by providing stakeholders with up-to-date information that they can use to make more informed decisions. For example, real-time traffic data can help architects and engineers design more efficient transportation systems.

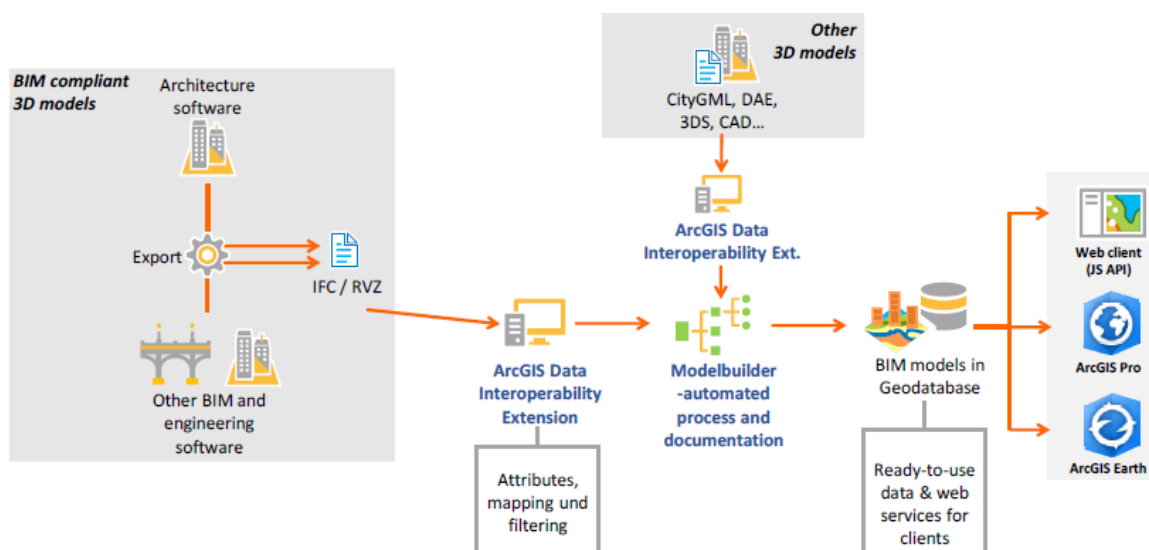


Figure 20: Integration of BIM models into ArcGIS using IFC-format and FME method (Source: Carstens 2019)

The use of 3D visualization tools like virtual reality (VR) and augmented reality (AR) (see Section 3.2.2) is improving the visualization of GIS and BIM data. These tools enable stakeholders to visualize and interact with spatial data in a more immersive way, improving communication and collaboration. As these technologies continue to develop, they are likely to play an increasingly important role in the integration of GIS and BIM technologies in the AEC industry.

There are two methods for the integration of the BIM model with GIS that can be found in the literature (Carstens 2019). The first method involves the transformation of Industry Foundation Classes (IFC) data with FME (Feature Manipulation Engine) software, which can integrate BIM models in IFC-format into ArcGIS with ArcGIS data interoperability extension see Figure 20. FME is a data integration software developed by Safe Software Inc. that can convert data between various formats and systems. According to a study by Wu et al. (2017), FME can be used to transform IFC data into GIS formats such as shapefile, Geodatabase, or KMZ. The study also highlighted the potential benefits of using FME for integrating BIM and GIS, including enhanced data interoperability, improved visualization, and more efficient decision-making processes.

The second method involves the direct read-in of BIM-Revit models (Autodesk Inc.) by ArcGIS Pro see Figure 21. This method allows BIM data to be directly accessed and utilized in GIS without the need for data conversion or transformation. According to a study by Abd et al. (2020), direct read-in can provide more accurate and detailed information for spatial analysis and modelling, which can support decision making in urban planning and management. However, this method requires specific software integration and may have limitations in terms of compatibility and interoperability with different BIM and GIS systems.

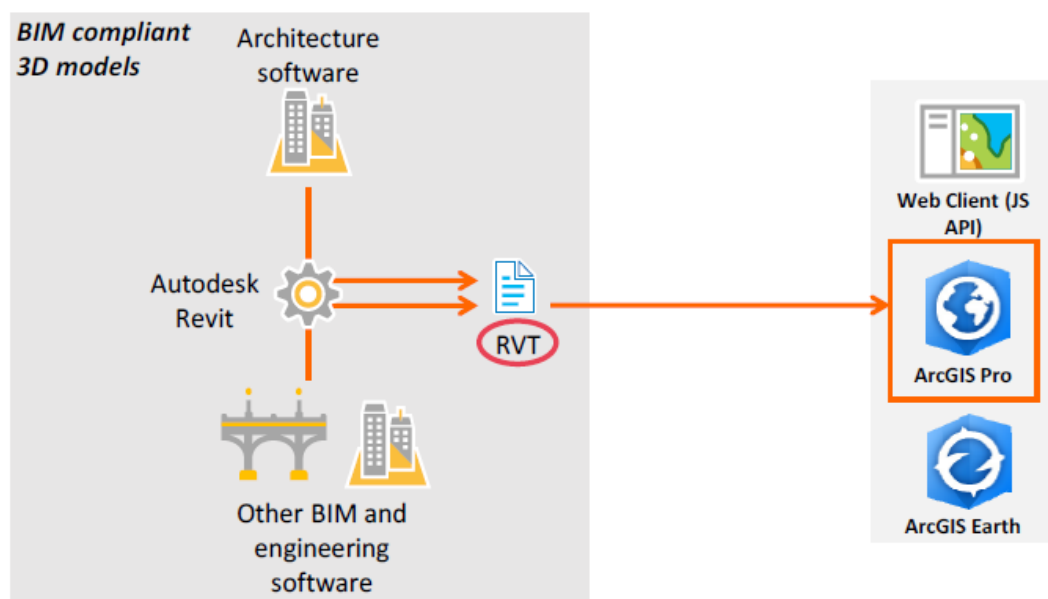


Figure 21: Integration of BIM models by direct read-in Revit model with ArcGIS pro (Source: Carstens 2019)

Both methods of integrating BIM models into GIS systems, i.e., the transformation of IFC data with FME and the direct read-in of BIM-Revit models by ArcGIS Pro, allow for the integration of BIM models with geographic data, including the attributive and metadata information. The integrated models can be utilized for various analysis, scenarios, and visualization purposes in GIS. Song et al. (2017) stated that by integrating BIM and GIS data using FME, the combined models can be utilized for spatial analysis, visualization, and decision-making processes. The integrated models can be used to support construction quality control, facility management, and asset tracking. Similarly, Zhu et al. (2018) noted that the direct read-in of BIM-Revit models by ArcGIS Pro allows for the integration of BIM and GIS data, including the attributive and metadata information. The integrated models can be used for urban

planning, asset management, and other applications that require spatial analysis and visualization. In the literature, GIS-BIM integration methods are also further categorized into three levels.

#### **4.1.1 Application-Level Method**

Application-level methods in integration generally involve modifying or rebuilding existing GIS or BIM tools to include additional functions. This approach can be costly and inflexible. Some examples of application-level integration methods include the work of Irizarry et al. (2013), who developed a BIM-GIS integrated model to improve construction supply chain management. They created a real-time visualization module using BIM-GIS to represent material availability and used GIS-based spatial analyses to manage supply chain logistics costs. Charef et al. (2018) employed a multi-disciplinary approach to review the state-of-the-art of BIM and GIS for collaborative design and identify areas in need of innovation. They described the composition of the research consortium, role distribution among partners, and research methodology at multiple levels.

#### **4.1.2 Process Level (Web Based Integration)**

At the process level, web-based integration methods are often used to connect different GIS or BIM tools through web services or APIs (Application Programming Interfaces) (Isikdag 2015; Tang et al. 2019). This approach allows for easier communication and data exchange between systems, without the need for modifying or rebuilding existing tools. Below are examples of works that used process level methods. El-Hallaq et al. (2019) proposed a web-based integration approach for BIM and GIS systems in the context of smart cities. They developed a web-based platform using open-source technologies that enabled BIM and GIS systems to exchange data through APIs. The platform included various features such as data visualization, querying, and analysis, and allowed for real-time data updates. Similarly, Bai et al. (2017) developed a web-based GIS-BIM integration platform for building energy performance analysis. The platform utilized web services and RESTful APIs to enable communication between BIM and GIS systems and provided various features such as data visualization, simulation, and analysis.

#### **4.1.3 Data Level Methods**

At the data level, integration methods focus on integrating data from different sources using data exchange formats such as Industry Foundation Classes (IFC) and Geography Markup Language (GML) (Beetz and Borrmann 2018; Sani and Abdul Rahman 2018). These formats allow for the exchange of data between different systems, enabling interoperability between GIS and BIM systems. For example, Yamamura et al. (2017) proposed a data-level integration method for linking BIM and GIS data in building energy performance analysis. They developed an IFC-GML mapping method that allowed for the exchange of data between BIM and GIS systems. The method was tested on a case study building, and the results showed that the approach was effective in linking BIM and GIS data for energy performance analysis. A data-level integration method for linking BIM and GIS data for urban flood simulation is also developed (Amirebrahimi et al. 2016; Zhu et al. 2018). Where a GML-based integration method that enabled the exchange of data between BIM and GIS systems and tested the approach on a case study of an urban flood event is proposed. Overall, data-level integration methods enable the exchange of data between different systems, facilitating interoperability between GIS and BIM systems.

## 4.2 Benefits of Integrating GIS-BIM

The authoring systems of GIS and BIM data are designed for different purposes and are technologically different from each other. However, in practical applications, there is a growing need to process the results of each system in joined workflows. The reason for this is that many BIM-related activities require spatial data for further solutions. For example, a BIM model of a building might need to be overlaid onto a GIS map to determine how the building fits into the surrounding environment or to analyse the impact of the building on local traffic patterns. In addition, BIM models may require GIS data to accurately represent the location and elevation of the building.

This need for integration is illustrated in Figure 22, which shows a more comprehensive illustration of the infrastructure lifecycle. The outer area of the figure represents the spatial data that is required for many BIM-related activities, such as site selection, environmental analysis, and urban planning. These activities involve a wide range of disciplines, including architects, engineers, urban planners, and environmental scientists, all of whom require access to both GIS and BIM data.

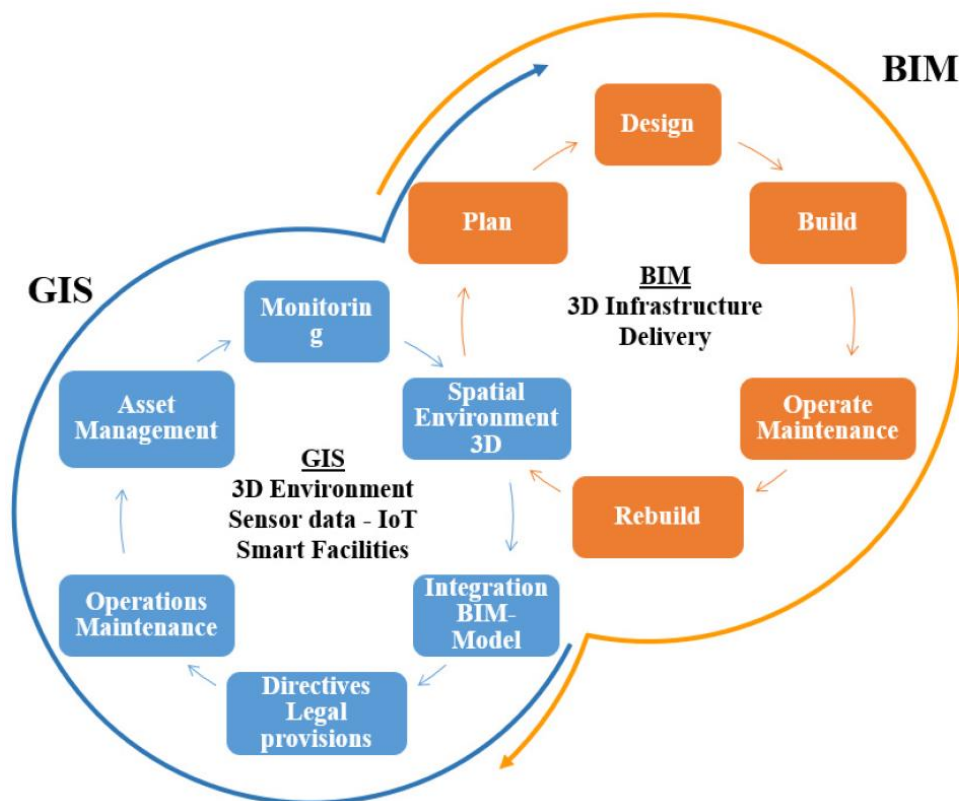


Figure 22: GIS and BIM Systems interacting in infrastructure lifecycle (Source: Carstens 2019)

Several studies have shown the benefits of integrating GIS and BIM technologies in the AEC industry. A study by Patten (2017) demonstrated that the integration of BIM and GIS can improve the accuracy and completeness of project information, reduce design errors and conflicts, and enhance communication and collaboration among project stakeholders. Similarly, a study by Kim and Park (2016) showed that integrating GIS and BIM technologies can help to improve the planning and design of infrastructure projects by providing a more comprehensive view of the project site and its surroundings. For instance, a study by Zhu and Wu (2022) highlights that GIS and BIM systems are

developed independently of each other, but their integration can support decision-making in construction projects. They argue that GIS and BIM data integration can enhance spatial analysis and improve the visualization of construction processes.

Similarly, the literature highlights that GIS and BIM data integration can support a range of activities across the infrastructure lifecycle, including design, construction, and operation (Isikdag 2015; Amirebrahimi et al. 2016; Bai et al. 2017). They argue that spatial data is crucial for a range of BIM-related activities, such as site analysis, building orientation, and energy simulation. These findings are supported by the work of El-Hallaq et al. (2019), who highlight the importance of GIS and BIM data integration in urban planning. They argue that the integration of spatial and non-spatial data can improve decision-making in urban planning by enabling stakeholders to visualize and analyse complex urban systems.

### **4.3 GIS-BIM Integration for Disaster Management**

One of the key benefits of GIS-BIM integration in disaster management is the ability to conduct simulations and analyses that can help identify potential hazards and vulnerabilities. This is particularly important for urban areas, where buildings and infrastructure are densely packed and may be susceptible to various types of disasters such as earthquakes, floods, and wildfires. With GIS-BIM integration, decision-makers can visualize and analyse the built environment in a way that helps them identify potential risks and develop effective disaster response strategies.

Another benefit of GIS-BIM integration in disaster management is improved communication and collaboration among stakeholders. By sharing a common platform, stakeholders such as emergency responders, planners, and engineers can work together more effectively to coordinate response efforts and develop solutions that address the needs of the community. This can help improve overall response times and reduce the impact of disasters on affected communities. Another study by Bi et al. (2013) explores the use of GIS-BIM integration for emergency management on a university campus in China. The study found that the integration of GIS and BIM provided more comprehensive data for emergency response planning and improved the efficiency and effectiveness of emergency management efforts.

### **4.4 GIS-BIM Integration for Flood Impact Assessment**

Flood impact assessment at the micro level such as the building level needs comprehensive information about the building and its different structural (walls, column, beams, etc.) and non-structural components (door, windows, HVAC, etc.), as well as information about its exposure to hazard along with hazard information (in this case its flood depth and velocity) itself. Therefore, due to advancements in the hydrodynamic simulation of floods and GIS, we can obtain spatially distributed flood hazards in terms of inundation depth and velocity within the GIS environment by employing various numerical hydrodynamic simulations. This spatially distributed hazard can be used to identify the exposure of various infrastructures i.e., buildings. Similarly, detailed information about the spatial reference of the building, its 3D virtual replica with its material properties, and information about its different structural and non-structural components can be obtained through BIM. By the integration of GIS (hazard) and BIM (exposed building), the vulnerability of different buildings' structural and non-

structural component to hazard can be achieved which ultimately provide a valid risk assessment of exposed infrastructure components' vulnerability to physical damage see Figure 23.

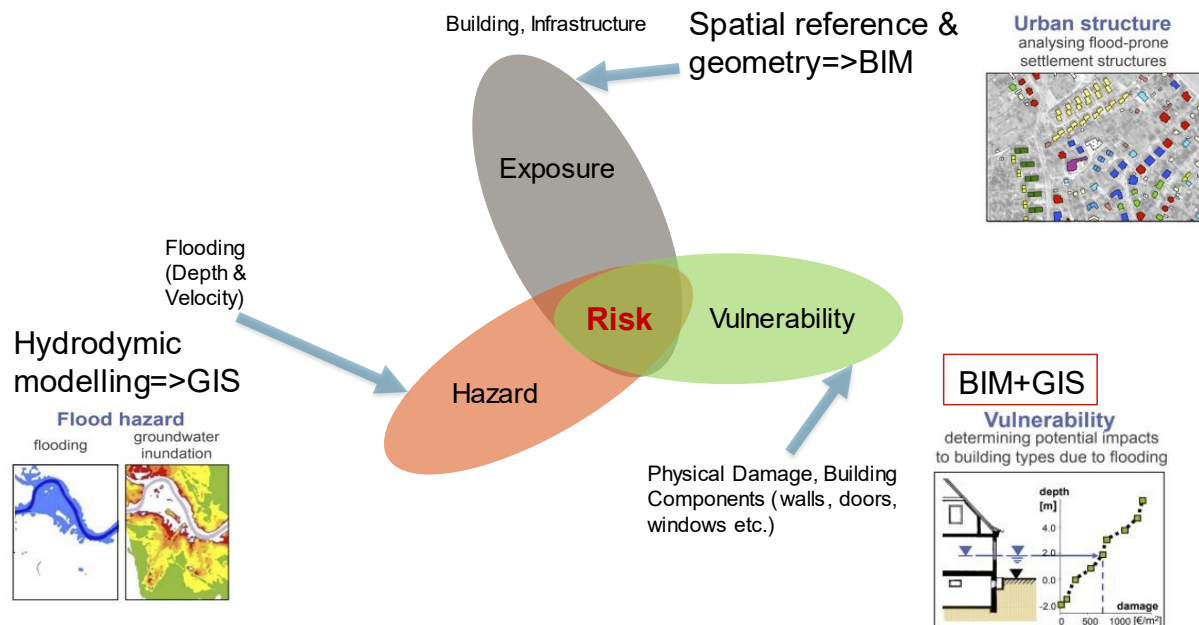


Figure 23: GIS-BIM integration benefits for flood risk assessment adopted from (Jacob 2015)

#### 4.5 Barriers to GIS-BIM Integration

GIS and BIM have been increasingly implemented in construction applications in recent years, resulting in several benefits, such as reduced design errors, improved design quality, shortened construction time, reduced costs, minimized information loss, and easier updating and transfer of data in 3D CAD environments. Similarly, several issues arise during this implementation, including problems with data sharing, data management, integrating GIS with BIM, and topology functions. BIM typically shares information as drawing files created as views of a building model, rather than sharing intelligent objects from the model, leading to poor information sharing and the need for users to rebuild the model to meet their requirements. Additionally, BIM's data structure is not ideal for performing "what if" scenarios for engineering design or providing 3D spatial and connectivity information required by building performance modelling (BPM) due to the lack of topology functions. Integrating GIS and BIM can solve many construction problems, but data mismatches occur due to the different data types and file formats used by each technology. GIS does not support all BIM primitives, which can cause geometry data loss during exporting, while GIS does not support semantic information, leading to semantic data loss during export. Transforming semantic information and spatial relationships from BIM's building model to a geospatial environment can also be challenging due to BIM's lack of object-oriented data structure, and the geospatial information provided by BIM is insufficient in representing 3D geometry and spatial relationships (Niu et al. 2015; Omirtay 2018; Tang et al. 2019).

GIS-BIM integration faces several challenges, including technical, organizational, cultural, and data quality barriers. Technical challenges arise due to differences in data structures, software platforms, and data exchange formats, while organizational challenges relate to coordination and communication between stakeholders. Cultural challenges are related to differences in language, terminology, and working practices between professionals, and data quality challenges arise due to differences in

standards, sources, and management practices (Isikdag 2015; Amirebrahimi et al. 2016; Kim and Park 2016; Abd et al. 2020).

The primary challenge in data integration is the mismatching of information due to the vast and complex nature of BIM data, which contains hundreds of different types of IFC objects with varying attributes and geometric expressions. This can lead to the loss of geometric data and ambiguities in the transformation process between GIS and BIM. While some solutions have been proposed for the transformation of 3D representations between GIS and BIM, there are still issues with semantic loss and mapping between them. The differences in definitions between IFC and GIS can also result in poor mapping, making it difficult to transform between different LOD. Shapefiles, which are commonly used in the GIS industry to support 3D geometry, are often neglected in the integration process due to their lack of defining LODs (Sadegh Khanmohammadi et al. 2020; Ruixue and Yicheng 2021).

The integration involves time-consuming and often manual methods of semantic information mapping, requiring domain experts in both fields. To address this issue, the automation of computer-aided semantic mapping is necessary, but full automation is challenging to achieve. Additionally, transferring information from BIM to GIS can result in information overload due to a large amount of data, making it difficult to handle complex models or entire city data. New technologies and methods are needed to reduce data size while maintaining complete information (Yamamura et al. 2017; Sani and Abdul Rahman 2018; Ruixue and Yicheng 2021). There is currently a lack of norms for the integration of GIS and BIM. Existing integration methods are mostly conducted in specific scenarios, leading to a lack of experience in industrial management practice. This has resulted in a lack of unified technical standards for GIS and BIM integration. Although new standards such as IndoorGML and InfraGML/LandInfra have been developed to complete the transformation, they do not fully meet the required transformation (Laakso and Kiviniemi 2012; Noardo et al. 2020).

There are several important considerations for integrating BIM and GIS, including the need for practitioners to have knowledge in both fields, the challenge of integrating older building data, the involvement of various stakeholders with different access rights, and the issue of privacy. These barriers must be addressed to develop effectively integrated methods and promote the development of the architecture, engineering, and construction industry (Laakso and Kiviniemi 2012; Amirebrahimi et al. 2016; Noardo et al. 2020; Ruixue and Yicheng 2021). Based on the available evidence, it can be inferred that numerous researchers have devised or adjusted procedural frameworks for incorporating GIS and BIM based on their specific requirements. Consequently, to effectively integrate, users must establish or embrace a tailored methodology for integration that addresses the difficulties associated with such integration, thereby achieving a favourable outcome.

## **Chapter 5**

---

# **Research Design and Methodology**



## 5 Research Design and Methodology

### 5.1 Research Design

The research design consists of four phases: i.e., background, model development, model testing and results. These phases are shown in Figure 24 which provides the linkages between the research questions and their corresponding chapters of this thesis.

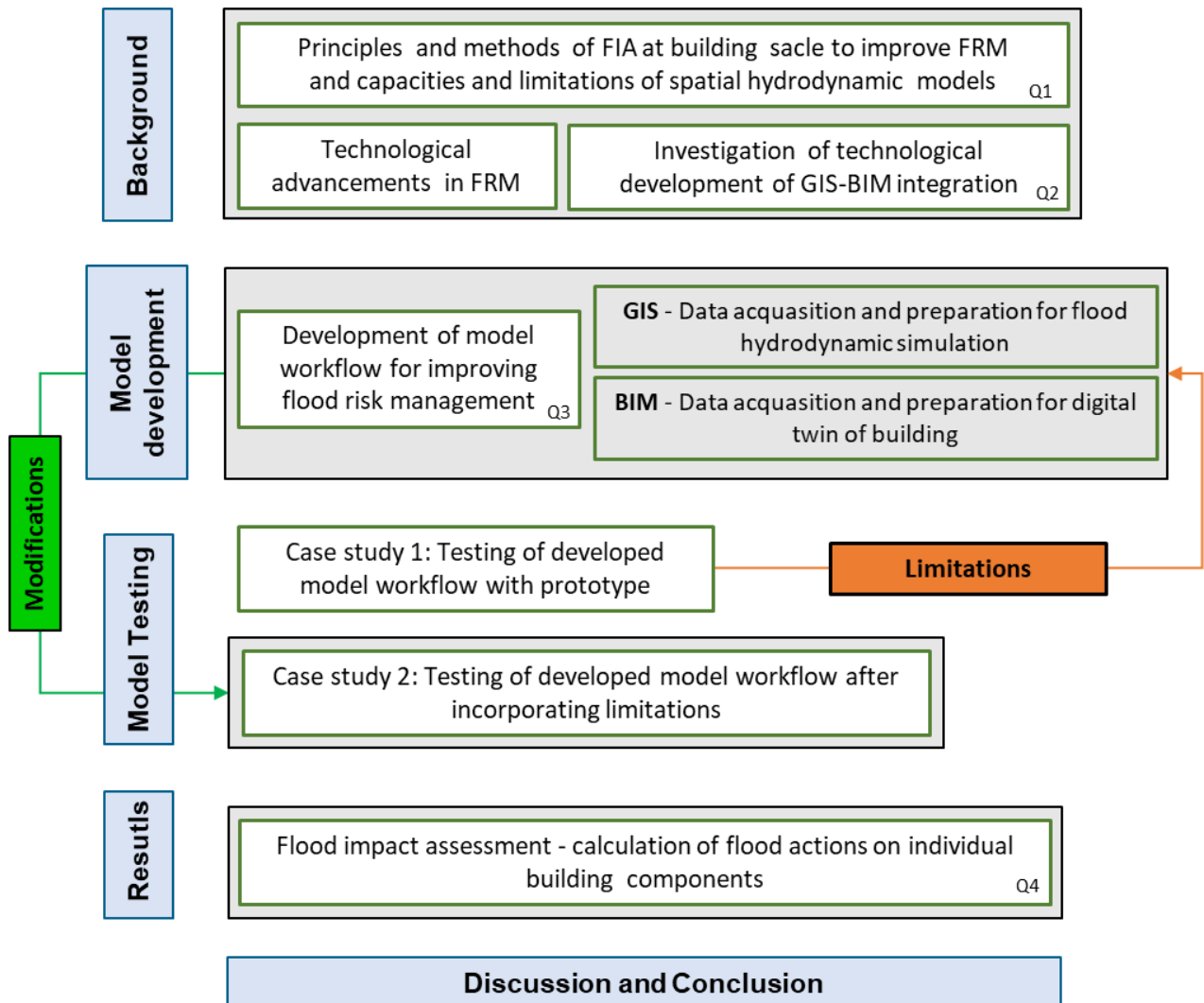


Figure 24: Research methodology with detailed phases

In the **background phase** several activities are undertaken to develop a knowledge base as a foundation for the development of the workflow in this research (see chapters 2, 3, and 4). These include:

- Understanding of principles and methods of flood impact assessment in FRM for abuilding to improve FRM approach in general. It also focuses on the existing literature available for performing FIA and their limitation in recent times with the advancement in technology as well as data inputs. Chapter 2 in this regard also provides insights into spatial hydrodynamic models

and methods to identify the capacities and limitations of existing models at building scale (chapter 2 deals with answering the first sub-research question).

- This research not only sheds light on the current state of FRM but also presents a compelling case for the adoption of advanced technological solutions to improve FRM practices. In chapter 3, the research methodically examines the major tasks involved in FRM and demonstrates how the integration of cutting-edge tools and techniques can improve FRM practices. By presenting a comprehensive analysis of the benefits that advanced technological solutions can bring to FRM, this research underscores the urgent need for their adoption to ensure more effective and sustainable management of flood risks.
- Chapter 4 represents a critical juncture in this research, as it delves into the integration of GIS and BIM techniques to enable more accurate and effective FIA at the building scale. By exploring the potential "reference domains" and technical developments in GIS-BIM integration, this chapter contributes to the development of a comprehensive knowledge base in this field. Moreover, by providing a thorough answer to sub-research question 2, this chapter establishes itself as a key component of this research, bringing clarity and insight into the complex interplay between GIS and BIM in FRM. Through its detailed analysis and rigorous methodology, chapter 4 makes a compelling case for the adoption of GIS-BIM integration as a critical tool for enhancing FIA and highlights its enormous potential for driving meaningful change in this field.

During the background phase, the activities are primarily carried out through qualitative review and assessment of existing knowledge by means of a literature review.

During the **model development phase**, numerous theories and methods were adopted (or developed if no previous method existed) based on the synthesis of knowledge gained during the conceptual phase, the model workflow was designed through logical integration and linking of these components. The model workflow mainly supports the generation of digital twins by creating a 3D flood and 3D building model to address sub-question 3 of the research (Section 1.4). This model workflow provides insights into the data input requirements, acquisition, and preparation for operationalization of the 3D FIA on various building components. To perform 3D FIA, this novel workflow addresses the challenges with advanced input data for creating 3D flood models based on 2D hydrodynamic flood simulations. It also provides insights into the 3D building model with its semantic properties which is developed using BIM. Finally, an integrated GIS-BIM approach is designed in this research to perform 3D FIA in a 3D environment. The design of the model workflow is explained in section 5.2. The model workflow is further tested in the next phase with two separate case studies.

During the **Model Testing phase**, it is essential to validate the functionality of each step involved in the model workflow. To begin with, a prototype case study is conducted, and the results are evaluated to identify any limitations or areas that need improvement. Chapter 6 provides a comprehensive explanation of how the prototype case study was implemented. Afterwards, a second case study is designed to address the limitations identified in the prototype case study. The improved methodology used in this case study helps to overcome the identified limitations, providing solutions that can be used to improve the overall workflow. Chapter 7 provides a detailed explanation of the second case study, including the methods used.

Finally, the **Results phase** will mainly provide improved spatial 3D visualization and communication possibilities of floods and buildings that are close to reality (digital twin). Automate the identification of structural and non-structural building components that are affected by floodwater. This also allows the evaluation and calculations of flood induced loads based on Eurocodes for building stability design partially automated in 3D interfaces that are integrated into the 3D digital twin. A first attempt is also made to transfer the results of this research to other media, i.e., structural analysis. A complete overview of the results is also given in chapter 7 in detail. Finally, the discussion and conclusion section with the future recommendation concludes this research see chapter 8.

## 5.2 Design of Model Workflow

The model workflow is designed based on the background phase where a review of available literature on different principles and methods of FIA at building scale, capacities and limitations of available hydrodynamic models, and novel technological advancements in FRM are thoroughly examined. The following Figure 25 provides an overview of the steps, required software, and models that are needed to perform a complete 3D flood impact assessment on a building in a digital twin environment. This model workflow consists of six distinct working Phases i.e., input data and processing, flood simulation, 2D FIA, 3D flood model (intermediate step), GIS-BIM integration (intermediate steps), and 3D FIA.

### 5.2.1 Input Data and Pre-processing

The first phase of the model workflow is the data acquisition, pre-processing, and preparation, which are critical steps in any case study. They ensure that the data used for analysis is reliable, consistent, and of high quality, which ultimately leads to accurate and reliable results. These steps are explained in detail in the specific case study sections to ensure that the reader understands the processes involved in this research (see Section 6.3 and Section 7.3).

### 5.2.2 2D Flood Simulations

The second phase is hydrodynamic flood simulation to calculate the inundation depth, flow velocity and flow direction of the selected study area. For this purpose, a model named "FloodArea" was selected based on license availability and field applicability on different projects specifically in Germany and abroad. Notably, 'FloodArea' stood out for its seamless integration as an ArcMAP extension, streamlining the simulation process without necessitating additional software. Its output in a map-ready format further simplified the interpretation and utilization of results, making it a pragmatic and efficient tool for flood simulation purposes. To generate spatially distributed hydrodynamic flood simulation, FloodArea requires the following information as input parameters: i) Digital Terrain Model (DTM) ii) Building Footprints iii) Water Bodies/Drainage System iv) Rainfall Data v) Land use and Landcover data. The simulation results of the FloodArea model produce a spatial 2D representation of a flood, which is essential in providing spatial inundation data, flow velocity, and direction of water movement around different structures and buildings. These parameters are crucial in estimating the impact of flooding on various infrastructures in a given region. The model generates raster data output which can be used as base data to generate 3D Flood. As ESRI ArcGIS Pro provides the opportunity to do spatial analysis on both raster and feature class data not only in 2D but now in 3D as well due to its immense developments. Also, the output data generated by FLOODAREA can easily be converted and visualized in 3D with ArcGIS Pro. It also delves into the details of flood

simulation requirements for each individual case study, focusing on them in their respective sections i.e., Section 6.4 and Section 7.4.

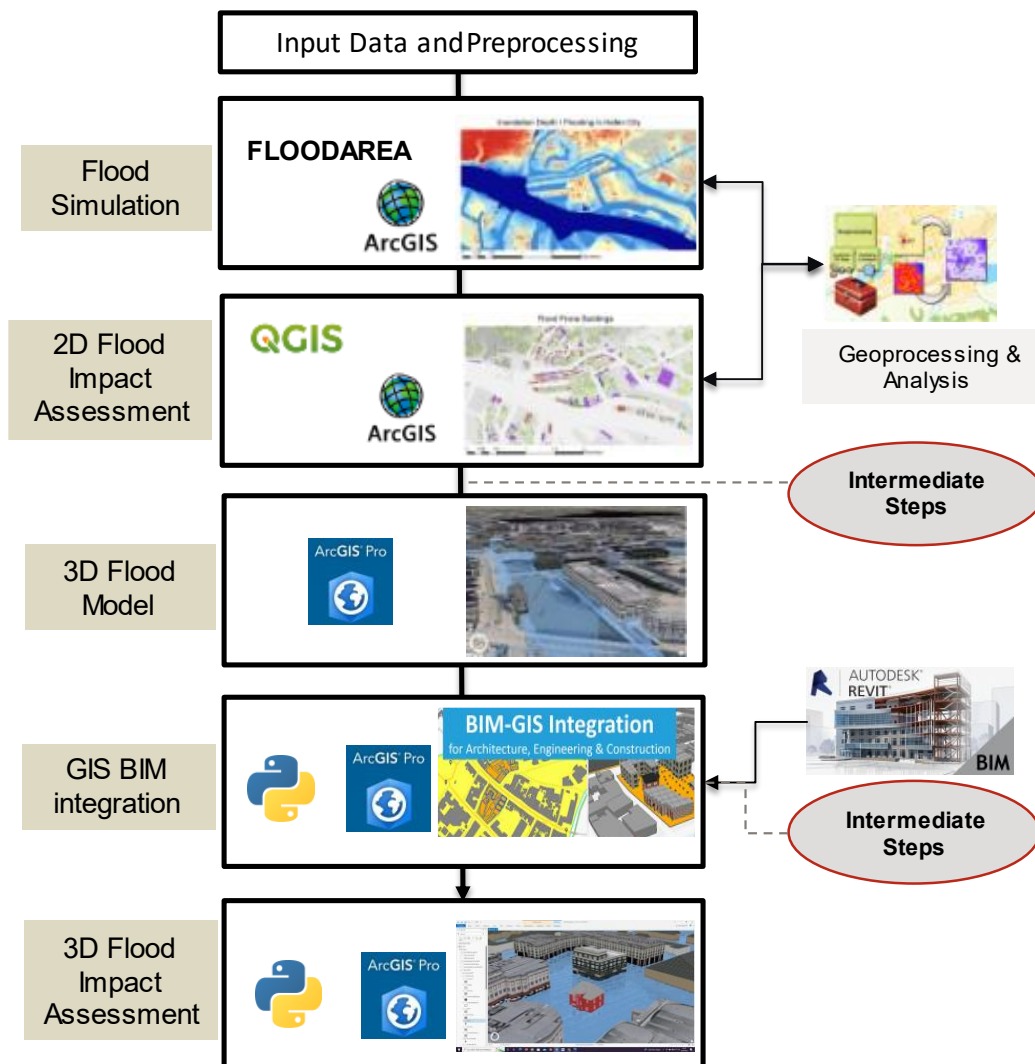


Figure 25: Model workflow for flood impact assessment in a 3D digital twin environment by integrating BIM and GIS approaches

### 5.2.3 3D Flood Model

The third phase entails the formulation of a 3D flood model through the utilization of innovative intermediate steps (see Section 6.6) to convert 2D data sets into 3D. The resulting output of the model comprises improved 3D visualization, 3D spatially dispersed inundation depths, and flow directions around distinct structures. These outputs are representable using color-coded maps, animations, and graphs. However, the application of this 3D model is limited to visualizations only, thereby impeding the potential for geospatial analysis. As a result, there has been a pursuit to investigate techniques that can enhance the capabilities of 3D flood modelling tools.

### 5.2.4 GIS-BIM Integration

To optimize the utilization and communication of information obtained from 3D flood models, it is imperative to establish a digital twin. This digital twin serves as a platform for geospatial analysis within

a 3D environment. In order to achieve this, it is necessary to integrate 3D flood models with 3D building components alongside their semantic properties, utilizing advanced technologies. Chapter 4 highlights that GIS-BIM integration offers a promising opportunity in this regard. By leveraging BIM, which provides building information and visualization, along with actual geometrical properties that are spatially georeferenced using real-world coordinates, it is possible to create a digital representation of a physical infrastructure. In brief, BIM serves as a digital representation of selected physical infrastructure, in this case, a building, which can be integrated with 3D flood models to facilitate geospatial analysis within a 3D geospatial environment.

The model workflow involves using Autodesk REVIT to create a BIM, which is a replica of a targeted building for a case study area. To generate a BIM model in Revit, comprehensive building plans or LiDAR scanned data are required. If there are no comprehensive building plans, LiDAR scanning can be used to create a BIM model, as demonstrated by Maiezza (2019) for historical buildings. LiDAR scanning provides point cloud data that contains detailed information on building features, which can be processed using Autodesk ReCAP software to create an accurate 3D building replica in REVIT (Lenac et al. 2017). The pre-processing and processing of this data are explained in detail in the case study section. Followed by 3D BIM based building model creation novel processing steps were formulated to integrate BIM data into GIS. This was done to perform geospatial analysis for risk assessment and identification of vulnerable building structural and non-structural components.

### **5.2.5 3D Flood Impact Assessment**

This phase of the model marks a significant advancement in flood risk management as it employs a novel approach that combines 3D building modelling and 3D flood modelling. By integrating the building model into a 3D GIS environment, the flood impact assessment on individual building components can be meticulously calculated. This comprehensive analysis provides detailed information on flood interaction, interacted area, and flood loads acting on each specific component, all in 3D. The benefits of this new workflow are abundant. It allows for an enhanced visualization of the flood-impacted components of buildings, which could lead to improved citizen participation during planning processes. Moreover, the data generated by this model can be used to create virtual reality (VR) or augmented reality (AR) simulations, aiding architects, and engineers in designing structures that conform to flood codes and are more resilient to disaster. Furthermore, the information obtained from this model can be exported for adaptation and structure stability analysis, cost estimation, and disaster preparedness scenarios and analysis, further strengthening the construction industry's ability to create safe and robust structures.

## **Chapter 6**

---

### **Prototype Testing: Case Study 1 – HafenCity, Hamburg**

## 6 Prototype Testing: Case Study 1 – HafenCity, Hamburg, Germany

This chapter describes the testing of the six phases of the developed model workflow. The purpose of this testing is to evaluate the effectiveness and performance of all phases of the model, including their intermediate steps. To perform this test, it is necessary to gather relevant data, which is crucial to the success of the model. Therefore, the prototype case study area is chosen based on the availability of open accessed geospatial data that met ISO<sup>1</sup> data quality standards and provided spatial richness and high resolution.

HafenCity (Hamburg) is selected as a prototype case study area due to several factors. For instance, HafenCity is a relatively new urban development area, which means that it has modern infrastructure and building designs that are constructed to withstand natural disasters such as floods. This makes it an ideal testbed for prototype testing, as it can provide insights into how newer building designs and infrastructure can respond to flood risk. Similarly, HafenCity is located in a low-lying area near the Elbe River, which is prone to flooding. This means that the area has a history of flooding and has already experienced flood events in the past, also providing a basis for the testing of flood related models.

In addition to its geographical location, HafenCity boasts a plethora of openly accessible geospatial data, which includes historical flood data, ground elevation data (e.g., Digital Terrain Model and LiDAR), and asset features (e.g., roads, bridges, and buildings) that meet the data quality standards specified in the ISO guidelines. As a result, the data is exceptionally reliable, accurate, and complete, making it an excellent resource for scientific applications and analyses. Consequently, HafenCity has been the focus of several previous research studies across various domains hence, it offers rich and reliable data (Krüger 2009; Serre et al. 2018). Overall, the combination of modern infrastructure, flood history, and availability of high-quality spatial data makes HafenCity a suitable case study area for prototype testing of model workflow.

### 6.1 HafenCity, Hamburg

HafenCity is a large-scale urban regeneration project located in the Hamburg-Mitte borough of Hamburg, Germany, on the Grasbrook island in the Elbe River. This area was formerly occupied by the Port of Hamburg and has undergone significant redevelopment since its formal establishment in 2008. The project includes the historic Speicherstadt district, which was recognized as a UNESCO World Heritage Site in 2015, along with the Kontorhausviertel. The main landmark of HafenCity is the Elbphilharmonie concert hall. The primary goal of the project is to Revitalize the "Grosser Grasbrook" area with new commercial, residential, and entertainment spaces. HafenCity is currently the largest urban regeneration project in Europe by landmass, covering an area of approximately 2.2 square kilometers (220 hectares) shown in Figure 26. The reduction in the economic significance of free ports in the era of European Union free trade and increased border security led to the reduction in the size of the Hamburg free port, which provided an opportunity for the development of HafenCity. The ground-breaking ceremony for HafenCity was held on 20 June 2001, and the first quarter of the

---

<sup>1</sup> ISO (International organization for standardization) provides guidance and recommendation for the selection of good quality data for research i.e., its completeness, logical consistency, spatial accuracy, thematic accuracy, temporal quality, and data usability. (ISO 8000-1:2022)

development, "Am Dalmannkai/Sandtorkai," was completed in 2009. The project continues to evolve, with the ongoing construction of new hotels, shops, office buildings, and residential areas.

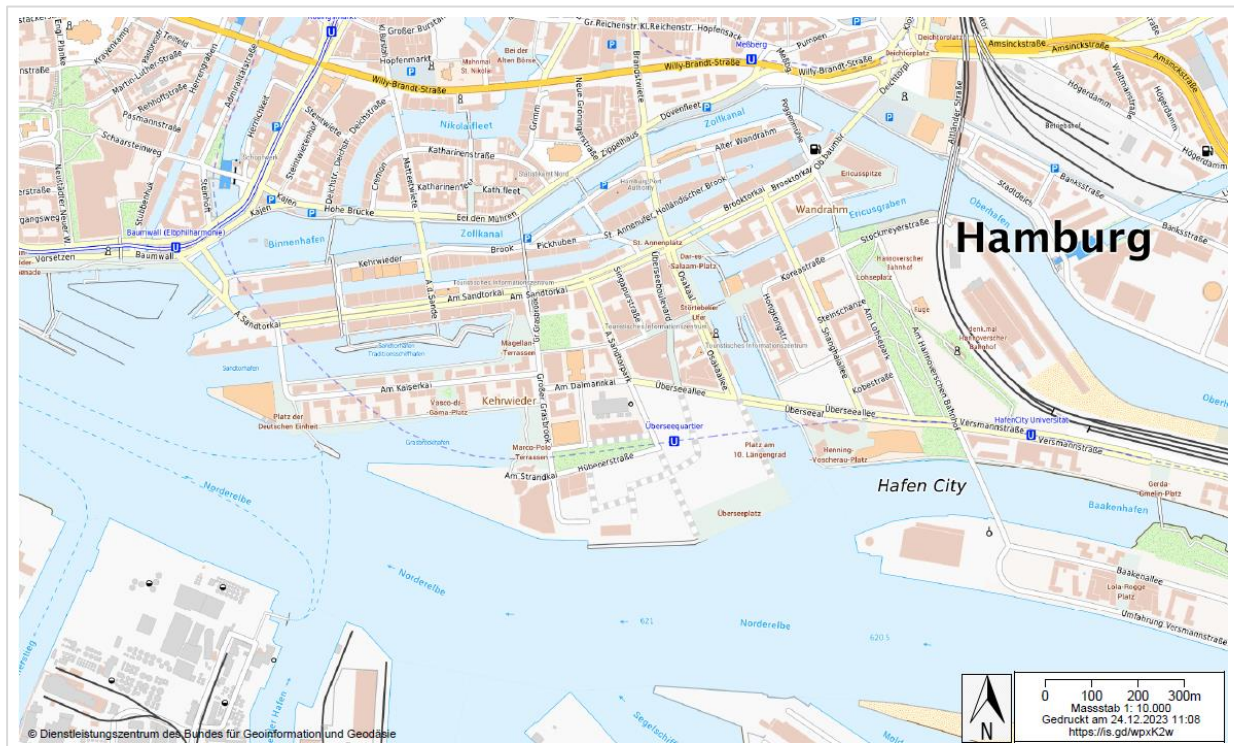


Figure 26: Selected case study area of Hafencity, Hamburg, Germany (Source: BKG)

## 6.2 Testing of Model Workflow

Model workflow is comprised of six interconnected phases that operate in a sequential manner, with each phase relying on the previous one. The phases consist of input data and pre-processing, hydrodynamic flood simulation, 2D flood impact assessment, 3D flood model, GIS-BIM integration, and 3D FIA. Each phase has its specific working steps, designed to achieve particular objectives. The testing of these phases and their intermediate steps was carried out through this prototype case study and explained in subsequent sections.

## 6.3 Data Collection and Pre-processing

This is the first and preliminary phase of the model workflow. This phase involves collecting and preparing data related to the case study area. This data can subsequently serve as input for the next phases. This includes collecting data on topography (digital terrain model), land use land cover, infrastructure (building footprints), and hydrological characteristics (water bodies) of the study area (Table 4). A detailed explanation of the collected data and the steps involved in its processing is given in subsequent subsections.



Table 4: Collected data types and sources for the case study area

Data	Type	Source
Digital Terrain Model	Raster (LiDAR)	BKG - Bundesamt für Kartographie und Geodäsie
Building Footprints	Polygon	Geodatenzentrum
Water Bodies	Raster	Extracted from DLM 1:250
Digital Landscape Model	DLM 1:250	Geoportal.de
Hydrograph	Text	BSH Hamburg - Bundesamt für Seeschifffahrt und Hydrographie
Roughness Coefficient	Report	DIN 3141
Water Inundation Depth	Raster	Self-generated by FloodArea
3D Buildings	Multi-patch	Self-generated by ArcGIS pro

### 6.3.1 Digital Terrain Model (DTM)

DTM is a high-resolution, digital representation of a terrain surface, which is created using data from various sources and processed using advanced algorithms. It is a valuable tool for analysing and modelling terrain characteristics and is widely used in many fields. In the prototype case study, the 2017 DTM of HafenCity was utilized, which was obtained in the form of LiDAR data from BKG in a raster format (see Figure 27). The DTM was provided in 1 km x 1 km tiles, with a resolution of 1 m x 1 m per pixel. To merge these tiles, the "merge raster" geoprocessing tool from ArcGIS was employed, followed by the assignment of a projection system using the "reproject tool" in ArcGIS. The ETRS 32632 projection system was selected for all raster datasets. The conversion of the projection system is a critical step and should be performed prior to subsequent analysis.

### 6.3.2 Building Footprints

Building footprints refer to the outline or boundary of a building's base or foundation, which provides valuable information regarding the exact location of a building (Meinel et al. 2009). In order to examine the impacts of flooding on buildings, it is important to consider the spatial distribution of building footprints. In this study, building footprints for the entire country of Germany were obtained in polygon format from Geodatenzentrum, and were subsequently filtered for the specific study area. The building footprint data was collected in 2015, and in instances where certain building footprints were missing, they were manually digitized by overlaying them on Bing maps. To accurately depict the flood inundation surrounding buildings, as opposed to the inundation directly on the building, as a subsequent step, a constant height of 5m was assigned to every building footprint in the study area to raise the buildings from their ground elevation. This was carried out to prevent the inundation depth from affecting the buildings. It was necessary to merge the building footprints with the Digital Terrain Model (DTM) prior to flood simulation. To achieve this, the building footprint (Figure 28) polygon file for the case study area was first converted into a raster using the geoprocessing tool "polygon to raster". The resulting file was then projected and merged with the DTM, effectively incorporating the influence of buildings into the DTM see Figure 29.



Figure 27: Digital terrain model (meters) of HafenCity with 1 meter resolution (Source: BKG)

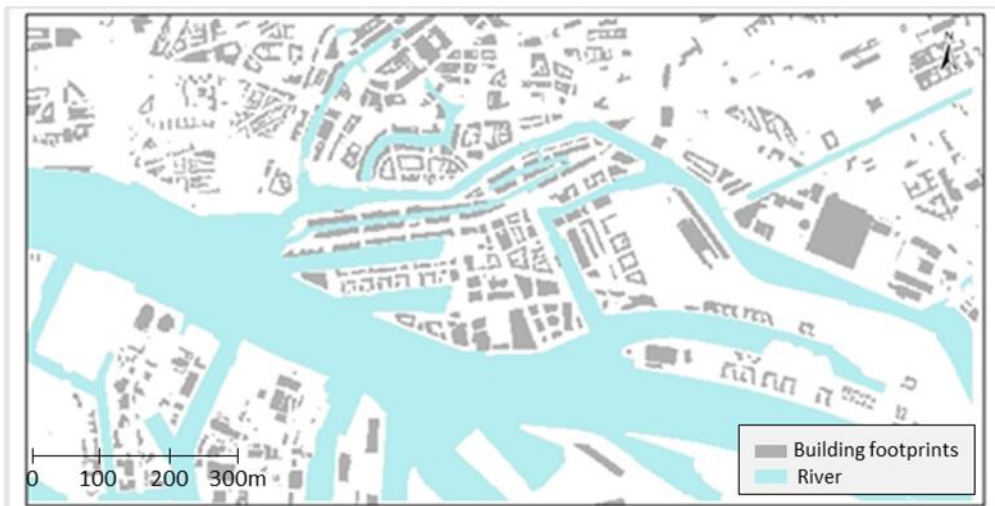


Figure 28: Building footprints and the water body of HafenCity (Source: Geodatenzentrum)

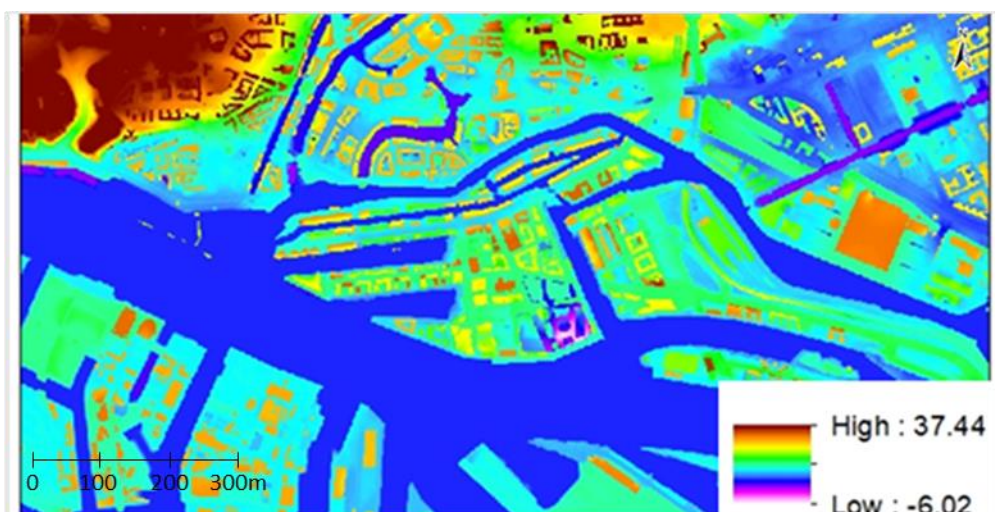


Figure 29: Merged DTM in meters with building footprints of HafenCity

### 6.3.3 Land Use and Land Cover Data

Land use and land cover (LULC) data refers to geospatial information that describes the types of land cover and their respective land use activities. This data typically includes categories such as paved grey infrastructure, bare soil, green areas, protected areas, and water bodies. In this study, LULC data was obtained in polygon format from Geodatenzentrum for the entire country of Germany. The HafenCity area was subsequently extracted from this feature class using the "select by location" geoprocessing tool within ArcGIS. Additionally, the LULC data for the study area was converted from polygon to raster format, and its projection was assigned. When combined with roughness coefficient values (obtained from DIN 3141) land use data can be used to estimate actual surface runoff. Therefore, roughness coefficient values were assigned manually to each individual land use category in the study area and are listed in the appendix. This raster file was later used as a surface roughness raster for numerical simulation with the surface roughness coefficients see Figure 30.

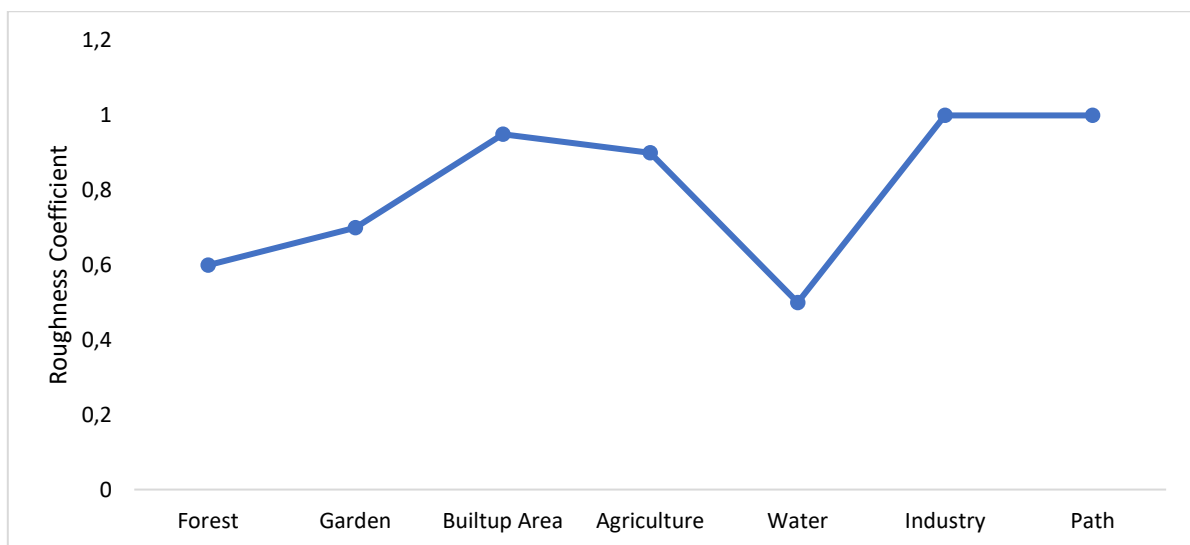


Figure 30: Roughness coefficients of each specific land use of HafenCity

Hydrological characteristics pertain to the physical attributes and dynamics of aqueous formations, including both natural and man-made bodies of water situated on the Earth's surface. The identification of water bodies within the proximity of the designated study area is achieved through the extraction of relevant data from the DLM obtained from Geodatenzentrum. The data collection process aimed to obtain information regarding the dimensions of water bodies in close proximity or immediate vicinity of the study area. Furthermore, the collected data underwent a rasterization process for further analysis.

### 6.3.4 Water Level Hydrograph

A water level hydrograph is a graphical representation of the variation in water level in a particular body of water over time. It shows the changes in water level with respect to time and is typically used to monitor water levels in rivers, lakes, and other bodies of water. The hydrograph typically displays the water level as a function of time, with the horizontal axis representing time and the vertical axis representing the water level. The graph may also include additional information such as rainfall data, flow rates, and other relevant data. For this research water level hydrograph was prepared shown in Figure 31 based on water level hydrograph obtained from BHS Hamburg (Federal Maritime and

Hydrographic Agency) for variable time intervals to feed the change in water level for hydrodynamic flood simulation software.

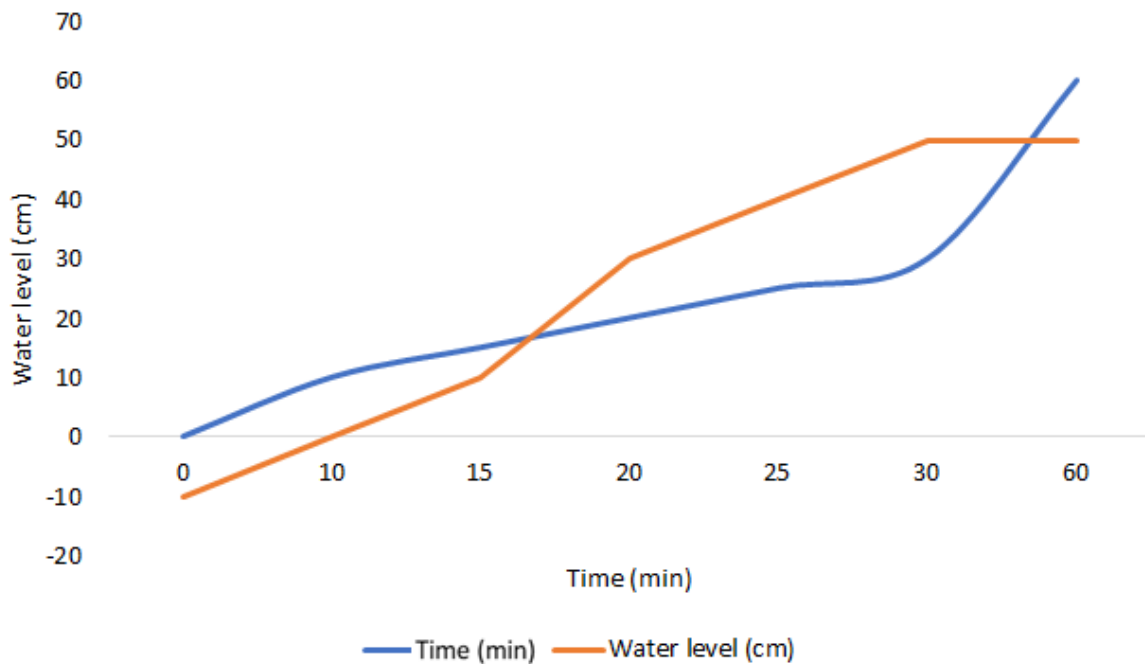


Figure 31: Water level hydrograph of HafenCity

#### 6.4 Hydrodynamic Flood Simulation

The second phase of the model workflow involves conducting a hydrodynamic flood simulation of the study area to obtain important information such as inundation depth, flow direction, and flow velocity. The hydrodynamic model known as "FloodArea" is utilized, as explained in the previous section, to compute runoff, flow concentration, flow velocity, backwater scenarios, and inundation depth for varying time intervals. The FloodArea hydrodynamic model is generally divided into two separate hydrodynamic simulation systems, namely riverine and rainfall. For the selected case study area, HafenCity, which is located on the Elbe River, the riverine flooding system was employed to execute the hydrodynamic flood simulation of the prototype area. The collected data, which was prepared and processed in the previous section, is utilized as input for this model, as shown in Table 4.

Subsequent to the preparation of essential input data for hydrodynamic flood simulation in FloodArea, the modelling process was initiated. This requires the installation of a licensed FloodArea extension that is compatible with ArcMap or ArcGIS Pro. In this work, ESRI ArcMap was utilized for flood hydrodynamic Simulation. The FloodArea toolbar and toolbox must be loaded in Arc Toolbox prior to launching the "Start FloodArea" tool with a graphical user interface (GUI). The tool necessitates input data that has been previously prepared from Section 6.3. The prototype model is configured for three distinct scenarios that correspond to relevant time intervals, specifically the 10-, 20-, and 30-minute periods. It is imperative to make a careful selection of the output switch since FloodArea offers four distinct flood simulation options, namely i) absolute water level, no flow direction/velocity, ii) absolute water level, with flow direction/velocity, iii) inundation depth, no flow direction/velocity, and iv) inundation depth, with flow direction/velocity. In this prototype case study, the output switch number



four (inundation depth, with flow direction/ velocity) was selected, as Additionally, the maximum exchange rate per mile was set to 5.

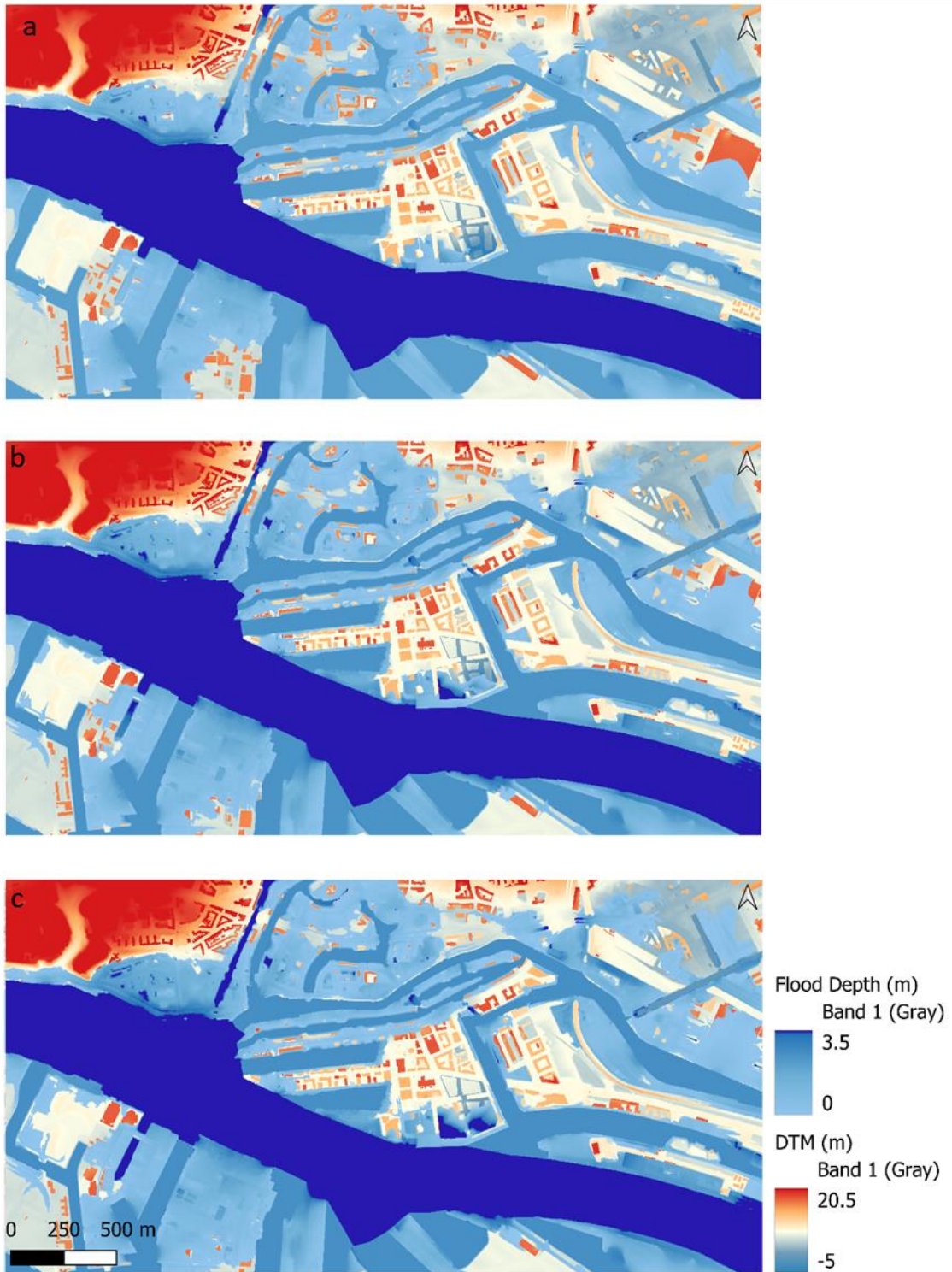


Figure 32: Spatial distribution of flood inundation depth after (a) 10 min (b) 20 min (c) 30 min simulation duration

This value determines the maximum amount of the current cell content that can be transferred to neighbouring cells during one iteration step (in promille). This value indirectly affects the simulation speed by reducing the duration of the iteration interval to meet this requirement. Large values of this

parameter may cause ripples in the model depending on environmental conditions. Such instabilities do not result in the termination of the simulation run but may interrupt it in extreme cases since high-water levels in individual cells can falsify the results. According to experience, values between 1 and 5 provide the most reliable results.

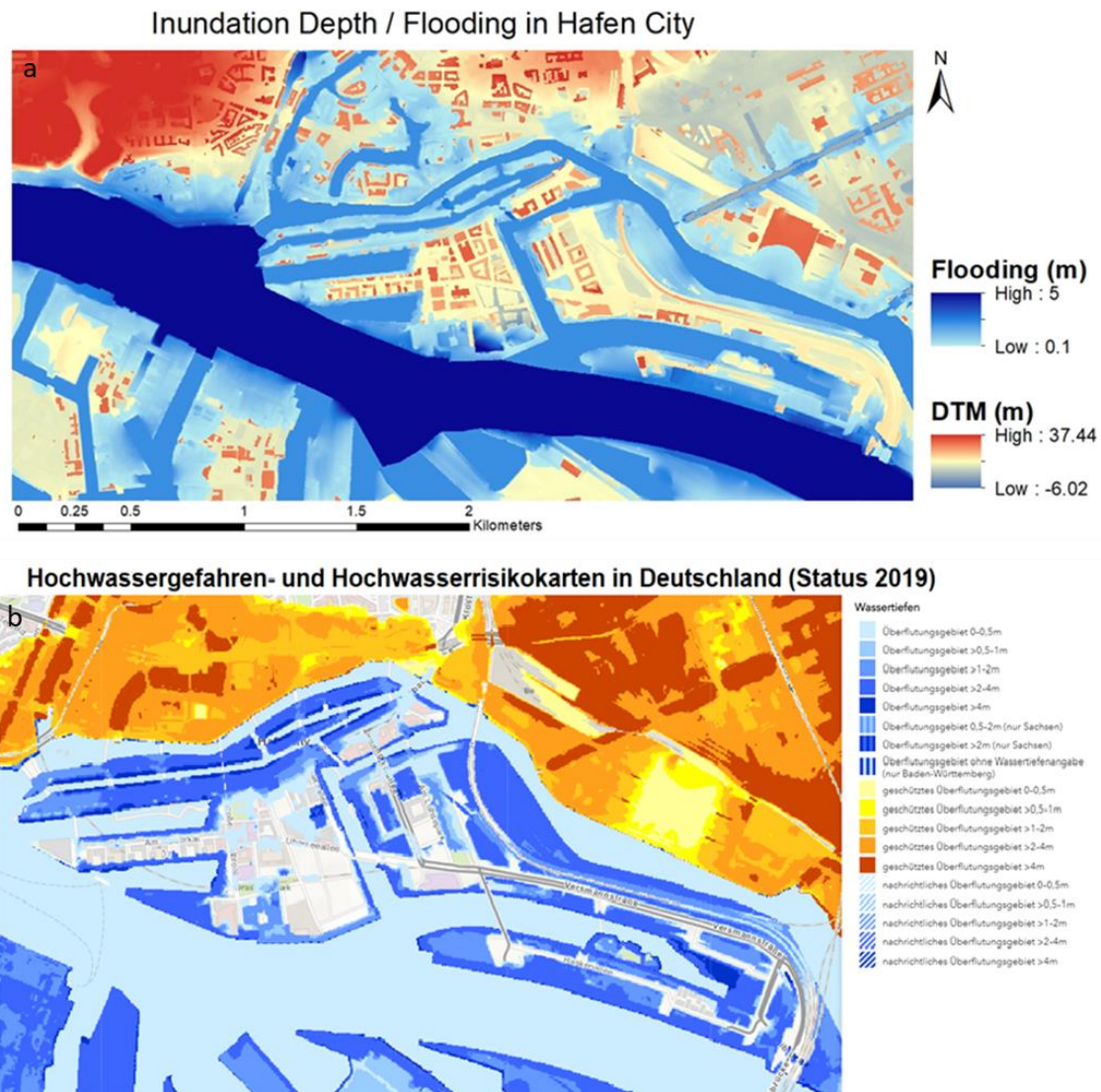


Figure 33: Comparison of (a) simulated flood inundation depth with the (b) available flooding map of 100 year flood (Source: Geoportal der Bundesanstalt für Gewässerkunde)

In the FloodArea tool, the minimum allowable input value is 1, corresponding to 0.1%. Larger exchange quantities up to a maximum of 100 (10%) are only useful if a quicker simulation time is desired, such as for a preview. However, in such cases, it is advisable to use a coarser grid. The tool is configured to have a maximum duration of 1800 seconds for the set scenarios, with a save interval of 600. Additionally, the roughness raster, digital terrain model, and drainage system raster are provided as input data and have been prepared with the same extent and coordinates to ensure the tool's environment is consistent. These parameters can be found in Table 4 and in the GUI shown in the appendix. Once all the necessary parameters have been set and the input data has been verified. The model is now ready to be executed for simulation. The duration of the simulation depends on various



factors, such as the input raster grid size, the maximum exchange rate per mille, the system specifications, and the number of cores used by the FloodArea tool (in this case, a minimum of 1 core was utilized).

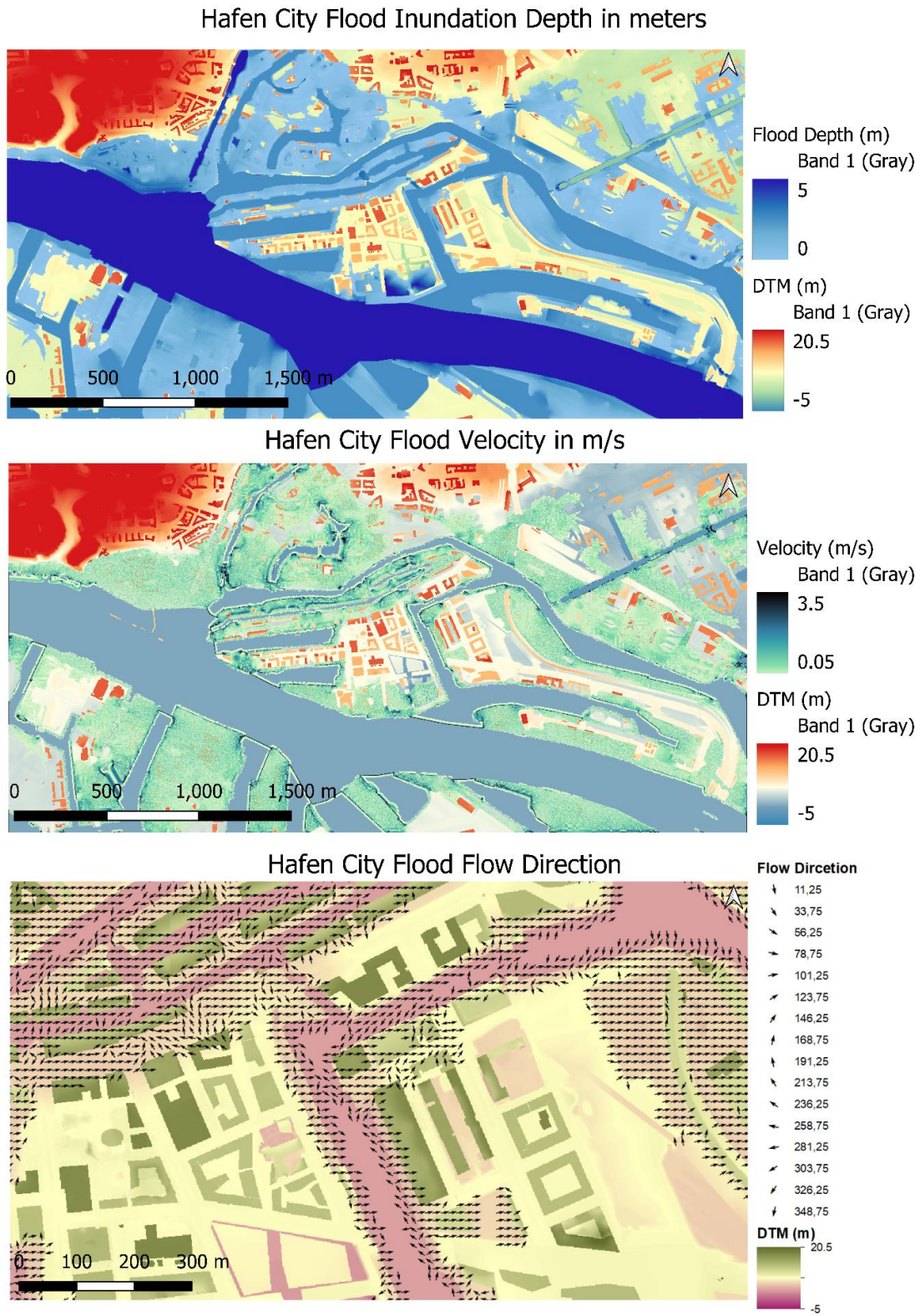


Figure 34: Spatial distribution of inundation depth, velocity and water flow direction

The simulation was run on a PC i7 with 64GB RAM and lasted for a duration of 5 hours. The successful completion of the simulation can be observed in the appendix, which displays all the data in XML format.

The simulation generates maps, which depict the spatiotemporal distribution of inundation depth for three equally distributed time intervals. An overview of the generated inundation maps is presented in Figure 32. It should be noted that the FloodArea model provides inundation, velocity, and direction maps in raster format. The output rasters from the hydrodynamic flood simulation were analysed in GIS for each time interval to facilitate proper interpretation and visualization. The results indicate that the simulated flood is in good agreement with the available flood maps for Hafen City. A comparison between the simulated and available maps (100 year floods) is presented in Figure 33. Furthermore, water velocities and direction were examined to verify the accuracy of the simulation, as illustrated in Figure 34.

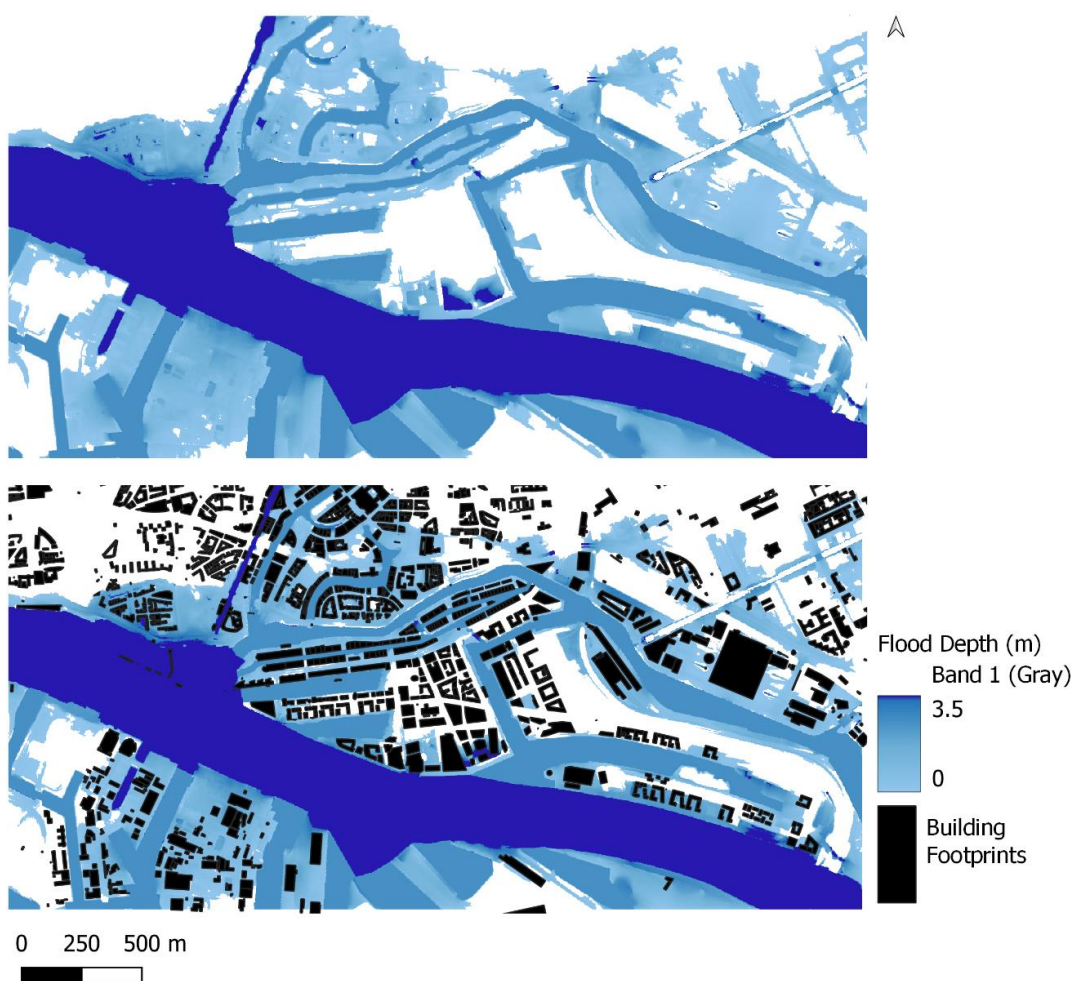


Figure 35: HafenCity flood inundation depth with and without building footprints

Furthermore, to investigate the influence of buildings on flood parameters, a simulation was conducted using a different geometry that did not include buildings, as illustrated in Figure 35. The results of the comparison revealed notable differences in the spatial distribution of water depth and velocity at the building location. This could potentially have a negative impact on the accuracy of FIA. As a result, only the outputs obtained from the simulation that considered buildings were utilized in this case study.



## 6.5 2D Flood Impact Assessment for Building Exposure

The third phase of the model workflow involves analysing the exposure of buildings to flooding. This analysis identified flood-prone buildings that are impacted by flood events. A simplified workflow with interdependent tasks was formulated and illustrated in Figure 36. The analysis of flood impacts requires two primary data sets, namely: (i) a feature class data of flood depth (inundation), and (ii) a feature class data of building footprints.

As described earlier, the inundation depth is in raster format, and thus, it needs to be converted into a polygon format. The same applies to the building footprint data. The conversion of both data sets was performed using the geoprocessing tool 'raster to polygon'. Following the conversion of the inundation depth and building footprints into a feature class (polygon format/shapefile), the next step involved merging the data into a single dataset. This was achieved using the spatial join tool from the Arc toolbox, which involved selecting the analysis tool, then overlay, and finally spatial join.

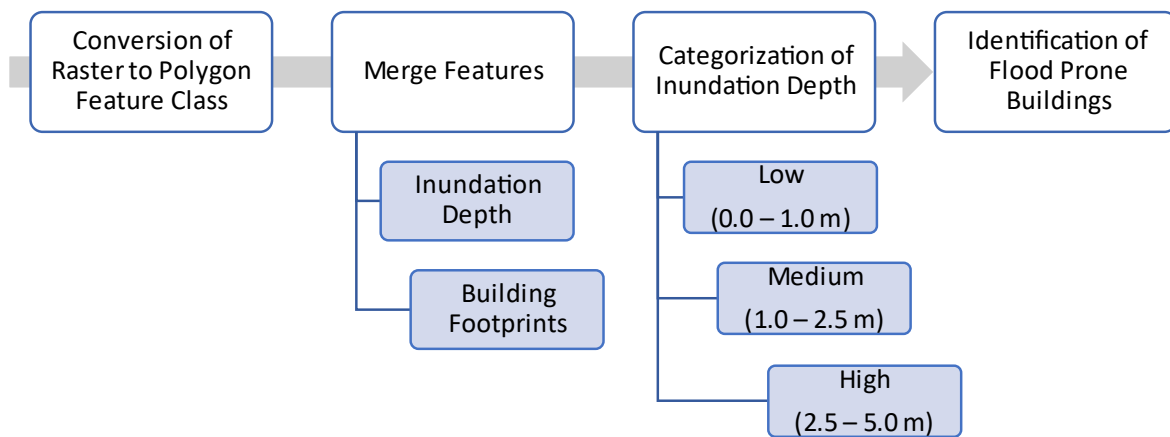


Figure 36: Processing steps for 2D flood impact assessment

Upon merging the two data sets, a classification-based approach was employed to define different flood depths. Specifically, the flood depths were categorized into three classes, namely: low, medium, and high intensity/depth. A flood depth of 0.0 – 1.0 meter was classified as 'low intensity', 1.0 -2.5 meters as 'medium intensity', and 2.5 – 5.0 meters as 'high intensity'. Using this classification, a spatially distributed map of the study area was generated by utilizing GIS. This map provides information on the spatial distribution of flood-prone buildings, considering different flood impact intensities (low, medium, and high), as shown in Figure 37.

The map presented in Figure 37 indicates that buildings in close proximity to the main water body are more severely impacted by floods compared to those located further away from the main water network. In general, a majority of the buildings are directly affected by flood depths of at least 1 meter or greater. The objective of this research is to conduct a flood impact analysis at a micro scale, specifically on individual buildings, including both structural and non-structural components. To accomplish this, a specific building was selected to serve as a prototype for upcoming phases. Although the selection criteria were random and simple, important factors were thoroughly considered. Firstly, the building had to have a variety of building components (e.g., walls, beams, columns, doors, windows, ventilation, stairs, facade) and characteristics (e.g., age, construction, material, and

occupancy type). Secondly, it had to be located in an area with a high flood hazard level and near a main water body. Lastly, data availability was also ensured, including the possibility of conducting a building survey and obtaining building construction plans if available. As a result, a commercial mix use building (commercial and semi-residential) located directly on the main riverbank was chosen. The building is surrounded by almost 3 meters of flood level, as depicted in Figure 37. Similarly, Figure 38 shows the location map and facade of the selected building.

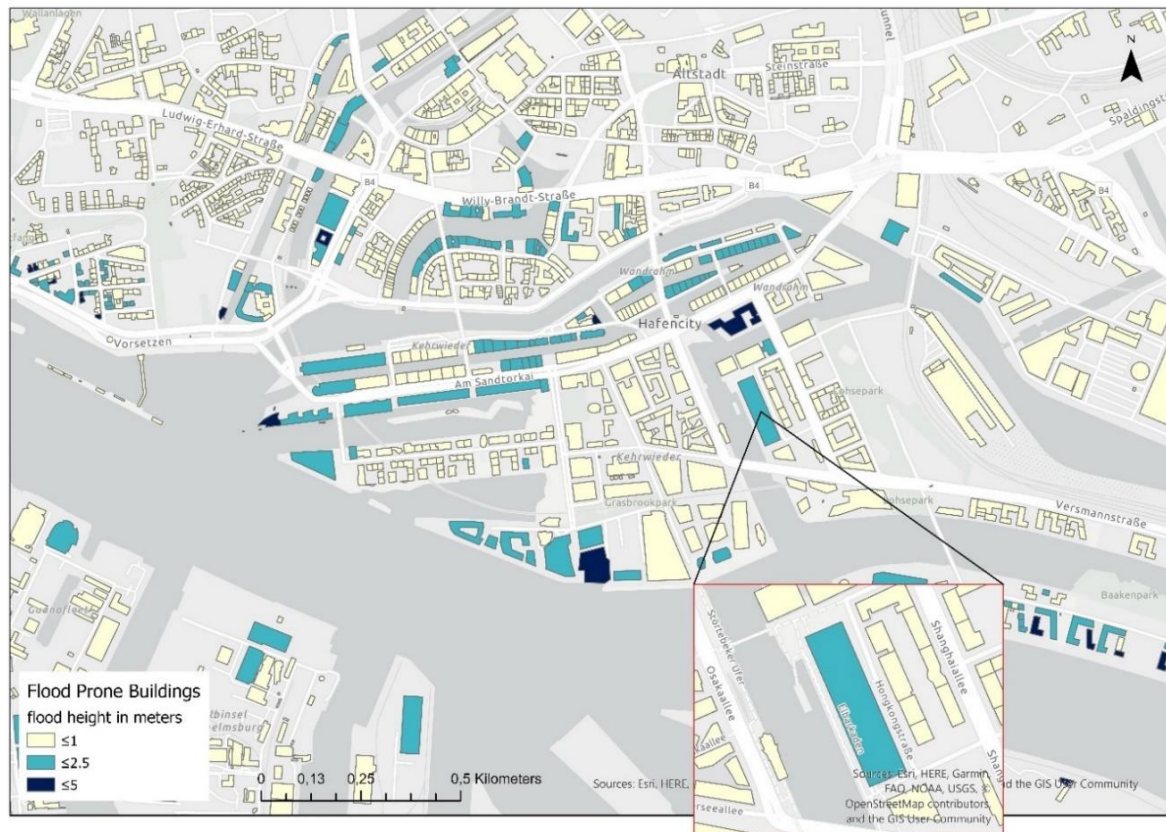


Figure 37: Flood prone buildings under different flood impacts in HafenCity and targeted building



Figure 38: Location of selected building and its facade image (Source: Google Images)

## 6.6 3D Flood Model

The fourth phase of the model entails generating a three-dimensional (3D) flood model for the prototype study area. This process involves using advanced modelling techniques to incorporate the 2D datasets into a 3D format, enabling more comprehensive and accurate visualization of the flood dynamics. To create a 3D flood model for enhanced visualization, a 3D city modelling technique is employed as the foundation (Biljecki et al. 2015). The terrain model, 2D flood inundation data, feature elevation, and building footprints are required for this step. They serve as the prerequisites for creating a 3D flood model. A framework consisting of three steps (preparation, processing, and modelling) has been developed to improve the understanding of the complex steps involved in the preparation of a 3D flood model see Figure 39.

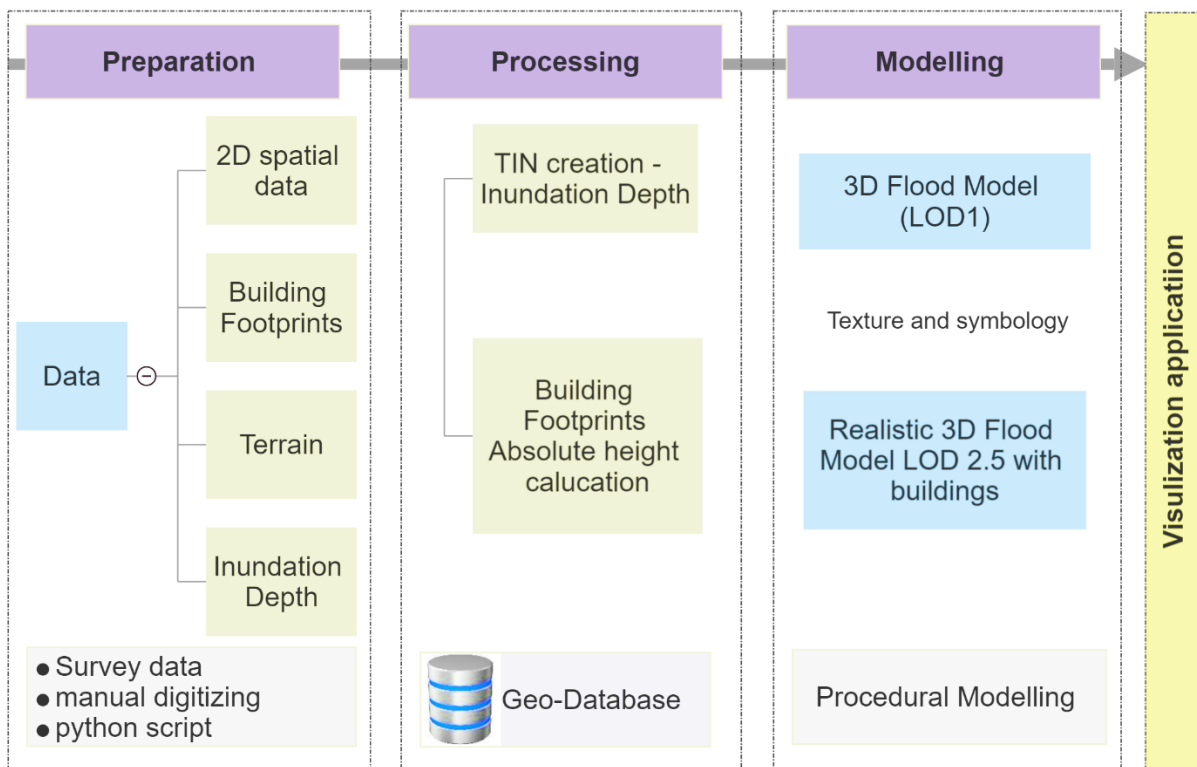


Figure 39: Framework to develop 3D flood model based on 2D datasets adopted from (Khayyal et al. 2022)

Initially, the required data is gathered and prepared followed by data processing where each dataset undergoes its individual pre-processing. These processing steps are compulsory for the data to be incorporated into the 3D interface of ArcGIS Pro as the 2D data format is not compatible with ArcGIS 3D interface to be visualized directly in 3D format. Using an innovative 3D modelling technique with intermediate steps, the data is then transformed into captivating 3D visualizations. A comprehensive explanation of intermediate steps for the 3D flood model, along with the specific dataset used, is described below.

### 6.6.1 Conversion of 2D Simulated Flood Inundation to 3D Flood

This step entails the transformation of 2D simulated flood scenarios into a 3D format. Although height data is available in numeric form in 2D flood maps, it lacks elevation properties. As such, the pre-

existing height values in 2D format need to be converted to a 3D format to incorporate elevation information.

There are several techniques available to convert two-dimensional data with a third numeric property into three-dimensional polygons. One such method is known as extrusion, where the numeric value is used to determine the height of the third dimension. This method creates a series of flat polygons that are then extruded vertically to create a 3D representation of the data. Another method is known as TIN (Triangulated Irregular Network) interpolation, where the data is triangulated into a set of non-overlapping triangles that can be used to create a surface. The height of each triangle is determined by the numeric value associated with the data. Additionally, Delaunay triangulation is another method that can be used to convert 2D data with a third property into a 3D representation.

In order to convert simulated flood scenarios from a 2D representation to a 3D representation, a technique for generating TIN is utilized. This approach was chosen based on its widespread application in transforming 2D DTMs into 3D representations, as well as its adaptability to multiple visualization methods, including colour gradients and topographic shading, for the purpose of depicting surface characteristics. Furthermore, TIN can also be utilized in combination with other 3D modelling techniques to produce intricate 3D models and visualizations.

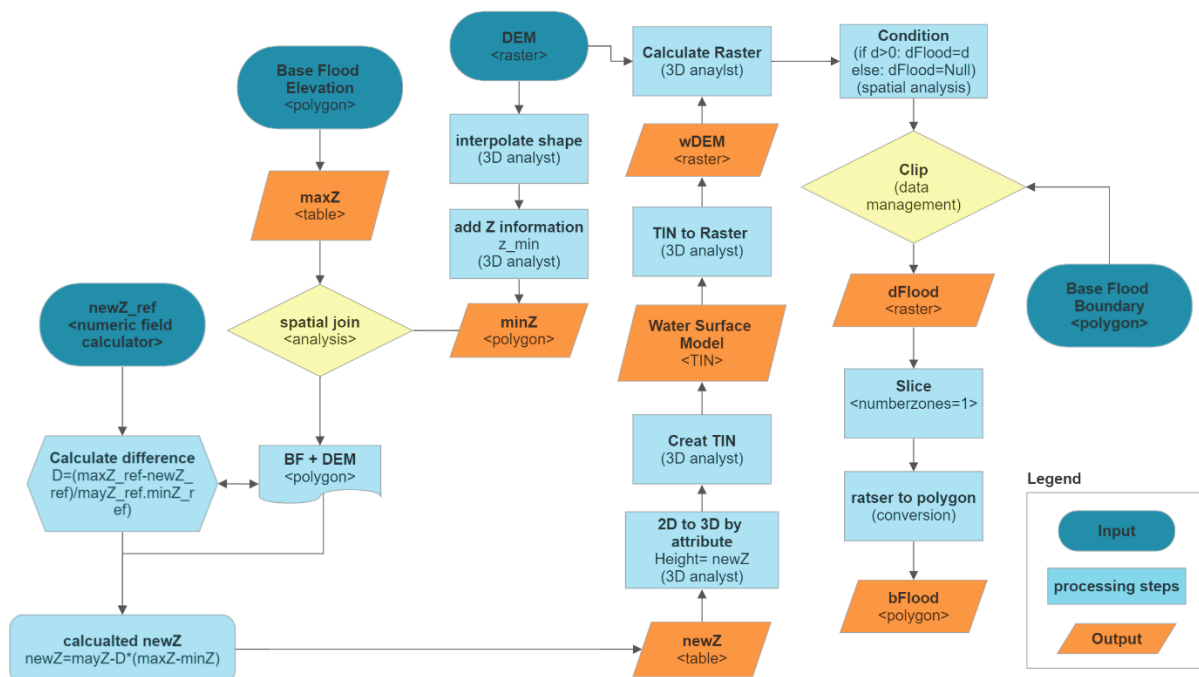


Figure 40: Steps involved in the conversion of 2D simulated flood inundation depth into 3D flooding adopted from (Javadnejad et al. 2017)

Figure 40 is showing the process adopted for visualization of the depth of flooding in a 3D context (Javadnejad et al. 2017). This process entailed dividing inundation depth data into a series of non-overlapping triangles, with the height of each triangle determined by the corresponding flood inundation depth value at the corresponding location within the flood simulation. The resulting TIN surface represents the continuous surface of flood inundation depth in 3D space Figure 41. This method enables the visualization of complex flood depths and their spatial patterns, allowing for a better understanding of the extent and severity of the flooding. To save computation time, the process



was performed using python console in ArcGIS Pro. This was done so that, the process can be automated and performed more efficiently than manually completing each step in the graphical user interface. This allowed for faster processing times and greater control over the TIN creation process, including the ability to adjust parameters and algorithms as needed. Additional details regarding the precise coding methodology employed for this procedure can be located in the appendix.

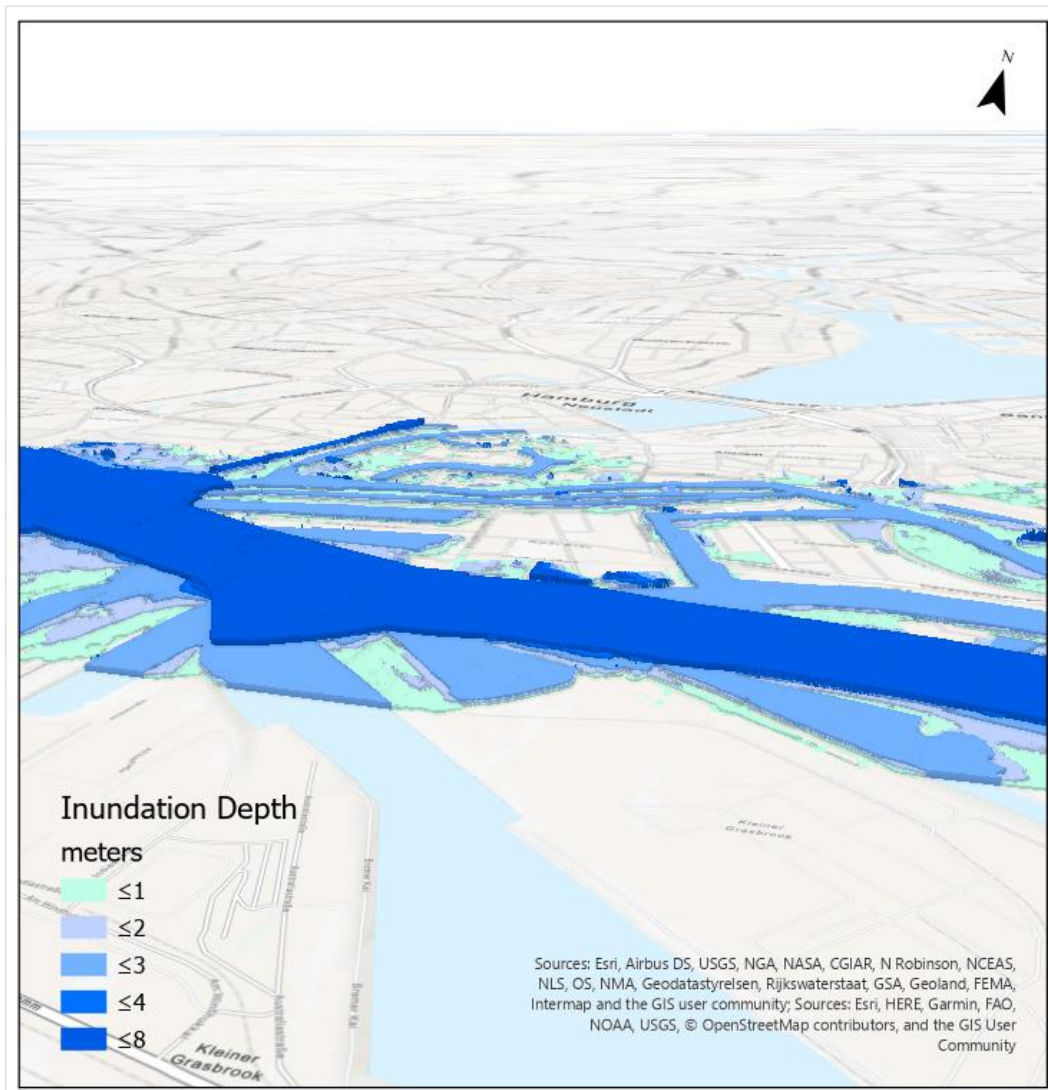


Figure 41: Triangular irregular networks of flood inundation in 3D space

It should be noted that creating a TIN from a 2D dataset requires careful consideration of the data inputs, algorithms used, and quality parameters to ensure accurate and meaningful results.

### 6.6.2 Conversion of 2D Building Footprints to 3D Building Blocks

Converting 2D building footprints to 3D building blocks in ArcGIS Pro is a complex process that requires a series of steps to create a realistic 3D representation of the buildings. This process typically begins with importing 2D building footprints as polygon features into the ArcGIS Pro software. To create 3D building blocks, these polygon features need to be extruded, which can be achieved in two ways i) Procedural modelling ii) Manual modelling.

### 6.6.2.1 Procedural Modelling

Procedural modelling is a technique used in ArcGIS Pro to automate the creation of 3D buildings based on pre-defined rules and parameters. This technique allows for the efficient and consistent creation of 3D models of buildings with varying levels of complexity, ranging from simple structures to highly detailed urban environments. Procedural modelling is based on the principles of computer graphics and involves the use of algorithms to generate 3D models of buildings.

There are several methods for procedural modelling in ArcGIS Pro, including the "Rule Package Editor", "CityEngine Integration", and "Python Scripting". The "Rule Package Editor" is a graphical interface that allows users to create rules and parameters for 3D modelling. The "CityEngine Integration" method involves the use of the CityEngine software to create procedural rules for the generation of 3D models in ArcGIS Pro. The "Python Scripting" method involves the use of Python programming language to write custom scripts for the creation of 3D models (Khayyal et al. 2022).

According to a study by Smelik et al. (2010), procedural modelling in ArcGIS Pro can significantly reduce the time and effort required for the 3D modelling of buildings compared to traditional manual methods. The study found that the use of procedural modelling tools in ArcGIS Pro can increase the efficiency of 3D modelling tasks by up to 70%. Similarly, a study by Jayaraj and Ramiya (2018) demonstrated that procedural modelling in ArcGIS Pro can be used to generate complex 3D models of urban environments with high levels of detail.

### 6.6.2.2 Manual Modelling

Manual modelling for 3D buildings in ArcGIS Pro involves the creation of 3D building blocks by incorporating height information of the building footprints. This method requires more effort and time compared to procedural modelling but provides more accurate and realistic 3D models.

This method involves a series of steps. The first step is to gather height information for the buildings from LiDAR data or other sources. The next step is to create a new 3D building feature class in ArcGIS Pro and add the building footprints as polygon features. The building footprints are then extruded to the height values obtained in the previous step using the "Extrude Between" tool in ArcGIS Pro. In order to compute the height of buildings, equations are utilized that incorporate the ground height, floor height, and number of floors. The height of a building is determined by the number of floors it possesses. The elevation is determined using Equation 12.

$$Bld\_Height = GFl\_Height + Fl\_Height \times N + 1.0 \quad \text{Equation 12}$$

Where, Bld\_Height represents the height of the building, GFl\_Height represents the height of the building's ground floor, Fl\_Height represents the height of the building's floors, and N represents the number of floors. Following this, a geodatabase is generated, and the calculated value of 'Bld\_Height' is assigned to the elevation attribute.

Once the basic 3D models are created, the models can be refined by adding more details such as roof shapes, windows, doors, and textures using the "Edit Vertices" tool and other editing tools in ArcGIS Pro. This method of manual modelling allows for more control over the final 3D model and can result in a more realistic representation of the buildings in the city.

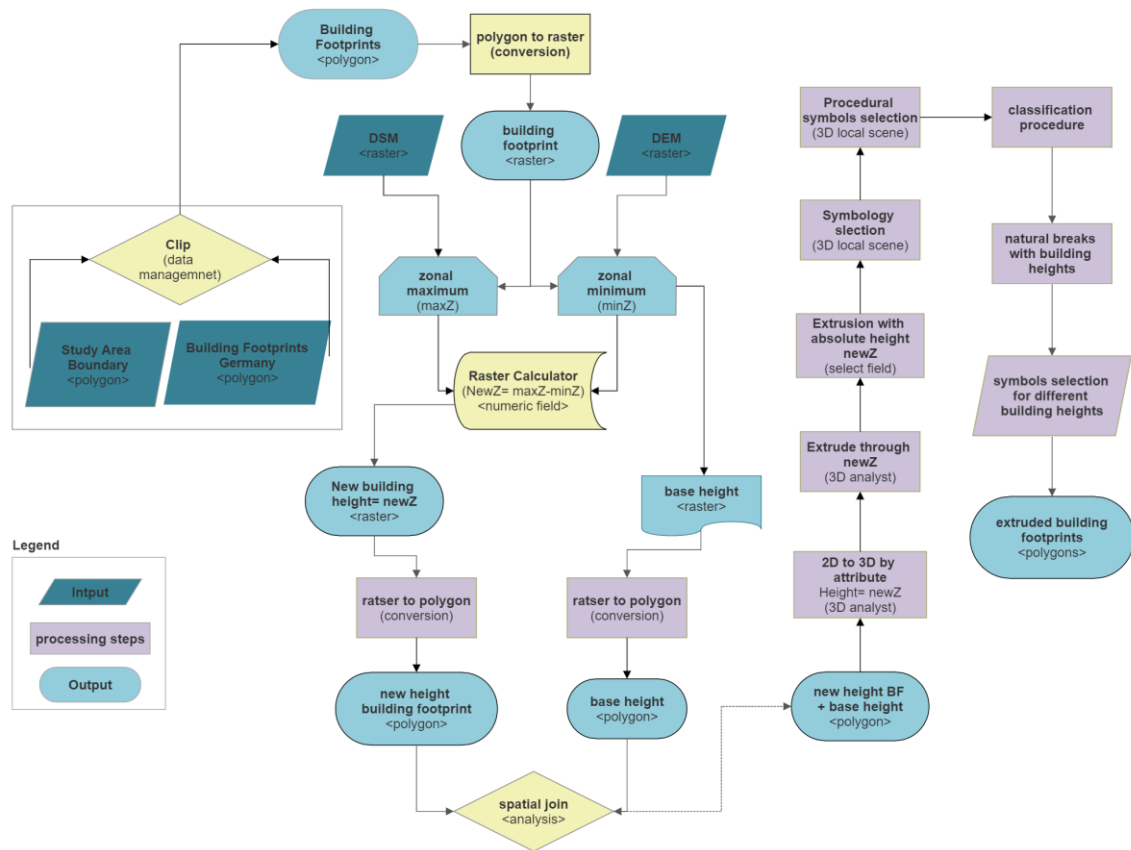


Figure 42: Steps for conversion of 2D building footprints to 3D building blocks with procedural modelling

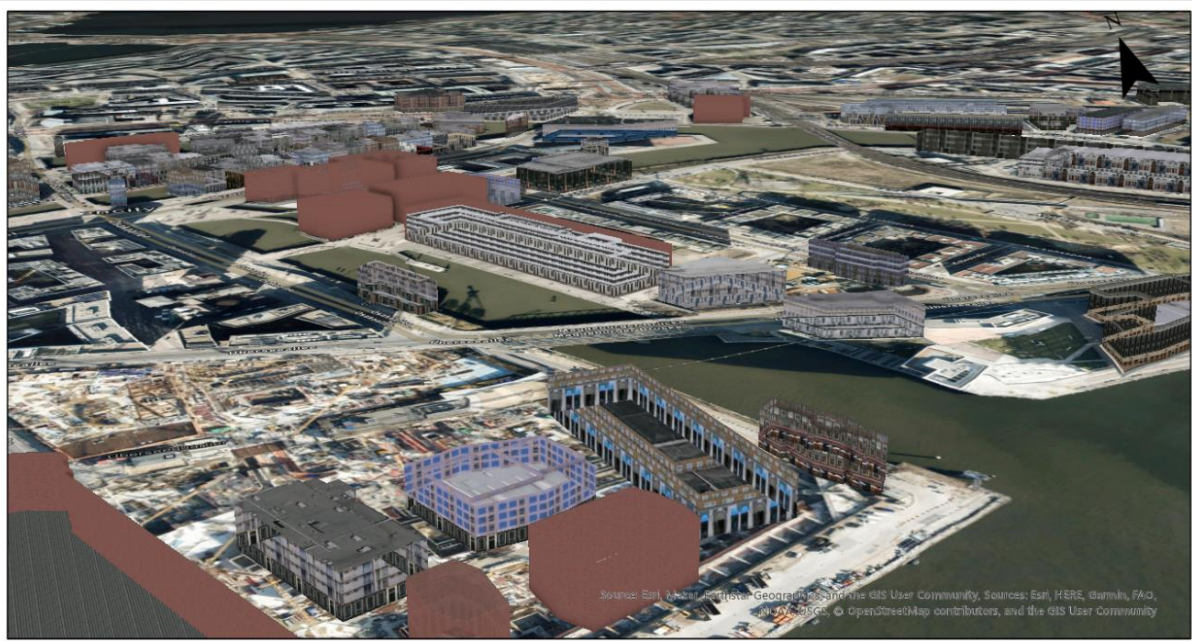


Figure 43: Visualization of 2D to 3D converted building blocks of HafenCity

There are several studies that have used manual modelling for 3D building creation in ArcGIS Pro. For example, a study by Jayaraj and Ramiya (2018) manually modelled 3D buildings from building footprints and LIDAR data in ArcGIS Pro for the purpose of urban heat island analysis. Similarly, Khayyal et al. (2022) manually modelled 3D buildings in ArcGIS Pro to create a realistic 3D city model for flood

analysis. After comprehensively understanding and evaluating the pros and cons of both methods for 3D building creation. The "Procedural Modelling" for this research is used. Its development process is shown in Figure 42 which is performed with python scripting to generate the 3D building models as shown in Figure 43. Python scripting with detailed information related to shapes, floor height, height expressions, roof shape expressions and colour parameters can be found in the appendix.

### 6.6.3 3D Visualization and Application

After the necessary data processing and conversions see Figure 39, the next step is creating a 3D flood model to visualize the flooding information in 3D alongside other topographic features such as buildings and terrain. For the purpose of creating a 3D flood model, ArcGIS Pro offers the ability to integrate and visualize various types of data, including terrain, buildings, and flood information, in a single 3D scene. This enables the user to gain a comprehensive understanding of the potential impact of the flood on the surrounding environment.

The user can overlay the flood information on top of the terrain and building layers to visualize the areas in 3D that are most vulnerable to flooding. ArcGIS Pro also provides a range of tools and features for customizing the display of the data, such as setting the extrusion properties for the building layer to give them height and adjusting the lighting and shadow properties to give the scene a more realistic look. These tools allow the user to create a highly customized and realistic 3D scene that accurately represents the potential impact of the flood on the surrounding environment in 3D. Furthermore, as previously explained ArcGIS Pro offers a range of analytical tools for analysing the impact of the flood on the environment, such as calculating the extent of the flood and the areas that are most affected by it. This helps the user to better understand the potential impact of the flood on the surrounding environment and plan for appropriate mitigation measures. Overall, creating a 3D scene in ArcGIS Pro involves adding 3D data layers to the scene, adjusting the display properties of each layer, and using tools and features to customize the appearance and analyse the data. With ArcGIS Pro, users can create immersive and informative 3D scenes that provide valuable insights into spatial relationships and patterns.

To create a 3D scene, particularly a 3D flood model, there are various ways to integrate the processed data into ArcGIS Pro. One way is to use the "Add Data" button in the "Layers" tab. This allows to select the processed data files from the user file system and add them to the scene. Another way is to use Python scripting, which provides more flexibility in how the data is added and processed. Python scripting can be used to add feature classes, rasters, TINs, point clouds, and other data types to the scene programmatically. Additionally, 3D files can also be imported into ArcGIS Pro to create a 3D scene. This includes 3D models created in other software, such as SketchUp or AutoCAD, which can be imported as a layer in the scene. Overall, the different ways to integrate processed data into ArcGIS Pro provide users with flexibility and choice in creating 3D scenes for various applications, including 3D flood models.

Therefore, for automating the process of adding data (processed in section 6.3) to the 3D scene python scripting was used, in order to save time and minimise the risk of errors or inconsistencies. As a result of the automation process, the complete 3D flood model of the prototype case study area was visualized, and the output can be seen in Figure 44. The use of this kind of 3D visualization technique in flood modelling and risk assessment is a significant advancement in this field. As can be seen from



Figure 44, the 3D model provides a more realistic and comprehensive understanding of the flooding impact on infrastructure such as buildings and roads. These models can provide information on the intensity and vertical velocity of flooding, which is essential for estimating the damage to infrastructure components. Moreover, 3D models allow users to see the rising velocity and transition of water levels at specific locations, providing a more intuitive representation of the flood impact. The developed 3D flood model visualization can be used by both experts and laypeople and can be scaled to different levels, allowing for a more comprehensive assessment of the impact of floods on individual towns, cities, and buildings. Overall, the use of 3D illustrated flood and building infrastructure visualizations can help in decision-making and risk management strategies. This 3D flood model visualization is a valuable tool for comprehending the complex nature of flood scenarios in built environments, as it enables stakeholders to examine and interpret flooding impacts from various perspectives.

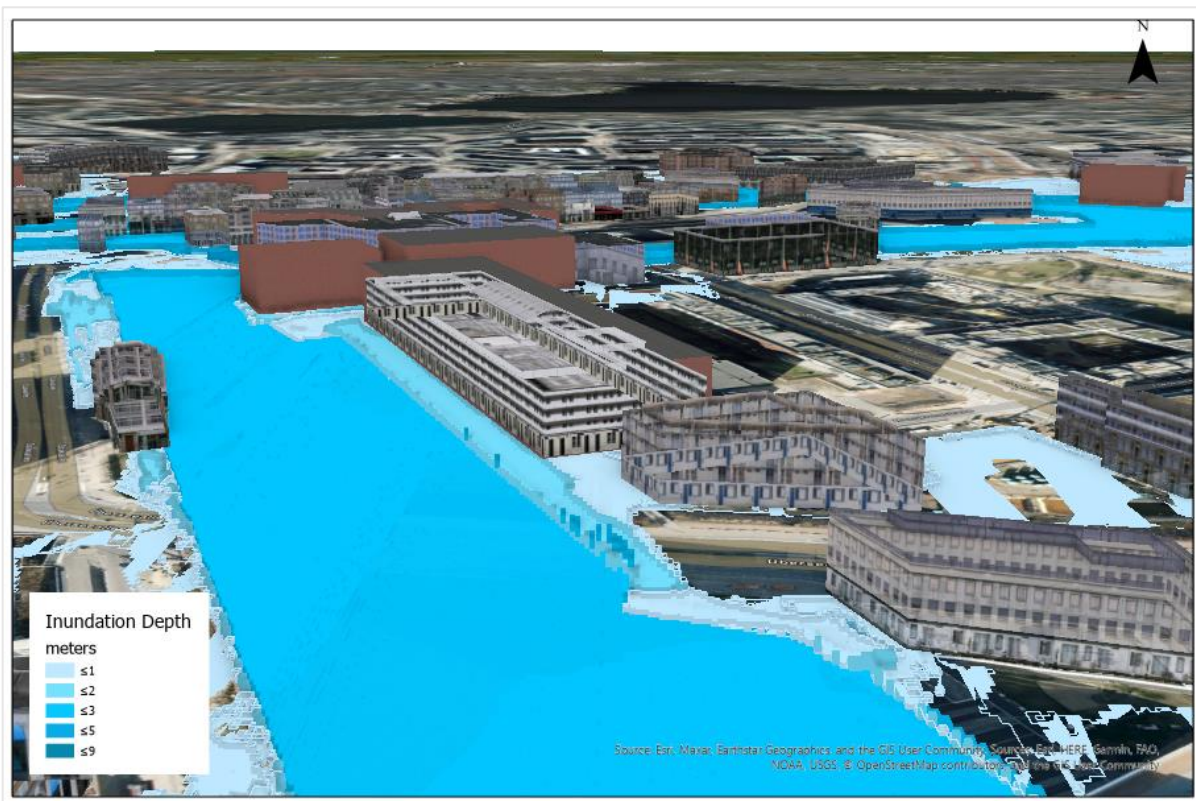


Figure 44: Visualization of buildings, terrain and flooding in 3D (3D flood model)

#### 6.6.4 Limitation of 3D Flood Model

After a thorough assessment and analysis of the developed 3D flood model, it was concluded that this kind of 3D visualization is a static type. This means this type of visualization can be utilized to observe flooding in three dimensions, by zooming in or out at specific points or by rotating the visualization 360 degrees to gain an all-encompassing view of the flooding situation around buildings. However, this type of visualization is incapable of generating the flood impact on individual building levels at the micro scale. To further elaborate, the 3D flood model visualization is limited in its ability to be used for geoprocessing analysis, as the 3D representations of floods and buildings are only 3D surface polygon blocks. While these are suitable for visualization purposes, they cannot be efficiently used with 3D analyst tools for further geoprocessing. For such tools to work effectively, the 3D polygons must be in a closed shape, which requires them to be in a volumetric (also known as Multipatch format) that acts

as a 3D volumetric element geometry. Volumetric elements are 3D representations of objects that have length, width, and height dimensions (Zhi et al. 2020).

The 3D flood model's building block representations are limited to LOD-2, meaning that they cannot adequately convey information about specific individual building components within the model. This results in a minimal amount of building detail being provided, and as previously noted, the geometry of the buildings and the 3D flood model is not closed, nor are they represented as volumetric components. These limitations underscore the need to improve the 3D flood model and its visualization to enable a more comprehensive analysis of flood impacts on infrastructure components.

## 6.7 GIS -BIM Integration

As a sixth phase, the integration of GIS and BIM represents a fundamental stage in the developed model. This stage serves as the core of the model as it facilitates crucial data integration and modifications through intermediary processes to establish the foundation for 3D flood impact assessment. Within ArcGIS Pro, it is possible to create 3D shapes and blocks in a volumetric format, which could allow for geoprocessing in 3D using the 3D analyst tool. However, this approach also has its own limitations. For instance, many building components, such as foundations, columns, beams, slabs, connections, and other structural aspects, are not modelled or represented by generic objects like "building installations" without the details of each specialized component and completely lacking IFC semantic properties (Nagel 2014; Noardo et al. 2020). Moreover, many of the building components are modelled using surfaces instead of actual objects, without IFC semantic properties. As an example, Figure 45 illustrates that the wall object in the ArcGIS pro standard is not explicitly defined and is instead represented by "wall surface" and "interior wall surface" objects, which is also the case for many other building elements like floors, ceilings, and roofs (Nagel 2014; Amirebrahimi et al. 2016).

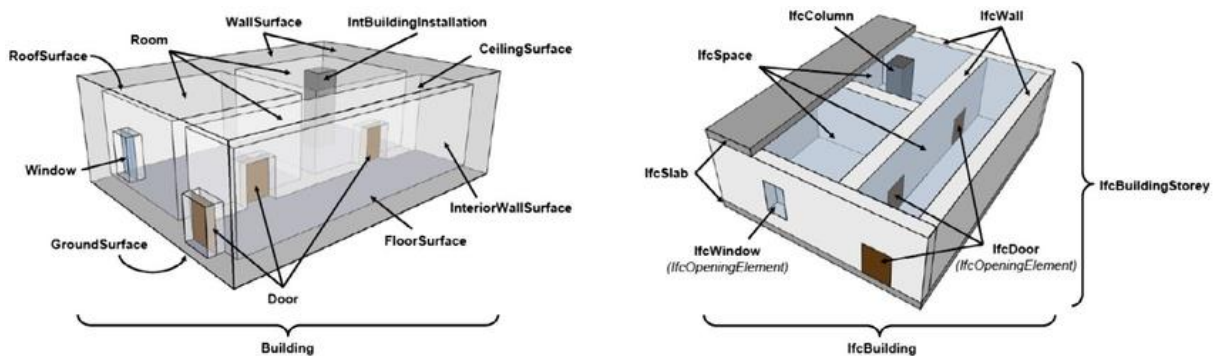


Figure 45: Comparison of representation of the building components in (left) CityGML and (right) IFC adopted from (Nagel 2014)

These limitations can result in confusion in the use of the full geometry of any of these elements and difficulty in the assignment of material properties. Therefore, it is important to continue to refine the modelling approaches to accurately represent building components and their relationships in the context of flood impact assessment. The limitations of ArcGIS Pro in creating detailed 3D volumetric models of buildings have led to the exploration of new technologies and methods to develop interactive flood impact assessments. This requires a detailed level of BIM in the form of LOD 3 or LOD 4, which is not currently possible within ArcGIS Pro. In the GIS environment, it is possible to visualize and query data from different LODs using various cartographic data from spatial data infrastructures

(SDIs) and regional and national portals. This includes LODs 0-1, LOD 2, or LOD 2.5, which can be integrated into ArcGIS Pro. However, to create detailed volumetric models, BIM is necessary. According to Amirebrahimi et al. (2016), the high level of detail of the model has a significant impact on the usefulness of the model for analyses and simulations. Similarly, Nagel (2014) believes, BIM models provide a comprehensive representation of the building and its components that can be used to evaluate flood risk and assess the impact of flooding on buildings. These studies also highlighted that integrating BIM models into the GIS environment requires the usage of object-oriented BIM software, which is capable of creating volumetric element models. BIM software enables the creation of detailed models of building components, such as foundations, columns, beams, and slabs, with specific attributes and material properties. These models can then be integrated into the GIS environment to evaluate flood risk and assess the impact of flooding on individual buildings and their components. An overview of the GIS-BIM integration process as a whole can be seen in Figure 46.

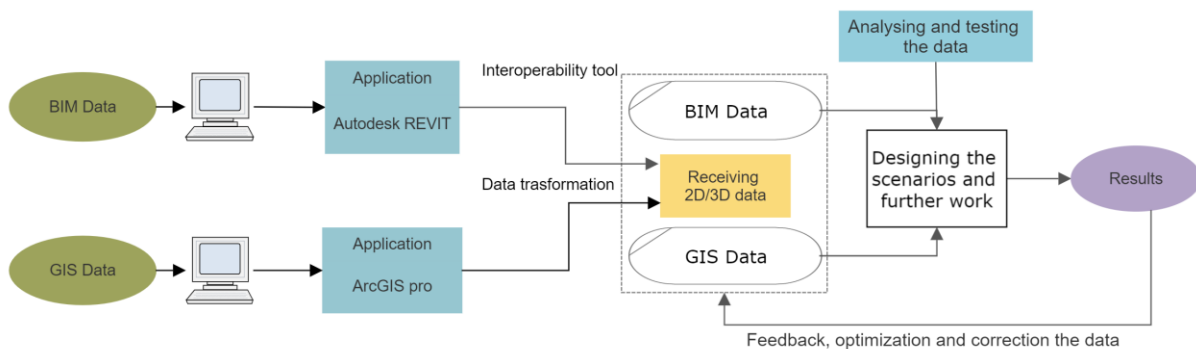


Figure 46: Overview of the GIS BIM integration process adopted from (Schaller et al. 2017)

In the following section, modifications are made to the existing 3D flood model to address its limitations. The visualization of the 3D flood model relied on a surface-based approach, which constrained the ability to generate volumetric models for both flood depth and building structures.

### 6.7.1 Adjustments to the 3D Flood Model

To enable 3D geoprocessing for flood impact analysis, certain adjustments must be made, such as creating detailed volumetric element models of buildings and converting generated TIN-based flood depth into closed volumetric elements (multipatch). To achieve this, a semantic LOD 4 building information model (BIM) in 3D must be generated, along with conversion of simulated inundation depth into closed volumetric elements. To develop a semantic building information model in 3D, Autodesk Revit is utilized due to its interoperability with ArcGIS Pro, while the conversion of the simulated flood into a volumetric element is performed in the ArcGIS Pro environment.

#### 6.7.1.1 1<sup>st</sup> Adjustment: BIM Generation of Targeted Building – A Digital Twin

To generate a detailed 3D building model, a BIM (Section 3.1.2) approach is adopted, which involves creating a replica of the selected building using actual coordinates and semantic information such as material properties and dimensions. Before starting the modelling process, certain prerequisites must be fulfilled, including the area of the structure, elevation, number of floors, height of floors, information about various structural components, openings for doors and windows, terrain information, and more. This information can be obtained in three ways: through building architectural

plans, manual surveying, or laser scanning (LiDAR) techniques. Obtaining this information is crucial in ensuring the accuracy and completeness of the 3D building model, which can then be integrated into a GIS environment for further analysis and visualization.

Due to the unavailability of an architectural plan for the selected prototype building and limited surveying resources, the observation method was employed to gather the necessary data to develop a BIM model. The observation method involves physically inspecting a building's exterior and interior to obtain information about its dimensions, openings, and other structural components. However, due to the pandemic (COVID-19) situation, detailed surveying of the building was not possible, and only a partial visual inspection of the first floor's interior was conducted using the naked eye. The information gathered from this survey was limited and not particularly useful for developing an accurate BIM model of the prototype building. Therefore, the BIM model developed may not be an exact replica of the desired edifice, and it may contain some inaccuracies. However, CADMAPPER, a freely available online application, was employed to acquire accurate information regarding the dimensions, area, height, coordinates, and topography surrounding the selected building. CADMAPPER can be used to obtain accurate building and topography information for BIM modelling when architectural plans or detailed surveying data is not available.

This tool allows users to obtain precise information about building dimensions and surrounding topography. It utilizes open-source data from sources such as OpenStreetMap, NASA, and the US Geological Survey (USGS) to generate 3D CAD files. This tool can be particularly useful in situations where there is limited access to architectural plans or surveying resources.

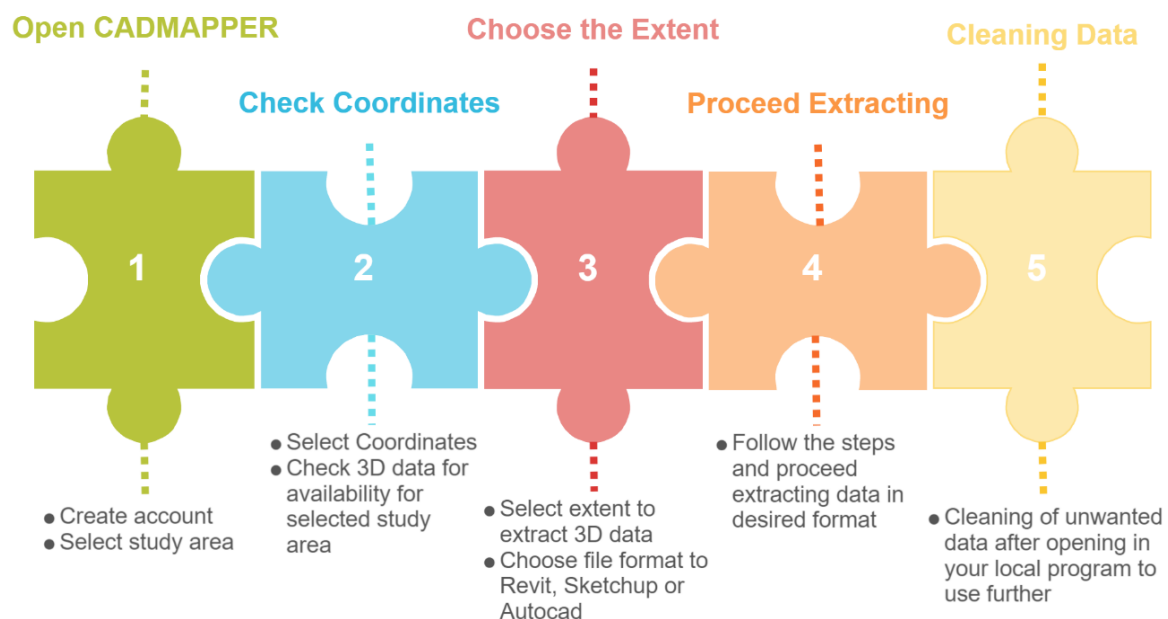


Figure 47: Processing steps for extraction of required data from the CADMAPPER tool

Basu and Bhattacharjee (2022) used CADMAPPER to extract building information for BIM modelling in an urban area in India. They found that the tool was able to provide accurate building dimensions and location information, which were useful for developing BIM models in the absence of detailed architectural plans. Similarly, Chen et al. (2021) utilized CADMAPPER to extract building information for BIM modelling in an urban area in China. They found that the tool was able to provide accurate building dimensions and location information, which was useful for developing BIM models in the



absence of detailed surveying data. With CADMAPPER, necessary data can be retrieved in a variety of forms, including CAD, DWG, and SKP. Figure 47 is showing the novel process developed for extraction the of required data with this tool. This tool provides three different kinds of data that are 2D, 3D and topography information. Figure 48 represents the 3D and topography data downloaded from CADMAPPER. This data was extracted for this study in the SketchUp format SKP.

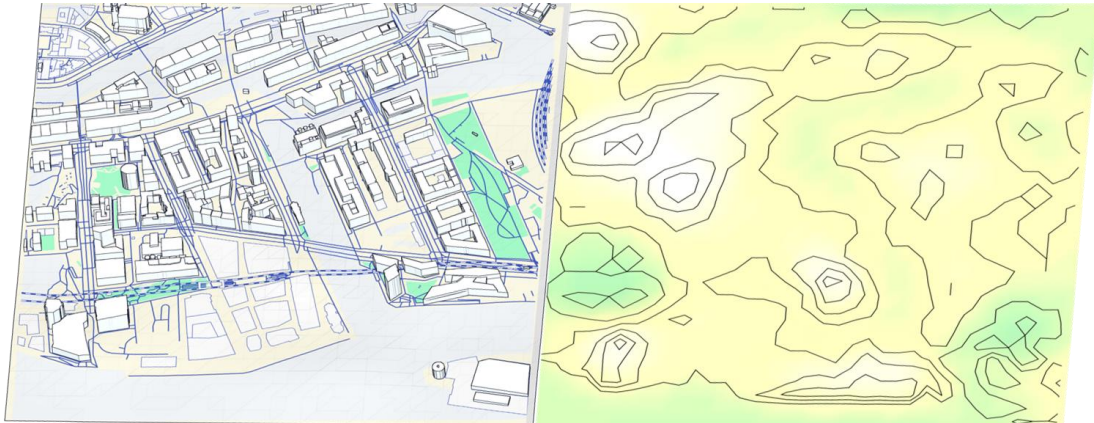


Figure 48: Extracted topography of the selected area with CADMAPPER (left-3D) and (right-2D)

In Figure 49, the intended prototype building is depicted in red. Before utilizing the data in SketchUp, it was necessary to clean and eliminate any extraneous data. Following this, the data was exported to Autodesk Revit to create a detailed 3D model with BIM attributes. To replicate the selected building's precise dimensions, data was imported into Autodesk Revit using the built-in tool for reading Sketchup (.skp) files. Setting the actual coordinates of the structure is crucial when beginning to model a structure in Autodesk Revit. Since the prototype building exists in the real world, its coordinates were obtained with the aid of CADMAPPER. These precise coordinates play a crucial role later on when importing data into ArcGIS Pro, ensuring that it is placed accurately in the intended location.



Figure 49: Targeted building data extraction with CADMAPPER

In order to create a realistic 3D model of a building, accurate information regarding the thickness of walls, window and door sizes, and floor heights must be available. This information can be obtained

through various methods, such as using the building's architectural plan or laser scanning (LiDAR). However, in the case of the prototype building in this study, only some of these values were assumed due to limited resources. The remaining dimensions, such as height, length, and width, were obtained from CADMAPPER, which was used to extract accurate data. With this information, a detailed virtual 3D model of the building was created in Revit. Figure 50 shows the key steps required to generate a 3D building model in Autodesk Revit.

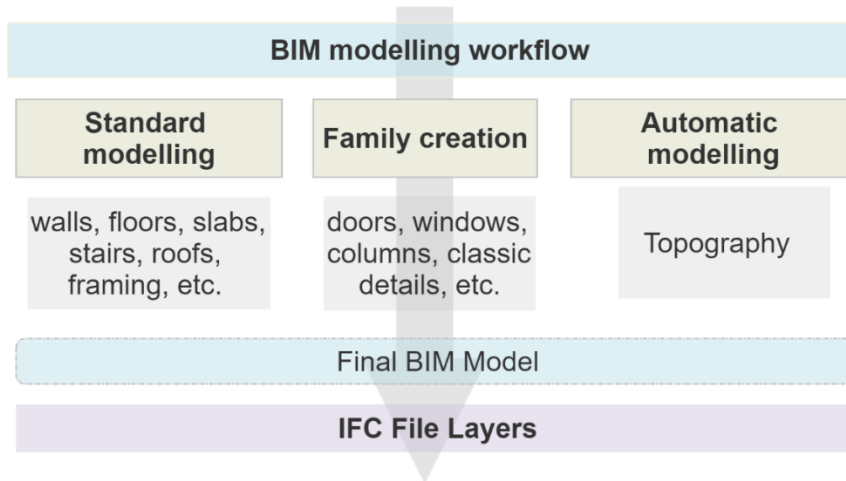


Figure 50: Key steps for 3D modelling with Autodesk Revit adopted from (Rocha et al. 2020)

Initially, a 2D floor plan was created using the intended building as a base, where walls, doors, windows, and other architectural elements were added. Floor levels were demarcated to indicate the number of floors and their corresponding heights. Additional floor plans were generated in 2D after establishing the levels and incorporating the floor-to-floor height. Semantically rich structural components were then constructed by attaching feature properties from the outside world. Once the 2D architectural plan and BIM components were ready, a 3D model shown in Figure 51 was created using the 2D model as a base. This was achieved by toggling to the Building Elevation Tab in the project window.

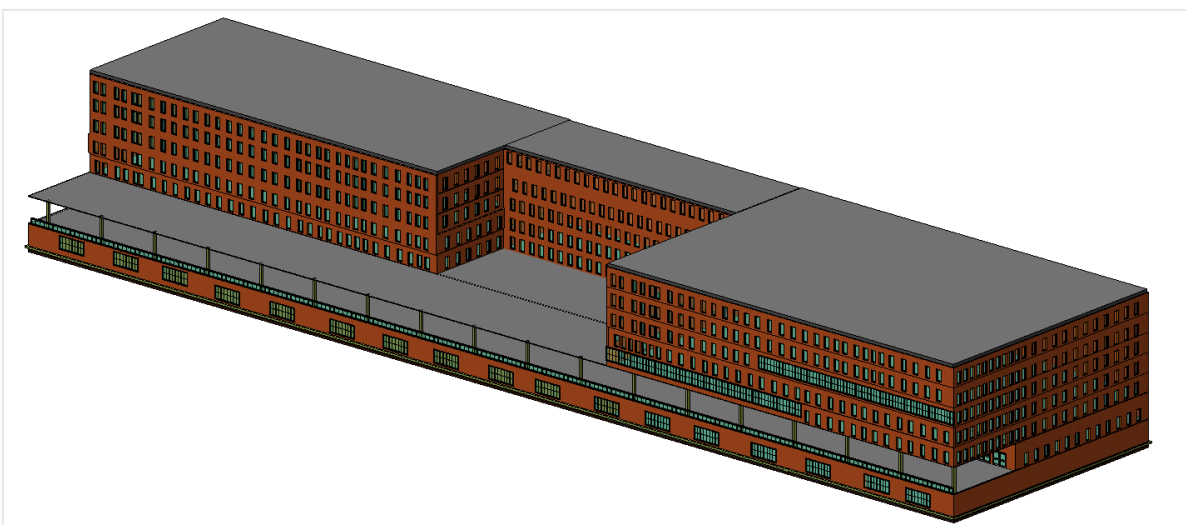


Figure 51: Generated BIM-IFC based 3D model of the targeted building

The utilization of object-oriented BIM software facilitates the production of volumetric element models. Hence, the 3D virtual representation of the structure, encompassing both its structural and non-structural components, inherently incorporates volumetric elements. The aforementioned entity possesses the potential for additional utilization in conjunction with GIS to facilitate further processing.

### 6.7.1.2 2<sup>nd</sup> Adjustment: Inundation Depth in 3D Volumetric Features

One way to represent the surface of the flooded area is by using a TIN (see section 6.6.1), which is a type of 3D dataset that represents a surface as a series of interconnected triangles. However, a TIN does not have a volumetric representation, which means that it does not provide information about the volume of water that has flooded the area. To overcome this limitation, it is necessary to convert the TIN into a volumetric format, such as a Multipatch, which is a type of 3D feature in ArcGIS Pro that can represent complex 3D objects with different geometries, such as buildings, bridges, or trees. By converting the TIN into a Multipatch, it is possible to combine the flood data with building data into a single format, which can be used for further geoprocessing and 3D analysis. To convert TIN based 3D flood inundation depth into volumetric component python scripting (see appendix) with the processing steps shown in Figure 52 was used.

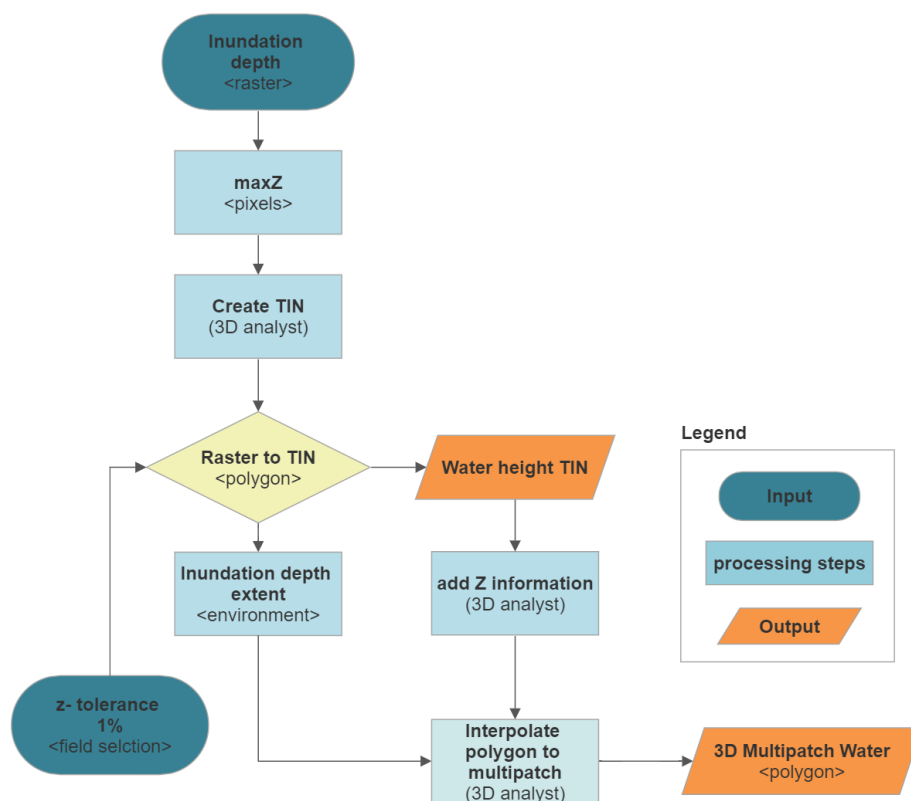


Figure 52: Processing steps for conversion of TIN into a volumetric component (multipatch)

After successfully running the model scripting, it was possible to visualize the TIN data as a volumetric object. It is necessary for the volumetric components or elements represented in multipatch format to be in a closed shape. This requirement is crucial for the effective utilization of such data in geoprocessing analysis, particularly in 3D analyst applications. The closed shape of the volumetric components or elements ensures that they are properly enclosed, with no gaps or overlaps in the data, which is essential for accurate and reliable analysis. Therefore, it is imperative to ensure that any

volumetric data represented in multipatch format meets this requirement before using it in any geoprocessing analysis. The completeness of the volumetric 3D flood inundation was evaluated using a built-in feature of ArcGIS Pro known as 'Is-Closed 3D' in 3D Analyst. This feature determines whether each volumetric feature completely encloses a volume of space. Volumetric features of the 3D flood inundation were tested using the Is-Closed-Feature tool in ArcGIS Pro. It confirmed that the volumetric 3D flood inundation was indeed completely closed. As a result, the TIN conversion into volumetric for 3D flood inundation was generated correctly and was suitable for further analysis, including modifications in the attribute table.

### 6.7.1.3 Integration of 3D Flood (GIS) and Building (BIM)

This step involves the integration of BIM-IFC based building into a GIS environment, in order to have building and flooding information into a single program operating in a homogeneous environment. This integration process is necessary to enable the seamless analysis and modelling of the impact of flooding on buildings and their components. By combining the two models into a single program operating within a consistent environment, it will be possible to conduct more accurate and comprehensive analyses that incorporate the interactions between the floodwaters and the built environment. The integration process likely involves the use of specialized software tools and scripting techniques to ensure that the two models are seamlessly integrated and can be utilized effectively for geoprocessing and modelling tasks.

A novel approach is proposed for integrating hydrodynamic simulations of the flood (GIS) and building (BIM) in 3D using a BIM-GIS integration methodology. This enables the execution of diverse spatial 3D geoprocessing analyses and assessments. As explained in section 4.1, it can be presumed that a multitude of researchers has either formulated or adapted procedural frameworks for the integration of GIS and BIM that cater to their specific needs. Therefore, to achieve a favourable outcome in the integration process, users must adopt or establish a customized integration methodology that addresses the associated challenges.

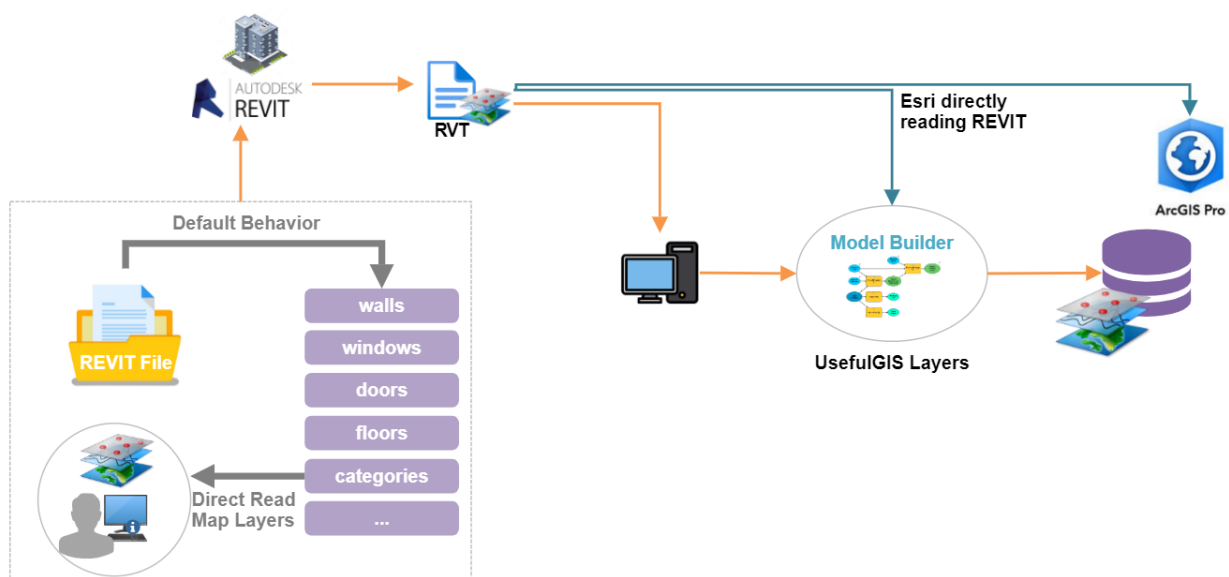


Figure 53: Modified GIS-BIM integration approach via direct read-in of BIM-Revit model to ArcGIS Pro (Carstens 2019)



Consequently, after evaluating two widely recognized approaches, namely, intermediate transformation using FME and direct read-in of the BIM-Revit model to ArcGIS Pro (see section 4.1), the latter was chosen for integration and modified according to this research needs, see

Figure 53. However, despite the selected method, several stages were still requisite for effectual data integration between BIM and GIS, and these stages and their corresponding procedures were contingent on the requirements and objectives of the end user. As a result, a novel process consisting of five steps shown in Figure 54 was developed for this research, with the aim of achieving a successful and meaningful integration between BIM and GIS data. This approach was formulated taking into consideration the particular requirements and objectives of the research, as well as the complexities and challenges inherent in the integration process.

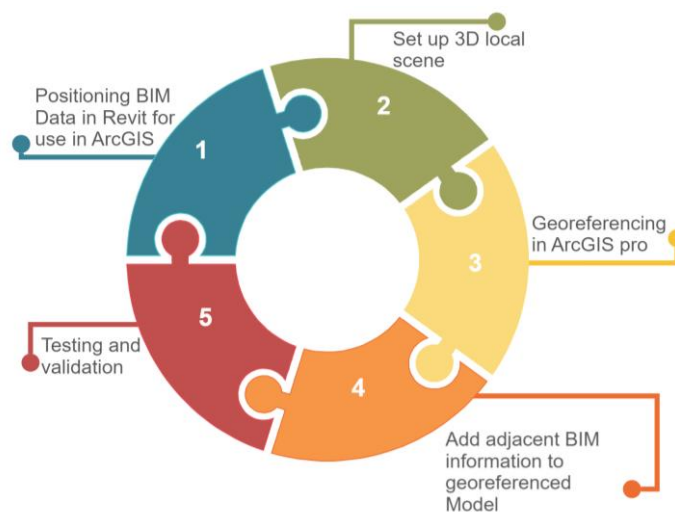


Figure 54: Five step data integration approach for GIS-BIM integration

The five-step approach is designed to be a systematic and rigorous method for data integration, providing clear guidelines and procedures to ensure that the integration is effective and reliable.

### Step 1: Positioning BIM Data in Revit for Use in ArcGIS

To position the BIM model generated by Autodesk Revit 2021, it is necessary to correctly position the source data of the BIM model. This will lead to opening the Revit data in ArcGIS Pro at the exact positions. Revit and ArcGIS Pro use different coordinate systems for representing geographical locations. Revit uses a Cartesian coordinate system to represent the position of elements within a building, while ArcGIS Pro uses a geographic coordinate system (GCS) or projected coordinate system (PCS) to represent the position of features on the earth's surface. To integrate Revit and ArcGIS Pro data, it is necessary to establish a connection between the two coordinate systems. This can be done by assigning a geographic location to the Revit model, which allows it to be properly georeferenced in ArcGIS Pro. In Revit, coordinates can be assigned to the model by specifying a location using latitude, longitude, and elevation data. This can be done manually or by importing a location data file. This process was done automatically due to importing the CADMAPPER file of the selected building (see appendix).

These coordinates were then used to generate the .prj file in QGIS. A projection (.prj) file is a file that contains the coordinate system information for a geospatial data file. The .prj file is used to define the projection or coordinate system of a spatial dataset, such as a shapefile, raster image, or geodatabase feature class. Without a .prj file, the spatial data would have no information about its location in space, making it difficult to interpret and analyse correctly. Therefore, it is important to ensure that a .prj file is included with any geospatial data file (in this case its Revit model) so that it can be properly integrated and analysed in GIS software. It should be noted that ArcGIS Pro use a .prj file to locate the Revit model in its exact location.

### **Step 2: Setting up 3D Local Scene in ArcGIS Pro**

Subsequently, the workflow transitioned to the ArcGIS Pro platform, wherein the initial stage involved creating a new project by choosing the Local Scene option. To work with local scenes in ArcGIS Pro, users need to have appropriate data available, including elevation data, 3D models, and other related content. Local scenes serve the purpose of exhibiting spatially referenced data within a projected coordinate system and have the capability of accommodating projects ranging from city-wide to building-specific scales. For the FIA at hand, local scenes were deemed appropriate. After creating a new local scene in ArcGIS Pro, certain parameters must be set. By default, each scene has an elevation surface called "Ground." However, additional surfaces, such as Geology 1, Geology 2, Ozone, and others, can be defined as needed. Each surface can have multiple data sources including raster's, TINs, and elevation services. Furthermore, thematic surfaces can be created from analytical results, such as sea surface temperature, and other layers can be draped on them. It is important to note that the "Navigate Underground" option should be enabled to ensure that buildings inserted into the scene do not become lost in the space beneath the ground surface.

### **Step 3: Georeferencing within Local Scene**

Georeferencing in ArcGIS Pro is the process of aligning geographic data to a known coordinate system so that it can be used in conjunction with other geographic data layers. This process involves identifying corresponding points on the geographic data and a reference layer with known coordinates and then transforming the geographic data to match the reference layer. Georeferencing can be done using a variety of tools, including the Georeferencing Toolbar, the Georeferencing Pane, and the Georeferencing Wizard. The process involves selecting control points on the geographic data and the reference layer, choosing a transformation method and adjusting the parameters of the transformation until the geographic data is aligned with the reference layer. Once georeferenced, the data can be saved as a new layer with a known coordinate system. The "Define Projection" tool in ArcGIS Pro is used to assign a known coordinate system to a dataset with an unknown coordinate system or to correct an incorrectly defined coordinate system. It is commonly used to properly georeference spatial data so it can be used for mapping, analysis, and visualization. The tool issues a warning when a dataset with a known coordinate system is included, but it can still be used. All feature classes in a geodatabase feature dataset should have the same coordinate system, and the coordinate system for a geodatabase dataset should be determined when it is created, as changing it after feature classes have been added can cause alignment issues. However, it is possible to reproject a geodatabase dataset to a different coordinate system if needed.

The Revit Model was initially projected in the WGS 84 Geographic Coordinate System, and it was necessary to convert it to the UTM zone 32N EPSG 25832 European projected coordinate system using the Define Projection tool. This conversion was required to accurately place the building on the base map using its true location. The Define Projection tool utilized the architectural plan components to select the desired projection of UTM zone 32N EPSG 25832 European projected coordinate system for the building's architectural plan. However, the initial projection resulted in a false location when the plan was brought into the local scene due to the previously defined WGS 84 coordinates in Revit. To correct this, the Manage tool was used to reproject and georeference the architectural plan, after which the exact location was obtained using the Locate tool in the Map tab of ArcGIS Pro. The full address of the building was required to locate it on the map using this tool. Similarly, the Georeferencing tab was also utilized to bring the BIM Model to the searched location. The "Move to Display" button was used to precisely reposition the geolocated BIM model and the necessary tools were provided to move it in all directions, as well as rotate and rescaled. By utilizing these tools, the BIM model was accurately positioned on the map at its true location. Figure 55 is showing the 3D BIM model of the building along 3D flooding.



Figure 55: 3D BIM-IFC based building inside ArcGIS Pro after integration

#### Step 4: Add Adjacent BIM Information to Georeferenced Model

The integration of Autodesk Revit files into local scenes enables the visualization of the built and natural environment. Incorporating these files into GIS content requires the use of a Data tool to establish a connection to the designated folder containing Revit BIM models. The ArcGIS Pro Catalogue pane facilitates a connection to the folder containing .gdb (geodatabase) conversions. To execute python scripts from the PyCharm interface, the FeatureClass To FeatureClass function must be

performed to convert each database file into a project geodatabase file. This allows successful conversion of the files while maintaining the Level of Information (LOI) of the Revit model. Georeferencing the model with its origin (Revit survey point) is accomplished by mapping it to the IFC Site (Longitude, Latitude) and subsequently transforming it into (Easting and Northing).

### **Step 5: Testing and Validation**

After meeting the initial requirement, the multipitch geometries underwent testing using both semantic and geometric geoprocessing methods. The semantic testing involved querying attribute table parameters, which were completely queryable based on the organization of geometry attributes. The geometric testing utilized the 3D Analyst geoprocessing to enable 3D intersection without errors, thereby satisfying the second requirement of the methodology which aimed to overcome geometric losses and problems resulting from 3D intersections. In case of any errors, the Check Geometry and Repair Geometry tools of ArcGIS geoprocessing were used as a workaround. To enable proper back-end management of BIM elements, a python script workflow was coded using arcpy libraries to merge feature classes using arcpy.Merge\_management, select categories simultaneously using arcpy.SelectLayerByAttribute\_management, and copy features from the input feature class or layer to a new feature class using arcpy.CopyFeatures\_management. After the successful integration of BIM data into ArcGIS Pro local scene the last phase of the developed model was tested.

## **6.8 Flood Impact Assessment in 3D**

Three-dimensional flood impact analysis is the last and most important phase of the proposed model workflow, involving a number of interlinked tasks to automate the calculation of flood actions, their pressures, and forces on building's structural and non-structural components and lastly their visualization in 3D. In order to perform 3D FIA prerequisites are spatial hydrodynamic 3D flooding, 3D buildings and terrains. Consequently, the previous section's integration of GIS and BIM was utilized to conduct a 3D FIA using a suitable method developed to test and calculate a justified subset of potential flood actions and their impacts. Based on the findings outlined in the literature section 2.6, Table 1 presents a comprehensive overview of the various flood actions that can impact buildings across different categories. To further support these findings, Table 5 showcases a selection of flood actions that were automated within the model for the purpose of rigorous testing and calculations. These results serve as compelling evidence for the significance of considering flood-related risks when designing and constructing buildings. Therefore, in order to check, if this phase will work and perform the intended results for this prototype case study, primarily flood action, and water interaction level was carried out. As can be seen from Table 5 in order to assess water interaction, spatial distribution of flood inundation depth as well as detail level of buildings (structural and non-structural) components are necessary. To assess which components of a building are being affected by flooding, it is important to determine which components are submerged in flood depth.

This is typically a challenging task because buildings have numerous components, and identifying the ones that will be damaged by flooding can be difficult. However, in the developed 3D flood model, all building components and their flooding depths are spatially available. Therefore, it only requires such geoprocessing that provides, which components of the building are fully or partially submerged in flood depth. To accomplish this, the 3D intersect tool in 3D Analyst can be used to determine which components of the building intersect spatially with the flood depth. Hence, python scripting has been

employed to perform 3D intersects (see appendix). The results of the intersected components can be viewed in Figure 56. This information can aid in determining the extent of damage caused by flooding to a building's components.

Table 5: Flood actions automated into digital twin for 3D flood impact assessment

<b>Flood action</b>	<b>Definition</b>	<b>Relevance</b>	<b>Predictability</b>	<b>Flood Parameters</b>
<b>Water Interaction</b>	Buildings (structural and non-structural components) directly or indirectly intersected with flood water	Highly Relative	Predictable	Above-floor inundation, Building Components Geometry (LODs)
<b>Hydrostatic Force</b>	Lateral forces imposed on building and its components by the mass of still water and created by the depth-differential on two-sides of a vertical component like wall. At any point, hydrostatic force is equal in all directions (irrespective of building or component orientation).	Highly Relative	Predictable	Inundation Depth, Building Components Geometry (LODs)
<b>Hydrodynamic Force</b>	Lateral forces that are generated by the flowing floodwater. Hydrodynamic forces can push or drag building and its elements depending on the local velocities.	Highly Relative	Predictable	Depth, Velocity, Building Components Geometry (LODs)
<b>Impact Force</b>	Also known as lateral-direction hydrodynamic force, it creates lateral pressure, localized changes in components can push or drag entire building or its components depending on the velocity.	Varies	Difficult	Depth, Velocity, Impact height Building Components Geometry (LODs)
<b>Debris Force</b>	The forces generated by flood-borne solids (debris) in the water or sediment deposition and aggradations against building components. These include the dynamic (former) and static (latter) debris actions.	Varies	Difficult	Velocity, Debris velocity, weight, geometry, impact height and duration
<b>Drag Side Effect</b>	These forces can drag building and its elements depending on the local velocities and its geometry.	Varies	Difficult	Depth, Velocity, Building Components Geometry (LODs)

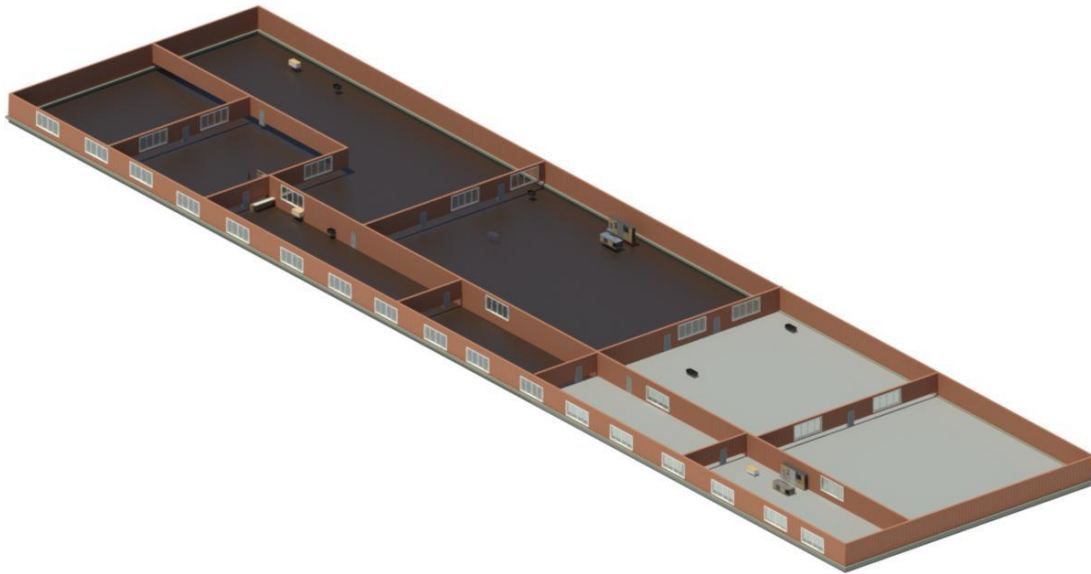


Figure 56: Flood intersected building structural and non-structural components

The thorough analysis of the intersected building components revealed that many of them were missed or ignored during the intersection process. This was despite the fact that these components were fully submerged during visual inspection. For example, a small opening near ground level was fully submerged but was ignored during the 3D intersection process. Similar issues were observed with many other building components. Further investigation showed that the problem was not with the intersection procedure or scripting. Therefore, the building and flooding data were thoroughly examined. It was discovered that during the hydrodynamic flooding simulation, the resolution of the digital terrain model (DTM) used was one meter by 1.0 meter pixel size. However, the different building components varied in size from millimetres to meters. This mismatch in resolution resulted in the problem. Although the building components were spatially present in the model, the flood pixels were much larger in size (1m by 1m), leading to their complete ignorance during the 3D intersection processing. However, the scope of the prototype case study was to check the model workflow functionality. After identifying the root cause of the problem and determining its extent and nature, a thorough assessment of the other flood actions in Table 5 was not carried out in the prototype case study. Instead, the methodology and datasets were improved to overcome the issue before testing them on the next case study.

### 6.8.1 Lessons Learnt and Limitations of Case Study 1

The purpose of conducting the prototype case study was to evaluate whether the developed novel model workflow for 3D flood impact assessment efficiently functioning with its intermediate steps. During the testing phase, several limitations and opportunities for improvement were identified.

#### Limitations in Dataset Properties

One of the key findings was that the 3D flood model visualization was not capable of generating FIA on buildings and their components. Although effective for visualization, the 3D surface polygon blocks of floods and buildings were inadequate for geoprocessing analysis. To effectively utilize 3D analyst tools, closed shape polygons were required, which could only be achieved through a volumetric



representation in a multipatch format with 3D volumetric element geometry. To address this issue, the 3D flood inundation depth was transformed into a volumetric element (multipatch).

### Limitation in Mismatching of Dataset Resolutions

Similarly, during testing last phase ‘3D Flood impact assessment’ of the model workflow, it was discovered that there is mismatching in dataset resolution detail. As for the case study, hydrodynamic flood simulation DTM data was low in resolution (100 by 100 cm pixel size) compared to building components resolution. Which resulted to ignore many building components during the assessment of water sensitive components. The resolution of a DTM refers to the size of each pixel or cell in the dataset. In general, a higher resolution DTM will provide more detailed information about the terrain, which can be beneficial for flood simulation. A 100-by-100 cm resolution DTM can be considered a relatively high resolution, as it means that each pixel in the dataset represents an area of one square meter on the ground. This level of detail can be suitable for many flood simulation applications, especially if the flood model is designed to work at a relatively large scale, such as over a regional or catchment area.

However, the suitability of a 100-by-100 cm resolution DTM for flood simulation ultimately depends on the specific requirements of the modelling application. For example, if the flood model needs to capture small-scale terrain features or flow paths with a high degree of accuracy, a higher resolution DTM may be necessary. Additionally, other factors such as the accuracy of the elevation data and the quality of the flood model itself will also play a role in determining the suitability of a given DTM for flood simulation. This can be better understood by following Figure 57.

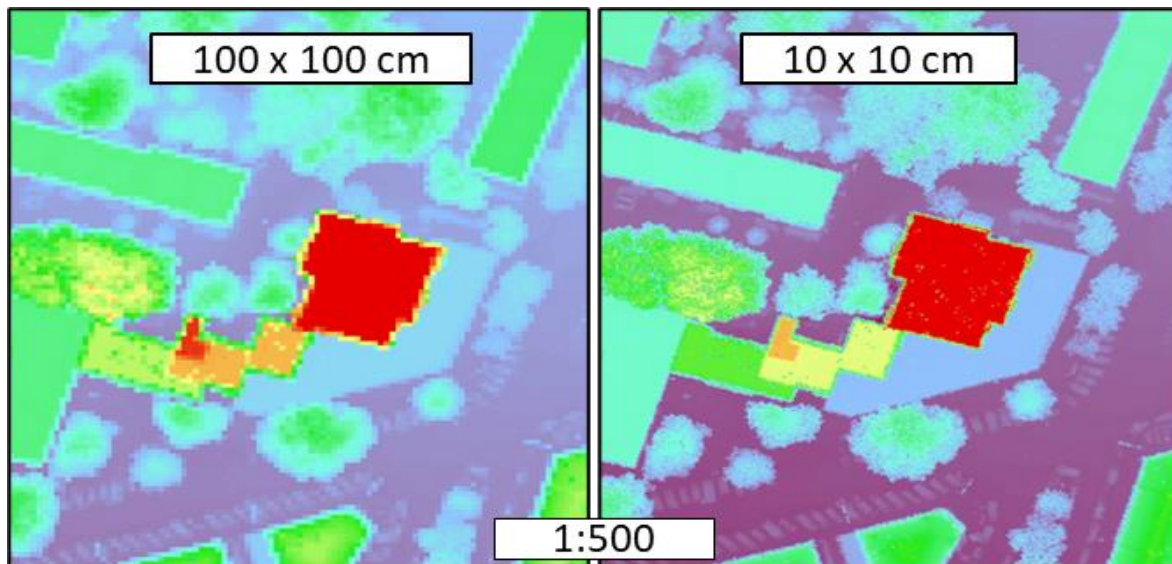


Figure 57: Comparison of DTM resolution 100-by-100 cm pixel size (left) 10-by-10 cm pixel size (right)

It can be seen that 100-by-100 cm resolution has coarser boundaries of the building and its surroundings, compared to high resolution, 10 by 10cm pixel size resolution data. Which has very refined resolution data which eventually provides detailed pixels of surroundings as well as of buildings that are up to 10 centimetres.

Even though according to many studies, 100-by-100 cm resolution DTM is considered good for flood simulations of urban areas, but this resolution is not enough for micro scale analysis such as individual building level. A 100 cm resolution DTM is adequate for flood modelling in small to medium-sized watersheds but suggested that a higher resolution DTM may be necessary for large watersheds or simulations requiring a high level of detail (Chen et al. 2012; Gioti et al. 2013). Similarly, Chen et al. (2012) described that 100 cm resolution DTM is sufficient for flood simulation in urban areas with moderate to high accuracy. However, the study also noted that a higher resolution DTM may be necessary for simulating floods in areas with complex topography, such as mountainous regions.

So, it can be concluded that the resolution of a DTM for flood simulation can depend on several factors such as the accuracy of the underlying elevation data, the extent and complexity of the study area, and the level of detail required for the simulation. This implies that the resolution of the DTM plays a crucial role in performing a 3D flood impact assessment on different building components, and it should be integrated based on the other datasets used for the analysis.

### **Limitations Regarding LODs of Building and Its Components**

BIM has been integrated into the workflow to produce high-detail (LOD) building components in volumetric form multipatch, as the ArcGIS built-in 3D modelling approach is currently incapable of generating LOD 3 or higher. The prototype BIM model used for this research had another limitation, regarding the modelling of 3D building and its components. In the case of the prototype case study, many components of the targeted building were assumed, leading to a 3D BIM model that deviated significantly from reality. For generating a digital twin of the flood scenario and calculating flood actions and structural loads, it is necessary to model the analysed building based on real-world geometry. This can be achieved either through architectural plans or by using survey methods such as laser scanning. By doing so, the generated impacts and loads can be applied to the building to evaluate its effectiveness in mitigating potential flood hazards. Therefore, accurate modelling of the building and its components is crucial for conducting an effective flood impact assessment.



## **Chapter 7**

---

### **Case Study 2: Testing and Implementation of Model Workflow**

## 7 Case Study 2: Testing and Implementation of Model Workflow

The importance of FIA cannot be overstated in today's world, where the frequency and intensity of floods are on the rise due to climate change. The prototype case study was previously conducted to test the novel 3D flood impact assessment model workflow and revealed several limitations and opportunities for improvement in datasets and methodology. One of the critical findings was the need to incorporate a higher resolution DTM to effectively assess the impact on different building components. Additionally, the prototype case study highlighted the significance of accurate modelling of buildings and their components to generate reliable digital twins of flood scenarios. Based on these limitations and lessons learned, an improved methodology and data were used in this case study to enhance the accuracy in calculations of 3D flood impact assessment through the developed model workflow. This case study aimed at a real-world scenario to demonstrate the improved workflow's efficiency and accuracy in generating 3D FIA on buildings and their components in a digital twin environment. Creating a digital twin requires accurate and precise input data, which is collected and prepared before the twin's creation. The input data should be reliable, relevant, and of sufficient resolution to model the real-world scenario with a high degree of accuracy.

To overcome the limitations identified in section 6.8.1 and to improve the methodology for creating a digital twin, the input data collection and preparation process is improvised in this case study. This includes using a higher resolution DTM (Airborne LiDAR) to capture more detailed terrain features and flow paths, as well as using survey methods such as laser scanning to accurately model the building and its components.

The selection of a suitable case study area is crucial for generating reliable and accurate FIA using a digital twin environment. The requirements for selecting the case study area were based on the limitations and lessons learned from the prototype case study. The University of Applied Sciences in Frankfurt am Main, Germany was chosen as the new case study area. This selection of the case study area is entirely random, and its purpose is solely to generate hypothetical flooding scenarios. These scenarios are entirely detached from real-world situations and serve as purely speculative exercises for the purpose of academic or experimental exploration. Another reason to select University of Applied Sciences Frankfurt is the availability of data necessary for creating a digital twin environment that could be utilized for conducting 3D FIA on a building and its components. Because the purpose of this research is to provide a workflow and process for dealing with FIA in the real world using a 3D approach. Therefore, the selection criteria for this case study were not based on a problematic area, but rather on the availability of data required for the creation of a digital twin environment for testing the developed model workflow for several flood scenarios.

### 7.1 UAS Frankfurt am Main

The Frankfurter University of Applied Sciences (UAS) is a public university located in Frankfurt am Main, Germany. It was founded in 1971 and has since then become one of the most renowned universities of applied sciences in the country. The university offers a wide range of undergraduate and graduate programs in fields such as engineering, business, social sciences, and media.

The university is spread across several campuses in the city, with the main campus located in the city center shown in Figure 58. The total area of the main campus is approximately 20,000 square meters,

with numerous buildings and facilities dedicated to various academic departments and administrative services. In addition to the main campus, the university has several other smaller campuses and facilities located throughout Frankfurt.

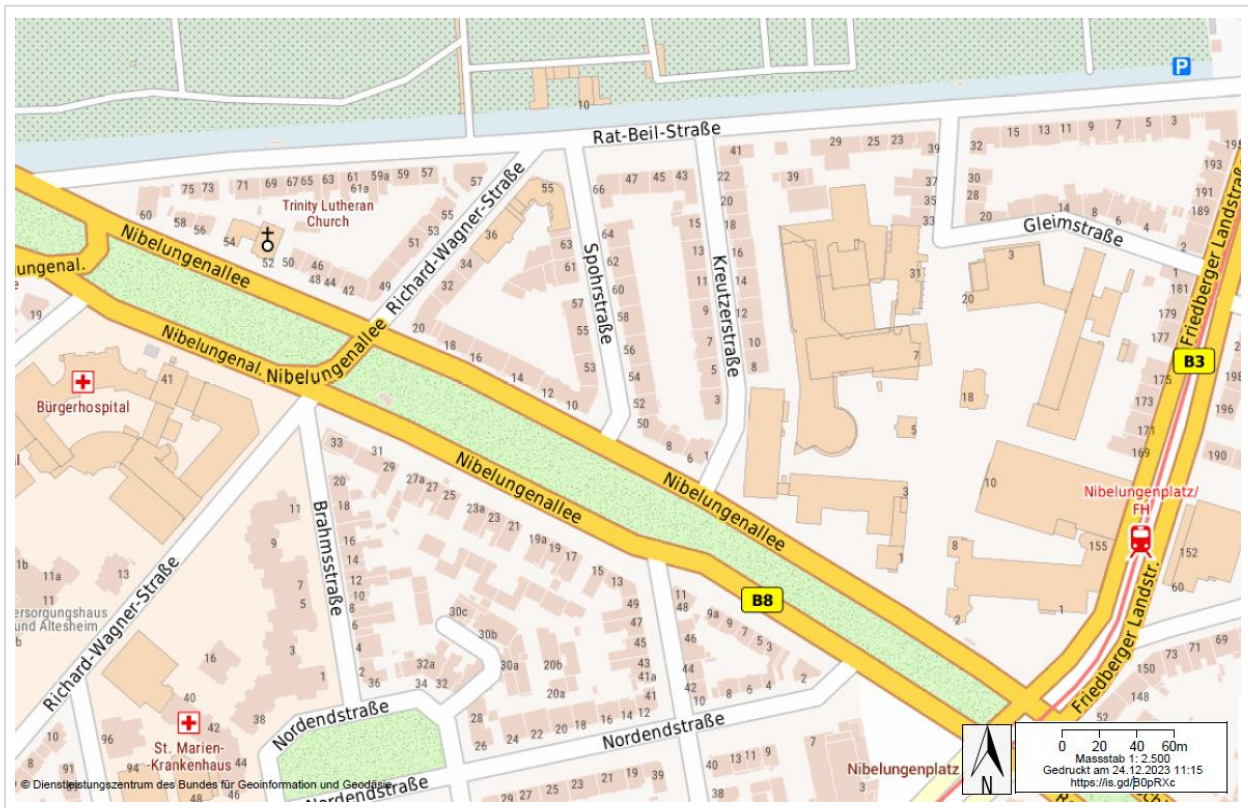


Figure 58: Selected case study area University of Applied Sciences (UAS) Frankfurt am Main (Source: BKG)

## 7.2 Testing of Model Workflow

The model workflow is structured as a sequence of six interconnected phases that are dependent on one another, as elaborated in section 5.2. These phases include input data and pre-processing, hydrodynamic flood simulation, 2D flood impact assessment, 3D flood model, GIS-BIM integration, and 3D flood impact analysis. Each phase is tailored to accomplish its distinct objectives and encompasses its own specific working steps. To validate the efficiency of these working steps, an improved methodology and datasets based on limitations and lessons learned from a prototype case study are implemented and tested in this case study. The subsequent sections will detail the testing and results of the improved methodology and datasets.

## 7.3 Data Collection and Pre-processing

This is the first and preliminary phase of the model workflow. This phase involves collecting and preparing data related to the case study area. This is the first and preliminary phase of the model workflow. This phase involves collecting and preparing data related to the case study area. This data can subsequently serve as input for the next phases. This includes collecting and preparing data on topography (DTM), land use (Corine land cover), infrastructure (building footprints), and hydrological

characteristics (water bodies) of the study area see Table 6. A detailed explanation of the collected data and the steps involved in its processing are provided below.

Table 6: Collected data types and sources for the case study area

Data	Type	Source
DTM	Laser Airborne Scan	UAS Frankfurt
Topography and Elevation	Laser Airborne Scan	UAS Frankfurt
Digital Landscape Model	Shapefile (DLM 1:250)	Geoportal.de
3D Building	Point Cloud	Self-generated
Building Footprints	Point Cloud	Self-generated
Roughness Coefficient	Report	DIN 3141

### 7.3.1 Digital Terrain Model

As stated previously, a DTM is necessary for accurate flood simulation and impact analysis. This is particularly important for small building components, such as openings and electrical utilities, which may have a significant impact on flood interactions and wetted perimeter calculations during 3D Flood impact assessment. To overcome the mismatching resolution limitations as identified earlier in section 6.8.1, the individual building components are modelled in BIM with high resolution and precision therefore a DTM is also required with a detailed high resolution and precision. So that it is capable of covering building openings up to 1.0 cm in size with high resolution. This means DTM should be of at least 1.0 x 1.0 cm resolution. While it can be difficult to obtain DTM at such a fine scale, drones and privately available airborne laser scanned data in LAS format can be used to create such a high-resolution DTM.

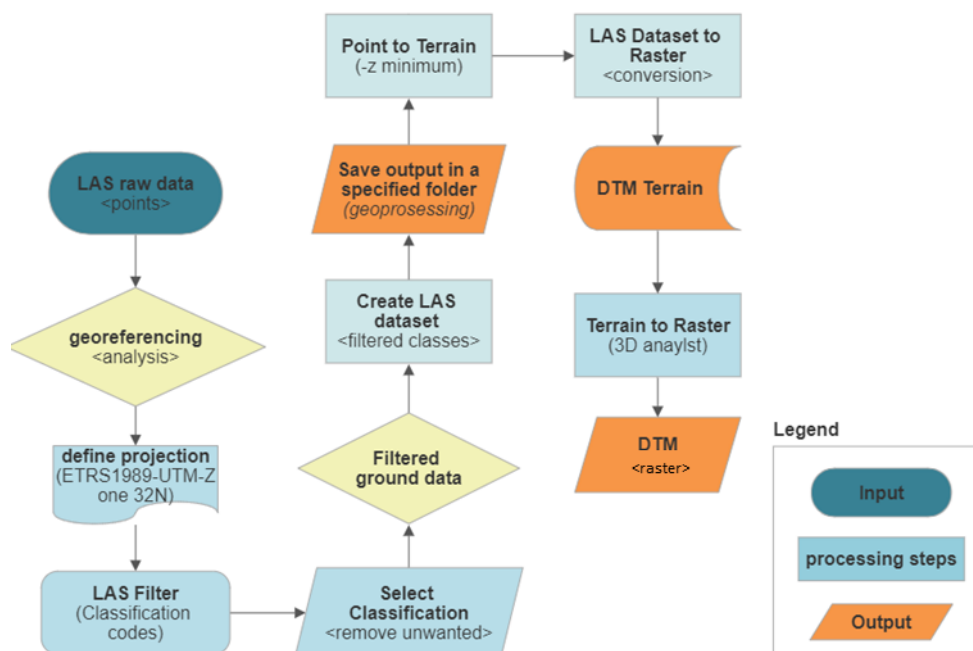


Figure 59: Processing steps for conversion of LAS data into DTM

However, obtaining this level of detailed data is not available easily, and pre-processing and processing are required to convert the data into an operational DTM format, in this case, should be suitable for

hydrodynamic flood simulation. In this case study, a drone-based LAS data set was obtained from the UAS Department of Geomatics for research purposes. This data set was composed of several 1.0 x 1.0 km tiles with a point density of approximately 20 points per square meter, covering the campus and surrounding areas. Before the LAS data can be used as DTM in hydrodynamic flood simulation using FloodArea, it must undergo two crucial steps: pre-processing and processing. These steps are necessary to convert the raw LAS data into a clean and usable GeoTiff format DTM that is suitable for the Hydrodynamic flood simulation. Figure 59 is showing processing steps to convert LAS data into an effective DTM.

### 7.3.1.1 Pre-processing

To create an accurate and reliable DTM from raw LAS data, the data must first undergo a crucial pre-processing step. During this step, any noise or anomalies present in the data are identified and removed. This process is essential to ensure the accuracy and reliability of the final DTM, which is necessary for hydrodynamic flood simulation. To achieve this, it is important to have a good understanding of the background and creation of the LAS data. Once this is understood, the LAS data was examined to identify any imperfections that may affect the accuracy of the DTM. In particular, the LAS data's elevation, intensity, and scanned location were analysed using software such as Autodesk ReCAP Pro, as shown in the appendix.

LAS data typically includes three main components: the x, y, and z coordinates of the points. The z coordinate represents the elevation value of each point, which is the height above a specified reference level. This elevation value is derived from the time it takes for the laser pulse to travel from the LiDAR scanner to the ground and back. The elevation values in LAS data are often used to create a DTM or digital surface model (DSM), which represents the bare earth or the ground surface and all features on it, respectively. Figure 60 is showing elevation values of LAS data.

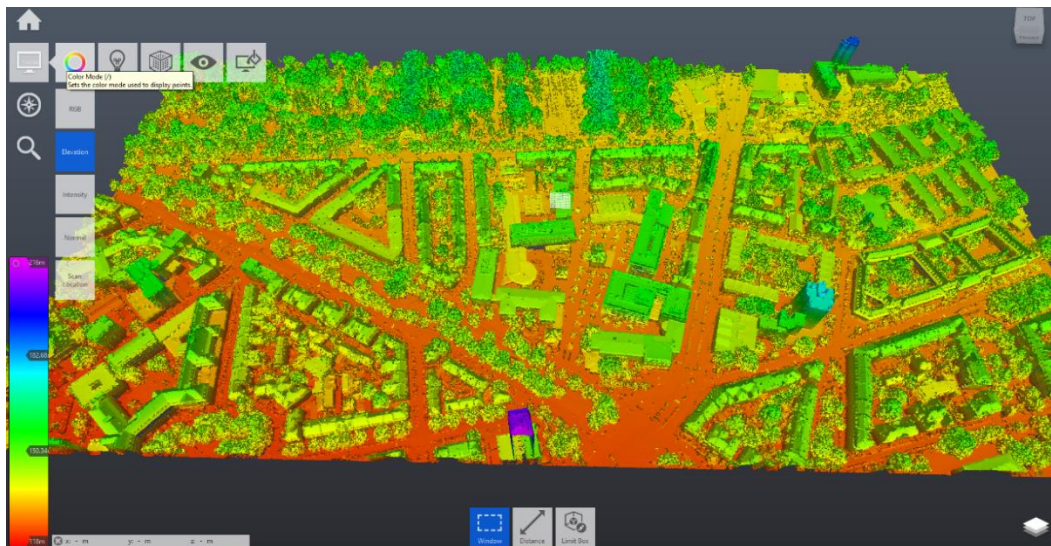


Figure 60: Information regarding elevations of case study area LAS data

The x and y coordinates of each point in the LAS data represent the location of that point in a two-dimensional space. These coordinates are often in the form of a projected coordinate system, such as UTM or State Plane, and are used to determine the precise location of each point on the ground. The scanned location of each point is determined by the location of the LiDAR scanner at the time the data



was collected. This information can be used to create a point cloud that accurately represents the topography and features of the area that was scanned. According to Jakovljevic et al. (2019), the intensity values in LAS data can be used as an additional source of information for feature extraction and classification. They explained that intensity values are related to the reflectance of the objects scanned by the LiDAR and can therefore provide useful information about the characteristics of the objects. They note that intensity-based classification can be especially useful when LiDAR data is acquired under less-than-ideal conditions, such as in areas with high vegetation cover or low light conditions. Furthermore, they also state that intensity values can be used as a substitute for aerial imagery when such data is unavailable. This is because intensity values can provide information about the brightness and contrast of the objects scanned by the LiDAR, which can be used to distinguish between different types of features.

By carefully examining and cleaning the raw LAS data during the pre-processing step, the user can create a highly accurate and reliable DTM that takes into account the intensity values of the scanned objects. This can be especially useful for hydrodynamic flood simulation, where accurate and detailed information about the terrain and features is essential for predicting the flow velocities, direction, and depth. The final step of the pre-processing stage involves defining the projection of the acquired LiDAR data. If the projection of LAS data is not defined, it cannot be accurately georeferenced to its correct location on the earth's surface. This means that any subsequent analyses or modelling using the data may be inaccurate or unreliable. Defining the projection is therefore a critical step in processing LiDAR data, as it ensures that the data is correctly positioned within a geographic coordinate system and can be integrated with other spatial data for further analysis.

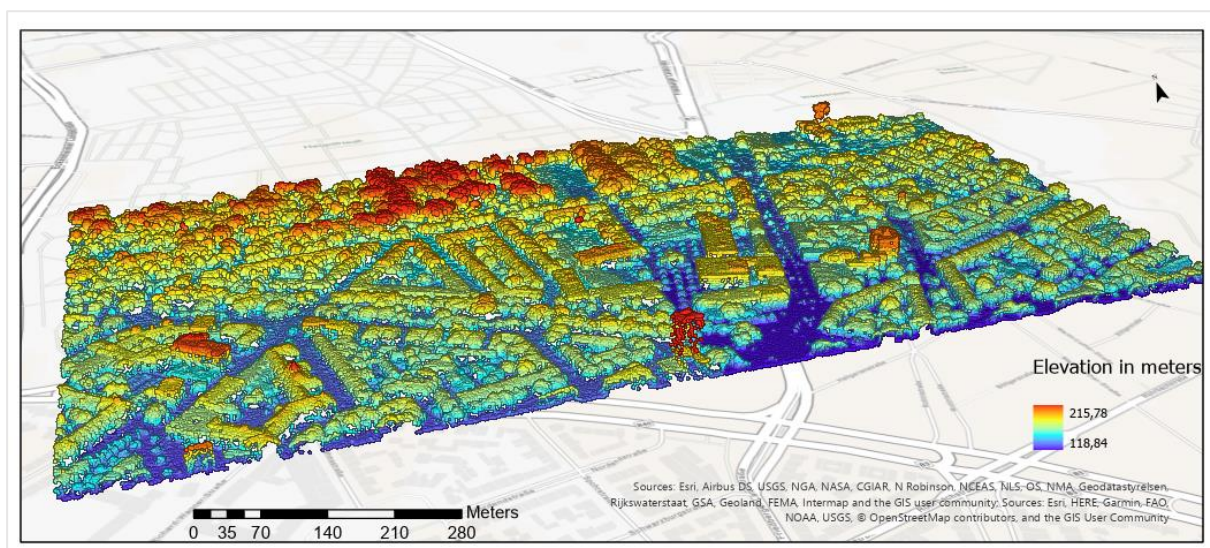


Figure 61: LAS data of study area import in ArcGIS local scene for processing and georeferencing

In order to properly georeferenced the acquired LAS data, the Local Scene feature in ArcGIS Pro was utilized. Initially, the data was opened in an incorrect location within France, which made it necessary to define the projection to its true location using the define projection tool in ArcGIS Pro. This involved defining the projection to ETRS 1989 UTM Zone 32N, which helped to bring the data to its actual location. The LAS data layers can be viewed in their true location within the 3D Local Scene window, as illustrated in Figure 61.

### 7.3.1.2 Processing

The analysis reveals that LAS data is abundant with 3D point information, which needs to be transformed into a DTM through a two-stage process. The first stage involves filtering the points to differentiate between ground and non-ground points. Several techniques have been researched and tested on various terrains to identify ground points, such as the lowest elevation sampling method, weighted linear least squares interpolation by Pfeifer, slope-based filtering by Vosselman, and mathematical morphology-based filtering (Lippert et al. 2018). In this study, ArcGIS Pro is utilized for filtering, as depicted in Figure 61, and the data set is prepared for a new LAS dataset.

In LiDAR data processing, each LiDAR point can be assigned a categorization code that corresponds to the type of surface or object from which the laser pulse was reflected. These codes are represented by numerical integers in the LAS files and are typically assigned using specialized classification software separate from ArcGIS Pro. The classification process involves setting parameters based on the topography and applying algorithms to identify the feature type of each point, with the resulting classification code recorded in the LAS file according to the ASPRS standard. The LAS files contain a number of predefined classification codes (see appendix), including ground, water, bare ground, and tree canopy tops. In this case study, the LAS filter dialogue box is used to select specific classes for the production of the final DTM. The selected classes include ground, low vegetation, low noise, model key reserved, water, road, rail, and others, as displayed in the appendix.



Figure 62: Generated DTM from LAS data of the study area

A new LAS dataset is then created using only the filtered classes for the final DTM generation. The filtered data set was converted to new LAS dataset without unnecessary information required for this research. Similarly, the LAS dataset was rendered using the LAS to Raster function. The function was used to add LAS dataset to a mosaic dataset, where both input and output properties were specified. Because of the resolution of the data and the time it can take to convert the point data to raster data, this function writes pre-processed raster data files to an output directory. Consequently, LAS dataset was converted into a raster format. where the output data type was floating point and cell size was 10 x 10 cm with the Binning Interpolation method. The conversion process took 3 minutes to complete for the 1.0 x 1.0 km LAS dataset with PC specifications of Core i7 RAM 64 GB. These generated rasters had a pixel size of 10 x 10 cm, which is three times larger than the average point distance of LAS

datasets. Generated DTM from LAS data is shown in Figure 62. The DTM is now ready to be used for further processing in flood simulation.

### **7.3.2 Preparation of Other Input Data for Hydrodynamic Flood Simulation**

For hydrodynamic flood simulation other types of data required such as building footprint, land use land cover, Discharge index grid and rainfall hydrograph follows the same procedures as mentioned in section 6.3 and additional details are in the appendix.

## **7.4 Hydrodynamic Flood Simulations**

In this case study, a hydrodynamic flood simulation was performed to assess the effects of different rainfall scenarios. Compared to a previous prototype case study that focused on riverine flooding, there are slight differences in the input data requirements for the FloodArea hydrodynamic flood simulation model. The process for this case study is similar to the prototype case study described in section 6.3, which involves preparing input data for hydraulic flood simulation in FloodArea and running the model. The model for this case study was configured for three different scenarios, each with a different time interval, and output switch four was selected to provide information on inundation depth, flow direction, and velocity. The simulation took 15 hours to complete. The simulation produced spatiotemporal raster maps on the distribution of inundation depth, flow velocity, and flow direction. An overview of the output spatial distribution of flood maps can be seen in Figure 63.



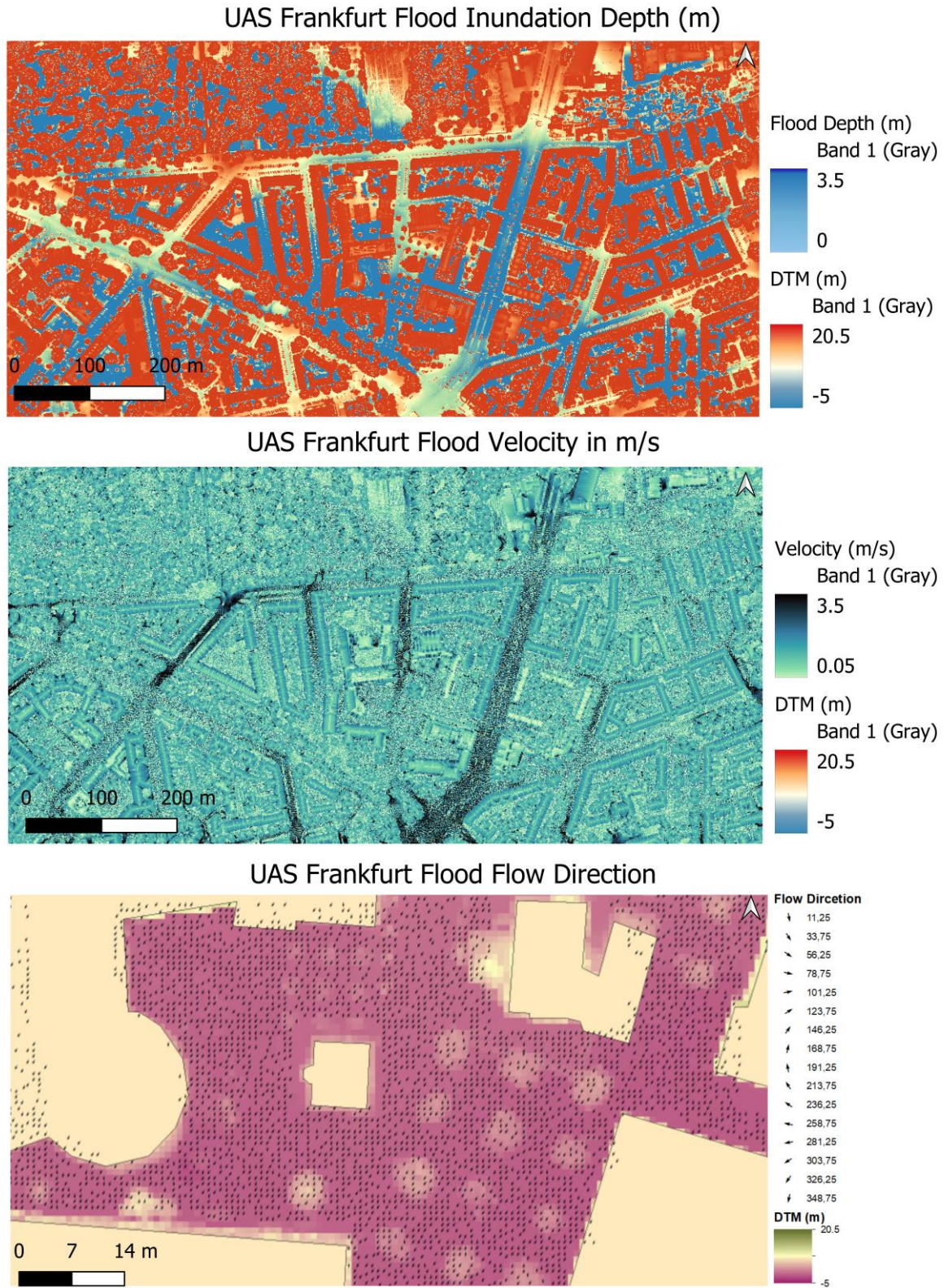


Figure 63: Spatial distribution of inundation depth, flow velocity and water flow direction

## 7.5 3D Flood Model

After the necessary data preparation, processing and hydrodynamic flood simulation, the next step was the creation of a 3D flood model to visualize the flooding information in 3D alongside other topographic features such as buildings and terrain shown in Figure 64. See section 6.6 for the processing steps required to develop a 3D flood model.

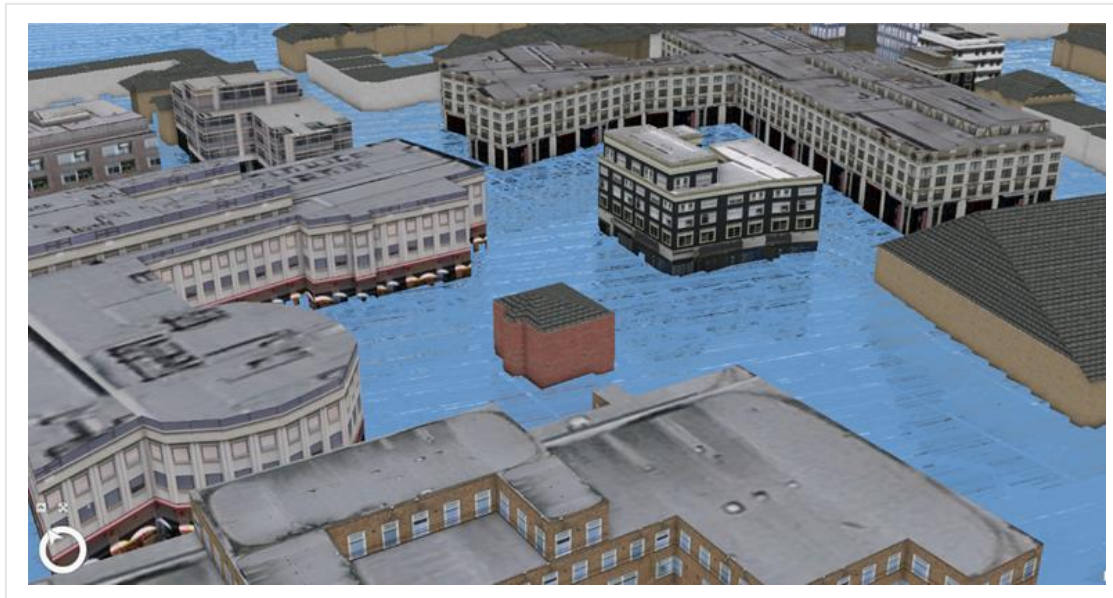


Figure 64: Visualization of buildings, terrain and flooding in 3D (3D flood model)

It was found during the prototype testing that relying solely on a 3D flood model is insufficient for in-depth analysis. Several critical parameters necessitate significant conversions, such as transforming the 3D flood inundation depth into a 3D multipatch format. Consequently, during the 3D inundation depth generation for this case study, the dataset was directly converted into the volumetric form using the procedure outlined in section 6.6.2. A further constraint recognized in the prototype testing (section 6.8.1) pertained to the extensive level of detail required for buildings and their components, specifically regarding real-world geometry, dimensions, and material properties. In response, the subsequent measures were implemented to tackle this limitation.

### 7.5.1 3D Building Generation

Upon completion of the 2D flood impact assessment for building exposure, as outlined in section 6.5 2<sup>nd</sup> phase of the model workflow, the Rotes Haus was selected as the building to undergo further analysis. This decision was based on the fact that it stands alone and is detached from surrounding buildings and infrastructure, as can be seen in Figure 65. The Rotes Haus is a two-story historical building with a basement, covering a gross built area of approximately 106m<sup>2</sup>. Its structure is a combination of masonry, concrete, stone, and metallic materials. Furthermore, it became evident from the limitations of the prototype that in order to create a digital twin of a building, it is essential to have the building's architectural plan or conduct a survey using a LiDAR equipped laser scanner. Since the Rotes Haus is a historical building and does not have a proper architectural plan, a detailed survey of the building was carried out using a LiDAR equipped laser scanning device.





Figure 65: Das Rotes Haus UAS Frankfurt am Main

Keeping this limitation in consideration, a new approach was developed Figure 66. This involved using IFC-based components, with accurate dimensions and properties of each individual building component, to create a digital twin of the building through precise scanning of the targeted structure. The proposed approach entailed the use of a BIM model to generate a digital twin of the selected building, which can be refined with an increased level of detail in the future if required.

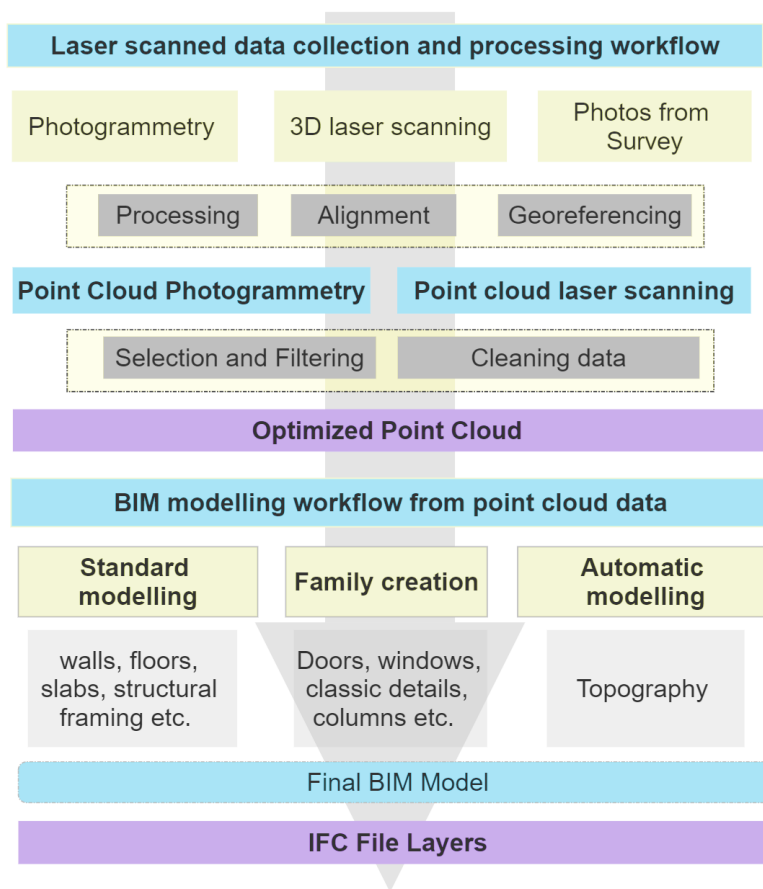


Figure 66: Processing steps for scan to BIM generation adopted from (Rocha et al. 2020)

As previously stated, high LOD is required for the building and its components in 3D flood impact assessment. Thus, stairs, doors, and windows were modelled with greater depth, achieving LOD 4, while other elements such as walls and floors were modelled at LOD 3.5. This is due to the challenge of scanning the components that make up the core of certain parts, resulting in a limited ability to distinguish between inner layers. Consequently, the final model was restricted to the shapes, sizes, locations, orientations, and finishing materials of the building's elements, without the ability to differentiate the inner layers. The model comprises all the elements arranged based on their usage, along with their finishing materials, and when feasible, structural and support components, in addition to the geometric reconstruction of the building. The LOD can be raised by updating both geometric and non-geometric data, such as physical and material performance characteristics, costs, manufacturers, compositions, and others, as needed because the BIM model is not static. Notably, since the 3D building model was constructed solely using IFC components, these components' original functionality can be preserved when integrated with ArcGIS by changing their characteristics to multipatch component/volumetric in nature. It is crucial to note that to perform geoprocessing analysis within an ArcGIS environment, BIM components must be in multipatch format, as identified during the prototype case study.

#### **7.5.1.1 Scan to BIM for Digital Twin**

The central methodology, as illustrated in Figure 66, utilizes the Scan-to-BIM workflow to create a 3D BIM model from a point cloud. This involves two main stages: 3D surveying with laser scanning and processing of the information gathered using various BIM authoring software. The surveying stage employs laser scanner technology, which utilizes electro-optical devices to map points in three dimensions to survey the surface of any object. To create the BIM model, a subsequent "reverse engineering" process was required, which involved shaping the surfaces of a 3D model on the points of the point cloud. Two main categories of 3D surfaces were utilized: (i) NURBS, which precisely and steadily describe complicated surfaces using mathematical equations, and (ii) Meshes, which are made up of polygons whose vertices are the cloud's points and whose sides are the segments that connect them and are ideal for using point clouds. A more realistic simulation was achieved by assigning unique textures to mesh surfaces using survey-related source photographs as the final step in 3D modelling. After the 3D surface model was recreated from the point cloud's trace, semi-automatic algorithms were used to manage the model's data and query it. Autodesk BIM-based computational codes, such as Recap Pro for handling survey data and Autodesk Revit for preparation and final rendering of BIM models, were employed as tools to ensure complete interoperability and success of the Scan-to-BIM technique. The Leica RTC360 model laser scanner was utilized for scanning, which operates by producing a laser pulse and determining the distance from the object detected by observing the laser pulse's roundtrip time.

After adjusting the resolution parameter, which determines accuracy and scanning speed, a single 360-degree scan was completed in 3 minutes and 50 seconds, resulting in a point cloud of nearly a million points. Each point's position is identified by coordinates  $[X, Y, Z]$ , determined by its distance from the instrument, inclination angle, and azimuth angle. To capture all shadow zones and cover an object from different angles, multiple scans using a terrestrial laser scanner were required (Intignano et al. 2021). The overlapping data from multiple scans were edited in Autodesk Recap. To ensure interoperability, the project was exported in a common format file, georeferenced using the Gauss-Boaga system, and scans were coordinated and checked individually. Three scans were performed for

the building chosen in this study, including the complete interior and exterior, outer facades, and two levels, with an additional scan for the storage room. Georeferencing of the LiDAR survey and photogrammetric point clouds was achieved using 11 GPS control points. Collecting various points around the building is crucial in reducing errors in the georeferencing procedure, and it is recommended to perform at least three scans forming a triangle of subsequent laser scanner positions (Rocha et al. 2020).

### 7.5.1.2 Database Managing and Point Cloud Editing

The point cloud database obtained from the three scans was managed and registered using the open-source model CloudCompare. Followed by exploration, checking, alignment, coordination, and georeferencing. Database managing and editing workflow are shown in Figure 67. Once completed, the data from the three scans were combined into a single point cloud file in the e57 format, which was imported into Autodesk Recap Pro. The point cloud was then processed and cleaned up in Recap Pro before being exported in Revit format files.

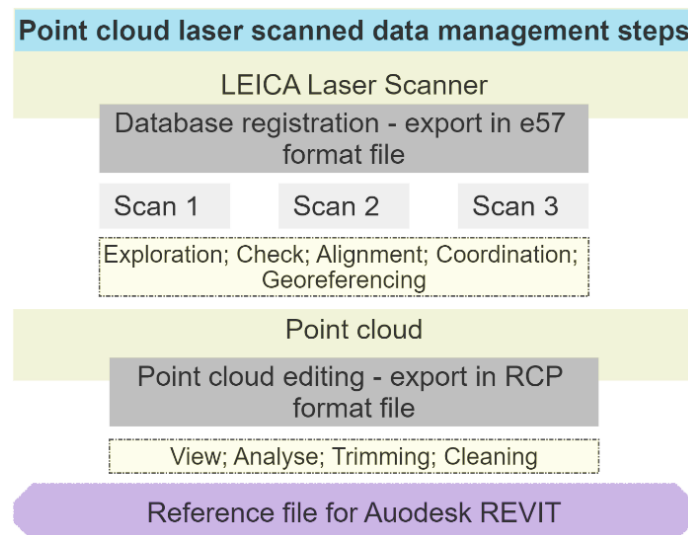


Figure 67: Processing steps for point cloud database editing and management adopted from (Intignano et al. 2021)

### Autodesk Recap Pro - Point Cloud Editing

Prior to commencing the creation of a 3D model of the building utilizing BIM software, it is crucial to conduct several processing steps on the scanned building point cloud data, including the reduction of noise, elimination of imprecise points, and removal of extraneous scene elements that are not relevant to the project (Rocha et al. 2020). The point cloud file was imported into Autodesk Recap Pro and a filter was applied to adjust its density and range. The software also provided the option to select the appropriate geographical coordinate system, with the software itself performing an automatic detection to ease the process. Additionally, the decimation grid, which determines the minimum distance between points, was set as a parameter.

The points in the scanned data were spaced 1mm apart and had a fixed radius of 0.5mm in CloudCompare. This provided an accurate perception of the surveyed items to the human eye. However, this level of detail is not necessary during the modelling phase, so a lighter database was

produced by setting the decimation grid to 5mm. This resulted in significant space savings. Due to the presence of vegetation and greater distance ranges, the accuracy and correspondence between scans for interior areas ranged between 0.50mm and 2.00mm, while exterior areas had accuracy and correspondence between scans ranging from 3.00mm to 5.00mm.

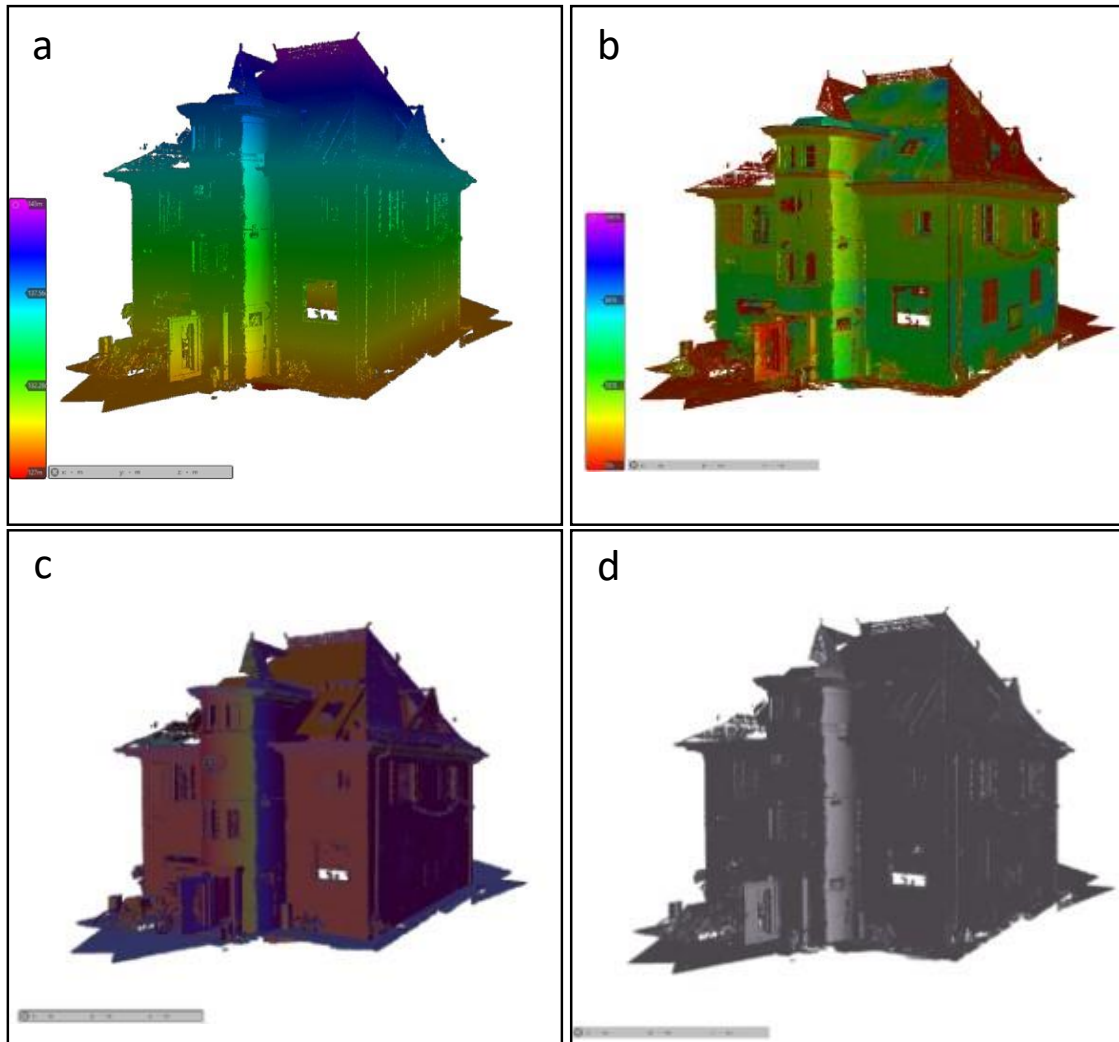


Figure 68: Colorization option; (a) elevation, (b) intensity, (c) normal, (d) scan location

Recap Pro offers several tools that can manipulate the background colour and simulate lighting effects. Here only a few selected were utilized in this research. Specifically, the colour setting tool, which can alter the colour of points based on various attributes such as elevation in Figure 68(a) was used. To highlight differences in height, and intensity see Figure 68(b) tool, and to indicate differences in point density RGB (Red, Green, Blue) tool was used. Moreover, to display the true colours of scanned objects RGB fundamentals, and normal direction see Figure 68(c) to assign the same colour to points lying on the same plane were used. Scan location in Figure 68(d) was also used to distinguish points originating from different scan files in order to obtain a single point cloud from multiple scans. From 'Selection Tools', to allow for the selection of points within a rectangular window, a closed polygon, a plane, or a limit box were basically used. These tools were used to isolate the areas essential for the modelling process, remove unnecessary points, streamline the model, and optimize the performance of the machine and graphic rendering.

The photogrammetric conversion process began by converting raw photos as shown in Figure 69 and ensuring that the white balance was appropriate while minimizing shadows and highlights. Artefacts and unwanted objects such as people, cars, and other elements were also masked. After these steps were completed, the point cloud data was cleaned and all noise and unwanted objects were removed, resulting in a clean 3D spatial point cloud data of necessary building components. While lens distortion correction is an essential component of accurate photogrammetric processing (Intignano et al. 2021), it was not performed in this research due to the internal calibration of the lens distortion.



Figure 69: Raw image from laser scan (left) and revealed image after cleaning (right)

This data can serve as a reliable reference model for creating BIM data. By using the point cloud data as a reference model, the creation of BIM data can be accomplished with a higher degree of accuracy and efficiency. Therefore, at this point cloud data is ready to be utilized for further purposes, such as creating BIM data in this research specifically.

### 3D Modelling of the Targeted Building

3D modelling of the targeted building involves a series of tasks that must be completed in a specific sequence to generate a BIM model (Figure 66). The initial step involves obtaining the coordinates of a point in the point cloud and setting the survey point in Revit to match these coordinates. This process ensures that the model is completed close to the internal origin coordinates to prevent performance issues that may occur when the model is distant from the origin. Revit employs two coordinate systems, the survey point, which represents a real-world position near the model, and the project base point, which establishes the origin of the coordinate project system at (0, 0, 0) (Rocha et al. 2020). The survey point was transferred to the origin without altering its coordinates to guarantee that the ground floor of the building would automatically be placed at level 0 within Revit when the point cloud was inserted. This eliminates the need for manual positioning adjustments, ensuring the accuracy of the model.

In the second step of the process, the point cloud (prepared in the previous section) is imported into Autodesk Revit. To ensure that the point cloud is positioned precisely according to the specified georeferencing coordinates, the shared coordinates option must be used. Furthermore, the point cloud must be fixed within the project to prevent unintended movement or rotation. Even if the point

cloud needs to be unloaded and then reloaded within the same project, these actions are essential to guarantee its consistent placement. By utilizing this positioning technique, users can divide large projects into smaller files and load only what is required at any given moment. The individual components of a partitioned point cloud will consistently load in the correct location thanks to the shared reference. Once the point cloud has been imported and fixed within Revit, the modelling process can commence by reorienting the building within the workspace and visually inspecting it to identify and generate the existing levels.

Defining a new orientation is a critical step in repositioning the building orthogonally within the work plane. Since most structures are built with walls perpendicular to one another, this approach aids in comprehending the geometry and avoiding discrepancies between the model and its intended design. To maintain the georeferencing integrity of the model, the internal project north should be rotated to achieve this new orientation, rather than changing the survey's true north. The determination and construction of the primary levels of the building using the reoriented model are crucial. These levels are necessary for the proper insertion of building elements, the construction of walls and floors, and overall building design. A practical approach should be taken to prevent the creation of unnecessary tiers that would complicate the operation (Rocha et al. 2020).

In the Rotes Haus case study, levels were generated for all floors, including the basement, ground, upper levels, and roofs, following the acquisition of scan data. A hard-coded knowledge-based technique was utilized to detect the building elements from the scan data. The RANdOm Sample Consensus (RANSAC) algorithm is employed to first recognize planes from the laser scan data. The RANSAC algorithm uses sample points from a dataset to iteratively create an estimated plane based on the sample points. Finally, the plane with the greatest number of points from the dataset is selected as the final estimated plane. The planes are then classified into floor, ceiling, walls, and openings (such as windows and doors) based on hard-coded knowledge that includes information on the size (e.g., approximately 11m x 9m for the floor), location (e.g., around 2.5m in height for the ceiling), and orientation (e.g., vertical for walls) of the various architectural elements.

In this study, a modelling strategy was adopted that prioritized the reconstruction of the building's geometry from a macro to a micro scale. The approach involved focusing on the most critical components such as walls, floors, and roofs before proceeding to create additional components and features. This well-structured and practical method enables decision-making and problem-solving efforts to be concentrated on a specific area of the building at a time. For example, when selecting wall-related properties like finish and thickness, there is no need to consider the insertion of doors, windows, or other openings. In multipurpose buildings, walls often exhibit non-uniform thickness, deviations, and non-perpendicular. This is also true for the Rotes Haus, where walls vary in thickness, with exterior shell walls measuring 24cm and internal partition walls measuring 17.5cm. non-perpendicular walls can impede BIM workflow, and thus it is crucial to consider this factor while developing a modelling strategy. Although internal walls at the Rotes Haus exhibited minimal deviations, enabling orthogonal modelling, the external perimeter walls were not entirely rectangular. One wall was found to deviate by over 5 cm from the intended perpendicular angle. In such cases, a model of the wall in its actual position with the appropriate deviation was created to maintain geometric accuracy. The walls were modelled with their respective thicknesses, with accuracy up to 1 cm tolerance. A pragmatic approach was adopted by prioritizing the critical components such as walls,



roofs, and floors before creating supplementary components and other features, facilitating decision-making and problem-solving efforts.

In order to enhance the precision and convenience of the modelling process, a decision was made to differentiate between interior and exterior finishes. This allowed for the generation of a schedule that specifically accounted for the number of finishes associated with each type of application, and it facilitated the implementation of various geoprocessing evaluations via ArcGIS Pro. The modelling approach was executed with careful attention to detail with regard to the integration of floors, beams, walls, and other building components, prioritizing precise intersections and a faithful depiction of the original structure. Nevertheless, certain areas of the model presented challenges due to conflicts, particularly at the junction between upper levels and roofs. These issues were attributed to limitations in the accessibility of these areas and were consequently more difficult to address with accuracy.

### **Family Creation within Revit**

A vast collection of family libraries in Autodesk Revit can enhance the modelling process for BIM workflow, resulting in more efficiency and quicker results. As these families are typically parametric elements, they can be customized to suit particular project demands, leading to enhanced productivity. Nonetheless, the dearth of libraries that cater to the demands of BIM projects involving old buildings necessitates the comprehensive modelling of these families. With Autodesk Revit, a highly versatile and advanced modelling software, we can create families either within the project or externally using the family editor. Regardless of the approach, the element can be categorized appropriately to ensure that it functions correctly within the project as a family designed for this purpose. For instance, in the case of the Rotes Haus project, all external doors, windows, and access hall doors were either modelled and created or adopted as per the specification. Additionally, internal doors were adapted from existing elements within the native software library. It is important to note that traditional point cloud file formats are not supported in the Revit family editor. Therefore, to incorporate it into the family editor, the points that pertain to the objects to be modelled have to be extracted and exported in dxf format, which was carried out by utilizing Autodesk Recap.

One additional challenge pertains to the default modelling of doors and windows in Revit, which involves a rectangular wall insertion cut. However, for old buildings with thick walls, the cut typically incorporates both horizontal and vertical chamfers. Consequently, the utilization of existing families is precluded, and novel ones must be generated utilizing various Boolean operations, such as sweep, extrude, revolution tools, and empty forms, to incorporate the different wall cut types. The process of creating customized families can be intricate and time-intensive, with highly parameterized elements necessitating a similar level of effort to that required for modelling an entire building. To optimize efficiency and minimize redundant labour, it is crucial to determine the intended function of the family before beginning the modelling process. At Rotes Haus, similar families were identified and subsequently modified based on requirements, with careful consideration given to which dimensions would need to be parameterized. This approach allows for the efficient use of the same window family in multiple scenarios, resulting in a reduction of modelling time. In addition to doors and windows, other elements such as roof and facade profiles, stairs, handrails, and columns were developed as specific families.

The structure features two internal staircases, each with its distinct design philosophy. One remarkable aspect is that each run possesses a unique floor height. Consequently, utilizing the default Revit tool to model the stairs, which ensures that every step has the same height, would result in a considerable discrepancy between the floor height and the central landing. To prevent such significant deviations, it was deemed necessary to divide the creation process into two phases. The first two runs were set at a floor height of 17.75 cm, while the third run had a floor height of 20 cm. Likewise, the non-uniform nature of geometry and the presence of imperfections in real-world structures must be taken into account when making decisions and selecting approaches. To ensure that the model accurately reflects the building's geometry and visual appearance and meets the desired requirements based on reality, it is critical to undertake the modelling process with care and meticulous attention to detail.

### **Automation in Topography Creation**

Despite the case study building's steady sloping topography and minimal deformations, the manual modelling process was still labour-intensive and prone to inaccuracies. To overcome these challenges and improve efficiency, an external Revit plugin known as "Scan Terrain" was utilized. This plugin automates the generation of a topographic surface using point cloud/LiDAR data, allowing users to specify various parameters such as crop size, point distance, and maximum surface point height (Messaoudi and Nawari 2020; Rocha et al. 2020). Although the use of this plugin minimizes effort, a visual inspection and manual correction of erroneously generated points is still necessary. The plugin algorithm can identify horizontal surfaces while avoiding vertical objects like walls and furniture. However, some features such as steps, floors, and plants may still be mistaken for topography. The plugin's performance can also be affected by irregularities in the point cloud, incomplete scanning of certain areas, and partial coverage of vegetation. Therefore, prior to using the plugin, it is crucial to clean the point cloud and eliminate unnecessary objects. This approach significantly enhances model quality and accuracy while reducing modelling time. Moreover, when the topography is adequately cleaned, it can be seamlessly integrated into GIS for further geoprocessing analysis without any issues.

### **Plausibility Check and Rendering (Model Processing)**

Upon completion of the modelling process, a BIM model was obtained with a high degree of accuracy and precision as depicted in Figure 70, containing a level of detail between LOD 3/3.5 in accordance with the Project Building Information Modelling Protocol Form (AIA 2013). Rocha et al. (2020) likewise utilized analogous verification measures in their investigation. The final model not only contained all architectural elements (with exact geometry and dimensions) but also included modelled structural building elements, the roof, beam columns, stairs etc. Parametric families for doors and windows were created, enabling their usage in similar projects, and simultaneously producing a verified library. Along with the BIM model, the complete set of plans with floor plans and elevations were generated (see appendix).



Figure 70: BIM-IFC based 3D model of the selected building – Das Rotes Haus

## 7.6 GIS-BIM Integration

The incorporation of BIM into GIS as the fifth phase is a crucial step in the model's development. This stage acts as the model's backbone, enabling essential data integration and modifications through intermediary processes, laying the groundwork for 3D flood impact assessment. Therefore, in this phase, all the prepared data, such as hydrodynamic flood simulations and scan-to-BIM data, are integrated into a single spatial medium to facilitate further processing and analysis.



Figure 71: 3D BIM-IFC based building inside ArcGIS Pro after integration

To achieve the integration of GIS and BIM, a novel methodology outlined in section 6.7 and illustrated in Figure 53 and Figure 54 was implemented. This approach enabled the successful integration of 3D flood spatial information with a spatial 3D BIM model. Figure 71 depicts the 3D flooding along with 3D BIM based building as well as 3D surface block geometry buildings representation.

## **7.7 Building Component Vulnerability Scenarios**

To assess building component vulnerability and impact, two scenarios were evaluated. In the first scenario, which was considered a block structure, floodwater was prevented from entering the building. The second scenario allowed floodwater to penetrate inside the building. The impact of floodwater, including pressure and forces, was calculated for both scenarios. Additionally, analytical methods were employed to evaluate the impact on external and internal walls, doors, windows, floor covering, utilities, eave lining, and ceilings.

## **7.8 3D Flood Impact Assessment with 3D Digital Twin (3D-FIA)**

3D flood impact analysis is carried out with a suitable method developed for the assessment and calculation of a justified subset of potential flood impacts on a building and its different components by creating a digital twin. This section describes how all flood actions (water contact/interaction, hydrostatic pressure, hydrodynamic pressure, debris effect, drag side effect and impact force), as explained in section 6.8, were partially automated through a novel workflow for 3D assessment and calculation. This approach not only identifies the building's structural and non-structural components that are directly or indirectly affected by floods but also visualizes them in 3D digital twin. Similarly, for every component impacted by flooding, the pressures and forces exerted by the different flood actions were measured and automatically visualized in 3D. Moreover, the calculated pressure and force are also exportable to other software for further analysis such as structural analysis for building stability and material analysis for water sensitive materials and components.

The followings are the procedures and methods utilized to automatize the developed digital twin for each flood action and perform 3D flood impact assessment on different building components. This means that each flood action, such as water contact/interaction, hydrostatic pressure, hydrodynamic pressure, debris effect, drag side effect, and impact force, is evaluated and integrated into this model for a comprehensive 3D assessment of the building components impacted by the flood. This also ensures that all possible flood scenarios are accounted for in the assessment, and the integration enables the visualization and calculation of the pressure and force exerted by each flood action on each component. The automation of the developed 3D digital twin for each flood action allows for a more accurate and detailed assessment of the potential impacts of flooding on the building and its components.

### **7.8.1 Floodwater Interaction**

This section presents a novel method for calculating and assessing the interaction between floodwater and buildings and their components in 3D. This interaction refers to the damage caused by floodwater, whether fresh or contaminated, coming into contact with water-sensitive elements of a building. These intersection components can provide valuable information for flood risk assessment and management, such as identifying areas of the building that are most vulnerable to flood damage.

According to various studies, water interaction is highly relevant see Table 1 in FRM and must be evaluated for effective management (Kelman and Spence 2004; Thieken 2006; Nadal et al. 2010; Moel et al. 2015). From section 2.6, it can be concluded that this action is predictable if proper flood parameters such as the spatial distribution of inundation depth and information about building components such as area, dimension, and material are available. As in the developed digital twin for this research, these necessary parameters, i.e., the spatial distribution of flood inundation depth and detailed building components with their semantic properties, are already integrated. Thus, a processing system can be developed to evaluate and assess this flood action automatically.

The use of digital twin technology enables the automation of assessing and visualizing flood influences on building components in 3D. This technology also allows for the automatic computation of the wetted parameter (surface area) of various building components (structural and non-structural) that directly interact with the flood water. This includes identifying the area of a specific wall that is affected by flooding. Additionally, the coding behind this process distinguishes between different components, allowing for the identification of overlaps, such as walls with openings for windows or ventilation. These openings were excluded automatically, and the intersected area of the wall without opening areas are presented. The model provides separately intersected areas of included windows, doors, or other components inside or over the wall. In order to perform flood interaction assessment in 3D, a 3D geoprocessing approach was chosen. "Intersect 3D" is a tool in ArcGIS Pro that enables the intersection of 3D features. To calculate the intersected areas, flood depth (multipatch) and BIM building components (multipatch) are used in conjunction, it then provides valuable information about the impact of flooding on buildings and their components. As explained in section 6.7.1 the flood depth multipatch file represents the height of floodwater in 3D, while the BIM building components represent the various components of the building. By using the Intersect 3D tool, these two datasets can be overlaid to identify the areas where the floodwater and building components intersect. Therefore, this 3D geoprocessing tool was incorporated into the developed digital twin.

The Intersect 3D requires important parameters to be considered. These parameters include input and output features, tolerance, join attributes, and output type. The accuracy and usefulness of the output features can be affected by these parameters, which can be optimized by choosing appropriate input features, tolerance, and output type. Similarly based on the limitations identified and lessons learned from the prototype case study (section 6.8.1). To work with the Intersect 3D tool, several additional requirements must be met. Firstly, the input datasets must be in "multipatch" format. Additionally, the multipatch element must be closed, which can be checked using the "Is Closed" tool. Finally, the georeferencing system and coordinates must be exact to perform accurate analysis. Following these requirements can ensure the proper functioning of the Intersect 3D tool.

To automate this process developed digital twin python scripting (see appendix) was used. The result of this process is a set of intersection components that shows the areas where the floodwater is in contact with the building components. For instance, the intersected output can be used to obtain the wetted perimeter or intersected area of the structural component walls. Figure 72 shows only intersected components (structural and non-structural) lying inside the area of flooding depth and Figure 73 shows intersected outer walls, windows, and doors.

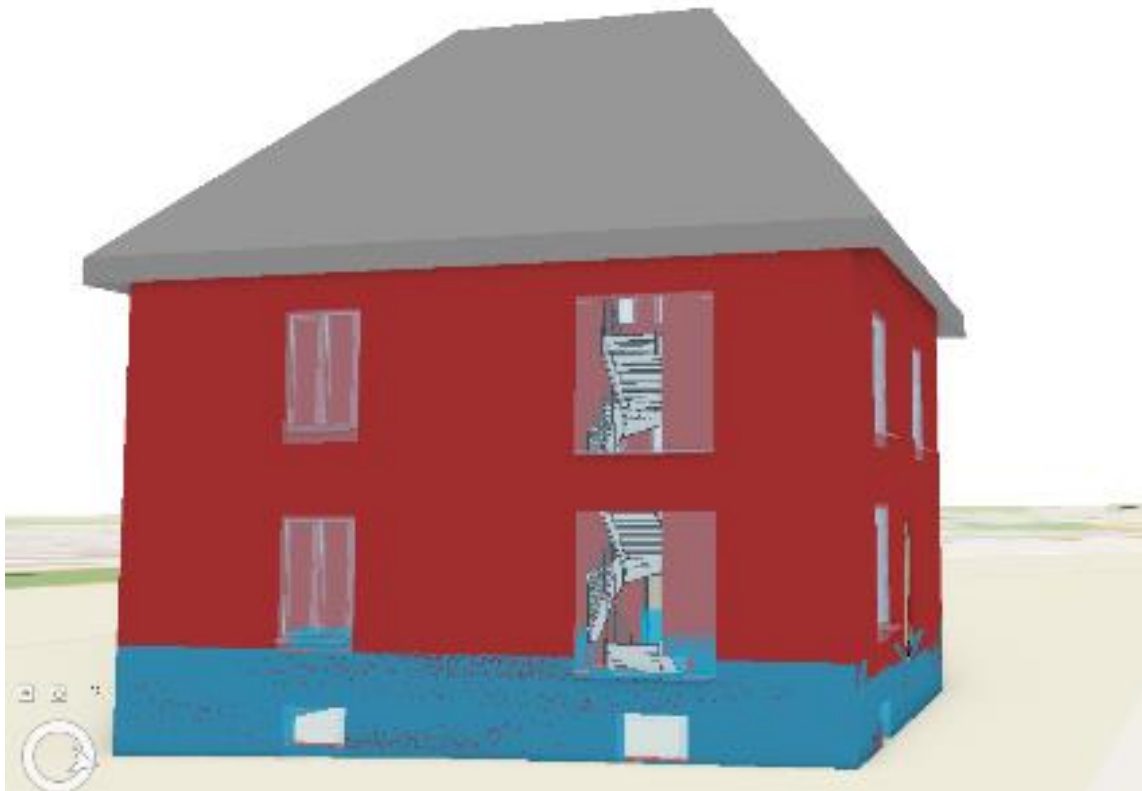


Figure 72: Intersected building components with simulated flooding

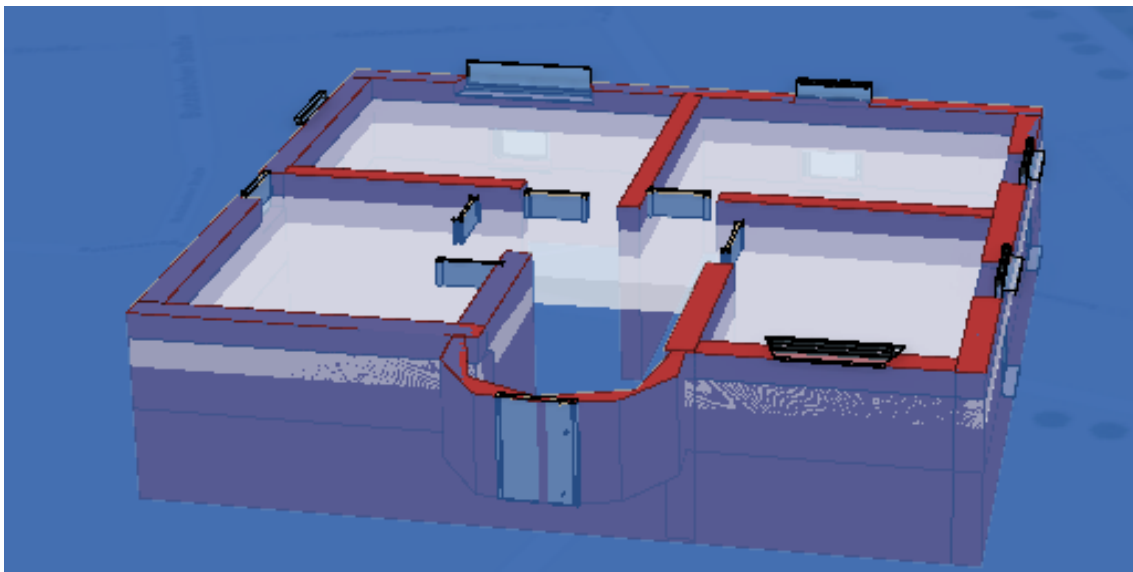


Figure 73: Intersected walls, doors, and windows of the building with simulated flooding

In order to simplify the analysis in this study, appropriate names were assigned to different building components. In hydrological terms, the side of the building facing the flow direction of the flood is referred to as the frontal side, which in this case study is the Northern side due to the North-South flow direction in the study area as depicted in Figure 74. This side is commonly known as the upstream side and is considered the most vulnerable side of the building to flooding. By performing hydrodynamic flood simulation in section 7.4, along with the outputs of flood depth and velocity, a comprehensive view of the flooding in the selected case study is obtained, as illustrated in detail in Figure 63.

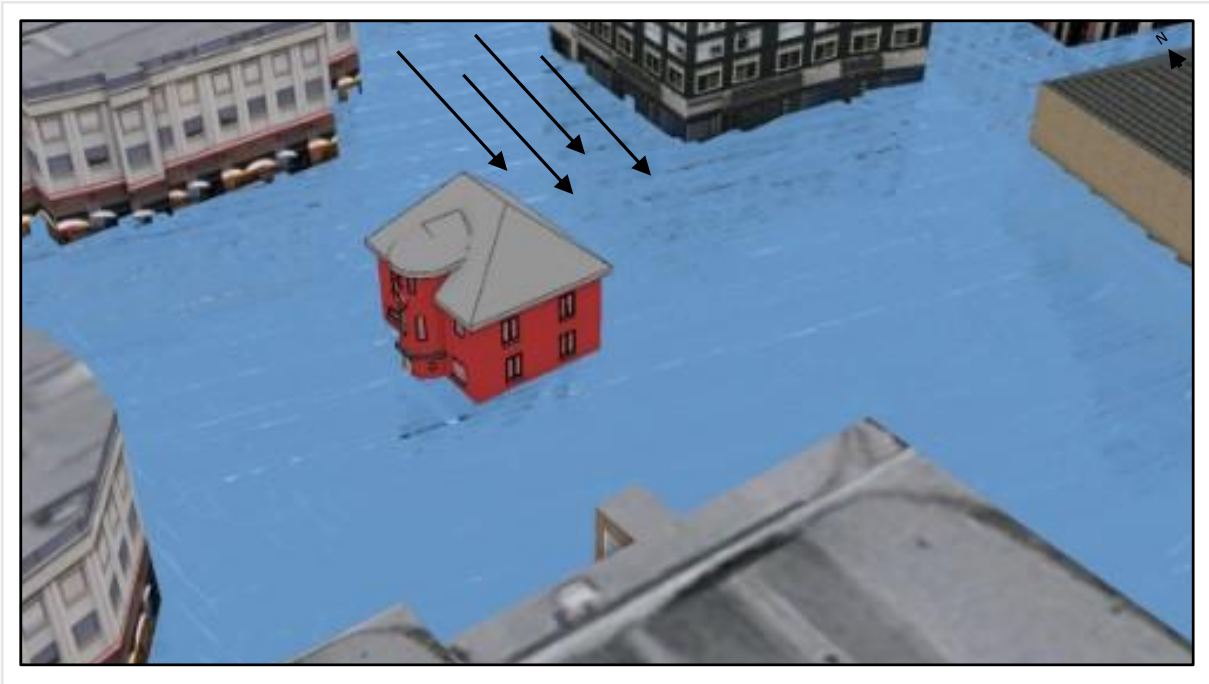


Figure 74: Flow direction of flooding in the study area with respect to targeted building

Three main walls on the frontal side of the building are most vulnerable to flooding see Figure 75a. These walls are outer facing walls at various height elevations. Of these three walls, two of them are basement walls, where one of the basement walls is exposed to flooding directly due to above the ground level. The detailed figures in the appendix represent the levels developed in the Revit BIM model for this building. The exposed basement wall is from level 0 to level 1. It also contains a ventilator as an opening. In this research, this basement wall from level 0 to 1 is called as front exposed basement wall. Similarly, the wall at ground floor level starts from level 1 to level 2 is called as front ground floor wall. Due to the fact that the front ground floor wall is partially exposed to the flooding. For all other side walls of the building similar distinctive names were given in order to avoid confusion.

Moreover, the opposite side of the frontal side is called a back side with similar levels of detail and names of the basement walls that are in accordance with the sides of the building. Thus, the southern side of the building is called as backside and all the walls on the backside are named as back basement wall, back exposed basement wall and back side ground floor wall and others Figure 75b. Similarly, the western side of the building is taken as the right side Figure 75c and the eastern side is taken as the left side Figure 75d of the building. The walls of these sides are named in accordance with the naming provided in this research. It is important to acknowledge that the depth of water in front of a building is significantly influenced by the terrain of the surrounding area, and this factor is automatically accounted for in the model.

### Total Surface Area of Walls

All the input parameters used in 3D intersect are volumetric elements (multipatch), therefore, flood intersected output is also in the form of volumetric element (multipatch). This also results in provision of volume of intersected walls with flood water. Therefore, the surface area of the wall intersected is based on all faces of the wall, which is added up to make the total surface area of the wall. In order to understand the total surface area, the following equation is determined:



$$\text{Total surface Area of a Wall } (SA_t) = W_o + W_i + W_l + W_r + W_d + W_u \quad \text{Equation 13}$$

Whereas  $SA_t$  is total surface area of the wall intersected with floodwater.  $W_o$  is the surface area of the outer face of the wall.  $W_i$  is the surface area of the inner face of the wall.  $W_l$  is the surface area of the left face of the wall.  $W_r$  is the surface area of the right face of the wall.  $W_d$  is the surface area of the down face of the wall.  $W_u$  is the surface area of the upper face of the wall. This is also illustrated in the following Figure 76.

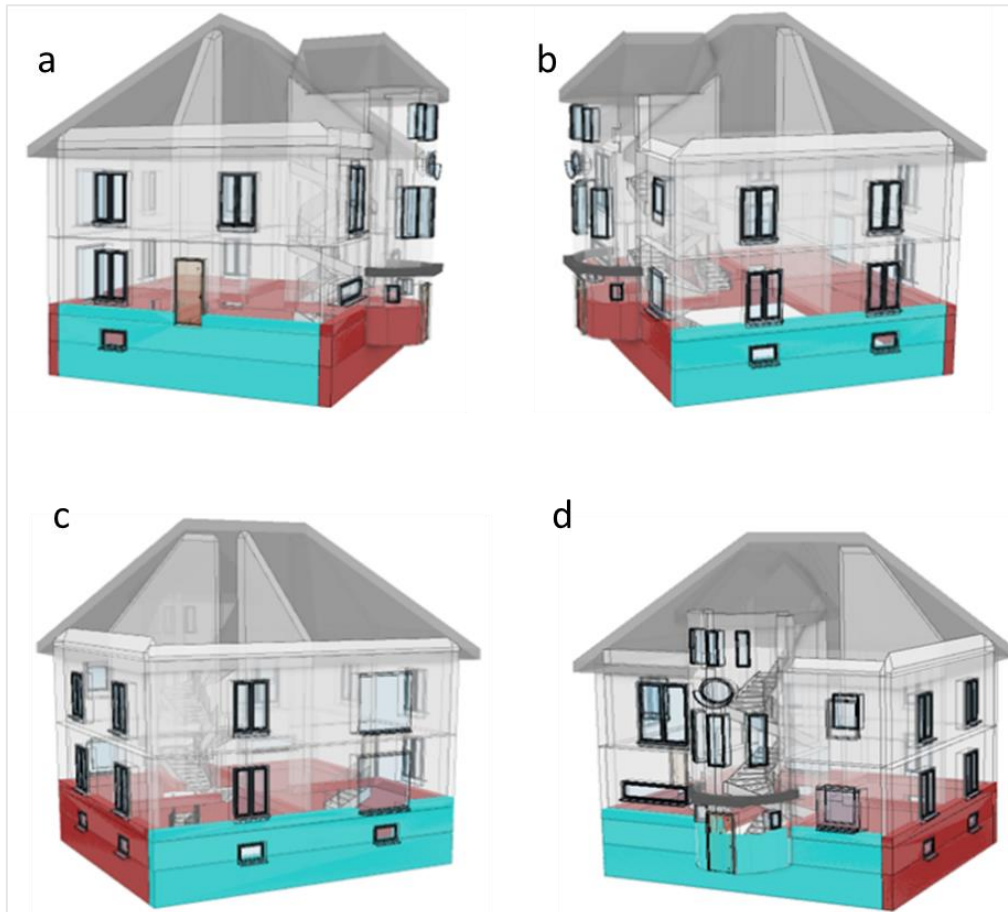


Figure 75: Building under investigation (a) frontal side (upstream side); (b) back side (downstream side); (c) left side (parallel to flow direction); (d) right side (parallel to flow direction)

Precise determination of the impacted areas on each wall due to various flooding actions is crucial for accurate evaluation. Accurate surface area calculations facilitate pressure assessments on the wall components to determine their capacity to withstand the applied pressure. Therefore, it is imperative to calculate the area of the wall that intersects with flooding. Despite the small size of the selected building, it has numerous outer walls, making manual calculation of this area a laborious and observation-intensive task. However, the 3D model used here automatically provides the surface areas of intersected walls following the interaction of floodwater with the building shown in Figure 77. This provides a powerful visual depiction of the walls that have been intersected, alongside a comprehensive comparison of the wetted perimeter (i.e., the surface area in contact with water) for each side of the affected building. By presenting this information in a clear and concise manner, the figures serve as a compelling reminder of the potential impact of flooding on building structures.

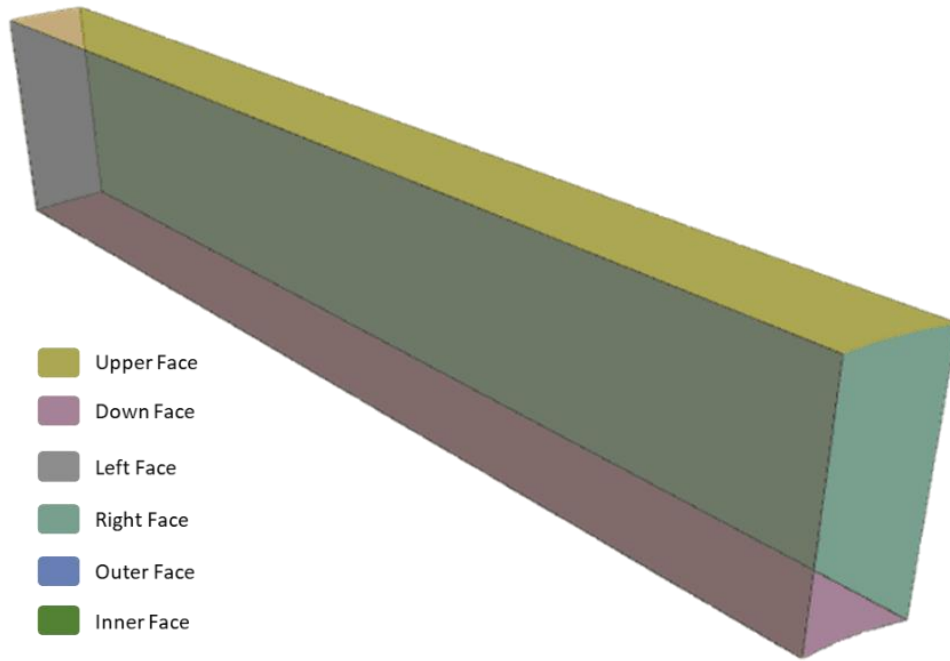


Figure 76: Visualization of volumetric components with information of all the faces

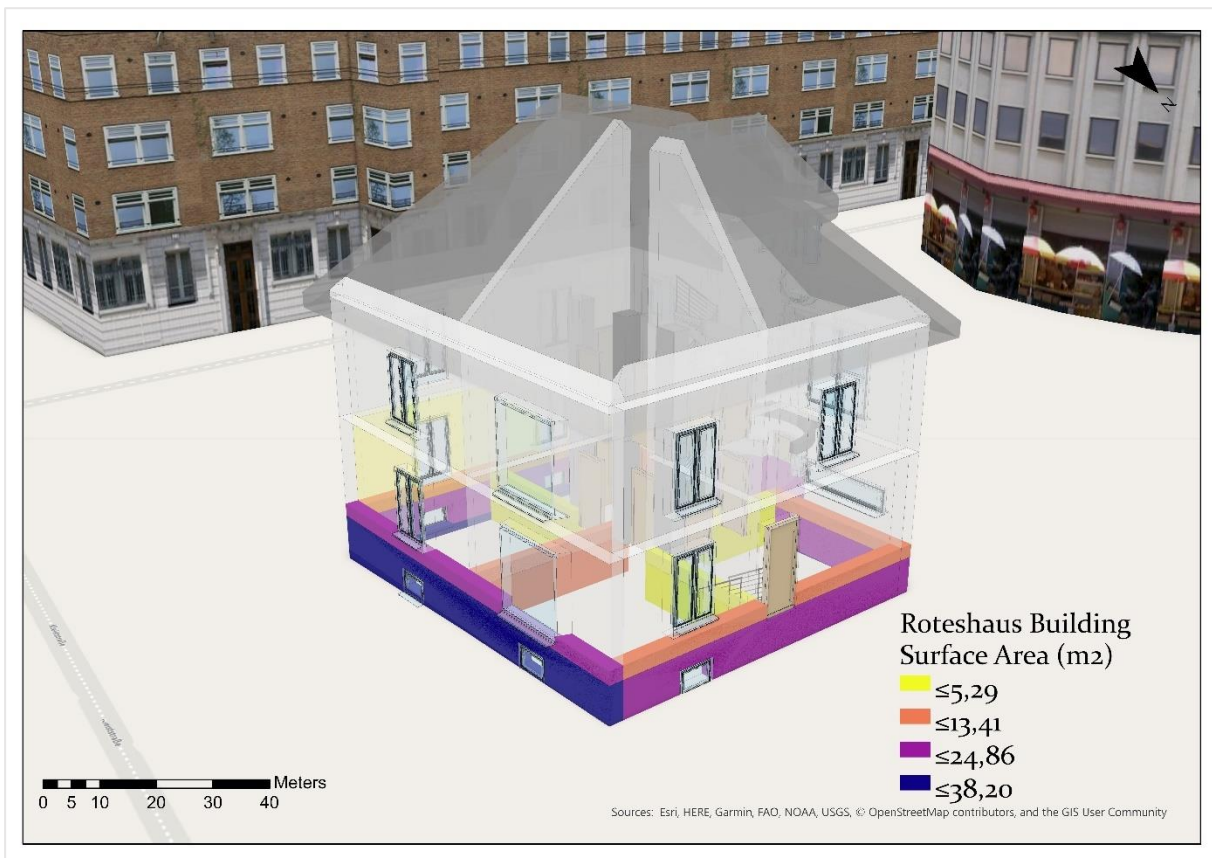


Figure 77: 3D visualization of surface areas of flood intersected walls

### Frontal Walls

The frontal side walls are most vulnerable due to direct flow impact. Therefore, their impacted area is crucial to know. A comprehensive understanding of the potential impact of flooding on walls is

important to consider. Therefore, Figure 78 offers a visualization of the frontal walls intersected by floodwater based on hydrodynamic flood simulation depth on the upstream side. Complementing this information, Figure 79 presents submerged surface area of each wall that is intersected, offering valuable insights into the magnitude of the potential damage. Together, these figures provide compelling evidence for the importance of considering flood-related risks in the design and construction of buildings, particularly when it comes to wall structures.

By default, the 3D model computes the total surface area of the front basement wall as 30.9 m<sup>2</sup>, and of the front exposed basement wall as 24.52 m<sup>2</sup>. Depending on the depth of the simulated flood upstream, the front wall of the ground floor is partially intersected with the flood, resulting in a total surface area of 12.05 m<sup>2</sup> for the intersected part of the front ground floor wall. It is important to note that this total surface area pertains to the respective building components and not the building as a whole.

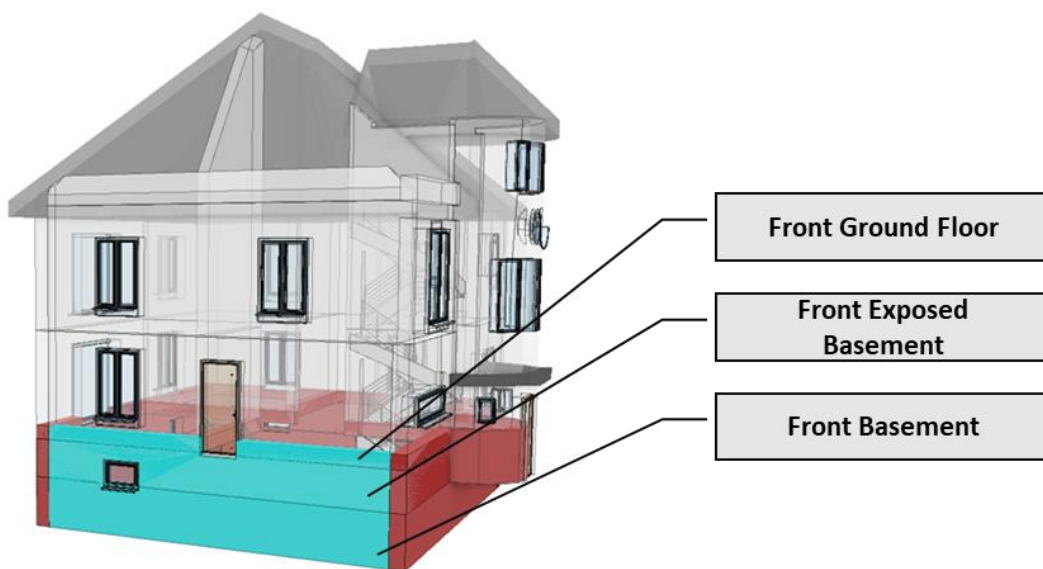


Figure 78: Highlighted frontal side (upstream side) flood intersected components (walls, ventilation, and door)

Moreover, the 3D digital twin model focuses on wall components and automatically excludes the surface areas of windows, doors, and ventilators from the total surface area of the intersected wall component. For instance, the surface area of a ventilation opening at Level 0 (Ground Level) is excluded from the total surface area of the exposed front basement wall in the developed 3D model. In the same vein, the model automatically excludes the surface area of the partially intersected door from the frontal ground floor wall. Additionally, the respective surface area of the partially intersected door and ventilation duct on the front side can be observed in Figure 80, as computed separately by the model.

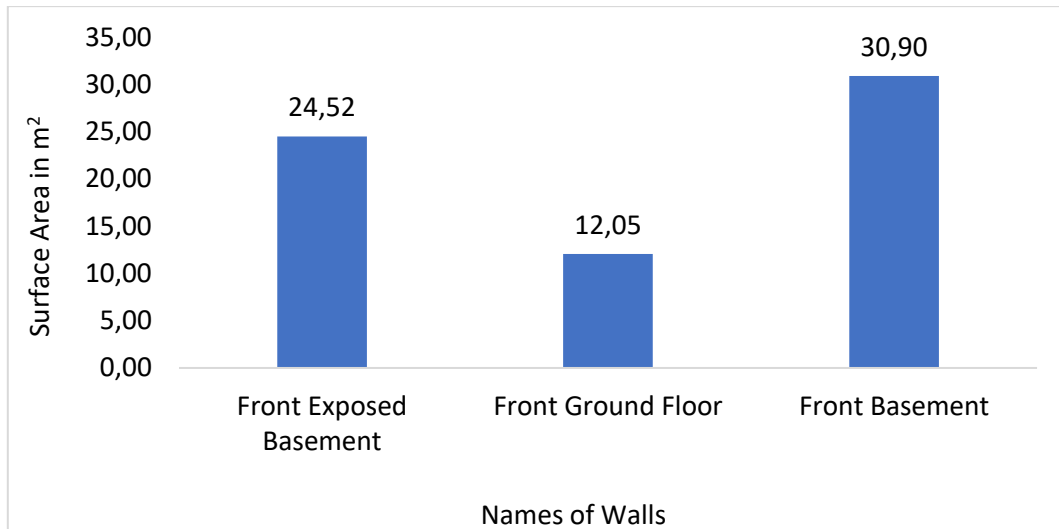


Figure 79: Comparison of surface area of flood intersected walls (frontal wetted perimeter)

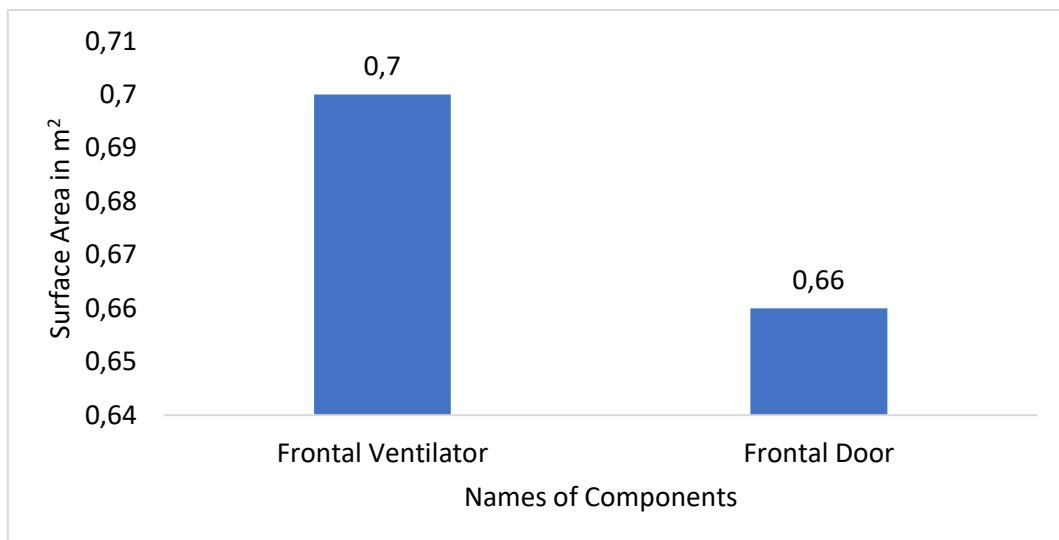


Figure 80: Comparison of outer frontal side non-structural components intersected surface area

### Backside Walls

The south face of the building is designated as the backside of the building as it is located opposite to the upstream side. Based on hydrodynamic flood simulation depth on the downstream side three walls, two ventilation ducts in the exposed basement wall, and two windows in the ground floor wall, all of which are intersected with the flood see Figure 81. Due to automatic computation, the 3D digital twin model determines the total surface area of the back basement wall as 32.15 m<sup>2</sup>, and of the exposed basement wall as 24.86 m<sup>2</sup> as shown in Figure 82. Similarly, the backside ground floor wall is partially intersected with an area of 13.41 m<sup>2</sup>. The intersected surface area of the ventilation and partially intersected windows can be observed in Figure 83.

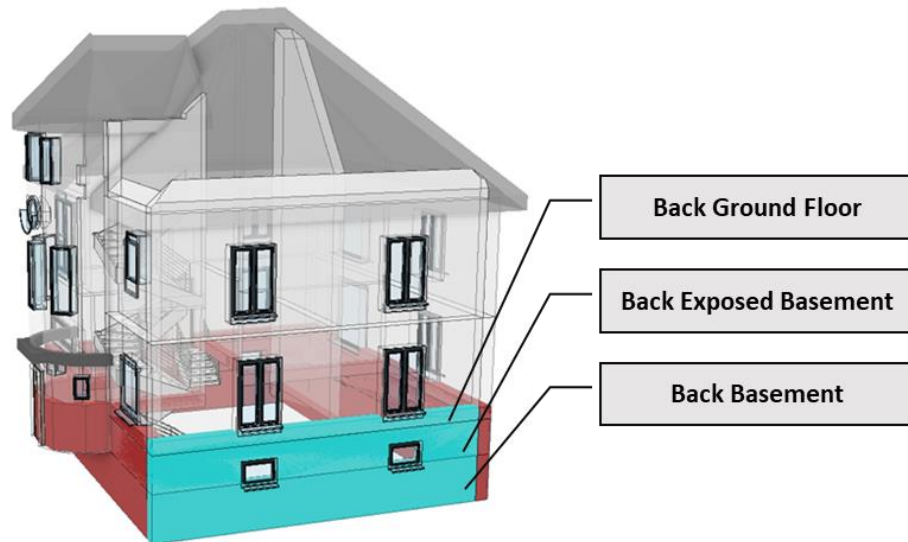


Figure 81: Highlighted back side (downstream side) flood intersected components (walls, ventilation, and windows)

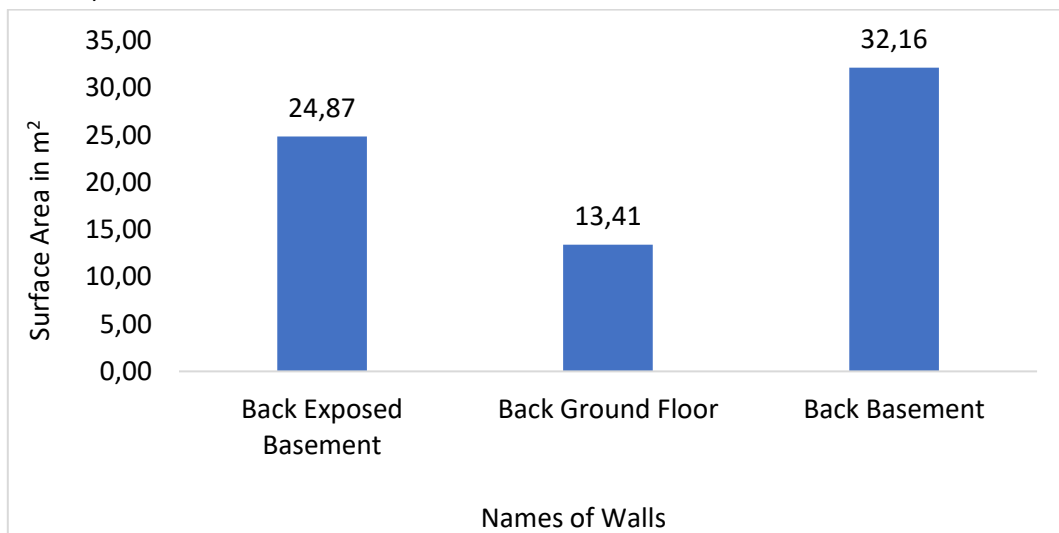


Figure 82: Comparison of surface area of flood intersected walls (backside wetted perimeter)

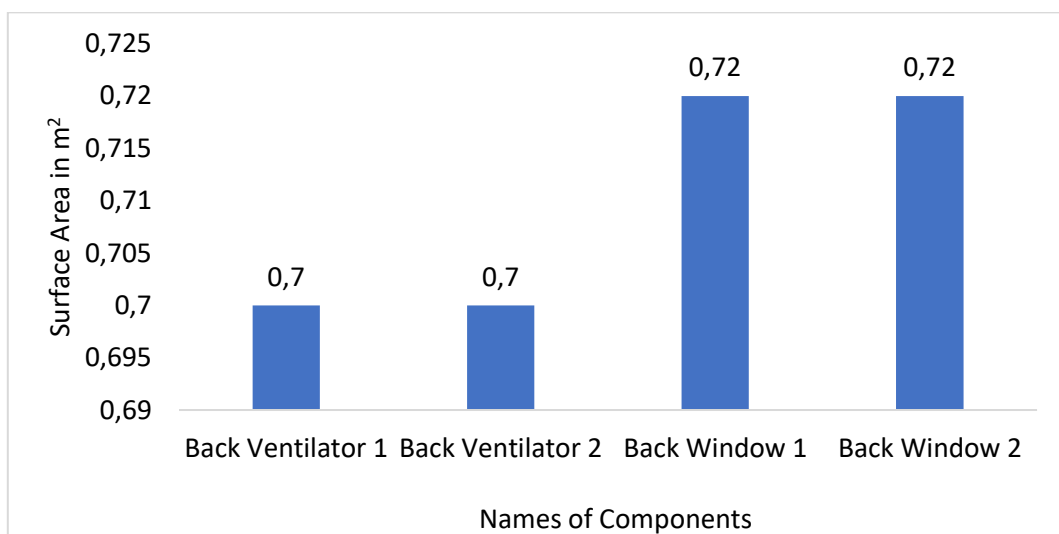


Figure 83: Comparison of outer back side non-structural components intersected surface area

### Left Side Walls

The east side of the building runs parallel to the flow direction, it is designated as the left side of the building. However, based on hydrodynamic flood simulation depth, this critical side of the building has suffered significant damage, with three outer walls, two ventilation ducts in the exposed basement wall, and two windows in the ground floor wall all being intersected by the flood, as clearly illustrated in Figure 84. Upon calculation, the 3D model determines the total surface area of the left basement wall as 38.20 m<sup>2</sup> and of the exposed basement wall as 29.863 m<sup>2</sup>. Similarly, the left side ground floor wall is partially intersected with an area of 15.53 m<sup>2</sup> (Figure 85).

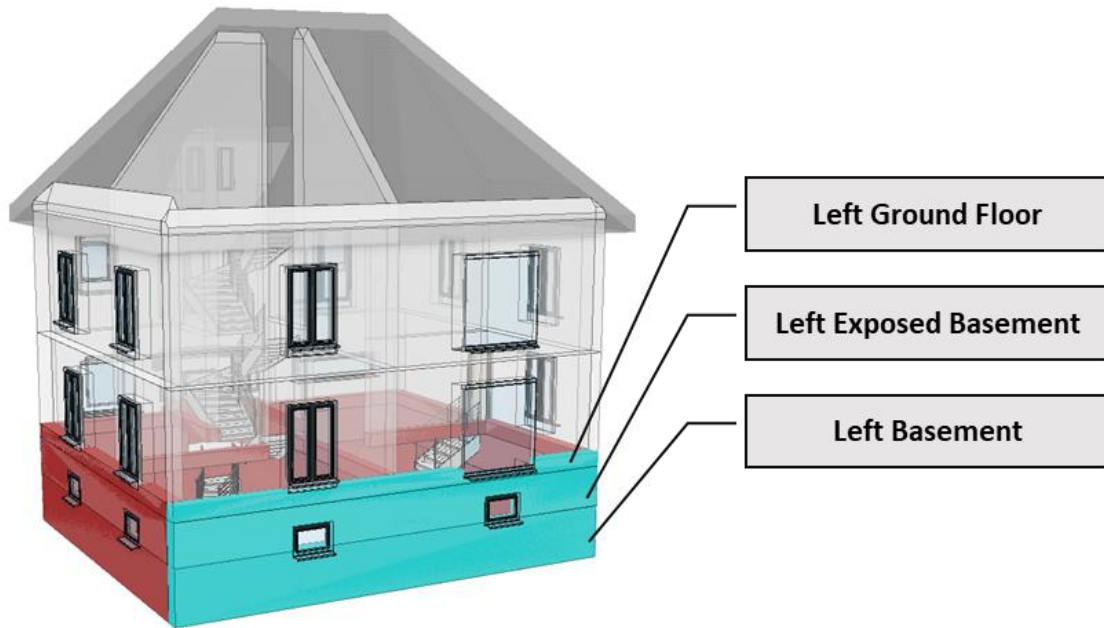


Figure 84: Highlighted left side (Parallel to flow) flood intersected components (walls, ventilation, and windows)

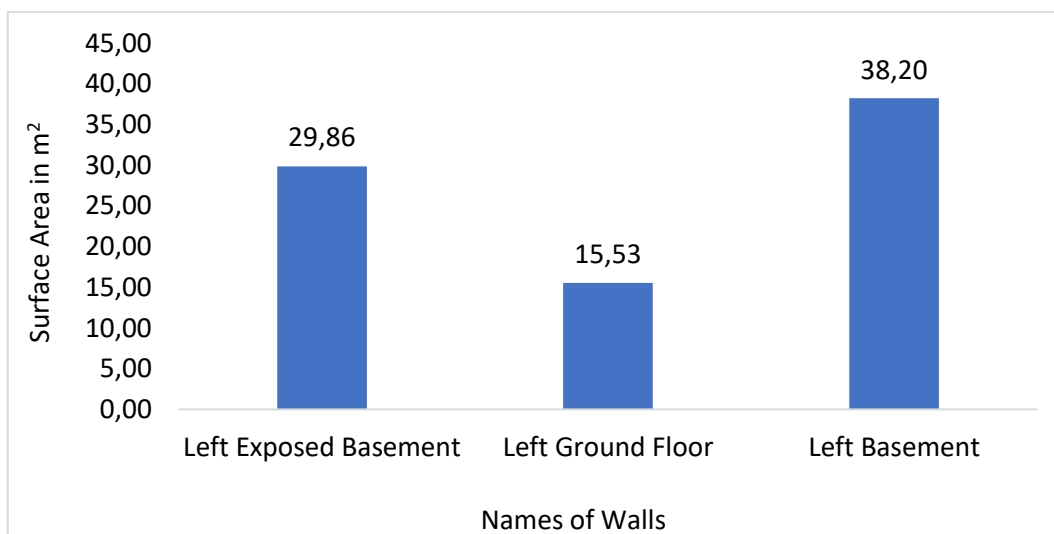


Figure 85: Comparison of surface area of flood intersected walls (left wetted perimeter)



Similarly, the intersected surface area of the ventilation and partially intersected windows can be observed in Figure 86.

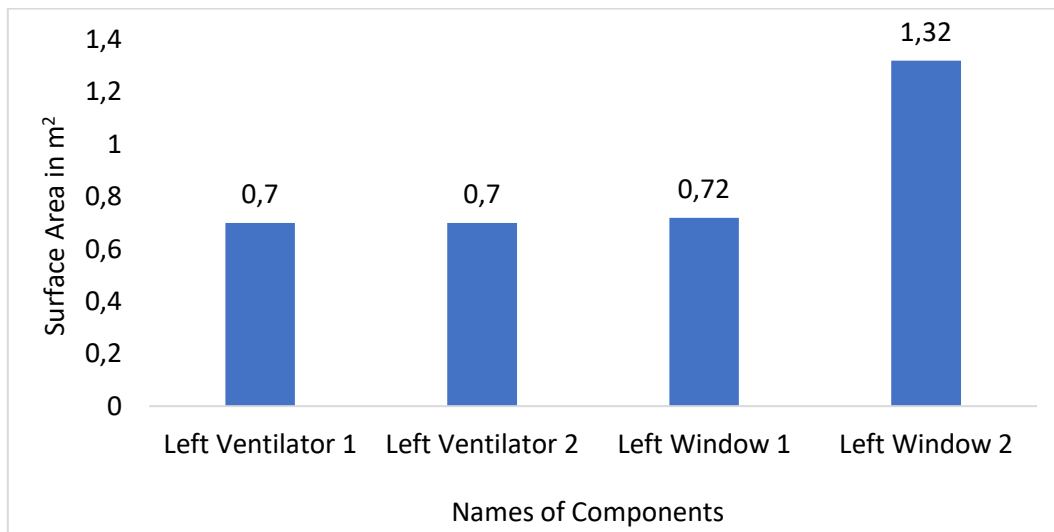


Figure 86: Comparison of outer left side non-structural components intersected surface area

### Right Side Walls

The West side of the building, which serves as the main entrance, is designated as the right side of the building due to its parallel alignment with the flow direction. This vital area of the building has suffered severe flood damage, with six exposed walls, one window in the ground floor right-side wall 1, and the entrance door all being intersected by floodwater in Figure 87.

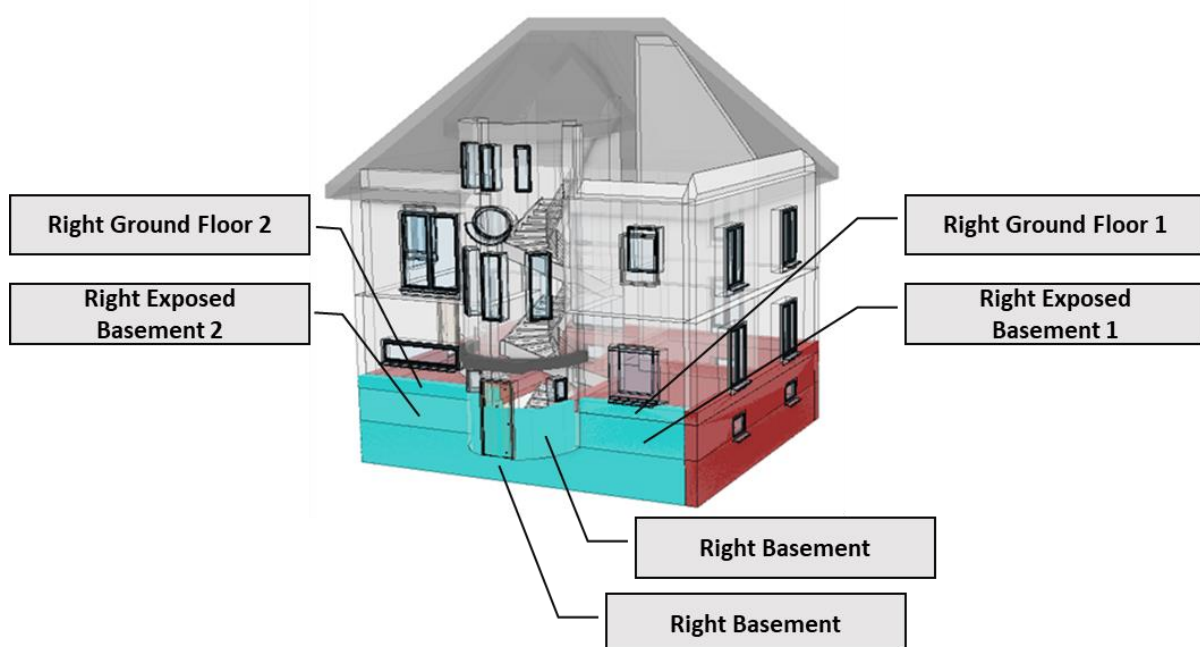


Figure 87: Highlighted right side (Parallel to flow) flood intersected components (walls, door, and window)

The intersected exposed basement walls around the entrance arc have a total surface area of 10.87 and 13.69 m<sup>2</sup>. Similarly, the ground floor walls have an intersected surface area of 5.01 and 7.04 m<sup>2</sup>, as depicted in Figure 88.



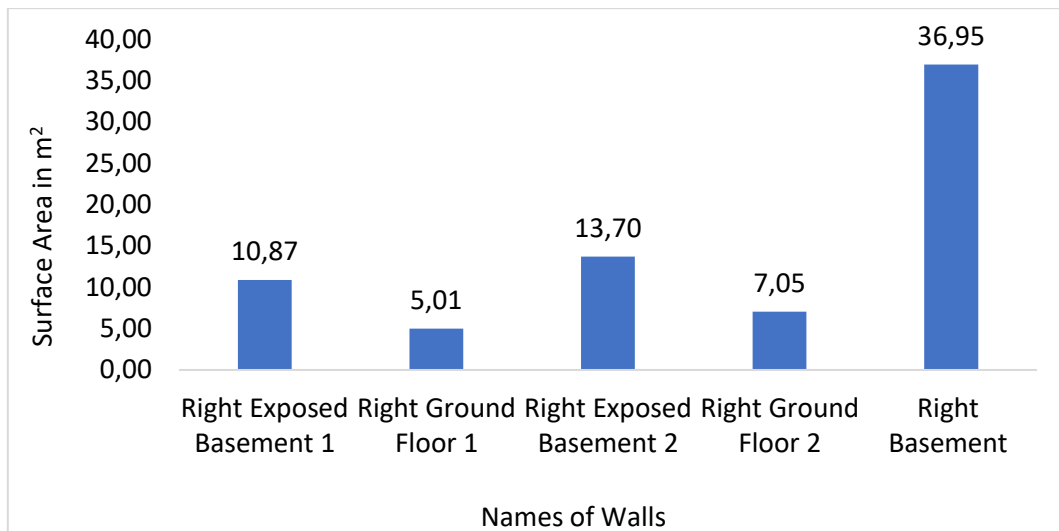


Figure 88: Comparison of surface area of flood intersected walls (right wetted perimeter)

Figure 89 provides critical information on the surface area of both the partially intersected door and window on the right side of the building.

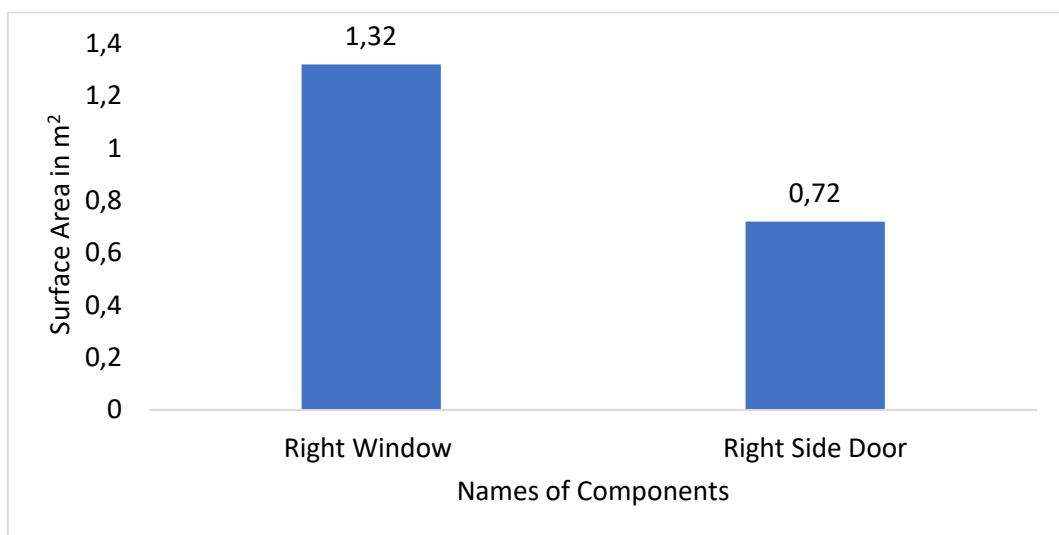


Figure 89: Comparison of outer right side non-structural components intersected surface area

#### 7.8.1.1 Adjustments to Extract Face Area

As previously mentioned, the default settings of the developed digital twin model calculate intersected areas based on all faces of the components, including outer, inner, upper, left, and right faces as shown in Figure 76. However, when evaluating the pressure on a wall, it is necessary to determine the surface area of either its outer face or its inner face, or both, since floodwater can interact with either or both faces of a building component. Therefore, it is necessary to calculate the surface area of the outer ( $W_o$ ) or inner ( $W_i$ ) face of a wall from the total intersected area of the wall. In this regard, after many iterations, an equation has been derived which is as follows:

$$\text{Outer/inner face Surface Area } (W_{o/i}) = \frac{SA_t}{2} - (SA_t \times 30\%) \quad \text{Equation 14}$$

Equation 14 denotes that the overall surface area of the intersected walls component takes into account the surface areas of all faces of the walls. Thus, to obtain the surface area of the outer face of a particular wall, it is necessary to remove the surface areas of the inner, upper, lower, left, and right faces of the wall. Whereas in this equation  $W_{o/i}$  is outer or inner face,  $SA_t$  is the total surface area of component, in this case, its total surface area (all sides) of a specific wall.

The inner face surface area is equal to the outer face surface area of the wall and can be easily calculated by dividing the total surface area in half. On the other hand, the surface areas of the left-right and up-down faces (see Figure 76) are calculated as 30% of the total surface area and are thus subtracted from the total surface area to determine the outer face surface area ( $W_o$ ). The equation mentioned above has been incorporated into a new field in the attribute table of the intersected walls in the digital twin model to compute their outer surface areas. This computation is done using the "Field Calculator/Calculate Field" feature.

### Verification of the face area extraction

In order to verify the validity of the derived equation, a basement upper wall that was fully submerged was selected. The calculated outer surface area ( $W_o$ ) in the ArcGIS attribute table was compared with the actual outer surface area in the Revit model during BIM modelling, as shown in Figure 90 and Figure 91. This comparison demonstrated that the computed surface area of the outer face of the wall using the derived equation was exactly the same as the geometry of the Revit model, which is accurate. A few more walls were also manually verified using this method to completely validate the equation.

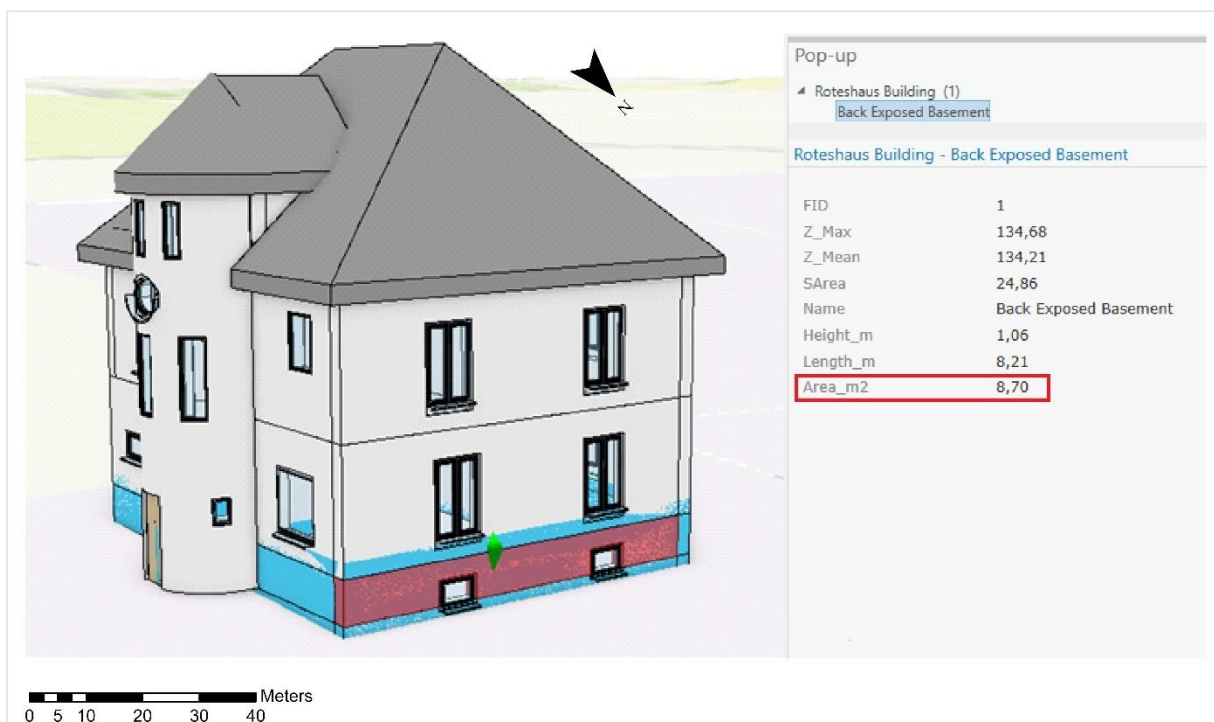


Figure 90: Left exposed basement wall outer face area in ArcGIS Pro

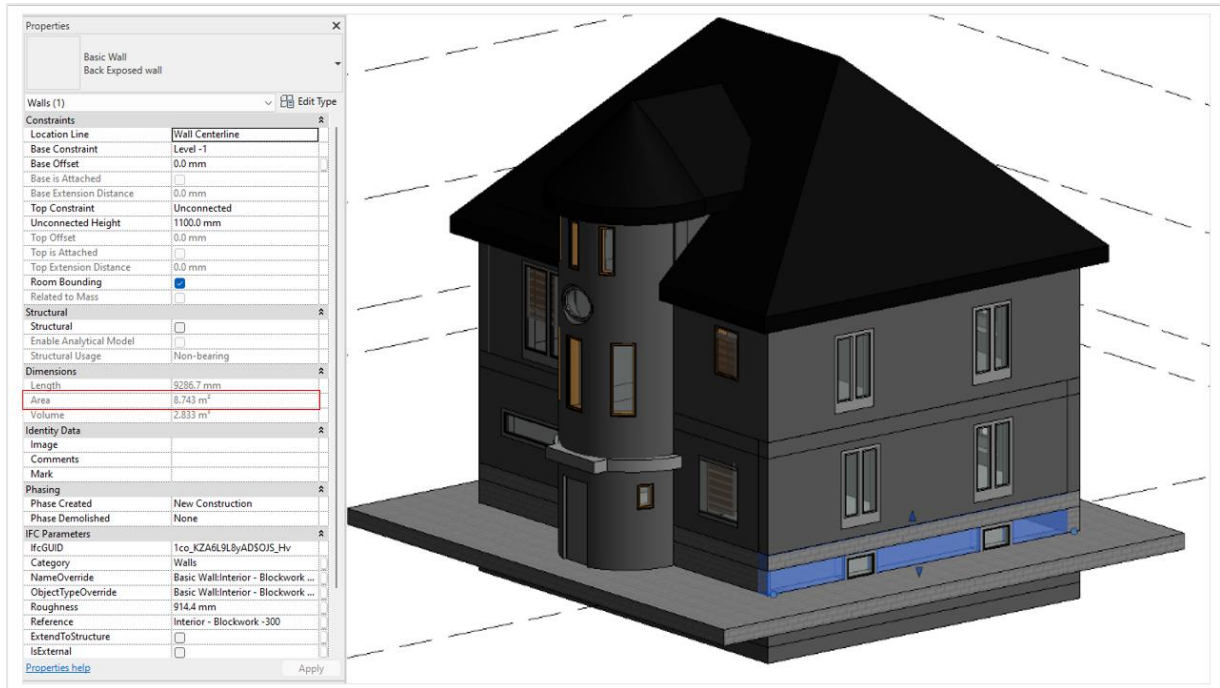


Figure 91: Left exposed basement wall outer face area in BIM model in Revit

As a next step, with Equation 14, the outer surface areas of all the intersected walls and other components were computed. Figure 92 is showing the comparison between the total surface area of the walls and the filtered, outer surface area of the intersected walls. It can be observed that the outer face area of each intersected wall is significantly smaller than the total surface area, which is due to the adjustment incorporated into the 3D intersected components.

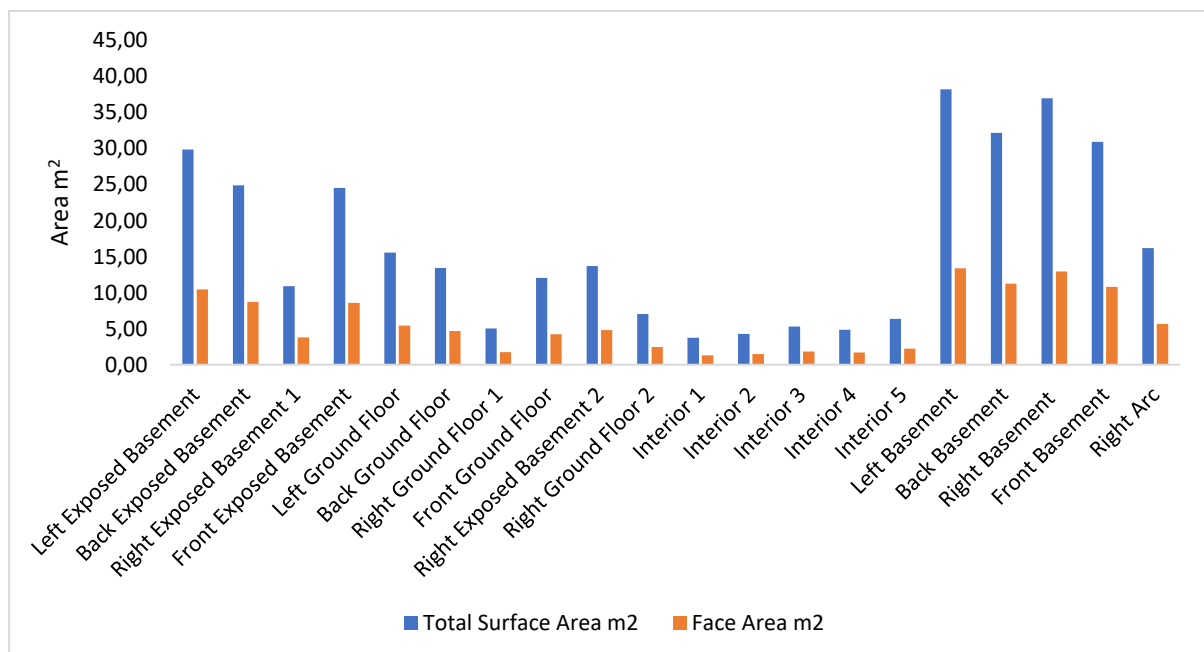


Figure 92: Comparison of total surface area (all the faces) and outer face area of flood intersected walls

### 7.8.1.2 Water Interaction Height

The Flood water interaction height of each wall is determined by computing the outer surface area of the wall and its length from BIM-IFC properties. Although the actual wall heights are provided in the semantic properties in BIM model, still after the intersection with flood the intersected height must be filtered in order to understand depth of the components inside flooding. The intersected height is then calculated using the basic area equation with the "Calculate Field Tool" in ArcGIS.

$$\text{Area} = \text{Length} \times \text{Height} ; \text{Height} = \text{Area}/\text{Length} \quad \text{Equation 15}$$

This intersected height reflects the water interaction level of each wall in the intersected building. The fully submerged walls are the exposed basement walls, while the ground floor walls are partially submerged. This automatic computation provides the corresponding submerged heights of these walls to the floodwater, as shown in Figure 93.

It is essential to accurately calculate the height of walls with respect to flooding inundation depth and surface area, as these are important factors to consider during pressure calculation. Manual survey and calculation of these values are labour-intensive tasks, and it is extremely difficult to manually calculate them accurately. However, due to the developed digital twin, this process can be automated, and by integrating the building with flooding, necessary values to effectively calculate flood actions pressure are ready to use further. Similarly, based on surface area, components can be visualized in 3D to determine how much they are submerged in water. With this process, electrical and furniture components can also be assessed and visualized in 3D to determine whether they have been damaged by flooding or not.

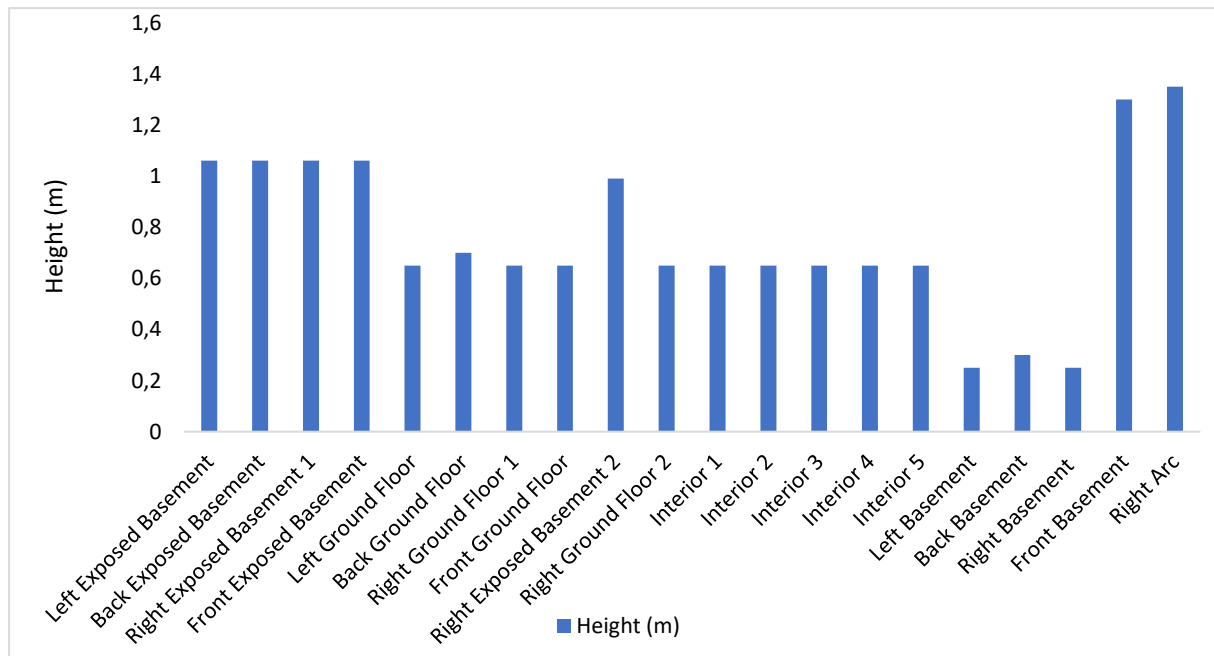


Figure 93: Flood submerged height of all the flood intersected walls

## 7.8.2 Hydrostatic Pressure

As described in literature section 2.6.2, a 3D hydrostatic pressure and force analysis can provide a more accurate understanding of the water pressures and forces on a building, allowing engineers to design structures that can withstand the forces exerted by water in all directions. However, it requires more detailed information about the building's geometry and the water pressure distribution, which may be more difficult to obtain in a 2D analysis. To calculate the hydrostatic force in 3D, the user would need to consider the three dimensions of the building and the pressure and direction of the water at each point on the building's surface, which involves more complex mathematical equations and numerical methods. To accurately calculate and assess hydrostatic pressure and force on individual building components, horizontal hydrostatic pressure (Equation 2), and force (Equation 3) equations were integrated into the developed digital twin model. These equations require information such as the area of the applied force or relative depth of water, which was obtained in the previous section with water interaction. In this section, this information (height, length, or surface area) was combined with other parameters (such as density of water or coefficient) to compute hydrostatic pressure and force. For the first scenario, where flood outside of the building was considered, lateral hydrostatic pressure and force were calculated without differentiating between inside and outside hydrostatic pressure.

In the developed model, the calculation of hydrostatic pressure and force is partially automated, meaning that every individual component receives its respective hydrostatic pressure and force acting on them automatically, based on the geometry, shape, and orientation of the component, which is directly linked to the density, height, width, and depth of flood water. Furthermore, components based on this computed pressure and force can be identified and visualized in 3D see Figure 94.

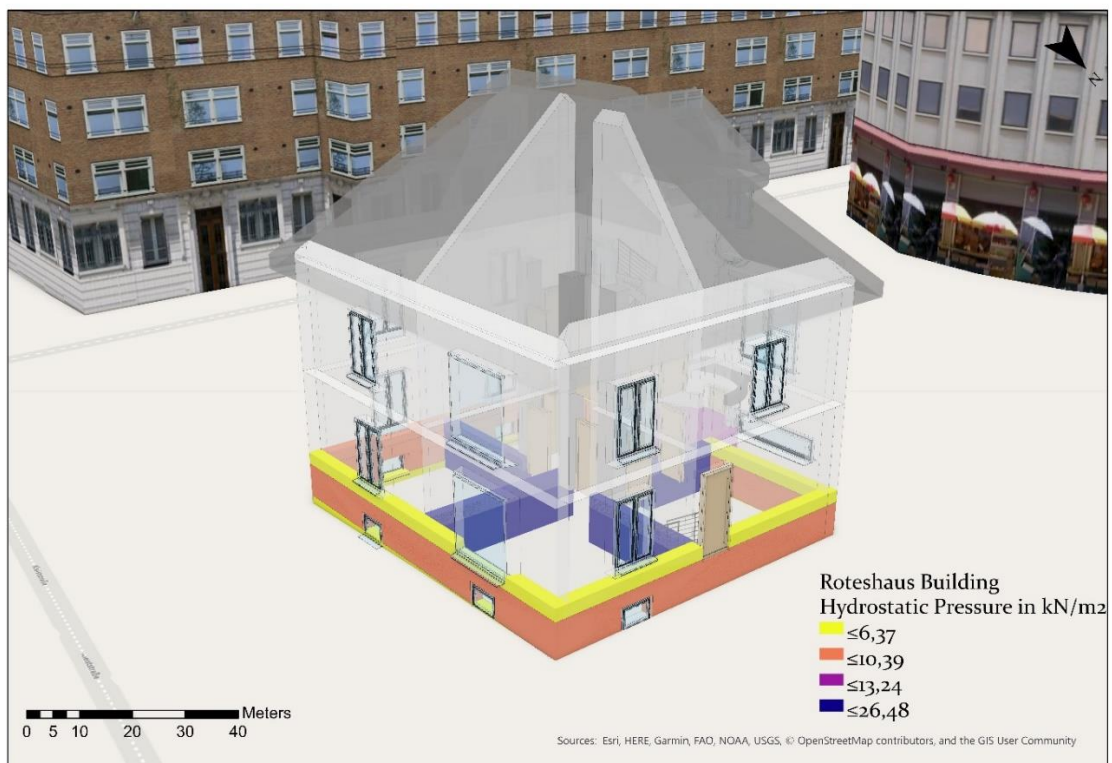


Figure 94: 3D representation of intersected walls, created using information on the hydrostatic pressure resulting from their intersections

The bar chart shown in Figure 95 represents the hydrostatic pressure on each individual wall of the building under the impact of flooding in a 3D environment. The maximum hydrostatic pressure is observed on the entrance arc wall, with a value of  $13.24 \text{ KN/m}^2$ , due to its large area being affected by flooding. The basement exposed walls follow with a value of  $10.39 \text{ KN/m}^2$ . On the other hand, for the remaining walls, only a marginal difference is observed as their surface area under flooding is very similar to one another. The maximum impact of hydrostatic pressure, with values ranging from 6-10  $\text{KN/m}^2$ , was observed for all other walls of the building.

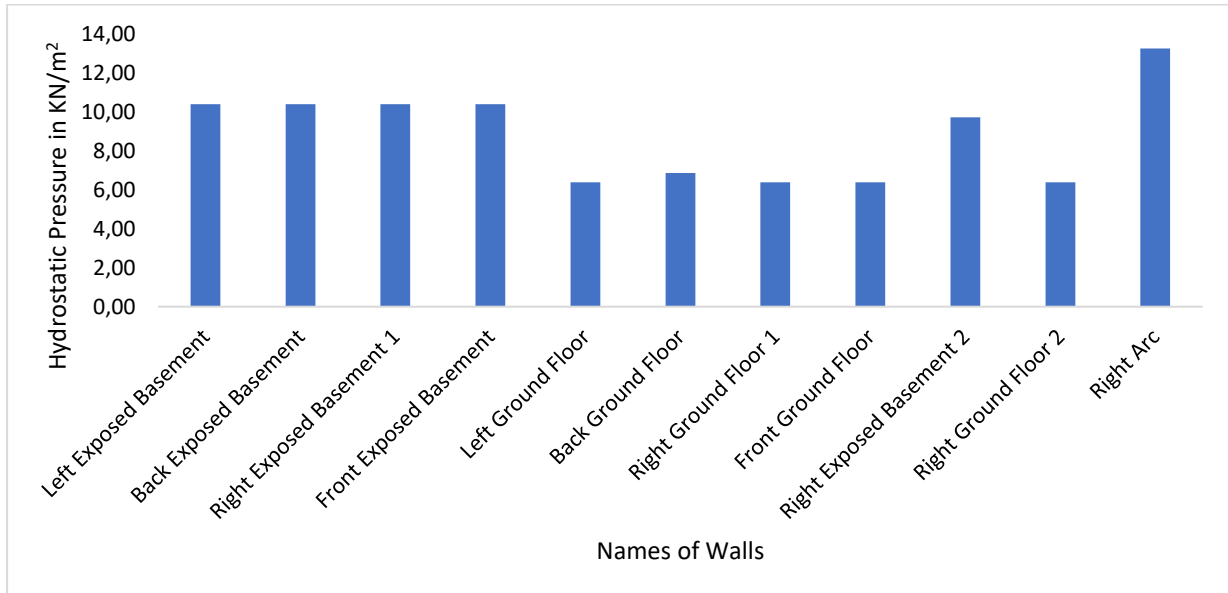


Figure 95: Comparison of hydrostatic pressure on different intersected walls

The maximum hydrostatic force was observed for the left exposed basement component with a distributed impact of almost 51 KN. The hydrostatic distributed force magnitude for the front side of the wall components reaches 42 KN at maximum. Similarly force magnitude for backside wall components reaches 43KN at maximum see Figure 96.

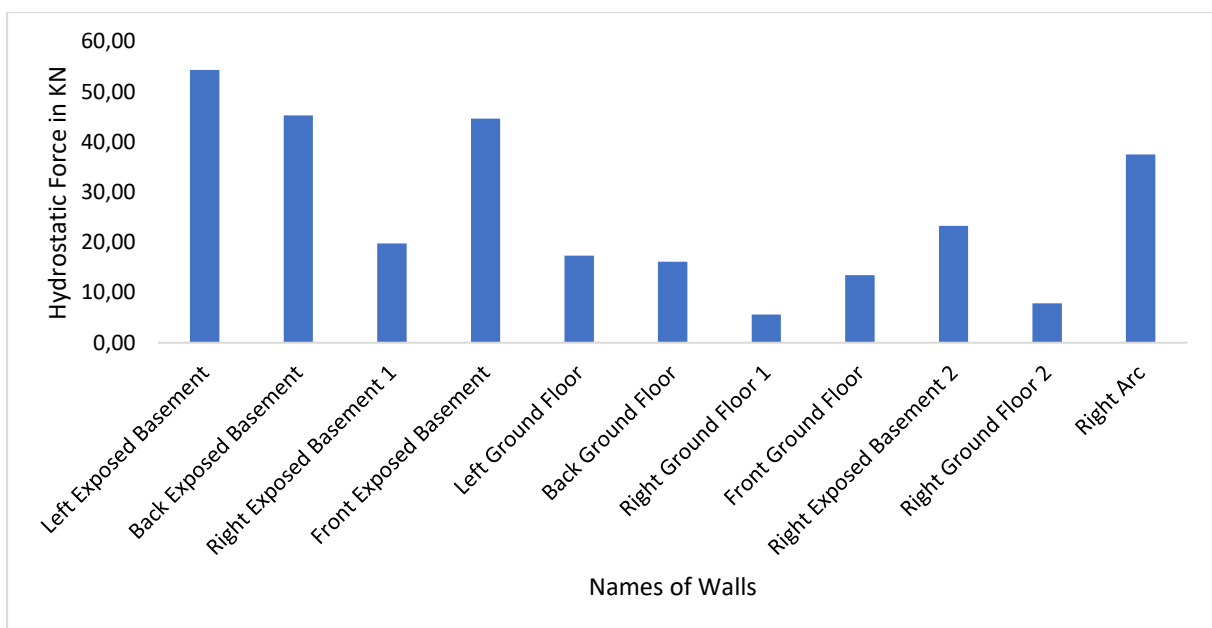


Figure 96: Comparison of hydrostatic force magnitude on different intersected walls

Moreover, Figure 97 represents the relationship between surface area and hydrostatic force for intersected wall components. If the intersected surface area is more that means the forces applied on the area are also high.

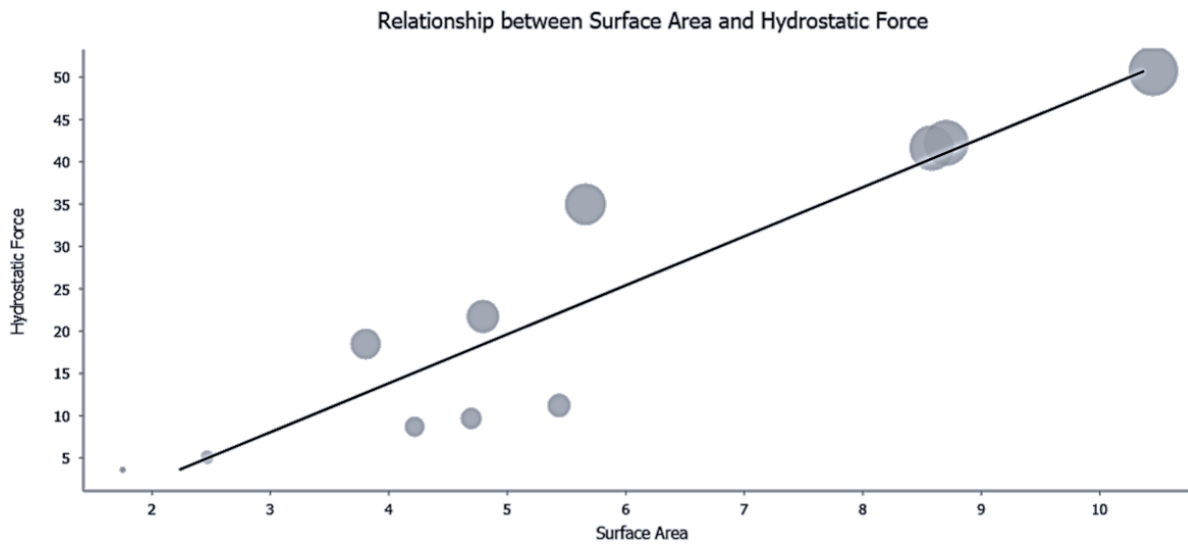


Figure 97: Relationship between surface area and hydrostatic force magnitude

Figure 98 displays the computed pressure acting on individual intersected areas of walls, as well as the hydrostatic force acting on individual walls based on their surface area. It is a well-known fact that pressure is directly proportional to the area, thus it can be observed in Figure 98 that the hydrostatic force is higher where the surface area of the intersected wall is greater.

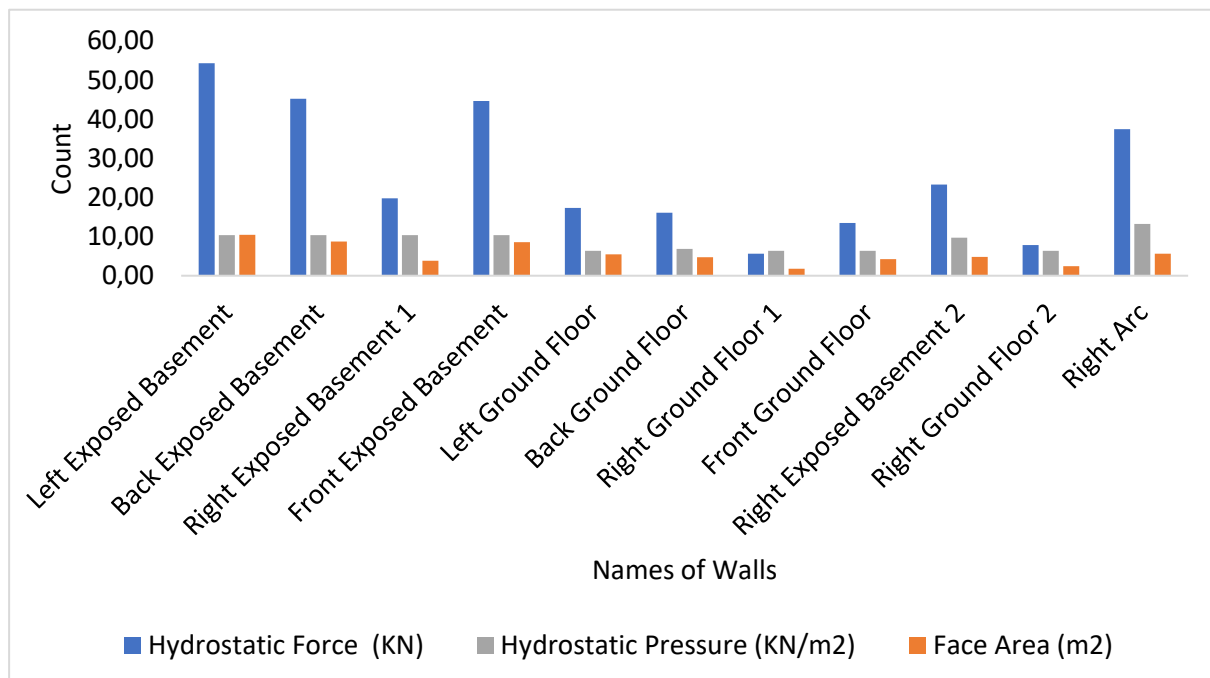


Figure 98: Comparison of hydrostatic pressure and force with respect to the intersected face area

For example, the left exposed basement wall has an intersected surface area of 10.45 m<sup>2</sup> resulting in a hydrostatic force of more than 51 KN compared to the left ground floor intersected surface area of



5.43 m<sup>2</sup> with a hydrostatic force of 13 KN. Therefore, a marginal difference can be observed for hydrostatic force among different intersected wall components.

In this section, hydrostatic pressure and force acting on walls are explained. The hydrostatic pressure and forces computed for other components, such as doors and windows, can be found in the appendix. In addition, the computed hydrostatic pressure and force can be utilized in other software or within the digital twin environment for further analysis and processing. For example, the hydrostatic pressure calculated for a particular section can be exported to Dlubal RFEM, which is a structural analysis software. This can be achieved by first importing the 3D BIM model of the building into the software via direct Revit to the RFEM interface. This is necessary because in the digital twin developed earlier, the building is a BIM model and all components of the building have their own associated name and semantic properties. These semantic properties help to identify the hydrostatic pressure associated with the components.

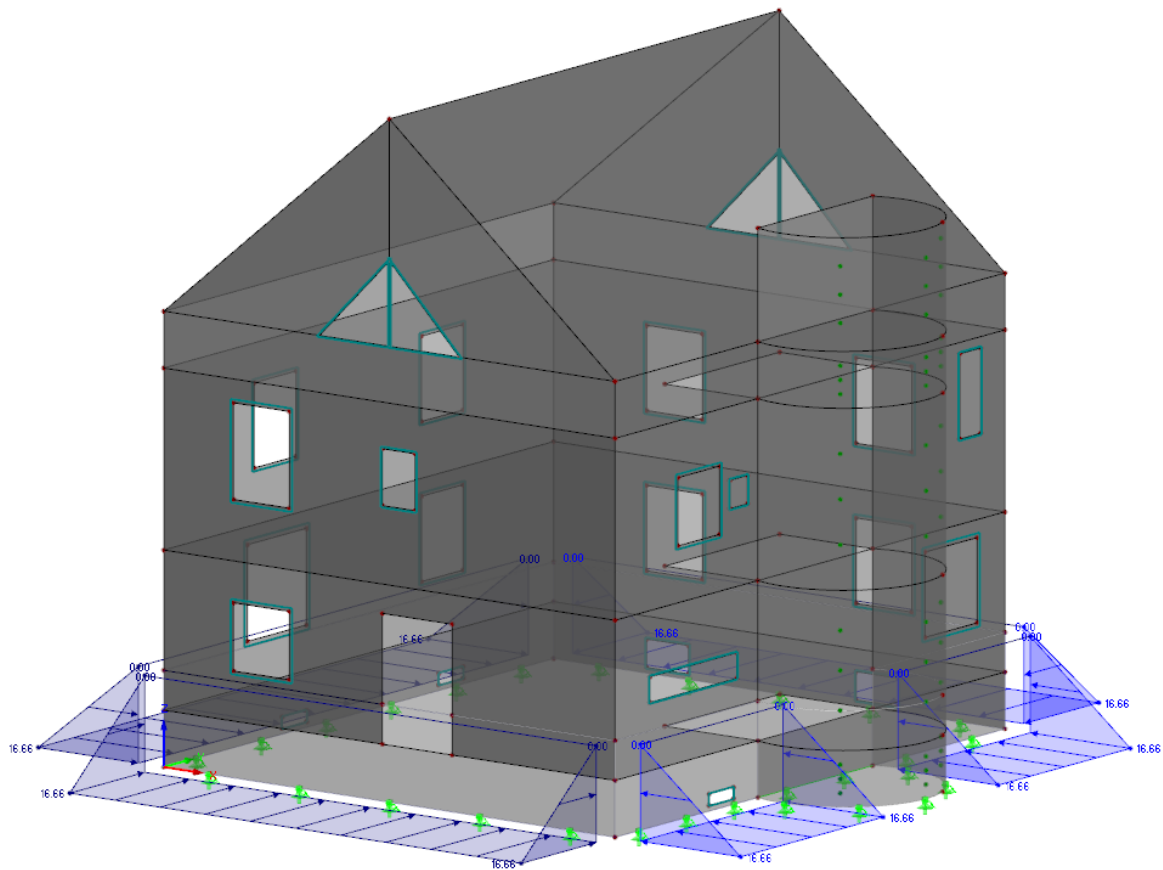


Figure 99: 3D Application of hydrostatic pressure on respective walls inside RFEM due to automation in digital twin

Furthermore, ArcGIS Pro provides hydrostatic pressure and force acting on individual components in the attribute table. This information can be exported into an Excel format (.xls) and later imported into RFEM, where the same BIM model with associated component names and properties has already been imported. Due to the same name and properties of the components, their associated hydrostatic pressures imported from ArcGIS Pro are automatically applied to their respective components (such as walls) in the structural analysis software, due to the same name and properties of the BIM model as shown in Figure 99. The magnitude of the hydrostatic pressure acting on a wall increases with the

depth of the water because the pressure at the bottom of the wall increases with depth. This increase in pressure results in an increase in the hydrostatic force acting on the wall. This information is already incorporated into a digital twin and can be seen in Figure 99. It is important to highlight that the current digital twin does not allow for the visualization of hydrostatic pressure on a specific component rather it shows components based on hydrostatic pressure or force. Thus, to gain insight into how hydrostatic pressure affects certain components, it is advisable to transfer this information from the digital twin to third-party software. It should be noted that this type of 3D visualization is also more flexible and can be customized to account for variations in terrain, location, and floodwater intensity.

### **7.8.3 Hydrodynamic Pressure**

As described in literature section 2.6.3, 3D hydrodynamic flood pressure calculations are essential for ensuring the safety and structural integrity of buildings in flood-prone areas. These calculations consider the impact of floodwater pressure on the foundation, walls, and other structural elements of the building, and help to identify the potential for damage or failure. Many studies have indicated that the hydrodynamic effects of flooding are highly relevant and crucial for managing flood risks in resilient buildings, as shown in Table 5 (Kelman and Spence, 2004; Nadal et al., 2010; Mason et al., 2012). These effects can be predicted but requires detailed parameters such as flood hazard data, structural details, and water properties for these calculations. This information also includes the frequency and intensity of flooding in the area, expected water levels during a flood event, building geometry, structural and non-structural components level of details and water properties such as velocity and depth. By taking into account these parameters, 3D hydrodynamic flood pressure calculations can help to design and construct buildings that can withstand the impact of flooding.

In the developed digital twin model, hydrodynamic pressure is automatized using hydrodynamic Equation 6, similar to hydrostatic calculation. The field calculator in the attribute table of intersected walls is used to determine the surface area, which is crucial in determining the 3D hydrodynamic pressure on individual building components. The building geometry, including the height, length, and area of the components, is also taken into account. Similarly, the hydrodynamic force was automatized using Equation 7. It should be noted that hydrodynamic force is the result of velocity (Kelman and Spence 2004). The maximum velocity around the building, which was computed to be approximately 3.5 m/s in the hydrodynamic flood simulation was used in this process see section 7.4 of the case study for more details.

The literature section 2.6.3 explains that when water flows around a building, it exerts pressure on the front side of the building and creates a suction or negative pressure on the backside of the building. Similarly, flood flow tries to drag the building along parallel to flow direction. As a result, the hydrodynamic pressure calculated for the backside of the building is considered to be half of the hydrodynamic pressure calculated for the front side of the building. Additionally, the backside walls of the building are only exposed to half of the hydrodynamic force in comparison to the frontal walls of the building. This is because the water flow around the building causes the hydrodynamic pressure to be distributed unevenly on the walls of the building, with the front side experiencing higher pressure than the back side. Accounting for this uneven distribution of hydrodynamic pressure is important in accurately assessing the potential for damage or failure of the building during a flood event. Therefore, this digital twin assesses this phenomenon automatically based on provided flow direction.

In addition, it is important to note that hydrodynamic pressure primarily acts above the ground surface (Mazzorana et al. 2014; Gems et al. 2016). Therefore, the underground components of the building were not taken into consideration in this scenario. Depending on flow direction two walls on the front side of the building were intersected (see section 7.8.1) where hydrodynamic pressure and force were calculated, as shown in Figure 100. The basement wall that is fully exposed to flooding experiences a higher hydrodynamic force than the ground floor wall. The computed hydrodynamic force for the basement wall is 742 KN as a distributed function, while for the ground floor wall, it is 365 KN as a distributed function.

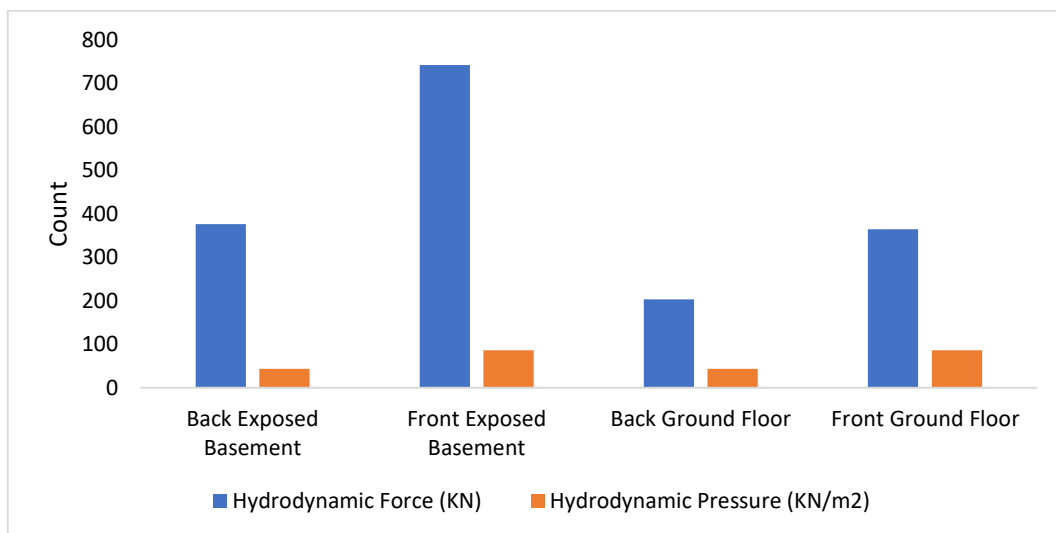


Figure 100: Comparison of hydrodynamic pressure and force on front and back side intersected walls

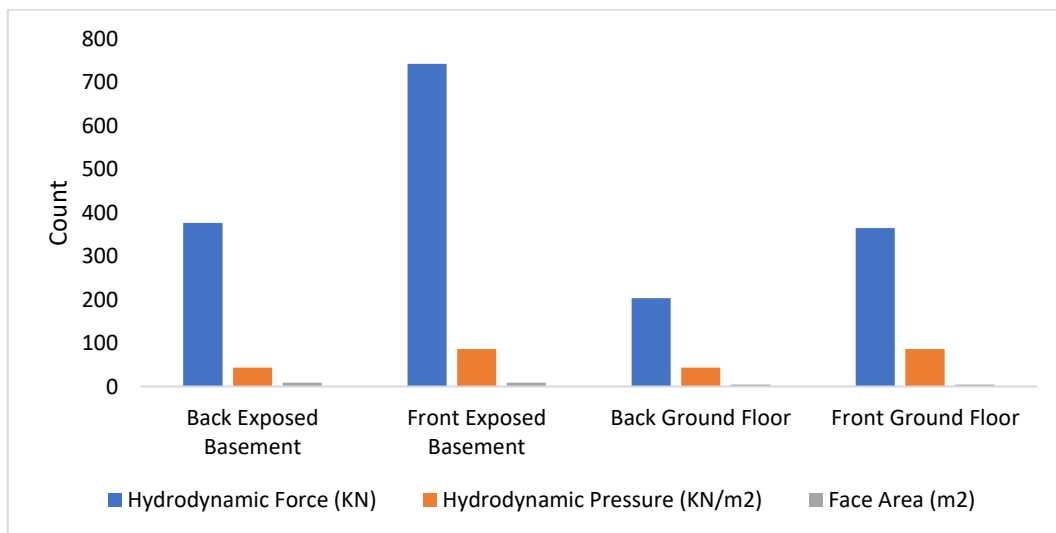


Figure 101: Comparison of hydrodynamic pressure and force with respect to intersected face area

The impacting hydrodynamic force on the front ground floor wall is generally lower than that on the front exposed basement wall. This is primarily because the intersected surface area of the front ground floor wall is smaller than the intersected surface area of the exposed basement wall. Similarly, the hydrodynamic force on the backside of the building is lower than the front side due to the comparatively lower velocities at the backside of the building. Figure 101 illustrates the relationship between hydrodynamic force, pressure, and intersected surface area. This figure provides a visual

representation of how the hydrodynamic force and pressure are influenced by the surface area of the building walls exposed to flooding.

Hydrodynamic forces are one of the primary causes of flood damage, and they can be significantly greater than the average hydrostatic force. This is supported by FEMA's report on flood damage (FEMA 2021). In this case study, the developed model has computed the hydrodynamic force, as shown in Figure 102, and it is found to be relatively higher than the hydrostatic force. This indicates that the hydrodynamic force is a significant factor in assessing the potential for damage or failure of the building during a flood event.

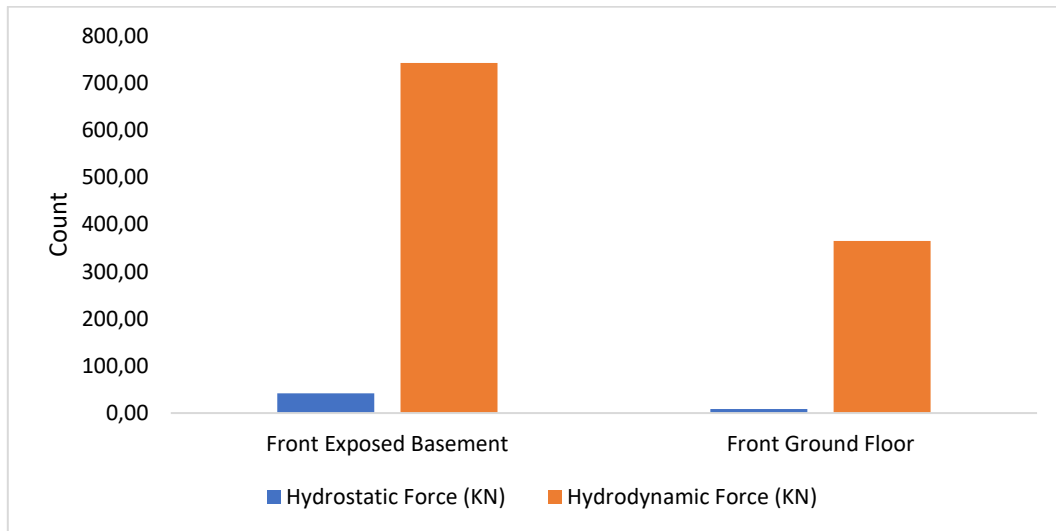


Figure 102: Comparison of hydrostatic and hydrodynamic force

The digital twin model provides a 3D visualization of the building and allows us to assess the risk of flooding by showing the hydrodynamic force acting on different building components. By analysing the figure that displays the damaged walls of the building with their respective hydrodynamic force, stakeholders can better understand the potential impact of flooding on the building and make informed decisions regarding risk assessment management. This approach can be more effective than traditional 2D models, as it provides a more comprehensive and detailed view of the building and its vulnerabilities to flooding. Figure 103 provides 3D visualization of intersected walls based on hydrostatic force depending upon their respective intersected face area with flood and flow velocity around them.

Likewise, the hydrodynamic force was transferred to the RFEM Structural analysis software to verify its application on relevant walls and visualize the hydrodynamic pressure acting on specific components. As stated in section 2.6.3, a hydrodynamic force acts uniformly on the relevant components in contrast to hydrostatic pressure, which can be observed in Figure 104. Currently, this type of pressure visualization based on direction is not possible in the developed digital twin, making it necessary to export the data to third-party software to visualize the magnitude as well as the direction of the pressure distribution on the components. However, it should be noted that based on the resulting pressure and force data, the components can be visualized in 3D within the developed digital twin Figure 103.



### 7.8.4 Debris Force

Based on various studies, the relevance of debris impact on flood-resistant structures (Table 5) differs depending on different scenarios and conditions (Jakob et al. 2012; Stolle et al. 2019; Kabir et al. 2023). Additionally, it is challenging to anticipate and necessitate considerations such as debris size, weight, properties, water depth, flow rate, terrain, building shape, impact height, and contact duration. Debris impact forces are a function of impact velocity and can be oblique and eccentric during flooding due to ripples in flowing water. To simplify the calculations in this particular case study, only Equation 10 based on Eurocodes for horizontal impact mentioned in 2.6.5 was partially automated into the digital twin.

Typically, in regular situations, the force of debris is greater on the side of a building that is facing upstream because the debris is more likely to accumulate on that side. However, in urban environments where there are various buildings and infrastructure, water waves and ripples can occur, causing debris to impact all sides of the building (Stolle et al. 2019; Kabir et al. 2023). It should be noted that the debris force is a distributed force that affects the overall component in a uniform manner (Jakob et al. 2012; Stolle et al. 2019).

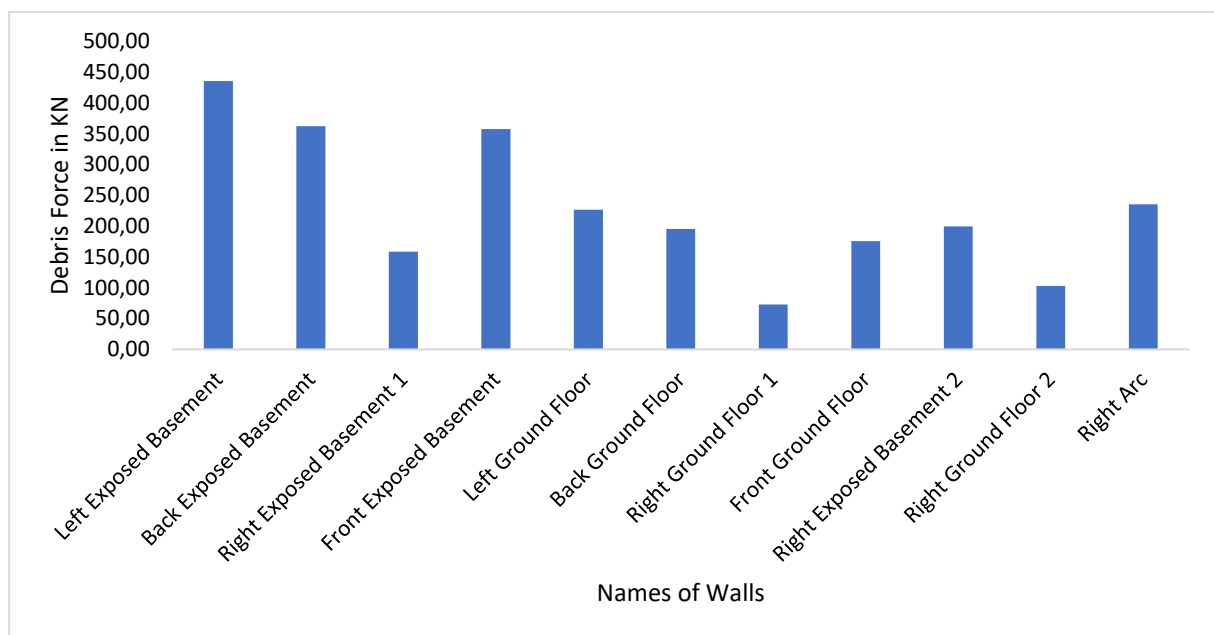


Figure 105: Comparison of debris force acting on different intersected walls

Figure 105 illustrates the computed debris force for each intersected wall component for the wetted perimeter of the building under investigation. The exposed basement wall on the left side of the building experiences the most significant amount of debris force. Additionally, it is observed that the magnitude of debris force decreases significantly based on the wetted perimeter of the walls. Consequently, the force magnitude is comparatively lower for the ground floor wall on the right side of the building because the area that intersected with the floodwater (wetted perimeter) was less.

Figure 106 displays a 3D visualization of walls intersecting with floodwater and the resultant debris force acting on them. This type of visualization is more vivid and provides a more accurate representation of the situation compared to 2D representations. Still, direction of pressure or force acting on walls due to debris angle and orientation is not possible to visualize in the developed model.







Similar to previous actions taken for flood impact, the debris pressure can also be exported to structural stability software to visualize direction of pressure distribution action on certain components in 3D. Accordingly, this also provides aids to assess the stability of the building and its components against the computed debris force in 3D. Additionally can also be visualized how the debris pressure acts on each component uniformly as a distributed force function see Figure 107.

### 7.8.5 Impact Force

As described in literature, the severity of the impact force on a building is influenced by several factors (Fauzan et al. 2019). One of the most significant factors is the mass and velocity of the object striking the building. An object with a higher mass or velocity will cause more damage upon impact than a lighter or slower object. The direction of the impact is also a critical factor. The force of impact can be more severe if the object strikes the building at a certain angle, such as perpendicular or at an oblique angle, rather than parallel to the building's surface. In this research, the impact force is simplified for calculation purposes. Specifically, it is assumed that the impact force acts perpendicularly to the surface of the building, and it is uniformly distributed in a perpendicular direction to the flow depth of the water. This simplification assumes that the impact force is evenly distributed across the building's surface area, regardless of the direction of the impact. While this assumption may make the calculations simpler, it may not accurately represent the true impact force experienced by the building in real-world scenarios. Therefore, based on the literature see section 2.6.4, the equations for accidental impact assessment were integrated into the digital twin model of 3D flood impact pressure and force calculation automatically (Fauzan et al. 2019).

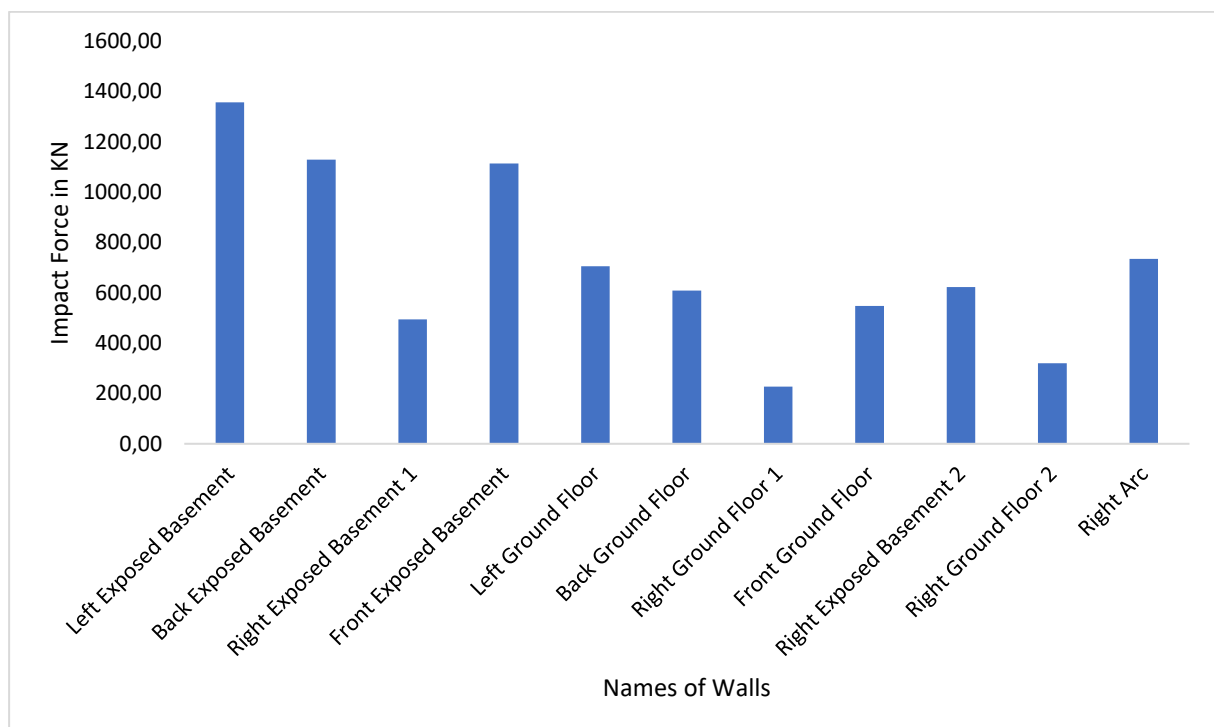


Figure 108: Comparison of impact force acting on different intersected walls



Like debris force, the impact force is also higher for the left exposed wall due to its higher wetted area (intersected area) followed by the back exposed wall see Figure 108. It should be noted that this force always acted as a distributed force upon the whole area. Moreover, in urban areas because of buildings and other infrastructure, flood water has back and forth effect, therefore, impact force should be computed for all sides of the impacted building or infrastructure. Figure 109 is showing building structural components in 3D based on the impact force. Similar to other flood actions, accidental impact pressure can also be exported to other software for further analysis and to visualize direction of pressure distribution acting on certain components in 3D as shown in Figure 110. Visualizing the impact force in 3D can help to communicate the potential risks and impacts of flooding to stakeholders and decision-makers in a more effective and understandable way.

### 7.8.6 Drag Side Effect

Calculating the drag force on a building during flooding can be a complex process. Numerous studies indicate that the significance of drag force in enhancing building resilience against flooding varies, and it is extremely challenging to accurately predict (see Table 5) (Kelman and Spence 2004; Nadal et al. 2010). It requires various factors for its calculation, such as the velocity and flow direction, the size and shape of the building, and the building's orientation in flooding. Along with many studies, Eurocodes also provide guidelines and methods to compute this force. Therefore, Equation 8 for the calculation of drag force from Eurocode is integrated into the digital twin for the computation of drag side effect automatically.

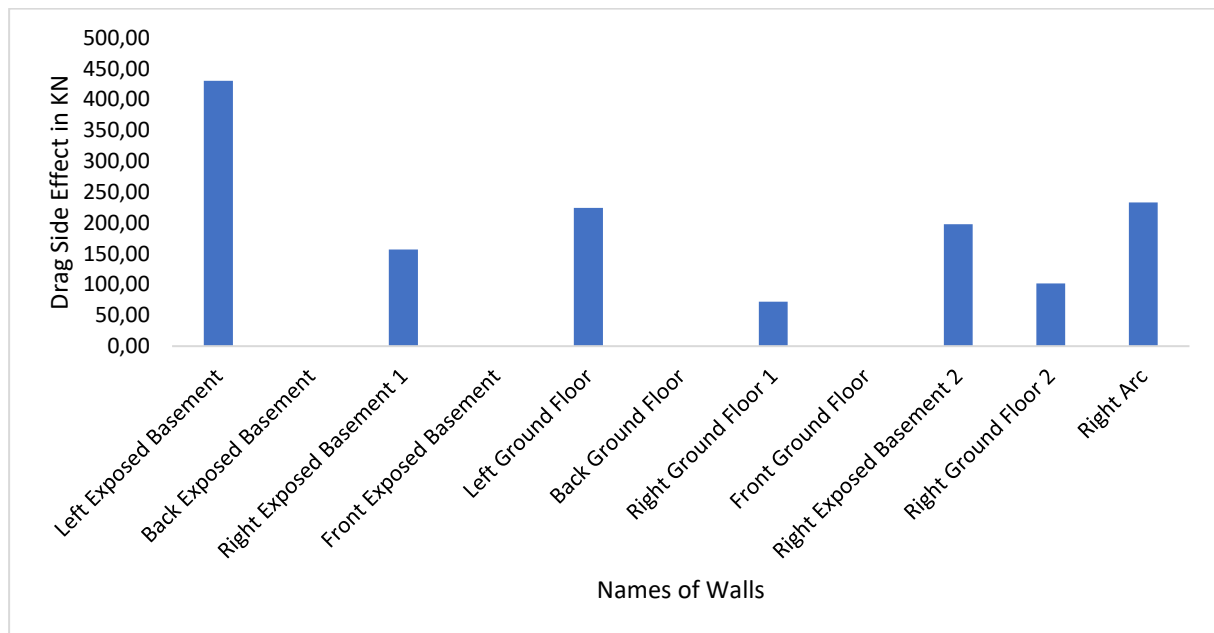


Figure 111: Comparison of drag force acting on different intersected walls

As described in the literature section 2.6.6 and illustrated in Figure 9 the drag force during flooding is known to act on the sides of a building that are parallel to the direction of the flow. In this study, the building being investigated has both its right and left sides parallel to the flow direction, as shown in Figure 75. The drag force is found to be slightly higher on the right side of the building, which is due to the difference in the exposed or intersected surface area of the outer walls.



However, when examining individual wall components, the left exposed basement wall experiences a higher magnitude of drag force because it has a larger wetted area, despite having two small ventilation openings. Figure 111 is showing comparisons of drag side effect on different walls of investigated building. 3D visualization of structural components based on different drag side force can be visualized in Figure 112. It is noted that the upstream and downstream sides of walls have zero drag side effect as it is always parallel to the flow of the direction. This also validates the automatic calculations done with this model. Figure 113 is showing 3D visualization of drag side pressure acting on respective structural building components after export to structural analysis software. Figure 113 provides a detailed visualization of the acting behaviour of the impacted drag side effect on the building walls.

## 7.9 Outcomes of 3D Flood Impact Assessment

The development of a 3D digital twin for 3D FIA has facilitated the automatic computation of flood actions on flooded building components, aiding in the evaluation of pressures and forces acting on both structural and non-structural elements of the building, as demonstrated in the previous section. This information is then presented in a comprehensive 3D format, enabling a detailed visualization of the building's response to flood-induced forces.

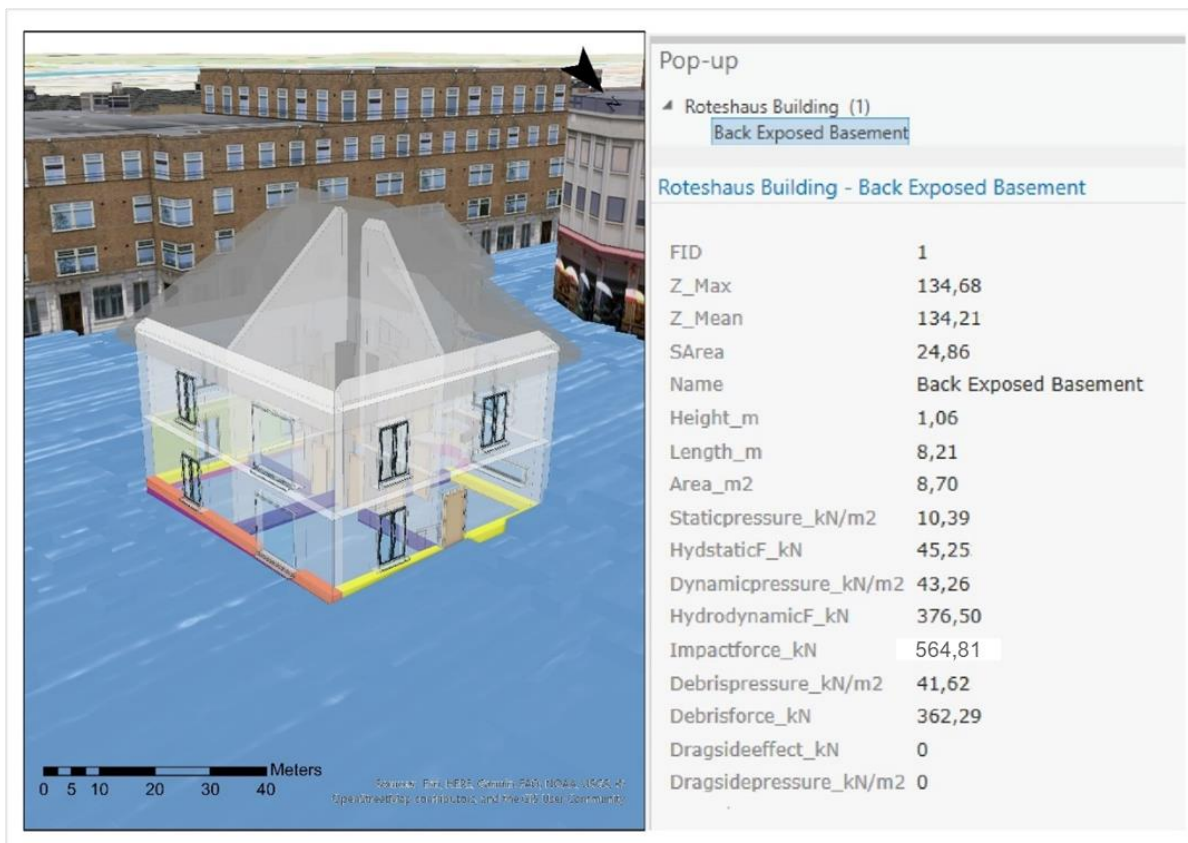


Figure 114: 3D visualization of intersected building components and necessary information pop-up window

This innovative technology allows for the automatic identification of water-sensitive components and visualization of the flood interaction area in 3D. This is particularly advantageous for complex buildings with numerous components that would require significant time and effort to manually compute flood



impact. By simply clicking or hovering over a specific component, the popup window displays comprehensive information on its name, material, dimensions, geometry, corresponding area impacted by flood, and the magnitude of force resulting from various flood pressures such as hydrostatic, hydrodynamic debris, drag side effect, and accidental impact see Figure 114.

Moreover, the developed digital twin automates the computation of various flood pressures for different building components, making the process less laborious and faster compared to traditional 2D methods. In addition, the study also highlights the exportability of computed pressure to other software for 3D analysis, such as structural and water sensitivity analysis for material, etc. The computed magnitude of forces acting on different walls based on their intersected area under flooding for various flood actions is illustrated in Figure 115. Overall, the developed 3D digital twin for 3D FIA provides a comprehensive and efficient solution for flood action computation and visualization on flooded building components.

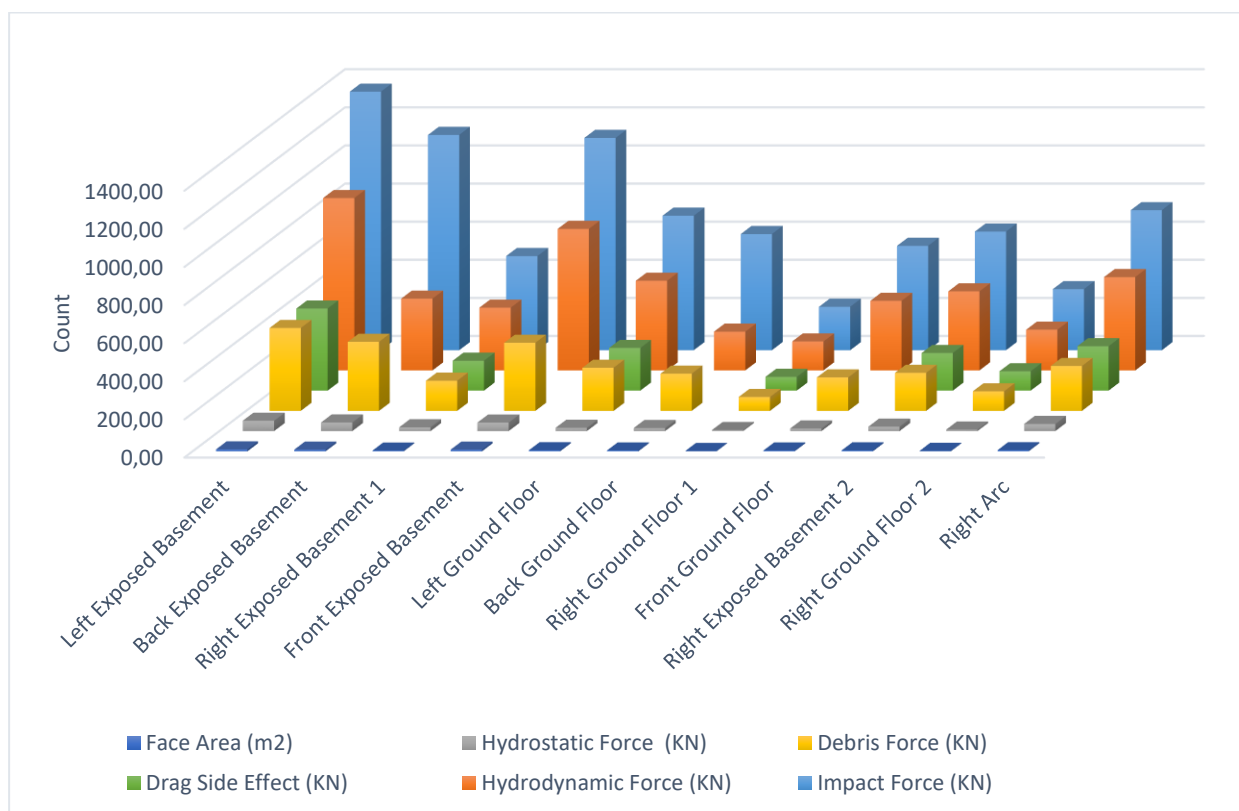


Figure 115: Comparison of all the forces computed on intersected walls with respect to their intersected areas

## **Chapter 8**

---

### **Discussion and Conclusion**



## 8 Discussion and Conclusion

This chapter provides a thorough and comprehensive overview of the research findings, addresses research questions in depth, identifies the limitations of this research, and suggests potential areas for future research.

### 8.1 Addressing the Research Questions

The main research question, as specified in chapter 1 was set out to

*“How GIS and BIM integration improve flood risk management (FRM) by creating 3D digital twin for flood resilient buildings, and would it provide support for flood impact assessment for structural and non-structural components of the building?”*

To answer the main research question, a novel multi-phase model workflow was developed in this research to improve FRM in the context of resilient buildings. This workflow was the main focus of the research and was developed using a combination of literature review, design science methodology, and data modelling techniques. The potential to improve FRM was based on a thorough literature review and a detailed overview of the principles and methods of FIA at the building scale, as discussed in chapter 2. The existing research gap and challenges were identified in this chapter as well. The capacities and limitations of various spatial hydrodynamic models were also highlighted, with a focus on their ability to assist in FIA at building scales with a high level of precision. In chapter 3, an investigation was carried out to observe the potential of novel tools and their opportunities in improving the FRM approach in general. The findings from this chapter led to an exploration of the state of the art of GIS-BIM integration potential for improving FRM with the 3D FIA approach in chapter 4. Various existing techniques were highlighted in this chapter. Eventually, in chapter 5, a multi-phase model workflow was developed based on the insights gained from the previous chapters. This workflow is intended to enhance FRM in the context of resilient buildings. A significant aspect of this model workflow is its integration of multidisciplinary information from both GIS and BIM to identify a common ground for improving FRM at the building scale with high precision, enhancing resilience against flooding. The combination of these approaches helped to ensure that the model workflow was grounded in existing knowledge and research, while also providing a new and innovative solution to the identified problem of FRM. The literature review and design science methodology provided the conceptual basis for the model workflow, while the data modelling techniques using case study ensured that the workflow was accurate and reliable.

Throughout the development process, the model has been designed to incorporate a range of features and functionalities that enable the creation of a comprehensive flood simulation for buildings. This simulation not only captures the various flood impacts against the building but also generates a 3D digital twin environment of the building, complete with all its associated flooding hazards. The 3D digital twin is presented in an easy-to-visualize 3D format, which enables users to view and interact with the model in a highly intuitive manner. The development of a 3D digital twin for 3D FIA has also facilitated the automatic computation of flood actions on flooded building components, aiding in the evaluation of pressures and forces acting on both structural and non-structural elements of the building.

Overall, the combination of GIS and BIM approaches has resulted in a highly reliable and efficient model workflow, which can significantly enhance FRM by generating a 3D digital twin for flood-resilient buildings. The model has the potential to inform the development of more effective FRM strategies and serve as a fundamental basis for further research in this field.

To thoroughly address the research question, a set of associated sub-questions were answered in detail.

### **1<sup>st</sup> sub-question**

*'What are the capacities and limitations of existing 2D and 3D spatial hydrodynamic flood simulation models at building levels to evaluate flood impact?'*

To investigate the hydrodynamic flood simulation in urban areas and more specifically for buildings, a comprehensive literature review was conducted in chapter 2. The study aimed to understand the working mechanism of spatial scale hydrodynamic flood simulation models and the type of data required to simulate flooding, particularly for individual building levels. The review found that 2D hydrodynamic flood simulation models provide detailed flood simulations around buildings but do not account for the vertical component of flooding. On the other hand, 3D hydrodynamic flood simulation models consider the vertical component of flooding but require input parameters such as flood depth and velocity to simulate flooding.

Research has revealed that while 3D hydrodynamic flood simulation models can successfully simulate vertical flooding, they do not possess the ability to integrate precise terrain and diverse surface conditions into the flood simulation model. Although initial input parameters, such as flood depth and velocity, enable 3D models to simulate the impact of flooding on buildings and their components, these models lack other important geoprocessing capabilities, including automatic detection of building components affected by flooding and assessment of the area of building components interacting with flooding. Furthermore, these models have limited reliability in terms of communicating and visualizing results.

After a thorough evaluation of the capacities and limitations of existing a 2D and 3D hydrodynamic flood simulation models (see appendix), 2D hydrodynamic flood simulation model was selected for the study to perform hydrodynamic flood simulation. The selected model provides detailed flood simulations around buildings, and its limitations are manageable within the scope of the study.

### **2<sup>nd</sup> sub-question**

*'What is the state-of-the-art of GIS and BIM technologies, and do they contain integration potential for improving flood risk management at building levels?'*

The question was addressed through a comprehensive examination of emerging tools for FRM that have been documented in the literature. Chapter 3 entails a thorough review of these tools, following their potential advantages were evaluated in order to assess how their integration could enhance FRM. The findings revealed that the integration of such novel tools can facilitate the implementation of more efficient and cost-effective strategies for mitigating flood risks.

Furthermore, research findings concluded that integrating tools like GIS and BIM can provide a comprehensive understanding of flood risks at the building level. This integration allows for a more comprehensive and accurate representation of the built environment, enabling better assessment of

flood risk and the development of effective flood management strategies. By using GIS to analyse data such as terrain, topography, and water flow, and BIM to create 3D models of buildings and infrastructure, potential flood hazards and vulnerabilities can be identified more effectively. The integration of GIS and BIM also facilitates better communication and collaboration among stakeholders, improving overall effectiveness.

However, research also concluded that combining GIS and BIM can be challenging due to different data models, standards, scale, software platforms, and complexity. Integration requires expertise, time, and resources. However, it is becoming increasingly important for accurate and comprehensive spatial data and can improve data quality, decision-making, and collaboration across disciplines.

### **3<sup>rd</sup> sub-question**

*“How GIS-BIM integration can be carried out and what practical challenges will emerge during integration steps for improving flood risk management?”*

In order to address this research question, the technological development of GIS and BIM was investigated in chapter 4, and based on the state of the art of methods for integration it was concluded that there are many ways to integrate GIS and BIM and many researchers have integrated GIS and BIM based on their need and requirements and therefore in order to integrate GIS and BIM for improving FRM a novel model workflow with supporting intermediate step was developed for this research in chapter 5 - 6.

Initially, the 2D hydrodynamic flood simulation information, along with topography and buildings within the study area, were transformed into a 3D model using innovative intermediate techniques specific to each of these processes. Subsequently, a 3D model of the buildings was created using BIM data, which was produced using object-oriented software. Lastly, this 3D building model was integrated into a 3D GIS environment using a novel approach.

To evaluate the practical challenges that may arise and to test how well the steps of the model workflow, a prototype case study was conducted. The goal of this case study was to identify any limitations in the developed model and to see how the different steps of the model work in practice. Various difficulties arose during and after the integration process, such as spatial resolution discrepancies between the datasets used for flood hydrodynamic simulation and 3D building creation, as well as disparities in database format. These difficulties helped to improvise overall methodology.

### **4th sub-question**

*“How does the integrated GIS-BIM approach support flood impact analysis on structural and non-structural buildings components?”*

This question was addressed in chapter 7, where the integrated GIS-BIM approach generated a 3D model that incorporated information on building components, such as walls, roofs, and floors, as well as data on the building's surroundings, such as terrain, floodplains, and drainage systems. The flood impact analysis was conducted on structural and non-structural building components by partially automating the calculations of flood pressures and forces on walls and identifying water-sensitive components. The system computed different flood pressures, such as hydrostatic, hydrodynamic, debris, impact force, and drag force, for different components.

The 3D digital twin was partially automated with the aid of Python scripting and manual modification, facilitating the rapid identification of building components under flooding. The impact of flooding in terms of pressures and forces exerted on these identified components was also obtained in a partially automated manner. The 3D model enabled the identification of the area of flood interaction and allowed for the visualization of the flood impact on building components, resulting in saving time and facilitating the communication of information through 3D visualization.

## **8.2 Limitations of the Study**

While the thesis has identified some limitations, it is important to note that these limitations serve as opportunities for further research and improvement. By acknowledging and addressing these limitations, future research can build upon the findings of this thesis to develop even more accurate and reliable methods for assessing flood risk and improving building resilience. First, the research requires high-resolution data with a minimum pixel size of 0.1m x 0.1m, which is challenging not only to obtain but also to process. A high-end workstation with specific components for data processing and model development, such as a workstation with a multi-core processor, high-end graphics card, and enough RAM would be sufficient to process the data used in this research. Creating a custom DTM based on airborne LiDAR data or other sources requires advanced GIS and data processing skills to effectively handle LAS or point cloud data. Similarly, the land use and topographic water bodies data required to merge with DTM for hydrodynamic flood simulation also need to be of such high resolution. Without this high-resolution data, the flood simulation may produce erroneous results.

Additionally, the integration of GIS-BIM is specific to performing FIA. The integration of GIS-BIM for other flood-related strategies may require some alteration in the working steps, limiting the model's reliability. Furthermore, the use of multiple software programs in the research means that users need to have extensive knowledge of software used in this research. The research possesses a limitation in the form of empirical validation of the results to understand the uncertainty and effectiveness of the model and its working steps.

Finally, the scale and scope of the research are limited as it considers only one building. Adding more buildings and increasing the scale may affect the accuracy and reliability of the model and results. This would broaden the applicability of the framework in space, time and to all flood events. Overall, these limitations highlight the need for careful consideration of data quality, expertise, and workflow when developing flood simulation models using GIS and BIM.

## **8.3 Future Recommendation**

There are continuous efforts to improve current flood risk management approaches. Traditionally, research has focused on assessing flood damage solely through water contact. However, this thesis presents a novel method for assessing flood impacts in a 3D digital twin environment. The approach specifically evaluates the hydrodynamic impacts of different flood actions on both structural and non-structural components of buildings. As a result, future efforts should concentrate on improving methodologies that should streamline the creation of 3D digital twins for 3D FIA for various building components. This would help reduce the number of steps required in the process.

### **Overcoming Computational Bottlenecks for Faster Simulations and Analysis**

In the future, it will be important to improve the computational power of automated flood load generation, particularly pressure and force calculations for various building components. Advances in these methods and models would facilitate real-time hydrodynamic flood simulation and digital twin environments. Uncertainty in computations is an important aspect to consider during such simulations, however, this study doesn't consider this aspect, providing an opportunity for future research. It is imperative to incorporate uncertainty into digital twin environments. This would allow the level of confidence in the flood impact assessment results to be assessed, thereby improving the accuracy of the predictions.

### **Validating 3D Digital Twin Models**

To achieve more effective validation of the developed model workflow, the outputs of laboratory experiments or previously collected empirical data can be compared with the generated outputs of the 3D digital twin model. This would help to validate the accuracy and reliability of the 3D digital twin model's predictions. By comparing the results of the laboratory experiments or empirical data with the model outputs, any discrepancies or inconsistencies can be identified and addressed, leading to further improvements in the model's accuracy and reliability.

### **Incorporating Additional Flood Actions and Expanding Hydrodynamic Outputs**

This study focused mainly on horizontal flood actions, however, integrating vertical flood actions into the model could be essentially useful. This would require suitable steps to integrate both horizontal and vertical flood actions, leading to a more comprehensive flood impact assessment. By incorporating vertical flood actions, the model's accuracy and realism can be improved, providing a better understanding of the impact of flooding on building components. The hydrodynamic action in this research was calculated using an average velocity vector for all depths. Although this approach can provide a reasonable input for damage assessment and has been used in previous flood impact assessment models, there may exist various factors that can affect the flow and result in variations in the magnitude and direction of velocity in the vertical axis in the vicinity of the building. Therefore, more efficient approaches, such as computational fluid dynamics (CFD) modelling, should be explored in future studies to model floods at a micro level and take into account potential variations. Where appropriate, these approaches should be incorporated into 3D digital twin for flooding.

### **Incorporating Other Building Component Properties for Resilience**

In future, further analysis of 3D digital twins should consider additional factors such as the age of the building, workmanship in its construction, previous damage from other events, fatigue in its elements, and precautionary measures. These factors would provide a more comprehensive analysis of the building's resilience against flooding. The high level of detail in the developed digital twin building and flooding information can be potentially used in the future for emergency response, evacuation plans, and rescue purposes. By providing detailed information about the building and flooding, emergency responders and rescue teams can make informed decisions, leading to more efficient and effective response times. Additionally, the high level of detail in the 3D modelling of the building and flooding can be used for future Technical Building Equipment (TBE) planning purposes to enhance the building's resilience against flooding damage. This research is limited to the permanent resistance of building

components and did not consider the influence of property-level features such as fences or walls that may potentially change the water flow, velocity, and impacts of flooding. In the future, an extension of the model would require such parameters to be accounted for in the modelling of floods and the analysis of their impact on the building. By incorporating property-level features into the model, the accuracy and realism of the 3D digital twin can be improved, providing a better understanding of the flood's impact on the building

### **Building Resilience Assessment via Structural Analysis in Digital Twins**

The research offers a comprehensive and detailed method and workflow for incorporating guidelines from Eurocodes and automating the process of flood action calculations. This is an impressive achievement that can significantly improve the accuracy and efficiency of flood risk management and building design practices. However, there is still much potential to further enhance the methodology by incorporating other available guidelines in a more comprehensive manner. The study presents an exciting opportunity to test and refine the developed model by incorporating additional guidelines, which can lead to even more effective and robust flood risk management and building resilience strategies. To comprehensively assess building resilience in terms of stability and response analysis, there is a need to incorporate complete structural analysis into the digital twin scenario. Although the study has provided an automatic estimation of flood load and their successful export to structure analysis software, the analysis of the building and its various components' response can be improved by incorporating their different resistance capacities. This would require a future research study that integrates structural analysis with digital twin scenarios to evaluate the building's resistance capacity under different flood induced loads. Additionally, the analysis should be extended to consider the interdependence of different building components, such as the foundation, walls, and roof, to provide a comprehensive assessment of the building's resilience. This information can be used to identify potential areas of weakness and develop strategies for improving the building's ability to withstand flooding events.

During the evaluation of the developed model workflow, it was acknowledged that users can benefit from the 3D visualization of impact mode and damage location. However, further research is required to conduct a comprehensive investigation of the advantages and limitations of this mode of communication from the user's perspective, and it is suggested as a future research direction. The practical synthesis presents a significant advancement despite challenges, serving as a pivotal proof of concept for future endeavors. Further research is recommended to conduct a comprehensive evaluation, exploring efficiency compared to traditional methods. Future research should also delve into interdisciplinary approaches to leverage burgeoning geospatial data availability, advancing our understanding and application of geospatial synthesis methodologies.

## **8.4 Conclusion**

This dissertation has developed a novel model workflow for improving flood risk management through the integration of GIS and BIM, resulting in the creation of a 3D digital twin for flood-resilient buildings. The developed 3D digital twin model facilitates partially automated flood impact assessment (pressure and force calculation) for various flood actions such as water interaction, hydrostatic and hydrodynamic forces, debris, flood impact, and drag side force. The developed model undergoes testing and validation through two distinct case studies. These case studies are conducted solely to

acquire data and assess the model workflow processes, regardless of their actual flooding conditions. The developed model with multiple phases offers a comprehensive approach to assess the resilience of buildings against flooding. Specifically, the second phase, which involves the analysis of flood impact in two dimensions, allows for the evaluation of flood effects on various buildings at different spatial scales, considering different levels of inundation. The third phase of the model proposes a novel methodology for creating a 3D flood model using 2D spatial data sets. This approach enhances the visualization of flood impacts on buildings and their surroundings and serves as an effective communication tool for decision-makers and stakeholders. The 3D flood model generates clear and compelling visualizations that can raise awareness and facilitate the mitigation of flooding effects.

In the subsequent phase, GIS and BIM are integrated into a single environment, resulting in increased efficiency by reducing the need to switch between multiple programs, saving time and resources, and simplifying data management and analysis. The integration enables geospatial analysis in a 3D digital twin scenario to facilitate building resilience against flooding. Various geospatial analyses are partially automated into the digital twin to identify and assess the impact of flooding on different building components, including flooded components, water pressure, and forces on structural and non-structural components. An important aspect of the 3D digital twin model to highlight is its ability to partially automate the identification of individual building components that are affected by flooding. Moreover, it calculates all the required flood action information in a 3D environment for each individual building component while providing 3D visualization and communication of these impacts on the building components. Furthermore, upon clicking on a component, a popup window displays its name, material, dimensions, geometry, and the area affected by the flood. The popup window also shows the pressure on the component, including hydrostatic, hydrodynamic debris, drag side effect, and impact force.

The data-rich outputs obtained from this approach have broad applications, including analyzing the material properties and structural stability of buildings and their components. Partially automated computation of pressure and force can be exported through an intermediate medium to various structural analysis software, reducing the risk of data loss and errors when calculating flood-induced loads for stability analysis against flooding. The developed model facilitates the exchange of these computed pressures and forces with structural analysis software, enabling more efficient and accurate analysis of the building's structural integrity. This can identify potential weaknesses and inform necessary adaptations or improvements to ensure the building's safety during a flood event. Automation through this technique significantly reduces the time and effort required to calculate flood-related pressures and forces, allowing engineers and architects to focus on other critical aspects of flood risk management and building design. Traditionally this process is highly complex and time consuming. The automation enabled by this technique is less prone to human error, further improving the reliability and validity of the results. Ensuring consistent methodology and parameters across different buildings and flood scenarios reduces the risk of mistakes or oversights that can compromise the accuracy of the calculations. This consistency and reliability are particularly important when assessing the impact of flooding on critical infrastructure, such as hospitals or power plants, where small errors can have significant consequences. Thus, automating the calculation of flood-induced loads can help to improve the overall effectiveness of flood risk management and building design. This information can be used to inform necessary adaptations or improvements to building design and construction practices, enhancing the safety and resilience of buildings in flood-prone areas. Although



there are challenges that need to be addressed in future studies, such as the need for high-quality data and the development of more sophisticated modelling techniques, this research provides a valuable contribution to flood risk management and building resilience. By leveraging the capabilities of the 3D flood impact assessment through the digital twin approach, engineers and architects can continue to develop more effective and sustainable strategies for managing flood risk and enhancing building resilience.

## **Chapter 9**

---

## **References**

## 9 References

- Abd AM, Hameed AH, Nsaif BM, 2020. Documentation of construction project using integration of BIM and GIS technique. *Asian Journal of Civil Engineering*, 21 (7), 1249–1257.
- Abdelkader M, Shaqura M, Claudel CG, Gueaieb W, 2013. A UAV based system for real time flash flood monitoring in desert environments using Lagrangian microsensors. 2013 International Conference on Unmanned Aircraft Systems (ICUAS). IEEE.
- Abdulrazzaq ZT, Aziz NA, Mohammed AA, 2018. Flood modelling using satellite-based precipitation estimates and digital elevation model in eastern Iraq. *International Journal of Advanced Geosciences*, 6 (1), 72–77.
- Aerts JC, Botzen WW, Moel H de, Bowman M, 2013. Cost estimates for flood resilience and protection strategies in New York City. *Annals of the New York Academy of Sciences*, 1294 (1), 1–104.
- AIA, 2013. Document G202–Project: Building Information Modelling Protocol Form. American Institute of Architects.
- Albano R, 2019. Investigation on Roof Segmentation for 3D Building Reconstruction from Aerial LIDAR Point Clouds. *Applied Sciences*, 9 (21), 4674.
- Amirebrahimi S, Rajabifard A, Mendis P, Ngo T, 2016. A framework for a microscale flood damage assessment and visualization for a building using BIM–GIS integration. *International Journal of Digital Earth*, 9 (4), 363–386.
- Anees MT, Abdullah K, Nawawi MN, Ab Rahman, Nik Norulaini Nik, Piah ARM, Zakaria NA, Syakir MI, Omar AM, 2016. Numerical modeling techniques for flood analysis. *Journal of African earth sciences*, 124, 478–486.
- Annis A, Nardi F, Petroselli A, Apollonio C, Arcangeletti E, Tauro F, Belli C, Bianconi R, Grimaldi S, 2020. UAV-DEMs for Small-Scale Flood Hazard Mapping. *Water*, 12 (6), 1717.
- Apel H, Aronica GT, Kreibich H, Thieken AH, 2009. Flood risk analyses—how detailed do we need to be? *Natural Hazards*, 49, 79–98.
- Aribisala OD, Yum S-G, Adhikari MD, Song M-S, 2022. Flood Damage Assessment: A Review of Microscale Methodologies for Residential Buildings. *Sustainability*, 14 (21), 13817.
- Aronsson-Storrier M, 2021. UN Office for Disaster Risk Reduction (2019). *Yearbook of International Disaster Law Online*, 2 (1), 377–382.
- Arruda Gomes MM de, Melo Verçosa LF de, Cirilo JA, 2021. Hydrologic Models Coupled with 2d Hydrodynamic Model for High-Resolution Urban Flood Simulation. *Natural Hazards*, 108 (3), 3121–3157.
- ARUP, 2019. *The City Water Resilience Approach*. ARUP International Development.
- ASCE, 2014. *Flood Resistant Design and Construction (24-14)*.
- Atyabi S, Kiavarz Moghaddam M, Rajabifard A, 2019. Optimization Of Emergency Evacuation in Fire Building by Integrated BIM and GIS. *The International Archives of the Photogrammetry, Remote Sensing and Spatial Information Sciences*, XLII-4/W18, 131–139.
- Awange J, Kiema J, 2019. *Light Detection and Ranging (LiDAR)*. Environmental Geoinformatics. Springer, Cham, p. 291–306.
- Bai Y, Zadeh PA, Staub-French S, Pottinger R, 2017. Integrating GIS and BIM for Community-Scale Energy Modeling. *American Society of Civil Engineers*, 185 p.
- Bakhtiari V, Piadeh F, Behzadian K, 2023. *Application of Innovative Digital Technologies in Urban Flood Risk Management*.

- Baldassarre GD, Kemerink JS, Kooy M, Brandimarte L, 2014. Floods and Societies: The Spatial Distribution of Water-Related Disaster Risk and its Dynamics. *Wiley Interdisciplinary Reviews: Water*, 1(2), 133-139.
- Bales JD, Wagner CR, Tighe KC, Terziotti S, 2007. Scientific Investigations Report. *Scientific Investigations Report*, 2007-5032.
- Basu A, Bhattacharjee A, 2022. Urban Expansion Around Kolkata: Evaluating Urbanogenic Interventions in New Town, Rajarhat. In: *Anthropogeomorphology: A Geospatial Technology Based Approach*. Springer, p. 571–603.
- Bates P, Roo A de, 2000. A Simple Raster-Based Model for Flood Inundation Simulation. *Journal of Hydrology*, 236 (1-2), 54–77.
- Bates PD, Horritt MS, Fewtrell TJ, 2010. A Simple Inertial Formulation of the Shallow Water Equations for Efficient Two-Dimensional Flood Inundation Modelling. *Journal of Hydrology*, 387 (1-2), 33–45.
- Bazan-Krzywoszańska A, Mrówczyńska M, Tront S, 2019. GIS technology, 3D Models and Mathematical Models as a Tool for Assessing Development Capabilities of Flood Risk Land to Make Arrangements of Municipal Planning Documents. *Journal of Ecological Engineering*, 20 (1).
- BBC News, 2021. Flooding Around the World, 2021. Accessed on 12.12.2021, <https://www.bbc.com/news/topics/c26xdmnee19t>
- Becker AB, Johnstone WM, Lence BJ, 2011. Wood Frame Building Response to Rapid-Onset Flooding. *Natural Hazards Review*, 12 (2), 85–95.
- Beetz J, Borrmann A, 2018. Benefits and Limitations of Linked Data Approaches for Road Modeling and Data Exchange. In: Springer, Cham, p. 245–261.
- Begum S, Stive MJ, Hall JW, 2007. *Flood Risk Management in Europe*. Innovation in Policy and Practice. Springer Science & Business Media.
- Beven K, Lamb R, Leedal D, Hunter N, 2015. Communicating Uncertainty in Flood Inundation Mapping: A Case Study. *International Journal of River Basin Management*, 13 (3), 285–295.
- Bhola PK, Leandro J, Disse M, 2020. Building Hazard Maps with Differentiated Risk Perception for Flood Impact Assessment. *Natural Hazards and Earth System Sciences*, 20 (10), 2647–2663.
- Bi XY, Wang J, Zhang JY, 2013. The Exploration of BIM Technology Application in the Building Fire Emergency Plan. *Applied Mechanics and Materials*, 357-360, 2473–2477.
- Biljecki F, Stoter J, Ledoux H, Zlatanova S, Çöltekin A, 2015. Applications of 3D City Models: State of the Art Review. *ISPRS International Journal of Geo-Information*, 4 (4), 2842–2889.
- Blanco-Vogt A, Schanze J, 2014. Assessment of the Physical Flood Susceptibility of Buildings on a Large Scale – Conceptual and Methodological Frameworks. *Natural Hazards and Earth System Sciences*, 14 (8), 2105–2117.
- Blaschke T, 2010. Object Based Image Analysis for Remote Sensing. *ISPRS Journal of Photogrammetry and Remote Sensing*, 65 (1), 2–16.
- Bodoque JM, Aroca-Jiménez E, Eguibar MÁ, García JA, 2023. Developing Reliable Urban Flood Hazard Mapping from LiDAR Data. *Journal of Hydrology*, 617, 128975.
- Boguslawski P, Mahdjoubi L, Zverovich V, Fadli F, Barki H, 2015. BIM-GIS Modelling in Support Of Emergency Response Applications. *Building information modelling (BIM) in design, construction and operations*, 149, 381.
- Bowker P, 2007. *Improving the Flood Performance of New Buildings: Flood Resilient Construction*. London: RIBA.

- Bozza A, Durand A, Confortola G, Soncini A, Allenbach B, Bocchiola D, 2016. Potential of Remote Sensing and Open Street Data for Flood Mapping in Poorly Gauged Areas: A Case Study in Gonaives, Haiti. *Applied Geomatics*, 8, 117–131.
- Brauneck J, Gattung T, Jüpner R, 2019. Surface flow velocity measurements from UAV-based videos. *The International Archives of the Photogrammetry, Remote Sensing and Spatial Information Sciences*. 42:221-6.
- Brett F. Sanders, 2017. Hydrodynamic Modeling of Urban Flood Flows and Disaster Risk Reduction. *Oxford Research Encyclopedia of Natural Hazard Science*.
- Brocchini M, Dodd N, 2008. Nonlinear Shallow Water Equation Modeling for Coastal Engineering. *Journal of Waterway, Port, Coastal, and Ocean Engineering*, 134 (2), 104–120.
- Brody SD, Zahran S, Vedlitz A, Grover H, 2007. Examining the Relationship Between Physical Vulnerability and Public Perceptions of Global Climate Change in the United States. *Environment and Behavior*, 40 (1), 72–95.
- Bubeck P, Kreibich H, Penning-Rowsell EC, Botzen WJW, de Moel H, Klijn K, 2017. Explaining Differences in Flood Management Approaches in Europe and in the USA – A Comparative Analysis. *Journal of Flood Risk Management*, 10 (4), 436–445.
- Bühlmann M, Boes RM, 2014. Lateral flood discharge at rivers: Concepts and challenges. *River Flow 2014*. 1799-806.
- Caleffi V, Valiani A, Zanni A, 2003. Finite Volume Method for Simulating Extreme Flood Events in Natural Channels. *Journal of Hydraulic Research*, 41 (2), 167–177.
- Cannon MG, Phelan JM, Passaro MA, 1995. Procedural Guidelines for Estimating Residential and Business Structure Value for use in Flood Damage Estimations, unpublished. Army Engineer Institute for Water Resources Fort Belvoir Va.
- Cantelmo C, Cuomo G, 2021. Hydrodynamic Loads on Buildings in Floods. *Journal of Hydraulic Research*, 59 (1), 61–74.
- Carstens A, 2019. BIM & GIS—New Dimensions of Improved Collaboration for Infrastructure and Environment. *Journal of Digital Landscape Architecture*, 4, 114–121.
- Charef R, Alaka H, Emmitt S, 2018. Beyond the Third Dimension of BIM: A Systematic Review of Literature and Assessment of Professional Views. *Journal of Building Engineering*, 19, 242–257.
- Chen AS, Evans B, Djordjević S, Savić DA, 2012. A Coarse-Grid Approach to Representing Building Blockage Effects in 2D Urban Flood Modelling. *Journal of Hydrology*, 426, 1–16.
- Chen K, Blong R, Jacobson C, 2003. Towards an Integrated Approach to Natural Hazards Risk Assessment Using GIS: with reference to bushfires. *Environmental management*, 31, 546–560.
- Chen K, Reichard G, Akanmu A, Xu X, 2021. Geo-Registering UAV-Captured Close-Range Images to GIS-Based Spatial Model for Building Façade Inspections. *Automation in construction*, 122, 103503.
- Chen S, Zeng Y, Majdi A, Salameh AA, Alkhalifah T, Alturise F, Ali HE, 2023. Potential features of building information modelling for application of project management knowledge areas as advances modeling tools. *Advances in Engineering Software*. 176:103372.
- Christodoulou SE, Vamvatsikos D, Georgiou C, 2010. A BIM-Based Framework for Forecasting and Visualizing Seismic Damage, Cost and Time to Repair. *eWork and eBusiness in Architecture, Engineering and Construction*, 33–38.
- Chung HC, Adeyeye K, 2018. Structural flood damage and the efficacy of property-level flood protection. *International Journal of Building Pathology and Adaptation*. 36(5):471-99.
- Coppock JT, 1995. GIS and Natural Hazards: An Overview from a GIS Perspective. *Geographical information systems in assessing natural hazards*, 21–34.

- Costa JE, 1988. Rheologic, Geomorphic and Sedimentologic Differentiation of Water Floods, Hyper Concentrated Flows, and Debris Flows. *Flood Geomorphology*, 113–122.
- CRED, 2022. EM-DAT: International Disaster Database. Accessed on 15.10.2022, <https://www.emdat.be/database>
- CSIRO, 2000. *Floodplain Management in Australia*. CSIRO Publishing.
- Cuomo G, Shams G, Jonkman S, van Gelder P, 2009. Hydrodynamic Loadings of Buildings in Floods. *Coastal Engineering* 2008. World Scientific Publishing Company.
- D'alpaos L, Defina A, 2007. Mathematical Modeling of Tidal Hydrodynamics in Shallow Lagoons: A Review of Open Issues and Applications to The Venice Lagoon. *Computers & Geosciences*, 33 (4), 476–496.
- Dai J-G, Gao W-Y, Teng JG, 2015. Finite Element Modeling of Insulated FRP-Strengthened RC Beams Exposed to Fire. *Journal of Composites for Construction*, 19 (2), 4014046.
- Dakhil A, Alshawi M, 2014. Client's Role in Building Disaster Management through Building Information Modelling. *Procedia Economics and Finance*, 18, 47–54.
- Dani AAH, Supangkat SH, 2022. Combination of Digital Twin and Augmented Reality: A Literature Review. In: 2022 International Conference on ICT for Smart Society (ICISS). IEEE.
- De Angeli S, Malamud BD, Rossi L, Taylor FE, Trasforini E, Rudari R, 2022. A multi-hazard framework for spatial-temporal impact analysis. *International Journal of Disaster Risk Reduction*. 73:102829.
- Defra EA, Flood EA, 2003. The Appraisal of Human-Related Intangible Impacts of Flooding. R&D Project.
- Dewals BJ, Giron E, Ernst J, Hecq W, Piroton M, 2008. Integrated Assessment of Flood Protection Measures in the Context of Climate Change: Hydraulic Modelling and Economic Approach. *WIT Transactions on Ecology and the Environment*, 108, 149–159.
- Dewan A, 2013. *Floods In a Megacity: Geospatial Techniques in Assessing Hazards, Risk and Vulnerability*. Springer.
- Dottori F, Salamon P, Bianchi A, Alfieri L, Hirpa FA, Feyen L, 2016. Development And Evaluation of a Framework for Global Flood Hazard Mapping. *Advances in Water Resources*, 94, 87–102.
- Douass S, Kbir MA, 2019. 3D Modeling of Flood Areas. In: Springer, Cham, p. 465–471.
- Dutta D, Alam J, Umeda K, Hayashi M, Hironaka S, 2007. A Two-Dimensional Hydrodynamic Model for Flood Inundation Simulation: A Case Study in The Lower Mekong River Basin. *Hydrological Processes*, 21 (9), 1223–1237.
- DWA, 2016. *Hochwasserangepasstes Planen und Bauen*. DWA-M 553. Deutsche Vereinigung für Wasserwirtschaft, Abwasser und Abfall e.V. (DWA). Hennef, Germany.
- El-Hallaq MA, Alastal AI, Salha RA, 2019. Enhancing Sustainable Development through Web Based 3D Smart City Model Using GIS and BIM. Case Study: Sheikh Hamad City. *Journal of Geographic Information System*, 11 (03), 321–330.
- Escobar Villanueva JR, Iglesias Martínez L, Pérez Montiel JI, 2019. DEM Generation from Fixed-Wing UAV Imaging and LiDAR-Derived Ground Control Points for Flood Estimations. *Sensors*, 19 (14), 3205.
- European Union, 2007. Directive 2007/60/EC of the European Parliament and of the Council on the Assessment and Management of Flood Risks, <https://www.eea.europa.eu/policy-documents/directive-2007-60-ec-of>
- Fauzan, Anas Ismail F, Siregar N, Al Jauhari Z, 2019. The Effect of Tsunami Loads on Pasar Raya Inpres Block III Building in Padang City based on FEMA P-646. *MATEC Web of Conferences*, 258, 3020.

- Fekete A, Sandholz S, 2021. Here Comes the Flood, but Not Failure? Lessons to Learn after the Heavy Rain and Pluvial Floods in Germany 2021. *Water*, 13(21):3016. <https://doi.org/10.3390/w13213016>
- FEMA, 2009. Quantification of Building Seismic Performance Factors. U.S. Department of Homeland Security, FEMA.
- FEMA, 2021. Building Resilient Infrastructure and Communities FY 2021 Subapplication and Selection Status.
- Flener C, Wang Y, Laamanen L, Kasvi E, Vesakoski J-M, Alho P, 2015. Empirical Modeling of Spatial 3d Flow Characteristics using a Remote-Controlled ADCP System: Monitoring a Spring Flood. *Water*, 7 (1), 217–247.
- Flood Resilience Portal, 2021. Climate Resilience Measurement for Communities (CRMC). Accessed on 02-11-2021, <https://floodresilience.net/frmc/>
- Forero-Ortiz E, Martinez-Gomariz E, Canas Porcuna M, 2020. A Review of Flood Impact Assessment Approaches for Underground Infrastructures in Urban Areas: A Focus on Transport Systems. *Hydrological Sciences Journal*, 65 (11), 1943–1955.
- Forkuo EK, Tsawo VA, 2013. The Use of Digital Elevation Models for Water-Shed and Flood Hazard Mapping. 2319-3484.
- Gallegos HA, Schubert JE, Sanders BF, 2009. Two-Dimensional, High-Resolution Modeling of Urban Dam-Break Flooding: A Case Study of Baldwin Hills, California. *Advances in Water Resources*, 32 (8), 1323–1335.
- Garvin S, Reid J, Scott M, 2005. Standards for the Repair of Buildings Following Flooding. CIRIA report C623, ISBN 0860176231.
- Gebrehiwot A, Hashemi-Beni L, Thompson G, Kordjamshidi P, Langan TE, 2019. Deep Convolutional neural network for flood extent mapping using unmanned aerial vehicles data. *Sensors*, 19 (7), 1486.
- Gems B, Mazzorana B, Hofer T, Sturm M, Gabl R, Aufleger M, 2016. 3-D hydrodynamic modelling of Flood Impacts on A Building and Indoor Flooding Processes. *Natural Hazards and Earth System Sciences*, 16 (6), 1351–1368.
- Geomer gmbH, 2017. FloodAreaHPC-Desktop – ArcGIS Erweiterung zur Berechnung von Überschwemmungsbereichen. User's Guide, Version 10.3, January 2017, Heidelberg
- Ghaith M, Yosri A, El-Dakhakhni W, 2022. Digital Twin: A City-Scale Flood Imitation Framework. Springer, Singapore, p. 577–588.
- Gilbuena Jr R, Kawamura A, Medina R, Amaguchi H, Nakagawa N, Du Bui D, 2013. Environmental Impact Assessment of Structural Flood Mitigation Measures by A Rapid Impact Assessment Matrix (Riam) Technique: A Case Study in Metro Manila, Philippines. *Science of the Total Environment*, 456, 137–147.
- Gioti E, Riga C, Kalogeropoulos K, Chalkias C, 2013. A GIS-Based Flash Flood Runoff Model Using High Resolution DEM and Meteorological Data. *EARSeL eProceedings*, 12 (1), 33–43.
- Golz S, Schinke R, Naumann T, 2015. Assessing the Effects of Flood Resilience Technologies on Building Scale. *Urban Water Journal*, 12 (1), 30–43.
- Gracia V, Sierra JP, Gómez M, Pedrol M, Sampé S, García-León M, Gironella X, 2019. Assessing The Impact of Sea Level Rise on Port Operability Using LiDAR-Derived Digital Elevation Models. *Remote Sensing of Environment*, 232, 111318.
- Gröger G, Plümer L, 2012. CityGML – Interoperable Semantic 3D City Models. *ISPRS Journal of Photogrammetry and Remote Sensing*, 71, 12–33.



- Grundý P, Thurairaja A, 2005. Some Reflections on The Structural Engineering Aspects of Tsunami Damage.
- Guidolin M, Chen AS, Ghimire B, Keedwell EC, Djordjević S, Savić DA, 2016. A Weighted Cellular Automata 2D Inundation Model for Rapid Flood Analysis. *Environmental Modelling & Software*, 84, 378–394.
- Gustafsson VS, Hjerpe M, Strandberg G, 2023. Construction of a National Natural Hazard Interaction Framework: The Case of Sweden. *Iscience*, 26(4).
- Guyo E, Hartmann T, Ungureanu L, 2021. Interoperability Between BIM and GIS through Open Data Standards: An Overview of Current Literature. *Sign*, 3, 5–9.
- Ha MC, Vu PL, Nguyen HD, Hoang TP, Dang DD, Dinh TBH, Şerban G, Rus I, Breţcan P, 2022. Machine Learning and Remote Sensing Application for Extreme Climate Evaluation: Example of Flood Susceptibility in the Hue Province, Central Vietnam Region. *Water*, 14 (10), 1617.
- Haberlandt U, 2010. From Hydrological Modelling to Decision Support. *Advances in Geosciences*, 27, 11–19.
- Hadimlioglu IA, King SA, Starek MJ, 2020. FloodSim: Flood Simulation and Visualization Framework Using Position-Based Fluids. *ISPRS International Journal of Geo-Information*, 9 (3), 163.
- Hailin Z, Yi J, Xuesong Z, Gaoliao J, Yi Y, Baoyin H, 2009. GIS-Based Risk Assessment for Regional Flood Disaster. 2009 International Conference on Environmental Science and Information Application Technology. IEEE.
- Hammond MJ, Chen AS, Djordjević S, Butler D, Mark O, 2015. Urban Flood Impact Assessment: A State-of-the-art Review. *Urban Water Journal*, 12 (1), 14–29.
- Haq M, Akhtar M, Muhammad S, Paras S, Rahmatullah J, 2012. Techniques of Remote Sensing and GIS for Flood Monitoring and Damage Assessment: A Case Study of Sindh Province, Pakistan. *The Egyptian Journal of Remote Sensing and Space Science*, 15 (2), 135–141.
- Hartmann T, and Juepner R, 2014. The European flood risk management plan: Between spatial planning and water engineering. *Journal of Flood Risk Management*, pp.1-2.
- Hartmann T, Jupner R, 2020. Implementing Resilience in Flood Risk Management.
- Hartmann T, Slavíková L, Wilkinson ME, 2022. Spatial flood risk management: Implementing catchment-based retention and resilience on private land. Edward Elgar Publishing.
- Hegger DL, Driessen PP, Wiering M, Van Rijswick HF, Kundzewicz ZW, Matczak P, Crabbé A, Raadgever GT, Bakker MH, Priest SJ, Larrue C, 2016. Toward more flood resilience: Is a diversification of flood risk management strategies the way forward?. *Ecology and Society*. 21(4).
- Hong L, Ouyang M, Peeta S, He X, Yan Y, 2015. Vulnerability Assessment and Mitigation for the Chinese Railway System Under Floods. *Reliability Engineering & System Safety*, 137, 58–68.
- Hossain AA, Jia Y, Ying X, Zhang Y, Zhu TT, 2012. Visualization of Urban Area Flood Simulation in Realistic 3d Environment. *World Environmental and Water Resources Congress 2011: Bearing Knowledge for Sustainability* (pp. 1973-1980).
- Hosseini FS, Sigaroodi SK, Salajegheh A, Moghaddamnia A, Choubin B, 2021. Towards a flood vulnerability assessment of watershed using integration of decision-making trial and evaluation laboratory, analytical network process, and fuzzy theories. *Environmental Science and Pollution Research*. 62487-98.
- Ibrahim A, Mahmood M, 2009. Finite Element Modeling of Reinforced Concrete Beams Strengthened with FRP Laminates. *European Journal of Scientific Research*, 30, 526–541.

- Intignano M, Biancardo SA, Oreto C, Viscione N, Veropalumbo R, Russo F, Ausiello G, Dell'Acqua G, 2021. Heritage-BIM Workflow for Stone Road Pavements Digital Reproduction. *Heritage* 2021, 4, 3032–3049.
- Irizarry J, Karan EP, Jalaei F, 2013. Integrating BIM and GIS to Improve the Visual Monitoring of Construction Supply Chain Management. *Automation in construction*, 31, 241–254.
- Isikdag U, 2015. BIM and IoT: A Synopsis from GIS Perspective. *International Archives of the Photogrammetry, Remote Sensing & Spatial Information Sciences*, 40.
- Isikdag U, Zlatanova S, 2009. A SWOT Analysis on the Implementation of Building Information Models within the Geospatial Environment. In: *Urban and Regional Data Management*. CRC Press, p. 27–42.
- Isma'il M, Saanyol IO, 2013. Application of Remote Sensing (RS) And Geographic Information Systems (GIS) in Flood Vulnerability Mapping: Case Study of River Kaduna. *International Journal of Geomatics and Geosciences*, 3 (3), 618–627.
- Jakob M, Stein D, Ulmi M, 2012. Vulnerability of Buildings to Debris Flow Impact. *Natural Hazards*, 60 (2), 241–261.
- Jakovljevic G, Govedarica M, Alvarez-Taboada F, Pajic V, 2019. Accuracy Assessment of Deep Learning Based Classification of LiDAR and UAV Points Clouds for DTM Creation and Flood Risk Mapping. *Geosciences*, 9 (7), 323.
- Jamali B, Löwe R, Bach PM, Urich C, Arnbjerg-Nielsen K, Deletic A, 2018. A Rapid Urban Flood Inundation and Damage Assessment Model. *Journal of Hydrology*, 564, 1085–1098.
- Javadnejad F, Waldron B, Hill A, 2017. LITE Flood: Simple GIS-Based Mapping Approach for Real-Time Redelineation of Multifrequency Floods. *Natural Hazards Review*. 18(3):04017004.
- Jayaraj P, Ramiya AM, 2018. 3D CityGML Building Modelling from LiDAR Point Cloud Data. *International Archives of The Photogrammetry, Remote Sensing & Spatial Information Sciences*, 42, 175–180.
- Jeong C, 2020. Development of a Flood Disaster Evacuation Map Using Two-Dimensional Flood Analysis and BIM Technology. *Journal of Korean Society of Disaster and Security*, 13 (2), 53–63.
- Jha AK, Bloch R, Lamond J, 2012. *Cities and Flooding: A Guide to Integrated Urban Flood Risk Management for the 21st Century*. World Bank Publications.
- Jia H, Chen F, Pan D, Du E, Wang L, Wang N, Yang A, 2022. Flood Risk Management in the Yangtze River Basin—Comparison of 1998 and 2020 Events. *International Journal of Disaster Risk Reduction*, 68, 102724.
- Jiang C, Yao Y, Deng Y, Deng B, 2015. Numerical Investigation of Solitary Wave Interaction with a Row of Vertical Slotted Piles. *Journal of Coastal Research*, 31 (6), 1502–1511.
- Jin X, Kranenburg C, 1993. Quasi-3D Numerical Modeling of Shallow-Water Circulation. *Journal of Hydraulic Engineering*, 119 (4), 458–472.
- Jodhani KH, Patel D, Madhavan N, 2021. A Review on Analysis of Flood Modelling Using Different Numerical Models. *Materials Today: Proceedings*.
- Johnson CL, Priest SJ, 2008. Flood Risk Management in England: A Changing Landscape of Risk Responsibility? *International Journal of Water Resources Development*, 24 (4), 513–525.
- Jongman B, Kreibich H, Apel H, Barredo JI, Bates PD, Feyen L, Gericke A, Neal J, Aerts J, Ward PJ, 2012. Comparative Flood Damage Model Assessment: Towards a European Approach. *Natural Hazards and Earth System Sciences*, 12 (12), 3733–3752.
- Jonkman SN, Kelman I, 2005. An Analysis of the Causes and Circumstances of Flood Disaster Deaths. *Disasters*, 29 (1), 75–97.

- Joseph R, Proverbs D, Lamond J, Wassell P, 2014. Application of the Concept of Cost Benefits Analysis (CBA) to Property Level Flood Risk Adaptation Measures: A Conceptual Framework for Residential Structural Survey.
- Joy CS, 1993. The Cost of Flood Damage in Nyngan. *Climatic Change*, 25 (3-4), 335–351.
- Jüpner R, 2018. Coping With Extremes - Experiences from Event Management During the Recent Elbe Flood Disaster in 2013. *Journal of Flood Risk Management*, 11 (1), 15–21.
- Jüpner R, 2019. Commentary: Effectiveness and Integrated Multi-use of Retention Measures—A Hydraulic Engineering Perspective. In: *Nature-Based Flood Risk Management on Private Land*. Springer Nature, Cham, p. 209–212.
- Jüpner R, Bachmann D, Fekete A, Hartmann T, Pohl R, Schmitt T, Schulte A, 2018. Resilienz im Hochwasserrisikomanagement. *Korrespondenz Abwasser. Abfall*. (11):656-63.
- Kabir SMI, Ahmari H, Dean M, 2023. Contribution of Debris and Substructures to Hydrodynamic Forces on Bridges. *Engineering Structures*, 283, 115878.
- Karagiorgos K, Thaler T, Hübl J, Maris F, Fuchs S, 2016. Multi-vulnerability Analysis for Flash Flood Risk Management. *Natural Hazards*, 82, 63–87.
- Karam W, Khan FA, Alam M, Ali S, 2021. Simulation of Dam-Break Flood Wave and Inundation Mapping: A Case study of Attabad Lake. *International Journal*, 9 (6).
- Karan EP, Irizarry J, Haymaker J, 2016. BIM and GIS Integration and Interoperability Based on Semantic Web Technology. *Journal of Computing in Civil Engineering*, 30 (3), 4015043.
- Kelman I, 2003. Physical Flood Vulnerability of Residential Properties in Coastal, Eastern England. University of Cambridge Cambridge, United Kingdom.
- Kelman I, Gaillard J-C, Lewis J, Mercer J, 2016. Learning from the History of Disaster Vulnerability and Resilience Research and Practice for Climate Change. *Natural Hazards*, 82, 129–143.
- Kelman I, Spence R, 2004. An Overview of Flood Actions on Buildings. *Engineering Geology*, 73 (3-4), 297–309.
- Keys C, 2006. The Evolution of Floodplain Risk Management and Real-Time Flood Management Planning in New South Wales. *Australian Journal of Emergency Management*, The, 21 (1), 3–8.
- Khan SI, Hong Y, Wang J, Yilmaz KK, Gourley JJ, Adler RF, Brakenridge GR, Policelli F, Habib S, Irwin D, 2011. Satellite Remote Sensing and Hydrologic Modeling for Flood Inundation Mapping in Lake Victoria Basin: Implications for Hydrologic Prediction in Ungauged Basins. *IEEE Transactions on Geoscience and Remote Sensing*, 49 (1), 85–95.
- Khayyal HK, Zeidan ZM, Beshr AAA, 2022. Creation and Spatial Analysis of 3D City Modeling Based on GIS Data. *Civil Engineering Journal*, 8 (1), 105.
- Kim JO, Lee JK, 2021. Urban Flood Inundation Simulation Based on High-Precision 3D Modeling. *Journal of Coastal Research*, 114 (sp1), 454–458.
- Kim KP, Park KS, 2016. Primary BIM Dataset for Refurbishing Flood Risk Vulnerable Housing in the UK. *Built Environment Project and Asset Management*, 6 (4), 365–378.
- Klapp J, Areu-Rangel OS, Cruchaga M, Aránguiz R, Bonasia R, Godoy MJ, Silva-Casarín R, 2020. Tsunami Hydrodynamic Force on A Building Using A SPH Real-Scale Numerical Simulation. *Natural Hazards*, 100, 89–109.
- Korzani MG, Galindo-Torres SA, Scheuermann A, Williams DJ, 2018. Smoothed Particle Hydrodynamics for Investigating Hydraulic and Mechanical Behaviour Of An Embankment Under Action Of Flooding And Overburden Loads. *Computers and Geotechnics*, 94, 31–45.

- Krishnan S, Crosby C, Nandigam V, Phan M, Cowart C, Baru C, Arrowsmith R, 2011. Open Topography. Proceedings of the 2nd International Conference on Computing for Geospatial Research & Applications - COM.Geo '11. ACM Press, New York, New York, USA.
- Krüger T, 2009. HafenCity Hamburg—Ein Modell für Moderne Stadtentwicklung? *Raumplanung* (146), 193–198.
- Kumar K, Ledoux H, Stoter J, 2018. Dynamic 3d Visualization of Floods: Case of The Netherlands. *International archives of the photogrammetry, remote sensing & spatial information sciences*.
- Kurnio H, Fekete A, Naz F, Norf C, Jüpner R, 2021. Resilience learning and indigenous knowledge of earthquake risk in Indonesia. *International Journal of Disaster Risk Reduction*, 62, 102423.
- Laakso M, Kiviniemi AO, 2012. The IFC standard: A Review of History, Development, and Standardization, *Information Technology. ITcon*, 17 (9), 134–161.
- Laat R de, van Berlo L, 2011. Integration of BIM and GIS: The Development of the CityGML GeoBIM Extension. *Advances in 3D Geo-Information Sciences*. Springer, Berlin, Heidelberg, p. 211–225.
- Lamond JE, Bhattacharya-Mis N, Chan FKS, Kreibich H, Montz B, Proverbs DG, Wilkinson S, 2019. Flood Risk Insurance, Mitigation and Commercial Property Valuation. *Property Management*.
- LAWA, 2018. Empfehlungen zur Aufstellung von Hochwassergefahrenkarten und Hochwasserrisikokarten. Bund-/Länderarbeitsgemeinschaft Wasser (LAWA), Ständiger Ausschuss Ständiger Ausschuss "Hochwasserschutz und Hydrologie" der LAWa (LAWA-AH). Weimar, Germany.
- Lemarié-Rieusset PG, 2018. *The Navier-Stokes Problem in the 21st Century*. CRC Press.
- Lenac K, Kitanov A, Cupec R, Petrović I, 2017. Fast Planar Surface 3D SLAM using LIDAR. *Robotics and Autonomous Systems*, 92, 197–220.
- Li C, Sun N, Lu Y, Guo B, Wang Y, Sun X, Yao Y, 2023. Review on Urban Flood Risk Assessment. *Sustainability*, 15 (1), 765.
- Li Y, Grimaldi S, Walker J, Pauwels V, 2016. Application of Remote Sensing Data to Constrain Operational Rainfall-Driven Flood Forecasting: A Review. *Remote Sensing*, 8 (6), 456, <https://www.mdpi.com/142062>
- Lim S, Thatcher CA, Brock JC, Kimbrow DR, Danielson JJ, Reynolds BJ, 2013. Accuracy Assessment of a Mobile Terrestrial LiDAR Survey at Padre Island National Seashore. *International Journal of Remote Sensing*, 34 (18), 6355–6366.
- Lippert F, Gradecak M, Petkanic P, 2018. Flooding Analysis based on LiDAR Point Cloud Data.
- Liu S, Zheng W, Zhou Z, Zhong G, Zhen Y, Shi Z, 2022. Flood Risk Assessment of Buildings Based on Vulnerability Curve: A Case Study in Anji County. *Water*, 14 (21), 3572.
- Liu W, He S, OnYang C, 2016. Dynamic process simulation with a Savage-Hutter type model for the intrusion of landslide into river. *Journal of Mountain Science*, 13 (7), 1265–1274.
- Lyu H-M, Shen S-L, Zhou A, Yang J, 2019. Perspectives for Flood Risk Assessment and Management for Mega-City Metro System. *Tunnelling and Underground Space Technology*, 84, 31–44.
- Ma Z, Ren Y, 2017. Integrated Application of BIM and GIS: an Overview. *Procedia Engineering*, 196, 1072–1079.
- Mahaffey S, 2018. A coupled hydrodynamic and discrete element method for modelling flash flood debris (Doctoral dissertation, Newcastle University).
- Maiezza P, 2019. As-built Reliability in Architectural HBIM Modeling. *International Archives of the Photogrammetry, Remote Sensing & Spatial Information Sciences*, 42, 461–466.
- Marvi MT, 2020. A Review of Flood Damage Analysis for a Building Structure and Contents. *Natural Hazards*, 102 (3), 967–995.

- Massaâbi M, Layouni O, Oueslati WBM, Alahmari F, 2018. An Immersive System for 3D Floods Visualization and Analysis. Springer, Cham, p. 69–79.
- Mazzorana B, Simoni S, Scherer C, Gems B, Fuchs S, Keiler M, 2014. A Physical Approach on Flood Risk Vulnerability of Buildings. *Hydrology and Earth System Sciences*, 18 (9), 3817–3836.
- McGraw Hill Construction, 2014. The Business Value of BIM for Construction in Major Global Markets: How Contractors Around the World Are Driving Innovation with Building Information Modeling. ICN Netherlands BV.
- McLachlan A, Defeo O, Jaramillo E, Short AD, 2013. Sandy Beach Conservation and Recreation: Guidelines for Optimising Management Strategies for Multi-Purpose Use. *Ocean & Coastal Management*, 71, 256–268.
- Meinel G, Hecht R, Herold H, 2009. Analyzing Building Stock Using Topographic Maps and GIS. *Building Research & Information*, 37 (5-6), 468–482.
- Merz B, Kreibich H, Schwarze R, Thielen A, 2010. Review article" Assessment of Economic Flood Damage". *Natural Hazards and Earth System Sciences*, 10 (8), 1697–1724.
- Merz B, Thielen AH, Gocht M, 2007. Flood Risk Mapping at The Local Scale: Concepts and Challenges. *Flood Risk Management in Europe: Innovation in Policy and Practice*, 231–251.
- Messaoudi M, Nawari NO, 2020. BIM-based Virtual Permitting Framework (VPF) for Post-Disaster Recovery and Rebuilding in the State of Florida. *International Journal of Disaster Risk Reduction*, 42, 101349.
- Messner F, 2007. Evaluating Flood Damages: Guidance and Recommendations on Principles and Methods. T09-06-01.
- Messner F, Meyer V, 2006. Flood Damage, Vulnerability, And Risk Perception – Challenges for Flood Damage Research. *Flood Risk Management: Hazards, Vulnerability and Mitigation Measures*. Springer, Dordrecht, p. 149–167.
- Meyer V, Messner F, Penning-Rowsell EC, Green CH, Tunstall SM, van der Veen A, Tapsell SM, Wilson T, Krywkow, Joerg, Logtmeijer C, Fernández-Bilbao A, Geurts P, Haase D, Parker DJ, 2009a. Evaluating Flood Damages: Guidance and Recommendations on Principles and Methods Executive Summary. European Commission.
- Meyer V, Scheuer S, Haase D, 2009b. A Multicriteria Approach for Flood Risk Mapping Exemplified at the Mulde River, Germany. *Natural Hazards*, 48 (1), 17–39.
- MIKE DH, 2012. 2D Modelling of Coast and Sea. DHI Water & Environment Pty Ltd.: Hørsholm, Denmark.
- Miller F, Osbahr H, Boyd E, Thomalla F, Bharwani S, Ziervogel G, Walker B, Birkmann J, van der Leeuw S, Rockström J, 2010. Resilience and Vulnerability: Complementary or Conflicting Concepts? *Ecology and Society*, 15 (3).
- Miro Govedarica, Gordana Jakovljević, Flor Álvarez-Taboada, 2018. Flood Risk Assessment based on LiDAR and UAV Points Clouds and DEM. *SPIE*, p. 66–76.
- Mirzaei K, Arashpour M, Asadi E, Masoumi H, Bai Y, Behnood A, 2022. 3D Point Cloud Data Processing with Machine Learning for Construction and Infrastructure Applications: A Comprehensive Review. *Advanced Engineering Informatics*, 51, 101501.
- Moel H de, Jongman B, Kreibich H, Merz B, Penning-Rowsell E, Ward PJ, 2015. Flood Risk Assessments at Different Spatial Scales. *Mitigation and Adaptation Strategies for Global Change*, 20 (6), 865–890.

- Moel H de, van Vliet M, Aerts JC, 2014. Evaluating the Effect of Flood Damage-Reducing Measures: A Case Study of The Unembanked Area of Rotterdam, the Netherlands. *Regional environmental change*, 14, 895–908.
- Moudrak N, Feltmate B, 2019. Ahead of the Storm: Developing Flood-Resilience Guidance for Canada's Commercial Real Estate. Intact Centre on Climate Adaptation.
- Muhadi NA, Abdullah AF, Bejo SK, Mahadi MR, Mijic A, 2020. The Use of LiDAR-Derived DEM in Flood Applications: A Review. *Remote Sensing*, 12 (14), 2308.
- Munawar HS, Hammad AWA, Waller ST, Thaheem MJ, Shrestha A, 2021. An Integrated Approach for Post-Disaster Flood Management Via the Use of Cutting-Edge Technologies and UAVs: A Review. *Sustainability*, 13 (14), 7925.
- Mustafa AS, Sulaiman SO, Al\_Alwani KM, 2017. Application of HEC-RAS Model to Predict Sediment Transport for Euphrates River from Haditha to Heet 2016. *Al-Nahrain Journal for Engineering Sciences*, 20 (3), 570–577.
- Nadal NC, 2007. Expected Flood Damage to Buildings in Riverine and Coastal Zones.
- Nadal NC, Zapata RE, Pagán I, López R, Agudelo J, 2010. Building Damage Due to Riverine and Coastal Floods. *Journal of Water Resources Planning and Management*, 136 (3), 327–336.
- Nagel C, 2014. Spatio-Semantic Modelling of Indoor Environments for Indoor Navigation.
- Nakazato H, Lim S, 2020. Interplay Between Social Support Tie Formations and Subjective Mental Health Conditions in a Community Currency System in Japanese Disaster-Affected Communities: The Ambivalent Effects of Social Capital. *International Journal of Disaster Risk Reduction*, 51, 101809.
- Nanditha JS, Kushwaha AP, Singh R, Malik I, Solanki H, Chuphal DS, Dangar S, Mahto SS, Vegad U, Mishra V, 2023. The Pakistan Flood of August 2022: Causes and Implications. *Earth's Future*. (3): e2022EF003230.
- Nasim M, Setunge S, Zhou S, Mohseni H, 2019. An Investigation of Water-Flow Pressure Distribution on Bridge Piers Under Flood Loading. *Structure and Infrastructure Engineering*, 15 (2), 219–229.
- Néelz S, Pender G, 2009. Desktop Review of 2D Hydraulic Modelling Packages, Science Report SC080035, Joint UK Defra/Environment Agency Flood and Coastal Erosion. Risk Management R&D Program.
- Néelz S, Pender G, 2010. Benchmarking of 2D Hydraulic Modelling Packages. 18491119.
- Néelz S, Pender G, 2013. Delivering Benefits thorough Evidences: Benchmarking the Latest Generation of 2D Hydraulic Modelling Packages. Report—SC120002.
- Nektarios NK, George PK, 2013. A Hydro-Economic Modelling Framework for Flood Damage Estimation and The Role of Riparian Vegetation. *Hydrological Processes*, 27 (4), 515–531.
- Nguyen TG, Joric C, Tran AP, 2009. A Method to Construct Flood Damage Map with an Application to Huong River Basin, In Central Vietnam. *VNU Journal of Science: Earth and Environmental Sciences*, 25 (1).
- Nistor I, Palermo D, Nouri Y, Murty T, Saatcioglu M, 2018. Tsunami-Induced Forces on Structures. In: *Handbook of Coastal and Ocean Engineering*. World Scientific, p. 481–506.
- Niu S, Pan W, Zhao Y, 2015. A BIM-GIS Integrated Web-Based Visualization System for Low Energy Building Design. *Procedia Engineering*, 121, 2184–2192.
- Nkwunonwo UC, Whitworth M, Baily B, 2020. A Review of The Current Status of Flood Modelling for Urban Flood Risk Management in the Developing Countries. *Scientific African*, 7, e00269.
- Noardo F, Harrie L, Arroyo Ogori K, Biljecki F, Ellul C, Krijnen T, Eriksson H, Guler D, Hintz D, Jadidi MA, Pla M, Sanchez S, Soini V-P, Stouffs R, Tekavec J, Stoter J, 2020. Tools for BIM-GIS Integration (IFC

- Georeferencing and Conversions): Results from the GeoBIM Benchmark 2019. *ISPRS International Journal of Geo-Information*, 9 (9), 502.
- Noh SJ, Lee J-H, Lee S, Kawaike K, Seo D-J, 2018. Hyper-Resolution 1D-2D Urban Flood Modelling Using LiDAR Data and Hybrid Parallelization. *Environmental Modelling & Software*, 103, 131–145.
- Novero AU, Pasaporte MS, Aurelio RM, Madanguit CJG, Tinoy MRM, Luayon MS, Oñez JPL, Daquiado EGB, Diez JMA, Ordaneza JE, Riños LJ, Capin NC, Pototan BL, Tan HG, Polinar MDO, Nebres DI, Nañola CL, 2019. The Use of Light Detection and Ranging (LiDAR) Technology and GIS in the Assessment and Mapping of Bioresources in Davao Region, Mindanao Island, Philippines. *Remote Sensing Applications: Society and Environment*, 13, 1–11.
- Oddo PC, Lee BS, Garner GG, Srikrishnan V, Reed PM, Forest CE, Keller K, 2020. Deep Uncertainties in Sea-Level Rise and Storm Surge Projections: Implications for Coastal Flood Risk Management. *Risk Analysis*, 40 (1), 153–168.
- Omirtay O, 2018. BIM-GIS Technologies In Analysing the Cost of Assets After Natural Disasters: Water Flood and Earthquake.
- Özgenç Aksoy A, Doğan M, Oğuzhan Güven S, Tanır G, Güney MŞ, 2022. Experimental and Numerical Investigation of the Flood Waves due to Partial Dam Break. *Iranian Journal of Science and Technology, Transactions of Civil Engineering*, 46 (6), 4689–4704.
- Papathoma-Köhle M, Schlögl M, Dosser L, Roesch F, Borga M, Erlicher M, Keiler M, Fuchs S, 2022. Physical Vulnerability to Dynamic Flooding: Vulnerability Curves and Vulnerability Indices. *Journal of Hydrology*, 607, 127501.
- Patten D, 2017. What Does Building Information Modelling (BIM) Really Look Like? Leeds Flood Alleviation Scheme, A Case Study. IABSE Conference, Bath 2017: Creativity and Collaboration – Instilling Imagination and Innovation in Structural Design. International Association for Bridge and Structural Engineering (IABSE), Zurich, Switzerland.
- Peiwei Xie, Vincent H Chu, 2017. Flood Wave Force on Infrastructure.
- Penning-Rowsell E, Johnson C, Tunstall S, Tapsell S, Morris J, Chatterton J, Green C, 2005. *The Benefits of Flood and Coastal Risk Management: A Handbook of Assessment Techniques*. ISBN 1904750516.
- Percival S, Teeuw R, 2019. A methodology for urban micro-scale coastal flood vulnerability and risk assessment and mapping. *Natural Hazards*. 97(1):355-77.
- Pistrika A, Tsakiris G, Nalbantis I, 2014. Flood Depth-Damage Functions for Built Environment. *Environmental Processes*, 1, 553–572.
- Pistrika AK, Jonkman SN, 2010. Damage to Residential Buildings due to Flooding of New Orleans After Hurricane Katrina. *Natural Hazards*, 54 (2), 413–434.
- Popat E, 2017. Flood Vulnerability Assessment for Building Inventories-The Case of the Municipality Bennewitz, Germany, unpublished. Master's thesis, Technische Universität Dresden.
- Pregolato M, Ford A, Wilkinson SM, Dawson RJ, 2017. The Impact of Flooding on Road Transport: A Depth-Disruption Function. *Transportation Research Part D: Transport and Environment*, 55, 67–81.
- Proverbs D, Soetanto R, 2004. *Flood Damaged Properties*. Wiley-Blackwell Publishing, London, UK.
- Qiu C, Zhou S, Liu Z, Gao Q, Tan J, 2019. Digital Assembly Technology based on Augmented Reality and Digital Twins: A Review. *Virtual Reality & Intelligent Hardware*, 1 (6), 597–610.
- Rehman K, Cho Y-S, 2016. Building Damage Assessment Using Scenario Based Tsunami Numerical Analysis and Fragility Curves. *Water*, 8 (3), 109.



- Rhee J, Park K, Lee S, Jang S, Yoon S, 2020. Detecting Hydrological Droughts in Ungauged Areas from Remotely Sensed Hydro-Meteorological Variables Using Rule-Based Models. *Natural Hazards*, 103 (3), 2961–2988.
- Robb DM, Vasquez JA, 2015. Numerical Simulation of Dam-Break Flows Using Depth-Averaged Hydrodynamic and Three-Dimensional CFD Models. *Proceedings of 22nd Canadian Society for Civil Engineering 22nd Hydrotechnical Conference* (pp. 1-10).
- Rocha G, Mateus L, Fernández J, Ferreira V, 2020. A Scan-to-BIM Methodology Applied to Heritage Buildings. *Heritage*, 3 (1), 47–67.
- Rong Y, Zhang T, Zheng Y, Hu C, Peng L, Feng P, 2020. Three-Dimensional Urban Flood Inundation Simulation based on Digital Aerial Photogrammetry. *Journal of Hydrology*, 584, 124308.
- Roussel J-R, Auty D, Coops NC, Tompalski P, Goodbody TRH, Meador AS, Bourdon J-F, Boissieu F de, Achim A, 2020. LiDAR: An R Package for Analysis of Airborne Laser Scanning (ALS) Data. *Remote Sensing of Environment*, 251, 112061.
- Ruixue L, Yicheng Z, 2021. Analysis of BIM and GIS Integration: Results from Literature Review and Questionnaire, unpublished.
- Rusca M, 2018. Visualizing Urban Inequalities: The Ethics of Videography and Documentary Filmmaking in Water Research. *WIREs Water*, 5 (4).
- Sadegh Khanmohammadi, Mehrdad Arashpour, Yu Bai, 2020. Applications of Building Information Modeling (BIM) in Disaster Resilience: Present Status and Future Trends.
- Sakuraba M, Nojima K, Takase S, 2020. Numerical Study on Behavior of Multiple Tsunami Drifting Object. Springer, Singapore, p. 261–268.
- Samali B, Kwok KC, 1995. Use of Viscoelastic Dampers in Reducing Wind-And Earthquake-Induced Motion of Building Structures. *Engineering Structures*, 17 (9), 639–654.
- Samuels P, Klijn F, Dijkman J, 2006. An Analysis of The Current Practice of Policies on River Flood Risk Management in Different Countries. *Irrigation and Drainage: The Journal of the International Commission on Irrigation and Drainage*, 55 (S1), S141-S150.
- Sani MJ, Abdul Rahman A, 2018. GIS and BIM Integration at Data Level: A Review. *The International Archives of the Photogrammetry, Remote Sensing and Spatial Information Sciences*, XLII-4/W9, 299–306.
- Schaller J, Gnaedinger J, Reith L, Freller S, Mattos C, 2017. GeoDesign: Concept for Integration Of BIM And GIS In Landscape Planning. *Journal of Digital Landscape Architecture*. 102.
- Schubert JE, Sanders BF, 2012. Building Treatments for Urban Flood Inundation Models and Implications for Predictive Skill and Modeling Efficiency. *Advances in Water Resources*, 41, 49–64.
- Serra-Llobet A, Jähnig SC, Geist J, Kondolf GM, Damm C, Scholz M, Lund J, Opperman JJ, Yarnell SM, Pawley A, Shader E, 2022. Restoring rivers and floodplains for habitat and flood risk reduction: experiences in multi-benefit floodplain management from California and Germany. *Frontiers in Environmental Science*. 9:778568.
- Serre D, Barroca B, Balsells M, Becue V, 2018. Contributing to Urban Resilience to Floods With Neighbourhood Design: The Case of Am Sandtorkai/Dalmanckai in Hamburg. *Journal of Flood Risk Management*, 11, S69-S83.
- Sertyesilisik B, 2017. Building Information Modeling as Tool for Enhancing Disaster Resilience of the Construction Industry. 1801-1764.
- Shahat E, Hyun CT, Yeom C, 2021. City Digital Twin Potentials: A Review and Research Agenda. *Sustainability*, 13 (6), 3386.

- Shirowzhan S, Sepasgozar S, 2019. Spatial Analysis Using Temporal Point Clouds in Advanced GIS: Methods for Ground Elevation Extraction in Slant Areas and Building Classifications. *ISPRS International Journal of Geo-Information*, 8 (3), 120.
- Shirowzhan S, Sepasgozar SME, Edwards DJ, Li H, Wang C, 2020. BIM Compatibility and Its Differentiation with Interoperability Challenges as An Innovation Factor. *Automation in construction*, 112, 103086.
- Singh H, Garg RD, 2016. Web 3D GIS Application for Flood Simulation and Querying through Open-Source Technology. *Journal of the Indian Society of Remote Sensing*, 44, 485–494.
- Sleigh P, Gaskell P, Berzins M, Wright N, 1998. An Unstructured Finite-Volume Algorithm for Predicting Flow in Rivers and Estuaries. *Computers & Fluids*, 27 (4), 479–508.
- Smelik R, Tutenel T, Kraker KJ de, Bidarra R, 2010. Integrating Procedural Generation and Manual Editing of Virtual Worlds. *Proceedings of the 2010 Workshop on Procedural Content Generation in Games*. ACM, New York, NY, USA.
- Smith AB, 2020. US Billion-Dollar Weather and Climate Disasters, 1980–Present (NCEI Accession 0209268). NOAA National Centers for Environmental Information, 10.
- Smith DI, 1994. Flood Damage Estimation-A Review of Urban Stage-Damage Curves and Loss Functions. *Water Sa*, 20 (3), 231–238.
- Snow M, Prasad D, 2011. Climate Change Adaptation for Building Designers: An Introduction. *Environment Design Guide*, 66, 1–11.
- Sohn W, Brody SD, Kim J-H, Li M-H, 2020. How Effective are Drainage Systems in Mitigating Flood Losses? *Cities*, 107, 102917.
- Song Y, Wang X, Tan Y, Wu P, Sutrisna M, Cheng J, Hampson K, 2017. Trends and Opportunities of BIM-GIS Integration in the Architecture, Engineering and Construction Industry: A Review from a Spatio-Temporal Statistical Perspective. *ISPRS International Journal of Geo-Information*, 6 (12), 397.
- Spekkers MH, Kok M, Clemens, F. H. L. R., Veldhuis JAE ten, 2014. Decision Tree Analysis of Factors Influencing Rainfall-Related Building Damage. Copernicus GmbH.
- Standard B, 2006. Eurocode 1: Actions on structures—. British Standard, United Kingdom.
- Stolle J, Goseberg N, Nistor I, Petriu E, 2019. Debris Impact Forces on Flexible Structures in Extreme Hydrodynamic Conditions. *Journal of Fluids and Structures*, 84, 391–407.
- Sultana P, Thompson PM, Wesselink A, 2020. Coping and Resilience in Riverine Bangladesh. *Environmental Hazards*, 19 (1), 70–89.
- Suppasri A, Pakoksung K, Charvet I, Chua CT, Takahashi N, Ornthammarath T, Latcharote P, Leelawat N, Imamura F, 2019. Load-Resistance Analysis: An Alternative Approach to Tsunami Damage Assessment Applied to the 2011 Great East Japan Tsunami. *Natural Hazards and Earth System Sciences*, 19 (8), 1807–1822.
- Taggart M, van de Lindt JW, 2009. Performance-Based Design of Residential Wood-Frame Buildings for Flood Based on Manageable Loss. *Journal of performance of constructed facilities*, 23 (2), 56–64.
- Taillandier F, Di Maiolo P, Taillandier P, Jacquenod C, Rauscher-Lauranceau L, Mehdizadeh R, 2021. An Agent-Based Model to Simulate Inhabitants' Behavior During a Flood Event. *International Journal of Disaster Risk Reduction*, 64, 102503.
- Tang S, Shelden DR, Eastman CM, Pishdad-Bozorgi P, Gao X, 2019. A Review of Building Information Modeling (BIM) And the Internet of Things (Iot) Devices Integration: Present Status and Future Trends. *Automation in construction*, 101, 127–139.
- Tariq Maqsood, Martin Wehner, Mark Edwards, Valdis Juskevics, 2014. Flood Vulnerability Research at Geoscience Australia.

- Teng J, 2020. Development and Application of an Effective and Robust Flood Inundation Model.
- Teng J, Jakeman AJ, Vaze J, Croke B, Dutta D, Kim S, 2017. Flood Inundation Modelling: A Review of Methods, Recent Advances and Uncertainty Analysis. *Environmental Modelling & Software*, 90, 201–216.
- Terry Cannon, John Twigg, 2003. *Social Vulnerability, Sustainable Livelihoods and Disasters*.
- Thieken A, Merz B, Kreibich H, Apel H, 2006. Methods for flood risk assessment: Concepts and challenges. *International workshop on flash floods in urban areas. Muscat–Sultanate of Oman*. (pp. 1-12).
- Tom RO, George KO, Joanes AO, Haron A, 2022. Review of Flood Modelling and Models in Developing Cities and Informal Settlements: A Case of Nairobi City. *Journal of Hydrology: Regional Studies*, 43, 101188.
- Tran-Cong S, Gay M, Michaelides EE, 2004. Drag Coefficients of Irregularly Shaped Particles. *Powder Technology*, 139 (1), 21–32.
- Trepekli K, Balstrøm T, Friberg T, Fog B, Allotey AN, Kofie RY, Møller-Jensen L, 2022. UAV-borne, LiDAR-Based Elevation Modelling: A Method for Improving Local-Scale Urban Flood Risk Assessment. *Natural Hazards*, 113 (1), 423–451.
- Tuan Hai D, Kim Hoang N, 2023. Maintenance Policies and Practices on Resilient Houses: Case Study from a Coastal Resilience Project in Vietnam. *Sustainability*. 15(7):5842.
- Ullah K, Witt E, Lill I, 2022. The BIM-based building permit process: Factors affecting adoption. *Buildings*. 12(1):45.
- UNDDR, 2019. *United Nations Office for Disaster Risk Reduction: 2019 annual report*.
- UNISDR C, 2015. *The Human Cost of Natural Disasters: A Global Perspective*.
- USACE, 2013. *Strategic Sustainability Performance Plan*, unpublished.
- Vaidya RA, Shrestha MS, Nasab N, Gurung DR, Kozo N, Pradhan NS, Wasson RJ, 2019. Disaster Risk Reduction and Building Resilience in the Hindu Kush Himalaya. *The Hindu Kush Himalaya Assessment*. Springer, Cham, p. 389–419.
- van Ackere S, Glas H, Beullens J, Deruyter G, Wulf A de, Maeyer P de, 2016. Development of a 3D Dynamic Flood WEB GIS Visualisation Tool. *Flood Risk Management and Response*, 106.
- Van der Veen A, Vetere Arellano AL, Nordvik JP, 2003. In Search of a Common Methodology on Damage Estimation. *Joint NEDIES and University of Twente Workshop, Report EUR (Vol. 20997)*.
- Veldhuis JA Ten, 2011. How the choice of flood damage metrics influences urban flood risk assessment. *Journal of Flood Risk Management*, 4 (4), 281–287.
- Viccione G, Izzo C, 2022. Three-dimensional CFD Modelling of Urban Flood Forces on Buildings: A Case Study. *Journal of Physics: Conference Series*, 2162 (1), 12020.
- Vojinovic Z, Seyoum SD, Mwalwaka JM, Price RK, 2011. Effects of Model Schematisation, Geometry and Parameter Values on Urban Flood Modelling. *Water Science and Technology*, 63 (3), 462–467.
- Volk R, Stengel J, Schultmann F, 2014. Building Information Modeling (BIM) for Existing Buildings—Literature Review and Future Needs. *Automation in construction*, 38, 109–127.
- Vorogushyn S, Merz B, Lindenschmidt K-E, Apel H, 2010. A New Methodology for Flood Hazard Assessment Considering Dike Breaches. *Water Resources Research*, 46 (8).
- Wadell H, 1934. The Coefficient of Resistance as a Function of Reynolds Number for Solids of Various Shapes. *Journal of the Franklin Institute*, 217 (4), 459–490.
- Wang C, Hou J, Miller D, Brown I, Jiang Y, 2019a. Flood Risk Management in Sponge Cities: The Role of Integrated Simulation and 3D Visualization. *International Journal of Disaster Risk Reduction*, 39, 101139.

- Wang H, Pan Y, Luo X, 2019b. Integration of BIM and GIS in Sustainable Built Environment: A Review and Bibliometric Analysis. *Automation in Construction*, 103, 41–52.
- Wang H, Zhou J, Tang Y, Liu Z, Kang A, Chen B, 2021. Flood Economic Assessment of Structural Measure based on Integrated Flood Risk Management: A Case Study in Beijing. *Journal of Environmental Management*, 280, 111701.
- White G, Zink A, Codecá L, Clarke S, 2021. A Digital Twin Smart City for Citizen Feedback. *Cities*, 110, 103064.
- Wittke S, Yu X, Karjalainen M, Hyyppä J, Puttonen E, 2019. Comparison of Two-Dimensional Multitemporal Sentinel-2 Data with Three-Dimensional Remote Sensing Data Sources For Forest Inventory Parameter Estimation Over A Boreal Forest. *International Journal of Applied Earth Observation and Geoinformation*, 76, 167–178.
- Wu J, Ye M, Wang X, Koks E, 2019a. Building asset value mapping in support of flood risk assessments: A case study of Shanghai, China. *Sustainability*, 11 (4), 971.
- Wu Y, Peng F, Peng Y, Kong X, Liang H, Li Q, 2019b. Dynamic 3D Simulation of Flood Risk Based on the Integration of Spatio-Temporal GIS and Hydrodynamic Models. *ISPRS International Journal of Geo-Information*, 8 (11), 520.
- Xu Z, Lu X, Zeng X, Xu Y, Li Y, 2019. Seismic Loss Assessment for Buildings with Various-LOD BIM Data. *Advanced Engineering Informatics*, 39, 112–126.
- Yalcin E, 2019. Two-dimensional Hydrodynamic Modelling for Urban Flood Risk Assessment Using Unmanned Aerial Vehicle Imagery: A Case Study of Kirsehir, Turkey. *Journal of Flood Risk Management*, 12, e12499.
- Yamamura S, Fan L, Suzuki Y, 2017. Assessment of Urban Energy Performance through Integration of BIM and GIS for Smart City Planning. *Procedia Engineering*, 180, 1462–1472.
- Yu D, Lane SN, 2006. Urban Fluvial Flood Modelling Using a Two-Dimensional Diffusion-Wave Treatment, Part 1: Mesh Resolution Effects. *Hydrological Processes*, 20 (7), 1541–1565.
- Zhang H, Wu W, Hu C, Hu C, Li M, Hao X, Liu S, 2021a. A Distributed Hydrodynamic Model for Urban Storm Flood Risk Assessment. *Journal of Hydrology*, 600, 126513.
- Zhang H, Wu W, Hu C, Hu C, Li M, Hao X, Liu S, 2021b. A Distributed Hydrodynamic Model for Urban Storm Flood Risk Assessment. *Journal of Hydrology*, 600, 126513.
- Zhi G, Liao Z, Tian W, Wu J, 2020. Urban Flood Risk Assessment and Analysis with a 3D Visualization Method Coupling The PP-PSO Algorithm and Building Data. *Journal of Environmental Management*, 268, 110521.
- Zhu J, Wright G, Wang J, Wang X, 2018. A Critical Review of the Integration of Geographic Information System and Building Information Modelling at the Data Level. *ISPRS International Journal of Geo-Information*, 7 (2), 66.
- Zhu J, Wu P, 2022. BIM/GIS Data Integration from the Perspective of Information Flow. *Automation In Construction*, 136, 104166.



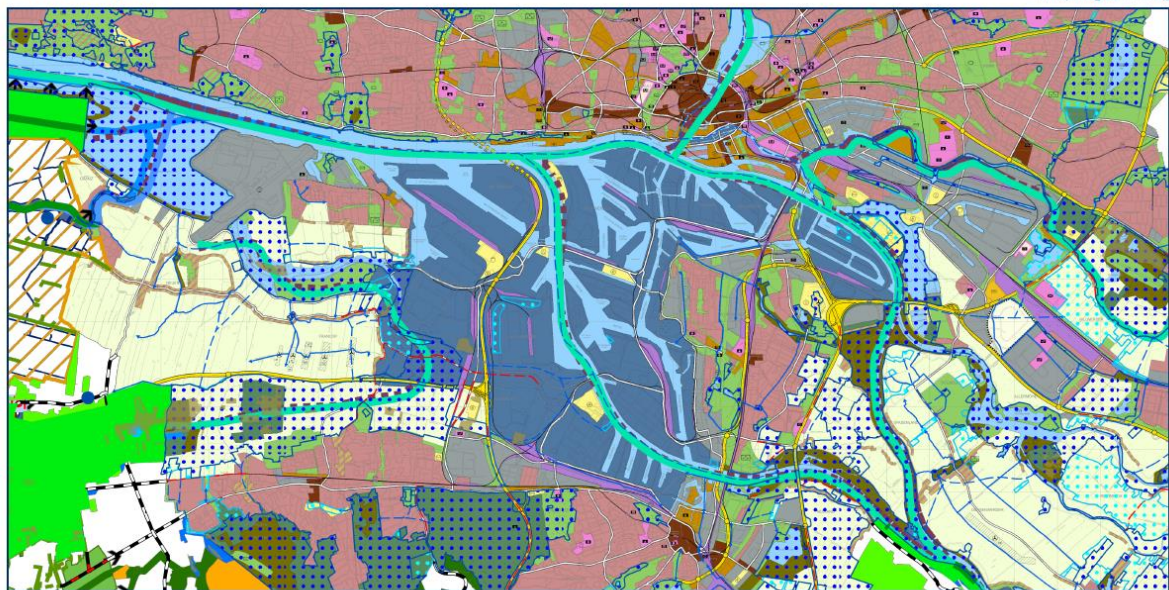
# Chapter 10

---

## Appendix

# 10 Appendix

Landuse plan



Herausgeber:  
 Geodateninfrastruktur der Metropolregion Hamburg – GDH-MRH  
 Kartengrundlage:  
 WebAtlasDE und Luftbilder © GeoBasis-DE/BKG  
 Karte 1:5000 © Auszug aus den Geobasisdaten der Länder:  
 Niedersächsische Vermessungs- und Katasterverwaltung – LGLN, Landesamt für Vermessung und Geoinformation Schleswig-Holstein  
 Landesvermessung für innere Verwaltung Mecklenburg-Vorpommern, Freie und Hansestadt Hamburg, Landesbetrieb Geoinformation und Vermessung  
 Geofachdaten und Copyright:  
 Alle Geodaten unterliegen dem Urheberrecht und anderen Gesetzen zum Schutz geistigen Eigentums. Datennutzung und  
 Datenweitergabe durch Dritte bedürfen der Genehmigung der zuständigen Kreis- und Landesverwaltungen.

0 1 2 3 4km  
 1:100000

Appendix Figure 1: Land use Plan of Hafen City

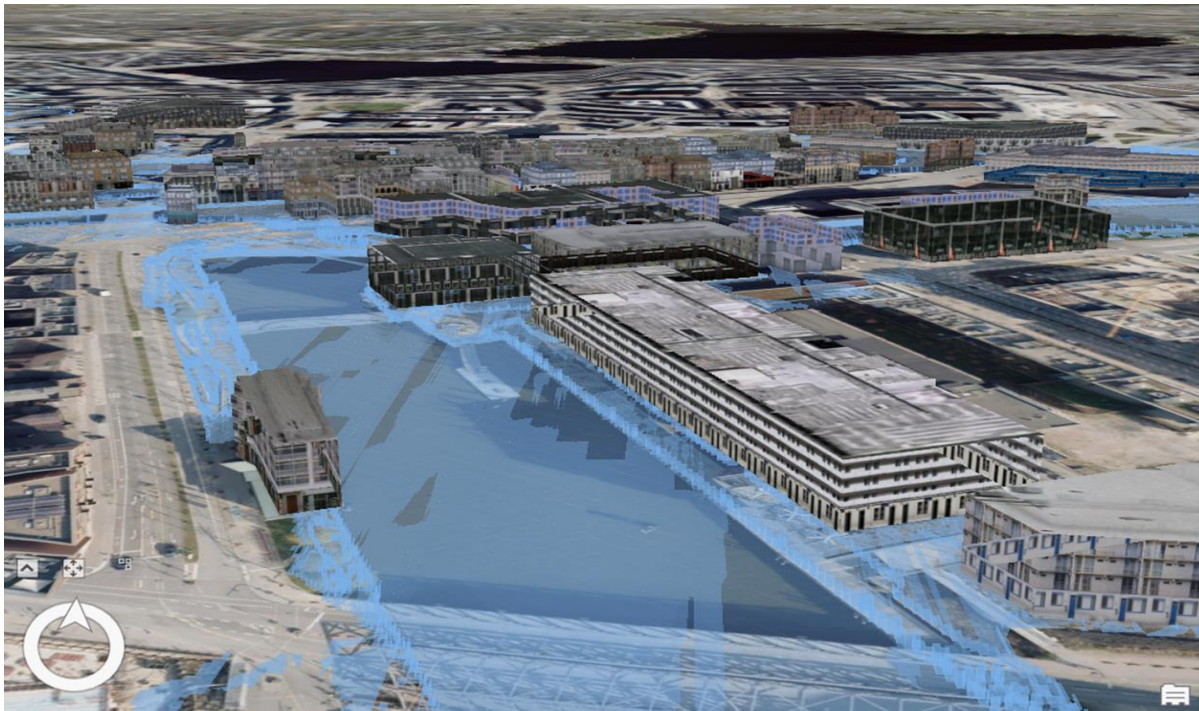
**Hinweise und Auszug aus der DIN 1986-100:2016-12 ( Abflußbeiwerte / Tabelle 9 )**  
 Die abflusswirksame Fläche  $A_u$  ergibt sich aus der Multiplikation der befestigten Fläche im Grundriss mit dem jeweils zugehörigen Abflussbeiwert  $C$  (Grundleitung:  $A_u = A \cdot C_s$ ); (Rückhaltung:  $A_u = A \cdot C_m$ ).



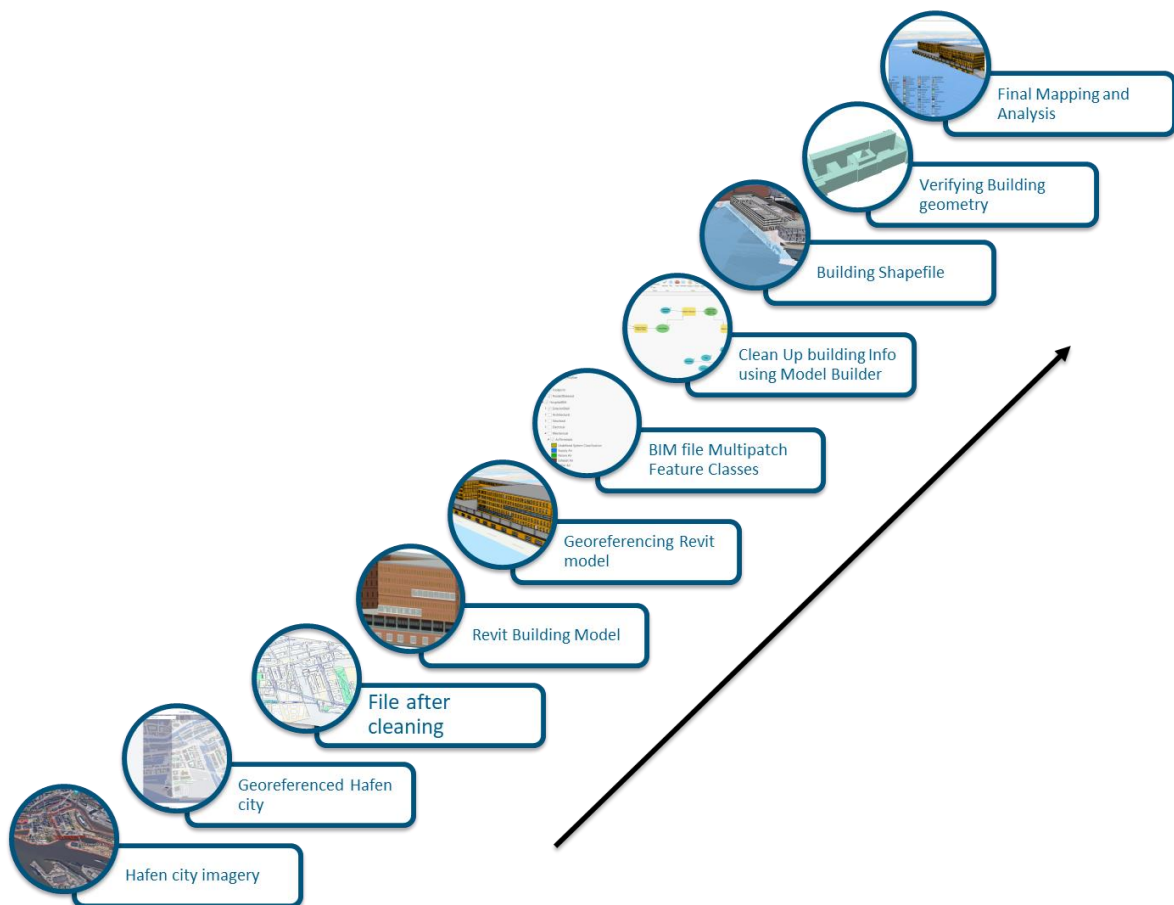
Nr.	Art der Fläche	Spitzenab-	mittl.
		fluß- beiwert $C_s$	Abfluß- beiwert $C_m$
<b>Wasserundurchlässige Flächen</b>			
1	<b>- Dachflächen</b>		
	<i>Schrägdach</i>		
	Metall, Glas, Schiefer, Faserzement	1,00	0,90
	Ziegel, Dachpappe, Abdichtungsbahnen	1,00	0,80
	<i>Flachdach (bis 3° / 5%)</i>		
	Metall, Glas, Faserzement	1,00	0,90
	Dachpappe, Abdichtungsbahnen	1,00	0,90
	Kiesschüttung	0,80	0,80
	<i>begrünte Dachflächen</i>		
	Extensivbegrünung (> 5°)	0,70	0,40
	Intensivbegrünung, ab 30 cm Aufbau (≤ 5°)	0,20	0,10
	Intensivbegrünung, ab 10 cm Aufbau (≤ 5°)	0,40	0,20
Extensivbegrünung, bis 10 cm Aufbau (≤ 5°)	0,50	0,30	
1	<b>- Verkehrsflächen (Straßen, Plätze, Zufahrten, Wege)</b>		
	Betonflächen	1,00	0,90
	Schwarzdecken (Asphalt)	1,00	0,90
	befestigte Flächen mit Fugendichtung (Pflaster mit Verguss)	1,00	0,80
1	<b>- Rampen</b>		
	Neigung zum Gebäude, unabhängig von der Neigung und der Befestigungsart	1,00	1,00
<b>Teildurchlässige und schwach ableitende Flächen,</b>			
2	<b>- Verkehrsflächen (Straßen, Plätze, Zufahrten, Wege)</b>		
	Betonsteinpflaster, in Sand oder Schlacke verlegt, Flächen mit Platten	0,90	0,70
	Pflasterflächen, mit Fugenanteil > 15 %, z. B. 10 × 10 cm oder fester Kiesbelag	0,70	0,60
	wassergebundene Flächen	0,90	0,70
	lockerer Kiesbelag, Schotterrasen z. B. Kinderspielplätze	0,30	0,20
	Verbundsteine mit Sickerfugen, Sicker- / Drainsteine	0,40	0,25
	Rasengittersteine (mit häufigen Verkehrsbelastungen, z. B. Parkplatz)	0,40	0,20
	Rasengittersteine (ohne häufige Verkehrsbelastungen, z. B. Feuerwehrzufahrt)	0,20	0,10
	<b>- Sportflächen mit Dränung</b>		
	Kunststoff-Flächen, Kunststoffrasen	0,60	0,50
Tennisflächen	0,30	0,20	
Rasenflächen	0,20	0,10	

Appendix Figure 2: Land use roughness coefficient values for different land use

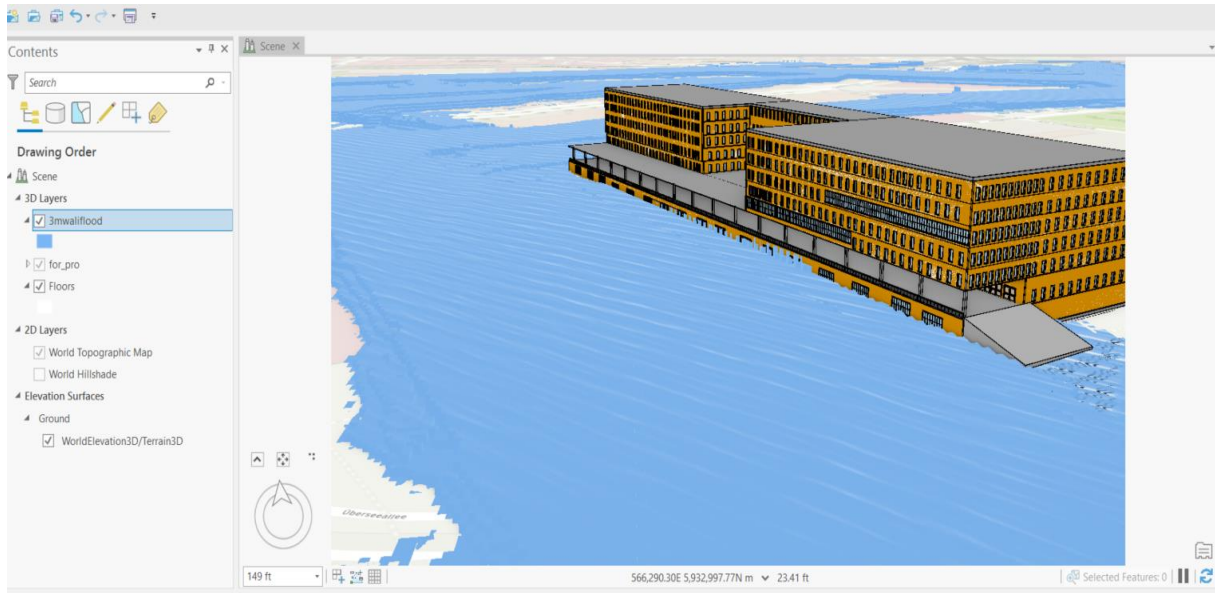




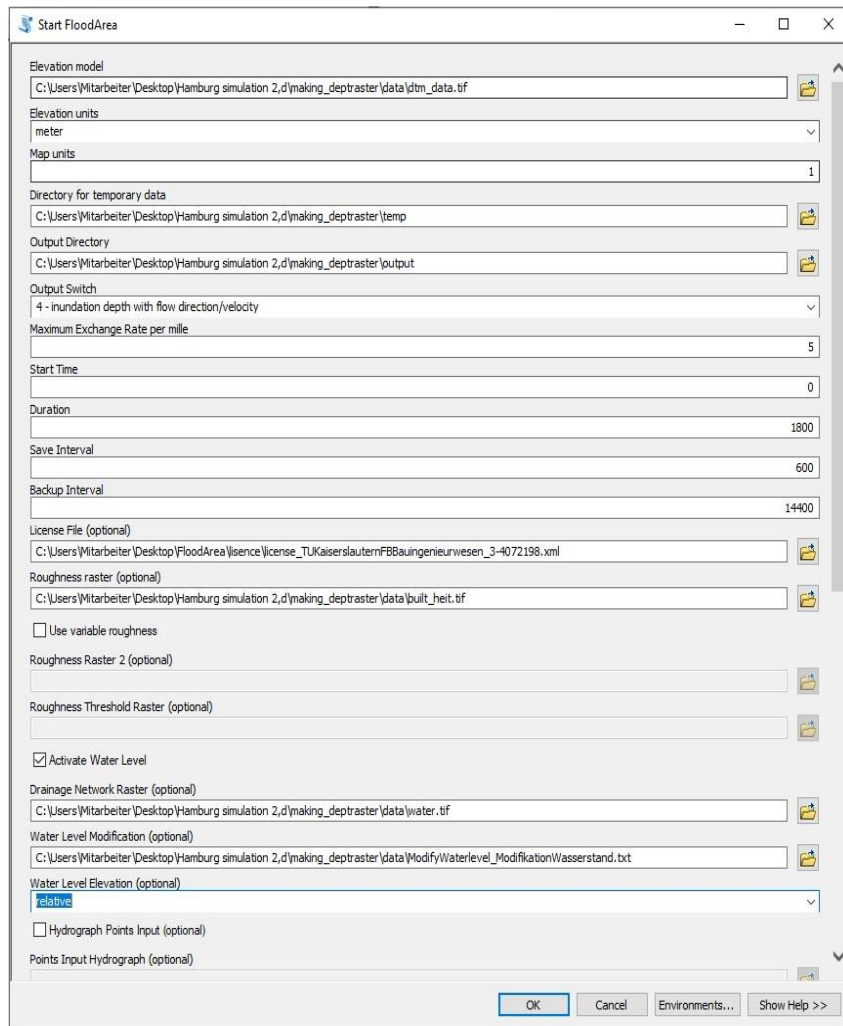
Appendix Figure 3: Developed 3D model of Prototype case study (Hafen City)



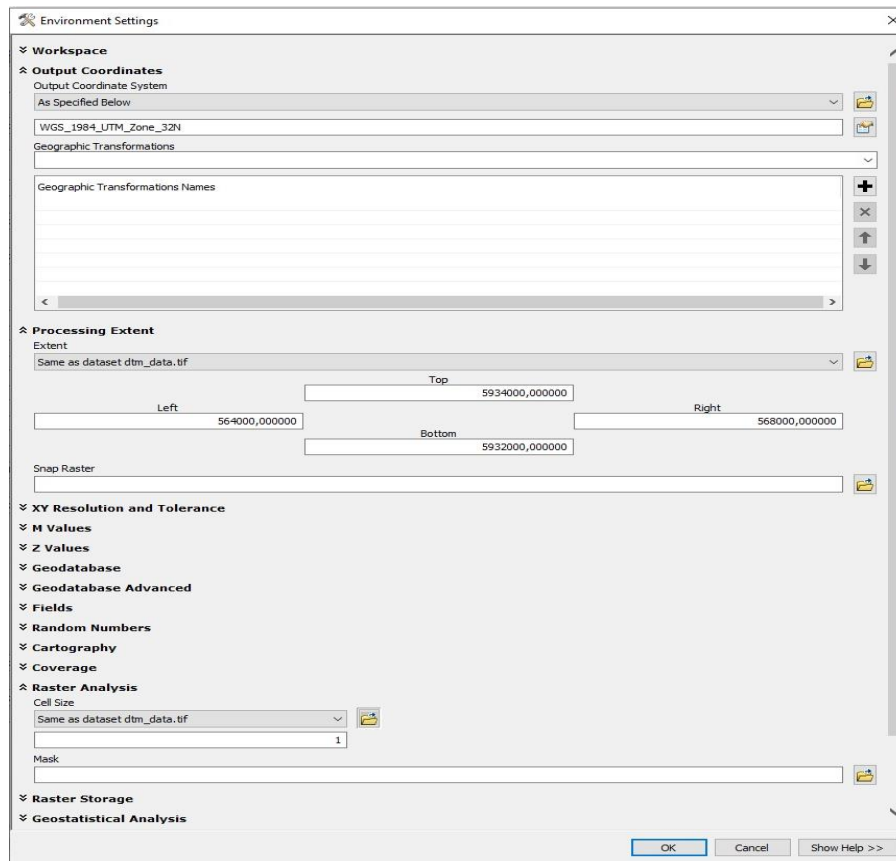
Appendix Figure 4: Processing Steps for a 3D Model to including integrate with GIS -BIM for prototype case



Appendix Figure 5: 3D BIM based building after integration into ArcGIS pro (3D-Digital Twin)



Appendix Figure 6: FloodArea Processing Dialogue Box for Hafen City



Appendix Figure 7: Environment and extent setting in FloodArea Dialogue Box

This XML file does not appear to have any style information associated with it. The document tree is shown below.

```

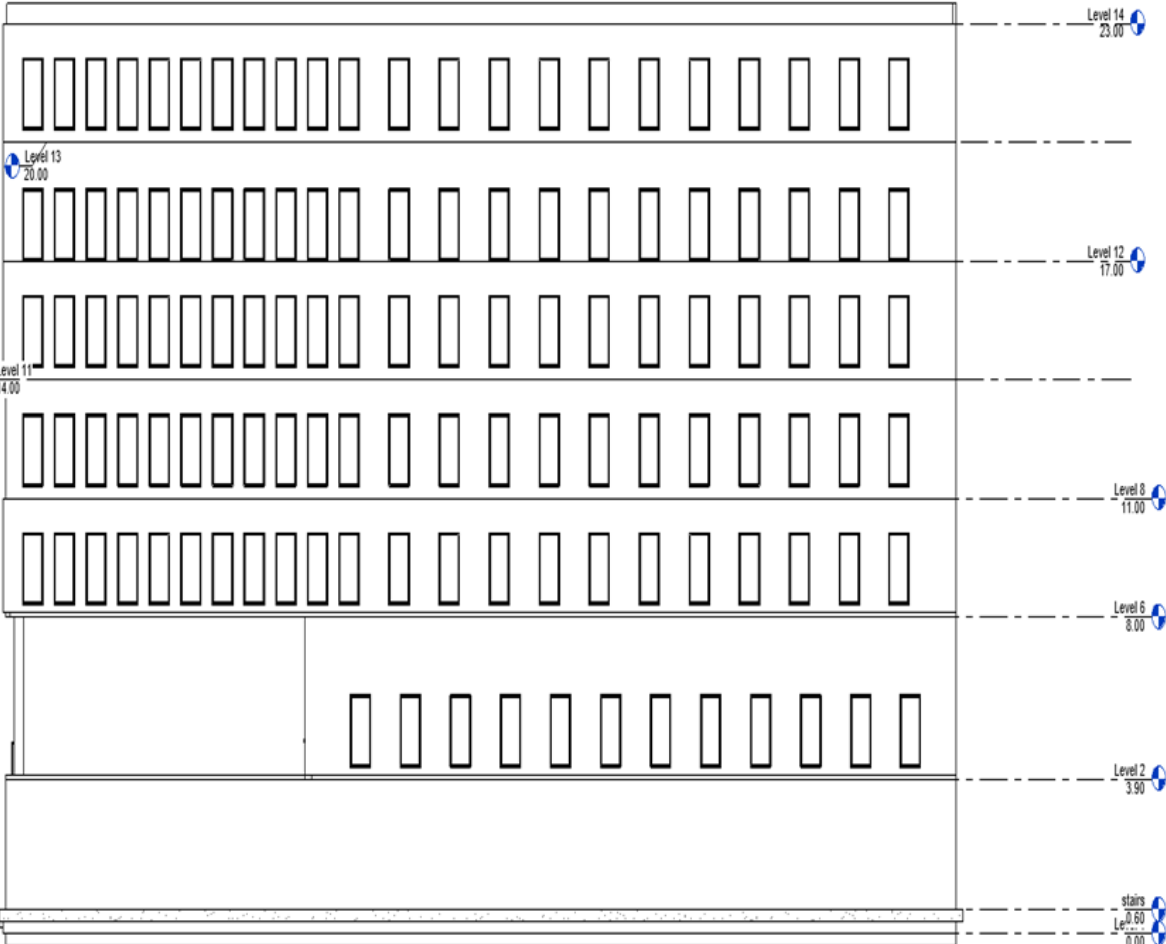
<config xmlns:xsd="http://www.w3.org/2001/XMLSchema" xmlns:xsi="http://www.w3.org/2001/XMLSchema-instance"
xsi:noNamespaceSchemaLocation="Config.xsd">
  <Citation>
    <Author>Mitarbeiter</Author>
    <Comment/>
  </Citation>
  <GeneralSettings>
    <ElevationUnits>meter</ElevationUnits>
    <RasterUnit>1.0</RasterUnit>
    <TileSizeInPixels>256</TileSizeInPixels>
    <OutputSwitch>4</OutputSwitch>
    <MaxExchangeQuantityPromille>5</MaxExchangeQuantityPromille>
  </GeneralSettings>
  <CalculationOption>
    <Rainfall>false</Rainfall>
    <HydrographPointsInput>false</HydrographPointsInput>
    <WaterLevel>true</WaterLevel>
    <CombineWithSewerNetworkModel>false</CombineWithSewerNetworkModel>
  </CalculationOption>
  <AdditionalOptions>
    <MultipleRainHydrographs>false</MultipleRainHydrographs>
    <UseVariableRoughness>false</UseVariableRoughness>
    <RainfallMode>MM_H</RainfallMode>
    <WaterLevelElevation>relative</WaterLevelElevation>
    <ContinuemodeHeight>relative</ContinuemodeHeight>
  </AdditionalOptions>
  <TimeSetup>
    <StartTime>0</StartTime>
    <BackupInterval>1440</BackupInterval>
    <SaveInterval>600</SaveInterval>
    <Duration>1800</Duration>
  </TimeSetup>
  <Paths>
    <DTM_ras>C:\Users\Mitarbeiter\Desktop\Hamburg simulation 2,d\making_deptraster\data\dtm_data</DTM_ras>
    <WaterLevel_ras>C:\Users\Mitarbeiter\Desktop\Hamburg simulation 2,d\making_deptraster\data\water</WaterLevel_ras>
    <WaterLevelModification_txt>C:\Users\Mitarbeiter\Desktop\Hamburg simulation
2,d\making_deptraster\data\ModifyWaterlevel_ModifikationWasserstand</WaterLevelModification_txt>
    <Output_dir>C:\Users\Mitarbeiter\Desktop\Hamburg simulation 2,d\output</Output_dir>
    <Temp_dir>C:\Users\Mitarbeiter\Desktop\Hamburg simulation 2,d\temp</Temp_dir>
    <LicenseFile_xml>C:\Users\Mitarbeiter\Desktop\FloodArea\lisence\license_TUKaiserslauternFBBAueningeurwesens_3-
4072198.xml</LicenseFile_xml>
  </Paths>
</config>

```

Appendix Figure 8: Output XML file to represent steps, data inputs and output and parameters for Hydrodynamic flood simulation

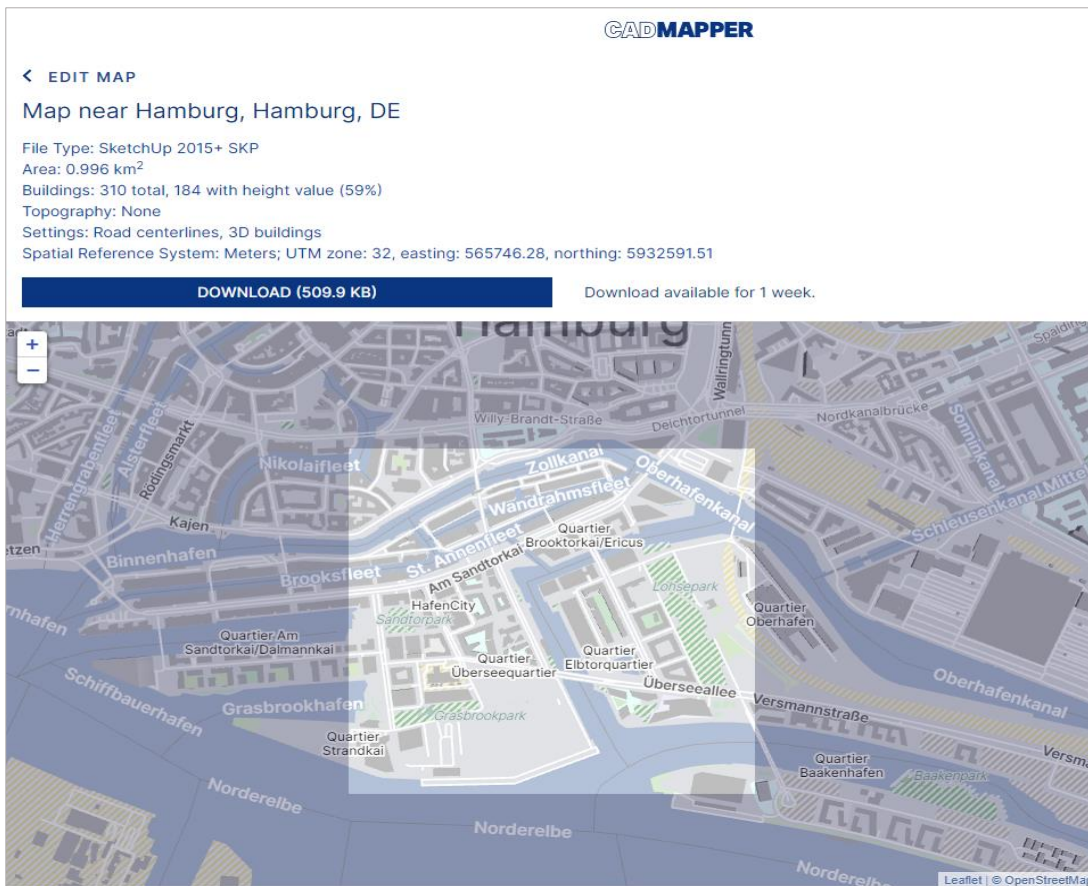


Appendix Figure 9: BIM based 3D model of the targeted building in Hafen City

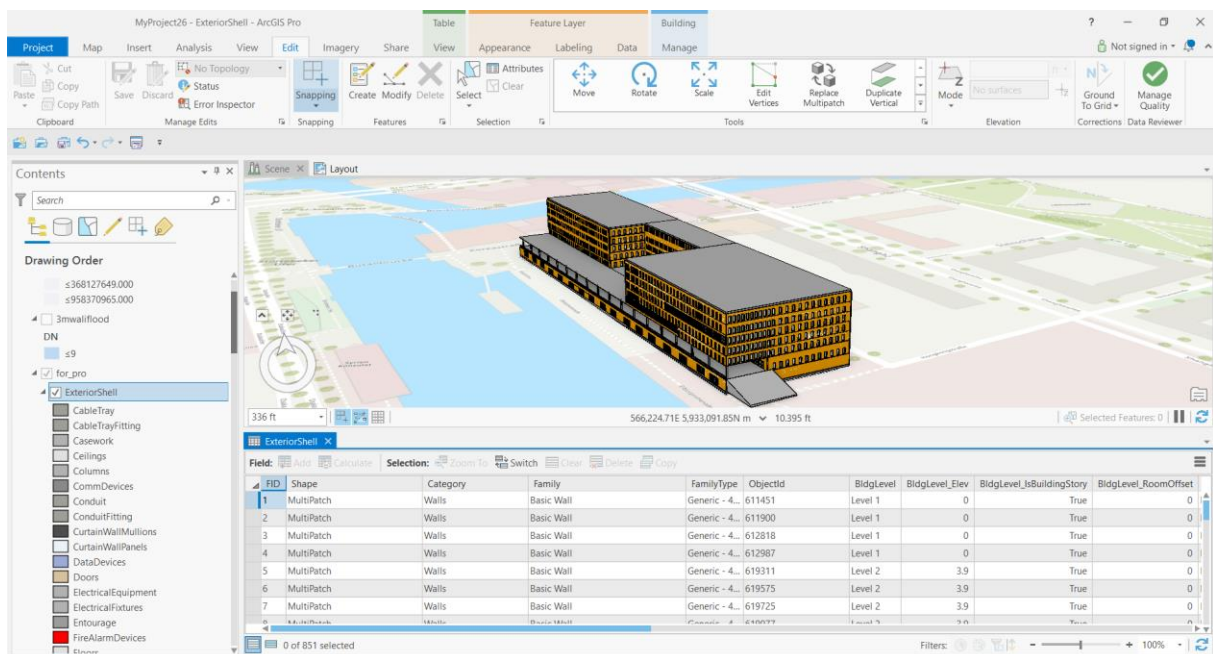


Appendix Figure 10: Level of floor for targeted building in Autodesk Revit

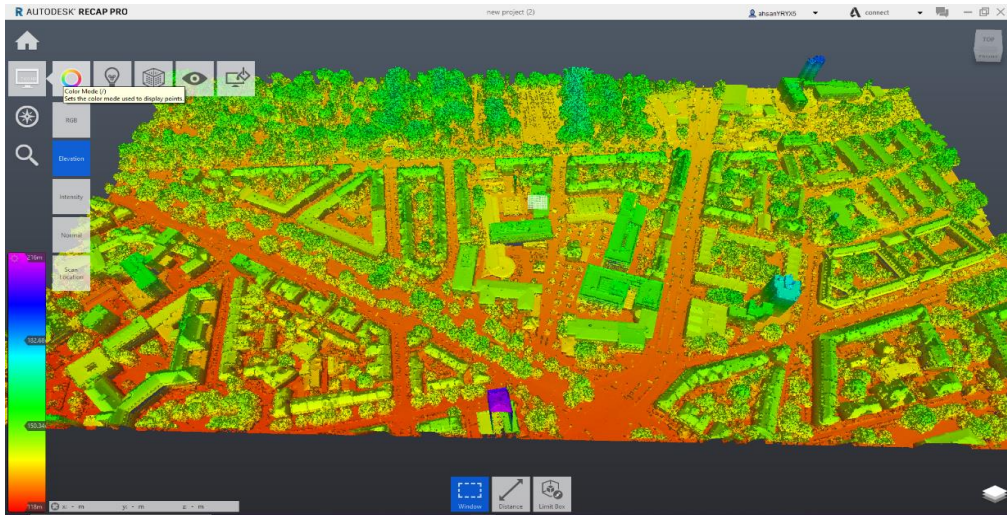




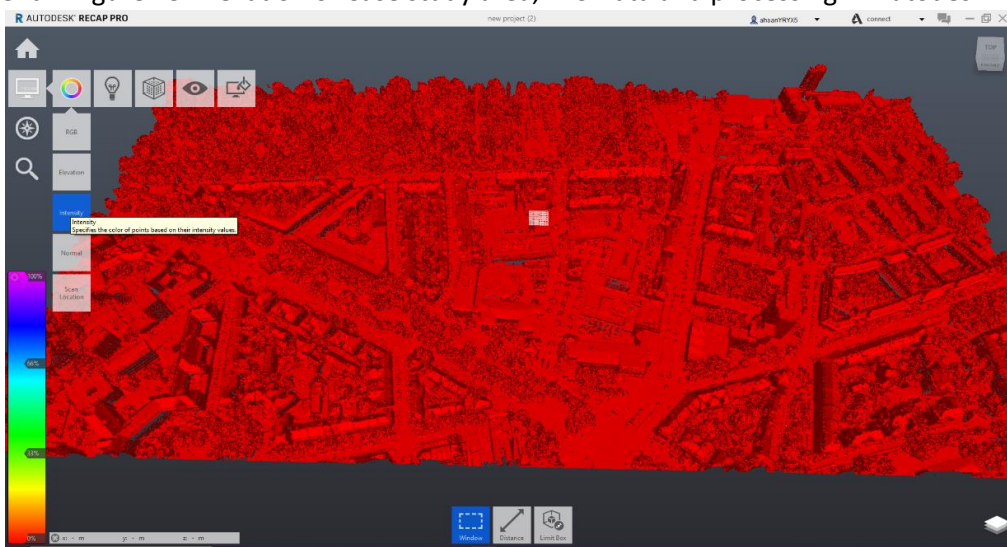
Appendix Figure 11: Extraction of 3D features and detail with CADMAPPER for prototype case study



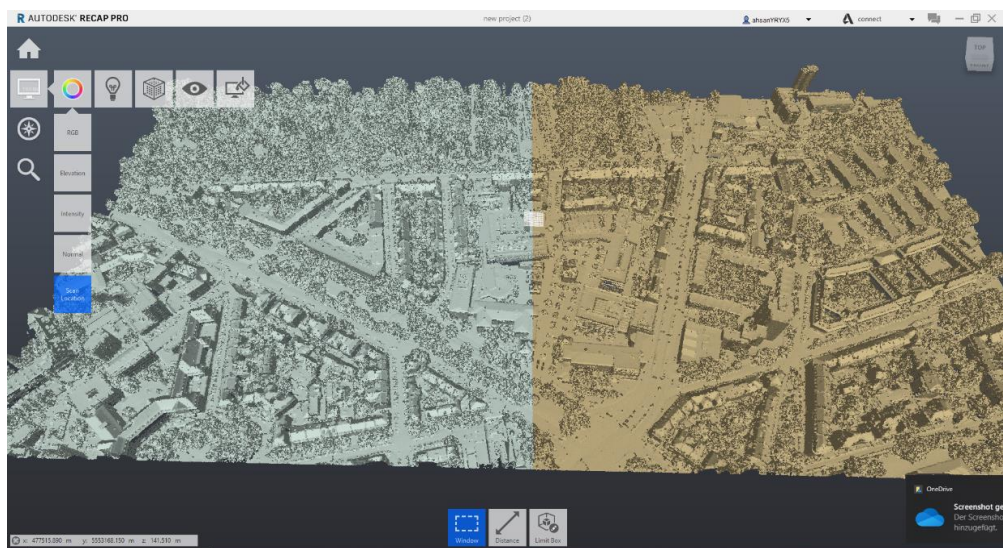
Appendix Figure 12: Successful integration of Revit BIM model into ArcGIS pro with semantic properties in attribute table



Appendix Figure 13: Elevation of Case study area, LAS Data and processing in Autodesk Recap.

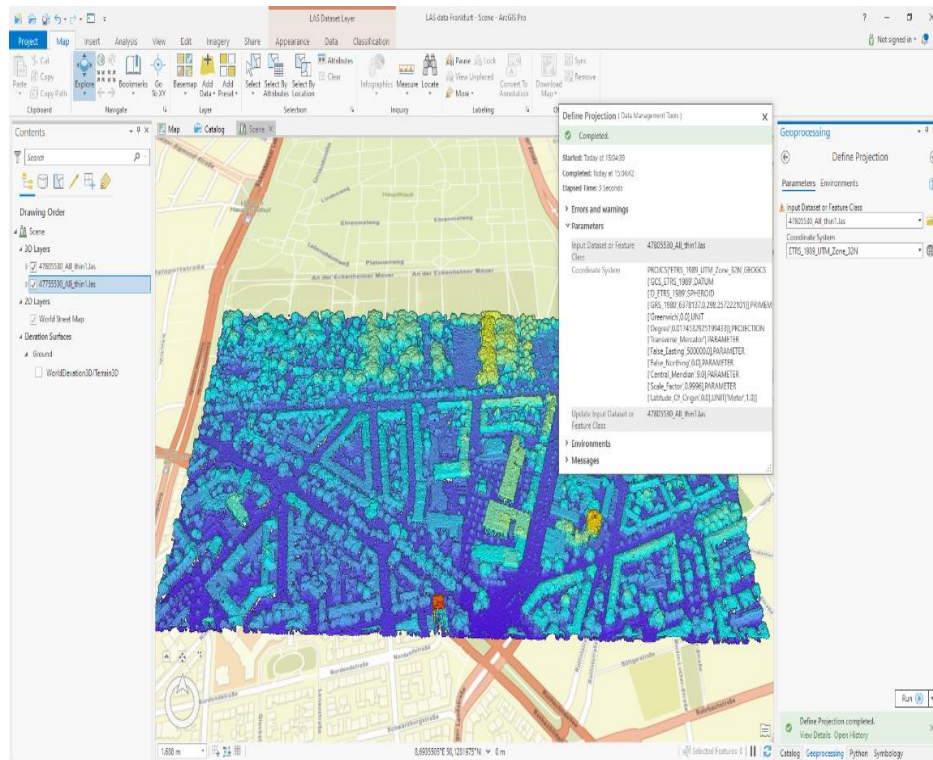


Appendix Figure 14: Intensity of LAS Data processing in Autodesk Recap.



Appendix Figure 15: Scan Locations of LAS Data processing in Autodesk Recap.



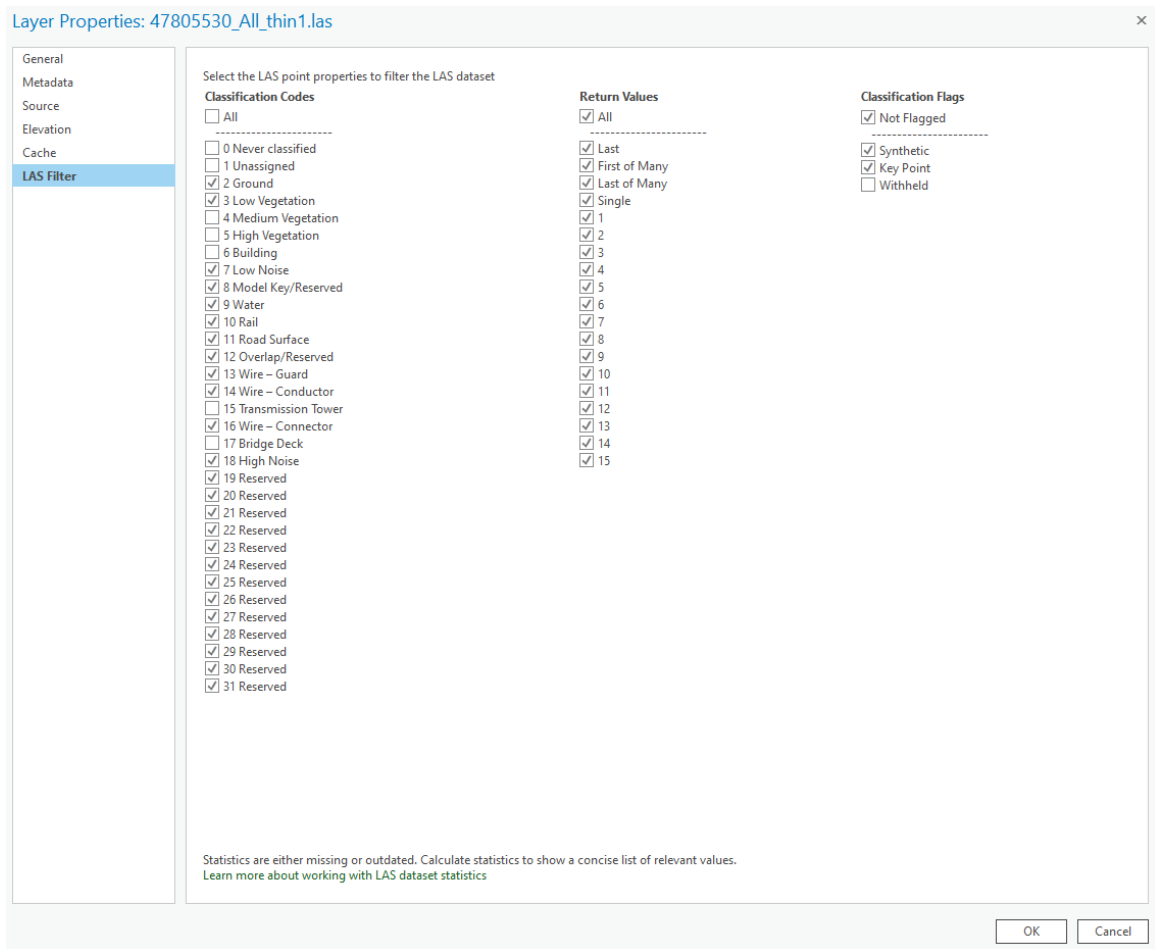


Appendix Figure 16: Defining projection of LAS data in ARCGIS Pro.

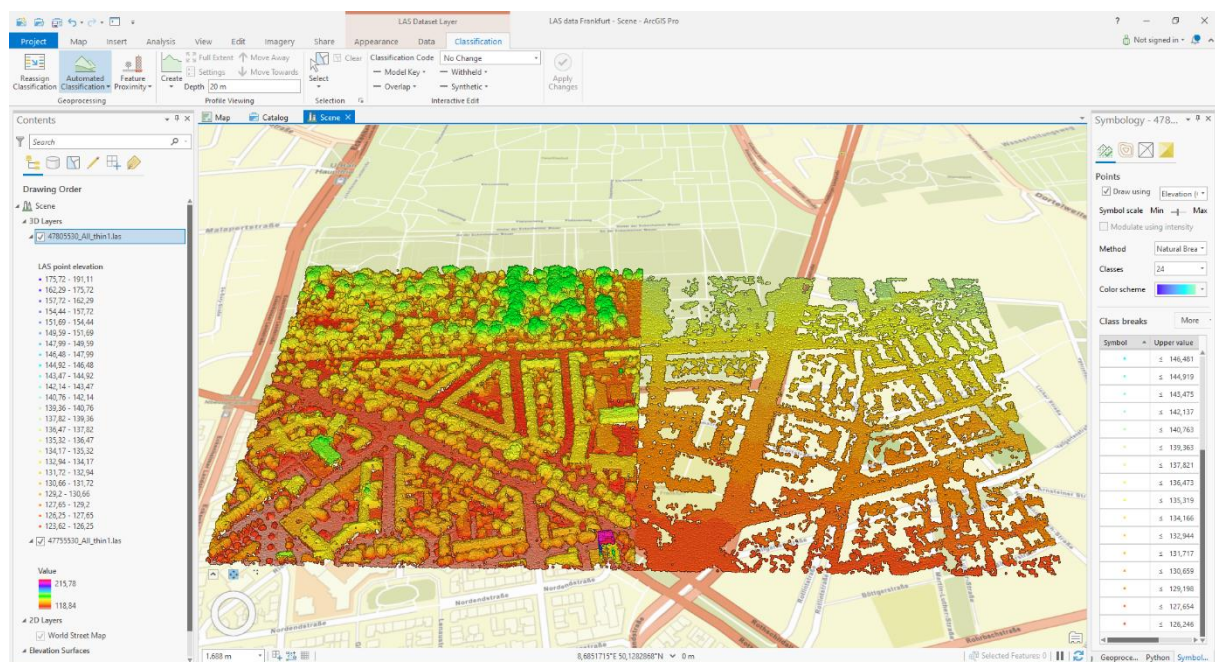
Never Classified	1
Unclassified	2
Ground	3
Low Vegetation	4
Medium vegetation	5
Tall vegetation	6
Buildings	7
Low point (noise)	8
Model key point	9
Water	10
Rails	11
Road Pavement	12
Reserved 12	13
Protective Wire	14
Wire - Conductor	15

Appendix Figure 17: Classification Codes for Processing LAS data into DTM

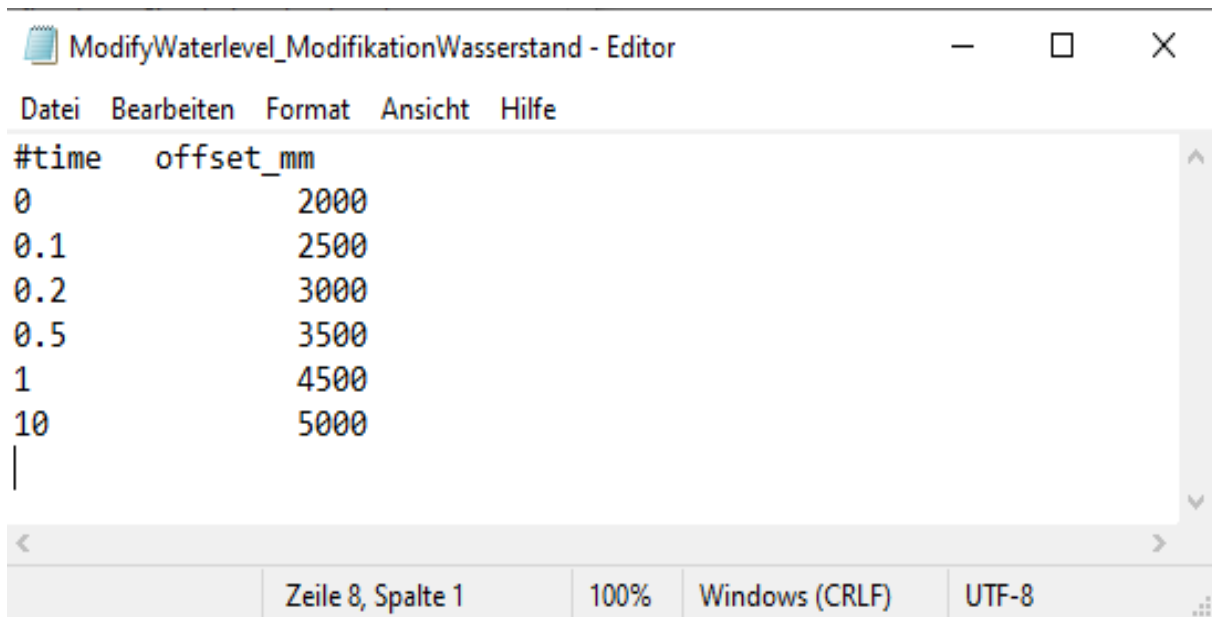




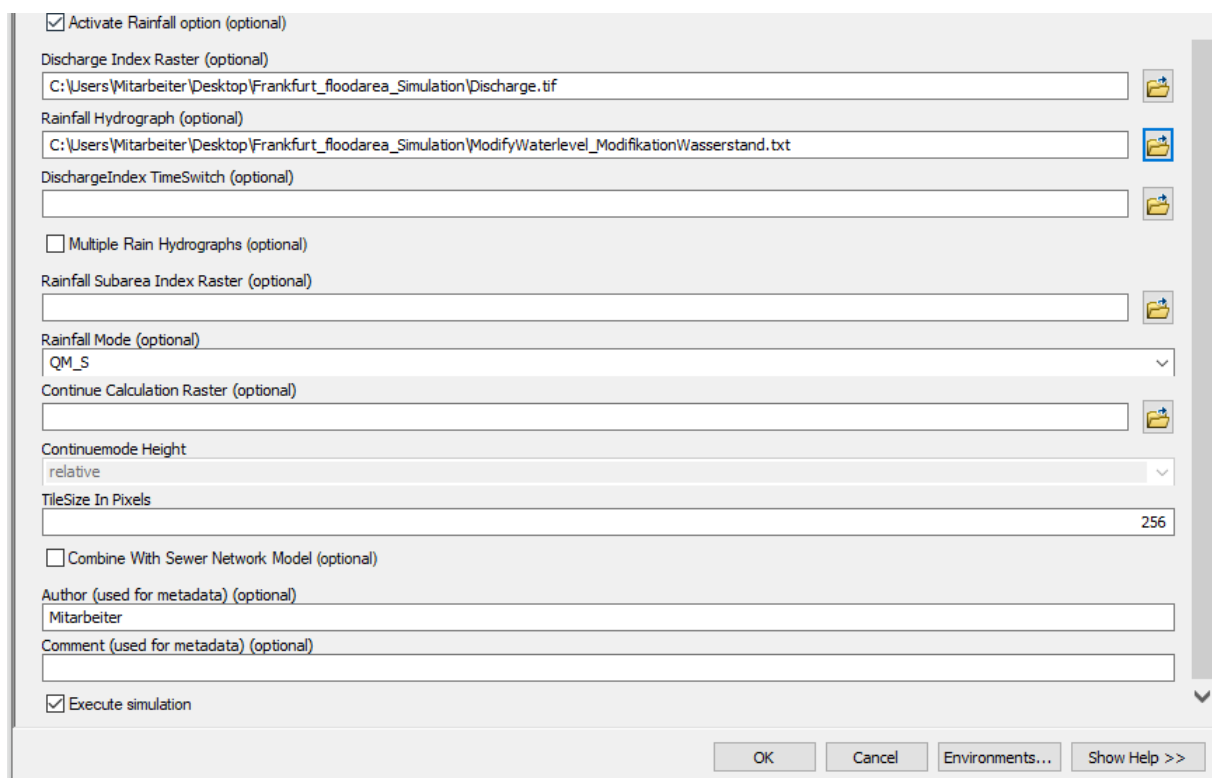
Appendix Figure 18: Assigning Classification Codes for Processing LAS data into DTM



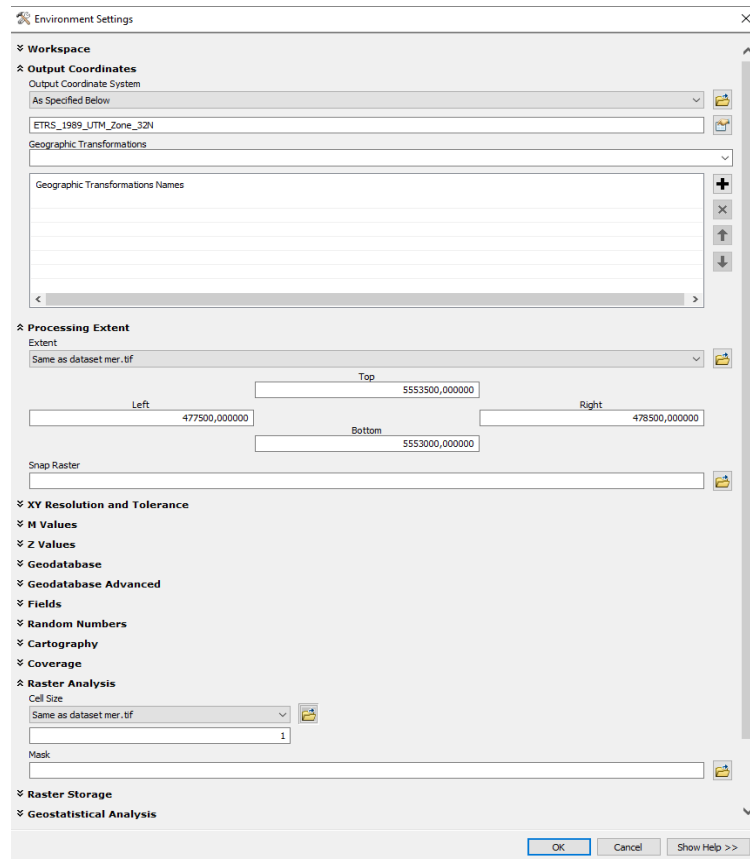
Appendix Figure 19: DTM generation from LAS data (left without filtering non ground point, right after filtration of non-ground points)



Appendix Figure 20: Hydrograph modification for FLOODArea Rainfall hydrodynamic flood simulation scenario



Appendix Figure 21: FloodArea Processing Dialogue Box for Frankfurt City



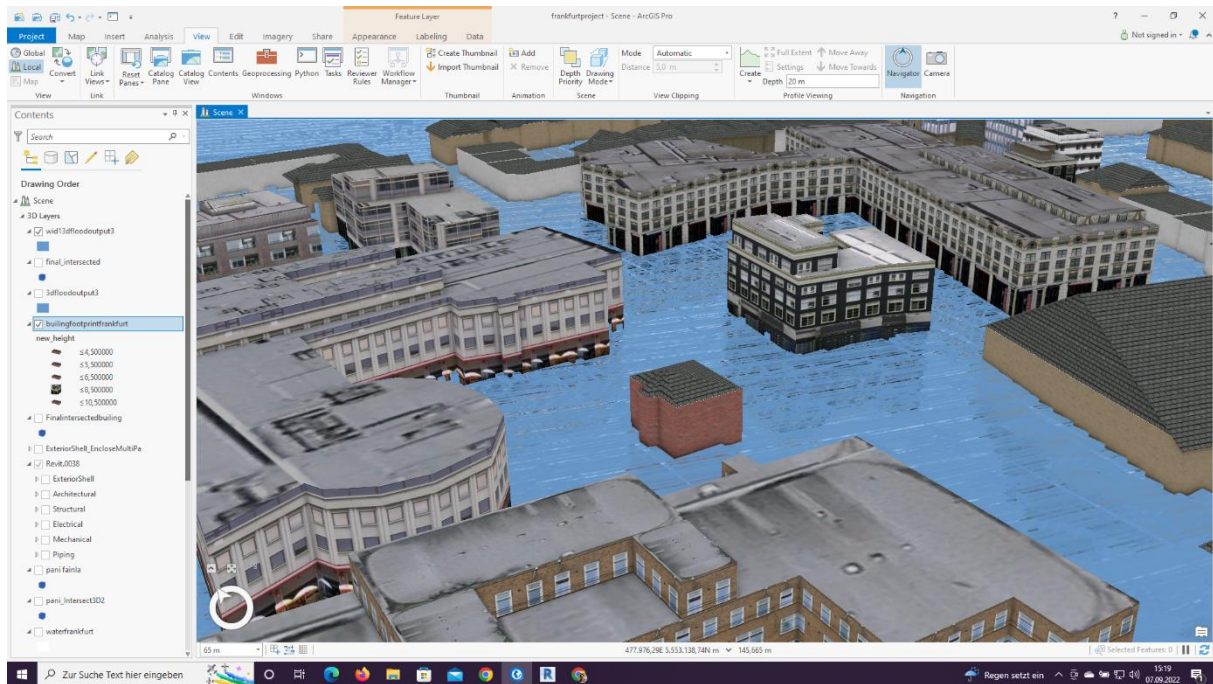
Appendix Figure 22: Environment and extent setting in FloodArea Dialogue Box

```

<?xml version="1.0" encoding="UTF-8" standalone="no" ?>
<config xmlns:xsd="http://www.w3.org/2001/XMLSchema" xmlns:xsi="http://www.w3.org/2001/XMLSchema-instance" xsi:noNamespaceSchemaLocation="Config.xsd">
  <Citation>
    <Author>Mitarbeiter</Author>
    <Comment/>
  </Citation>
  <GeneralSettings>
    <ElevationUnits>meter</ElevationUnits>
    <RasterUnit>1.0</RasterUnit>
    <TileSizeInPixels>256</TileSizeInPixels>
    <OutputSwitch>4</OutputSwitch>
    <MaxExchangeQuantityPromille>5</MaxExchangeQuantityPromille>
  </GeneralSettings>
  <CalculationOption>
    <Rainfall>true</Rainfall>
    <HydrographPointsInput>false</HydrographPointsInput>
    <WaterLevel>false</WaterLevel>
    <CombineWithSewerNetworkModel>false</CombineWithSewerNetworkModel>
  </CalculationOption>
  <AdditionalOptions>
    <MultipleRainHydrographs>false</MultipleRainHydrographs>
    <UseVariableRoughness>false</UseVariableRoughness>
    <RainfallMode>NM_H</RainfallMode>
    <ContinuumHeight>relative</ContinuumHeight>
  </AdditionalOptions>
  <TimeSetup>
    <StartTime>0</StartTime>
    <BackupInterval>1440</BackupInterval>
    <SaveInterval>400</SaveInterval>
    <Duration>1200</Duration>
  </TimeSetup>
  <Paths>
    <DTM_ras>C:\Users\Mitarbeiter\Desktop\Frankfurt_floodarea_Simulation\mer\DTM_ras
    <DischargeIndex_ras>C:\Users\Mitarbeiter\Desktop\Frankfurt_floodarea_Simulation\Discharge\DischargeIndex_ras
    <RainfallHydrograph_txt>C:\Users\Mitarbeiter\Desktop\Frankfurt_floodarea_Simulation\ModifyWaterLevel_ModifikationWasserstand\RainfallHydrograph_txt
    <Output_dir>C:\Users\Mitarbeiter\Desktop\Frankfurt_floodarea_Simulation\output\</Output_dir>
    <Temp_dir>C:\Users\Mitarbeiter\Desktop\Frankfurt_floodarea_Simulation\temp\</Temp_dir>
    <LicenseFile_xml>C:\Users\Mitarbeiter\Desktop\FloodArea\license_TUKaiserslauternFBBauingenieurwesen_3-4072198.xml</LicenseFile_xml>
  </Paths>
</config>

```

Appendix Figure 23: Output XML file to represent steps, data inputs and output and parameters for Hydrodynamic flood simulation



Appendix Figure 24: 3D flood model of Frankfurt case study area



Appendix Figure 25: 3D Lase scan Point cloud data of scanned building

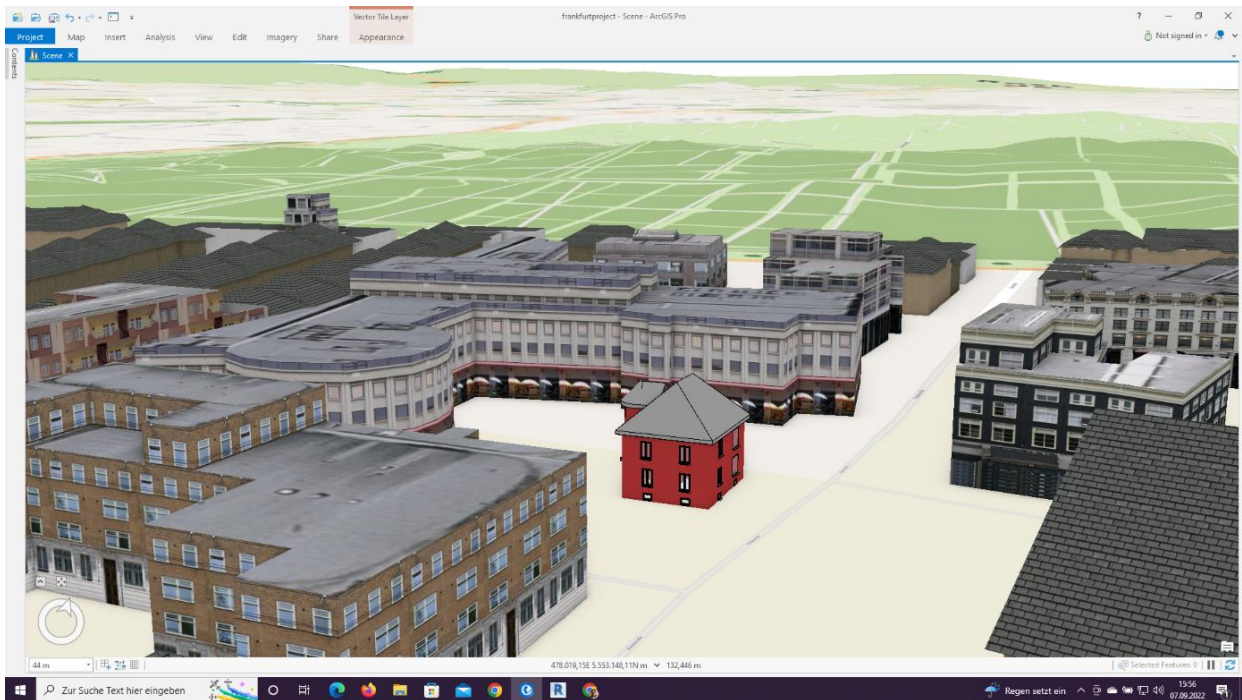




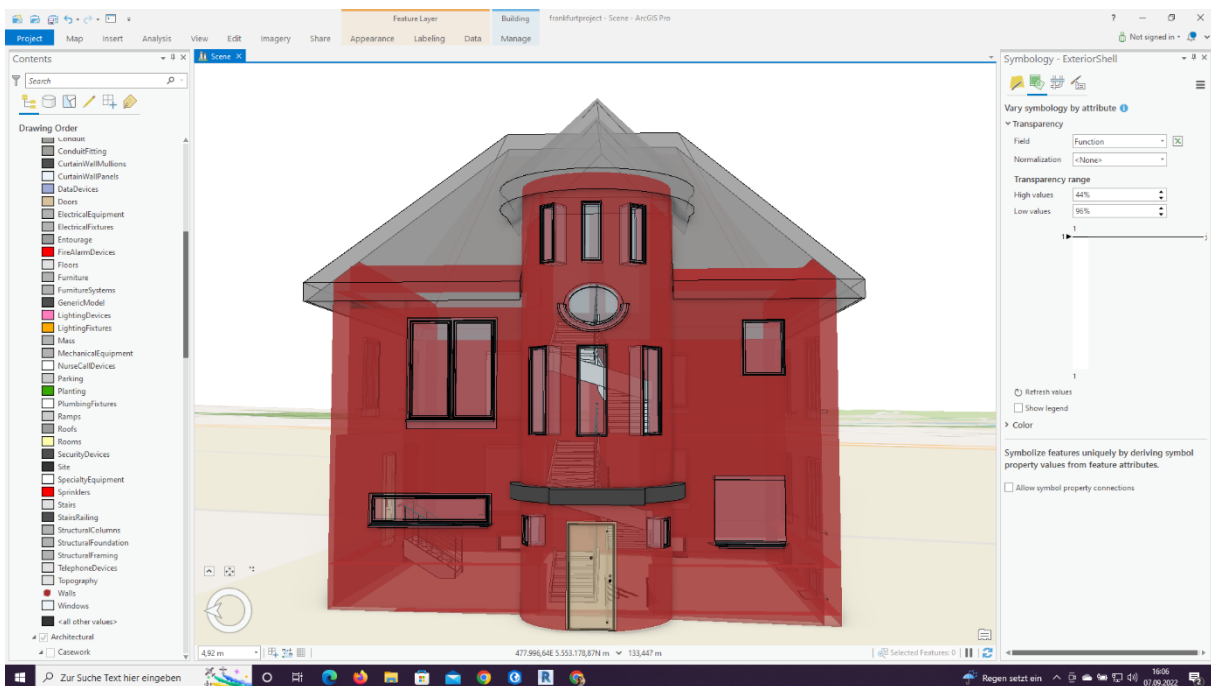
Appendix Figure 26: 3D Scan to BIM model (BIM modelling based on lase scan data geometries)



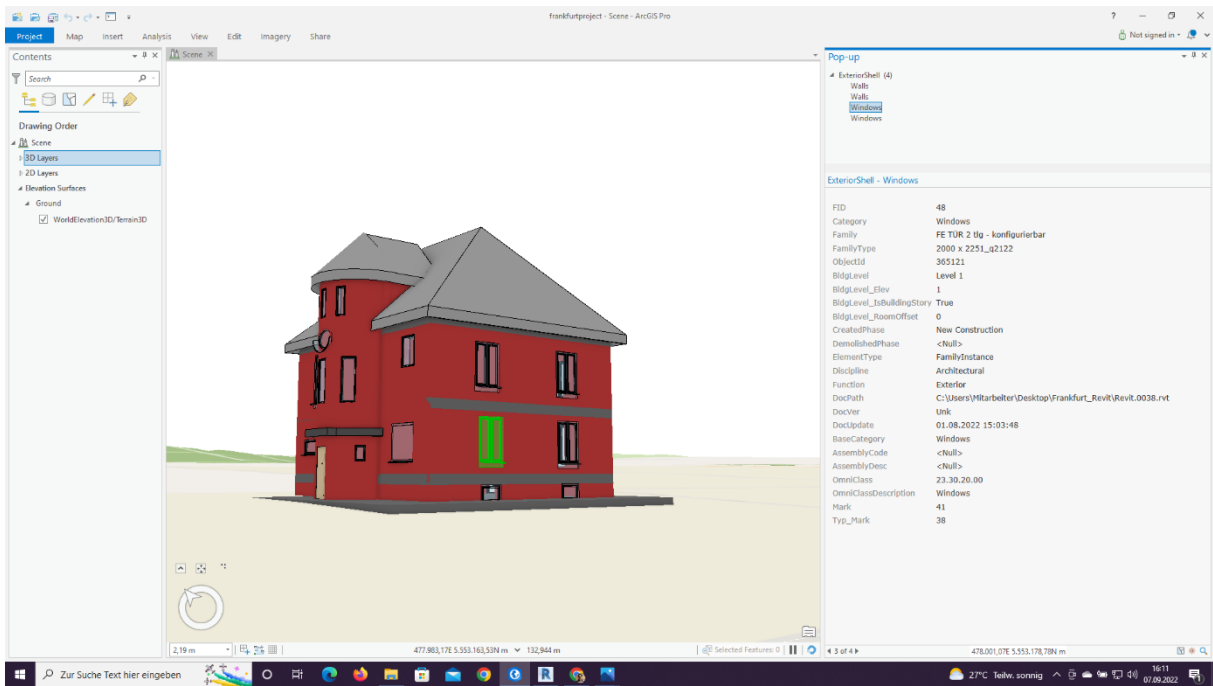
Appendix Figure 27: Level of Elevation for the 3D building model in Revit



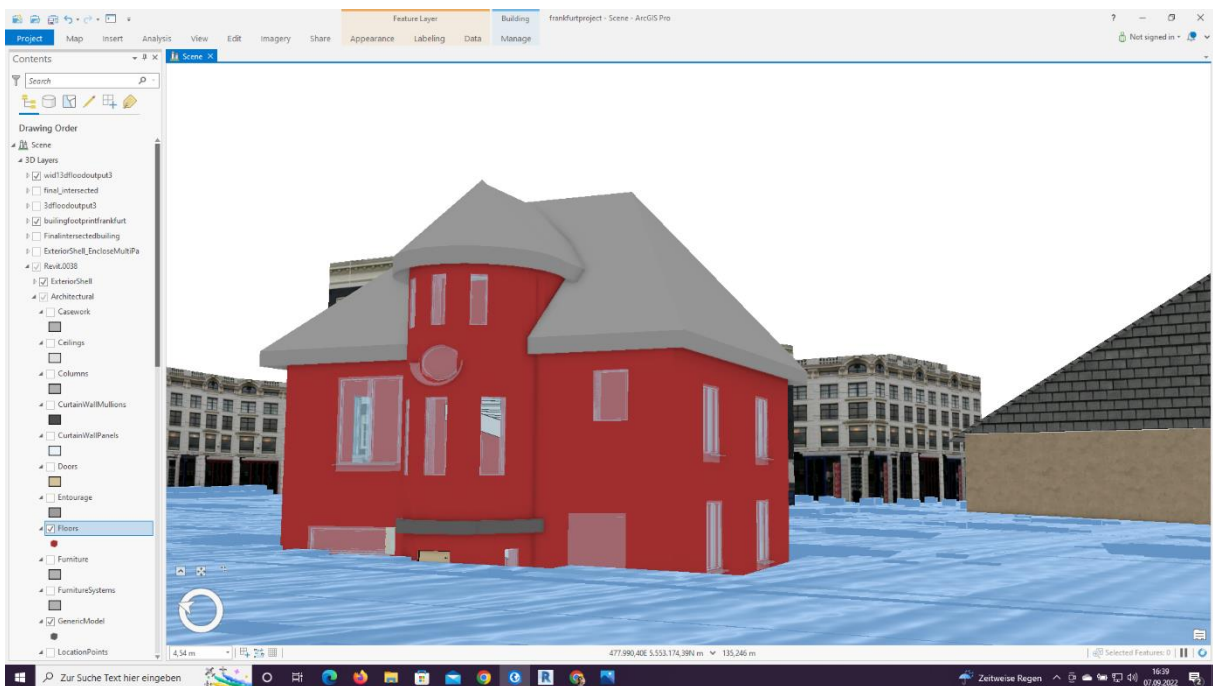
Appendix Figure 28: 3D BIM based building after integration in to ArcGIS Pro for the study area



Appendix Figure 29: 3D BIM based Building with its actual BIM properties into ArcGIS Pro after GIS-BIM integration

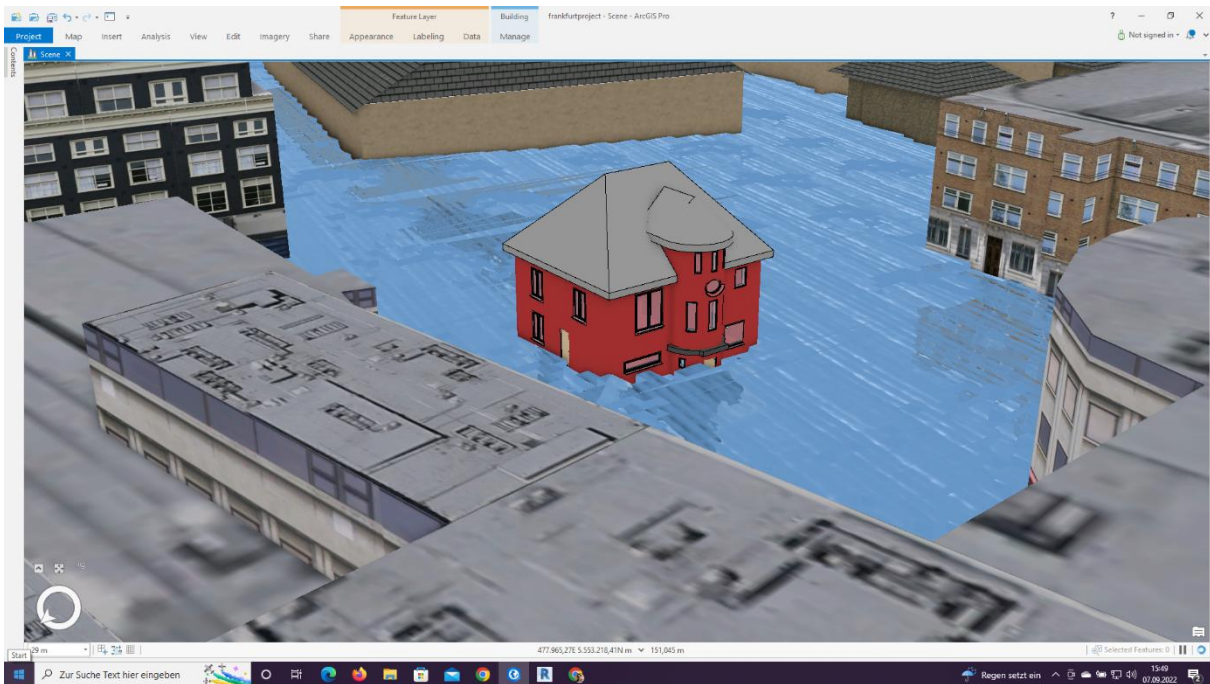


Appendix Figure 30: 3D BIM based Building with its actual BIM properties into ArcGIS Pro after GIS-BIM integration (BIM material and geometrical properties intact after integration for instance for window)

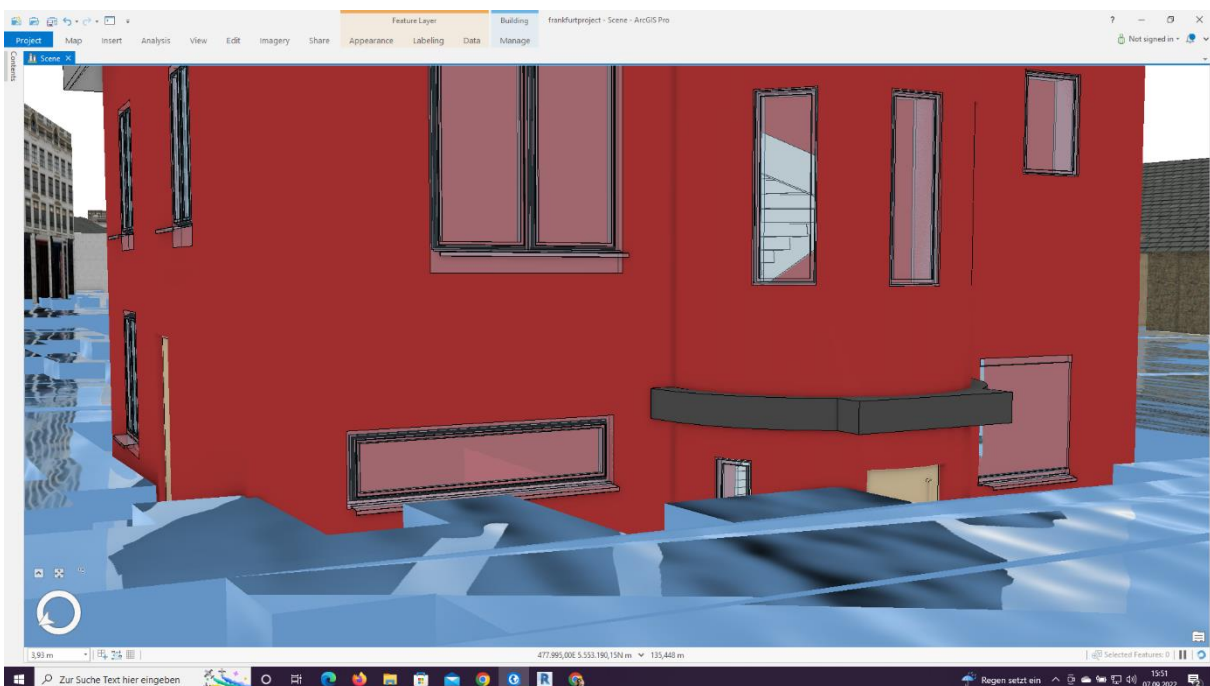


Appendix Figure 31: 3D Digital Twin of Frankfurt case study (with Flood inundation and BIM based 3D Building)

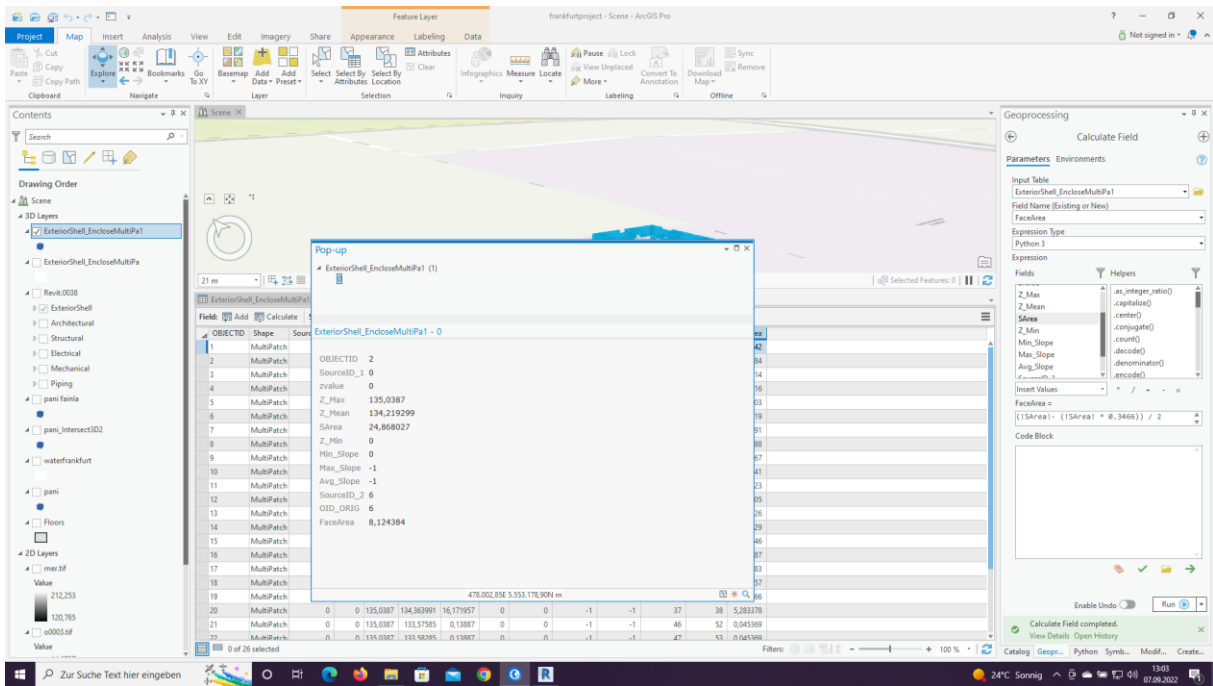




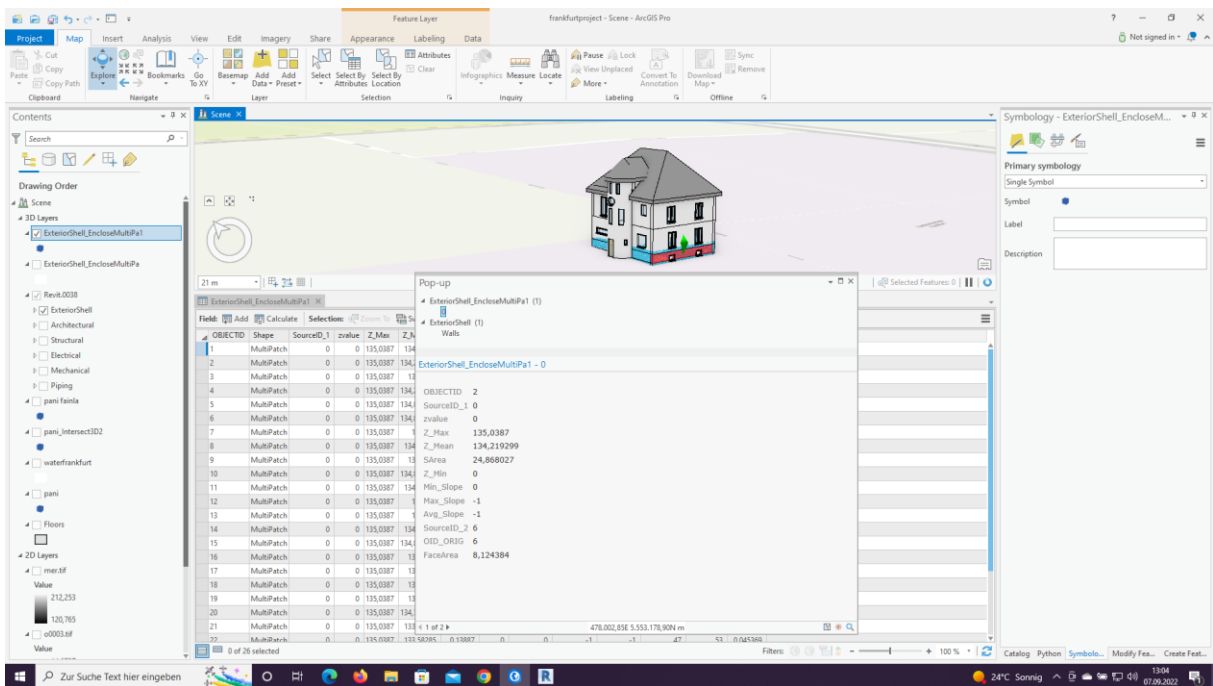
Appendix Figure 32: 3D Digital Twin of Frankfurt case study (with Flood inundation and BIM based 3D Building and block format surrounding buildings)



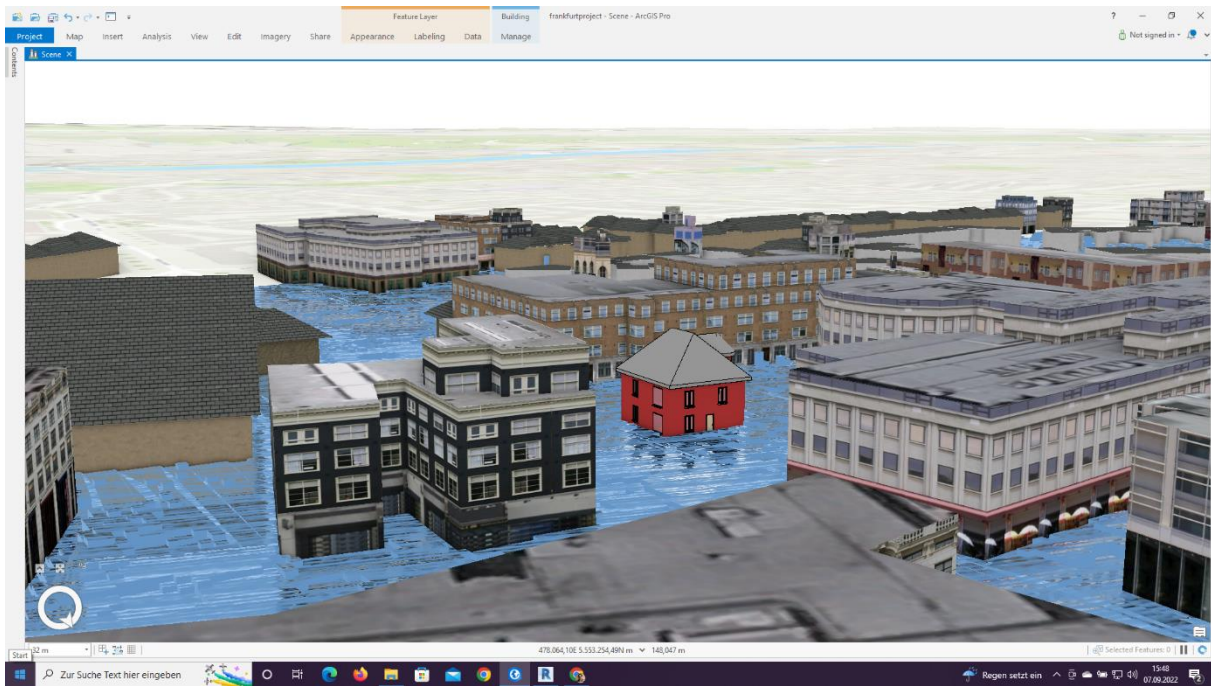
Appendix Figure 33: 3D Digital Twin of Frankfurt case study (with TIN based 3D Flood inundation and BIM based 3D Building)



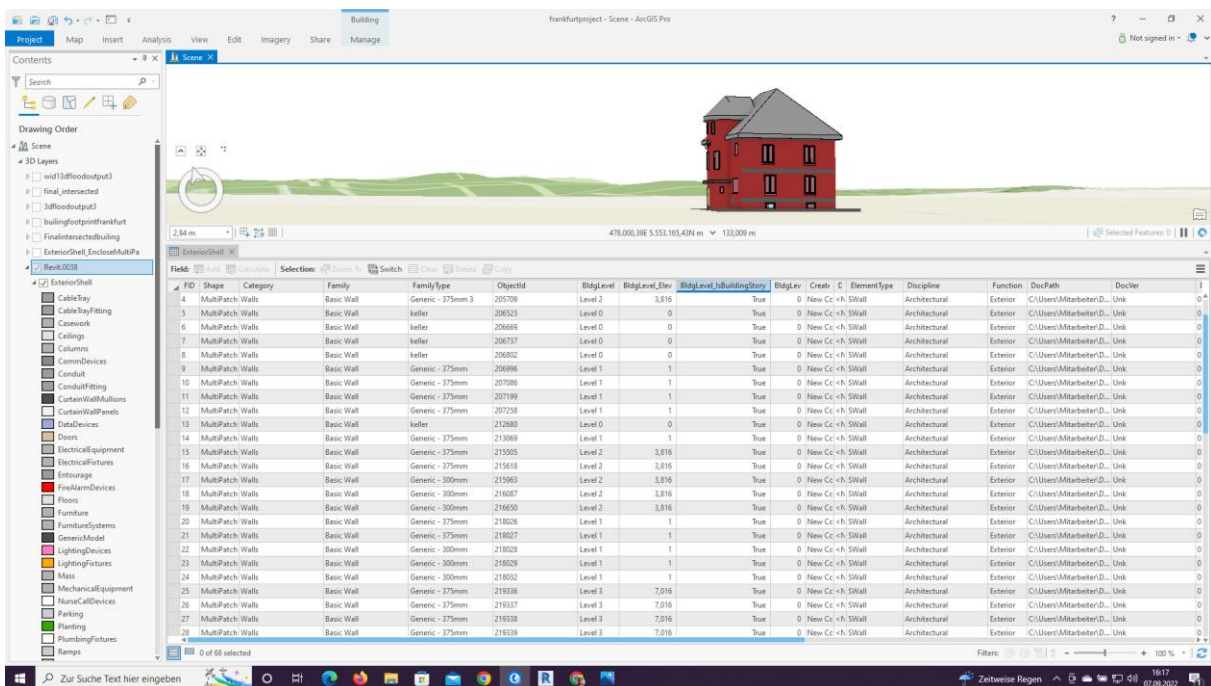
Appendix Figure 34: Flood intersected walls attribute Table



Appendix Figure 35: Flood intersected information before Computation of Pressures

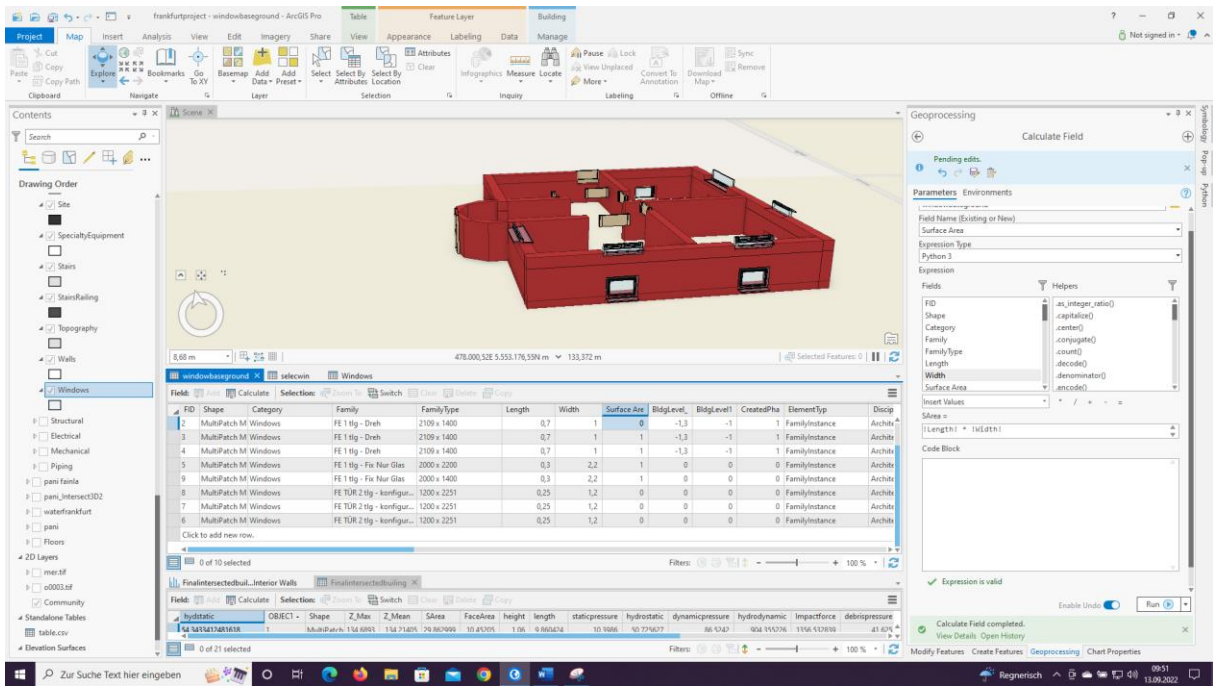


Appendix Figure 36: 3D Digital twin with surround information

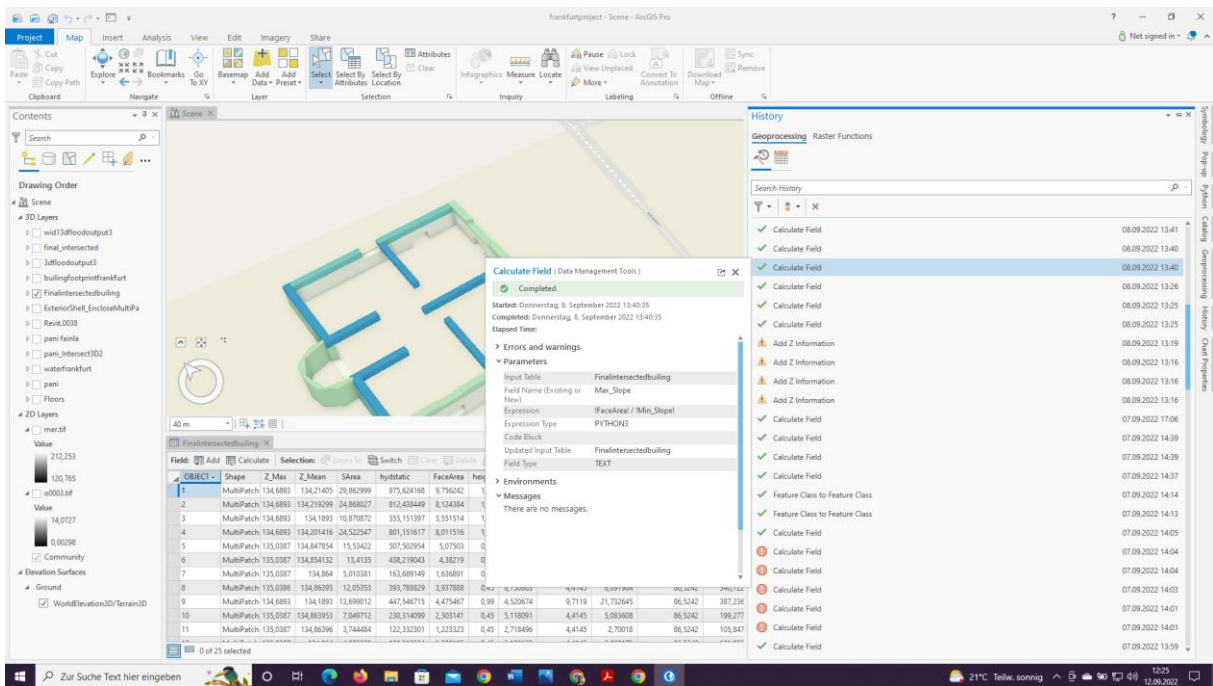


Appendix Figure 37: Attribute Table showing building Geometrical information from BIM model intact after integration into Arcgis Pro





Appendix Figure 38: 3D flood intersected building components with their attribute table in ArcGIS Pro



Appendix Figure 39: Showing successful integration of equations in attribute table for Automation

```

import arcpy
from arcpy.sa import *

# Set the workspace
arcpy.env.workspace = "C:/path/to/workspace"

# Convert building footprint data to ETRS 89 Zone 32N
input_features = "building_footprint.shp"
output_feature_class = "building_footprint_ETRS89.shp"
out_coor_system = arcpy.SpatialReference(25832) # ETRS 89 Zone 32N
arcpy.Project_management(input_features, output_feature_class, out_coor_system)

# Convert digital topography model to ETRS 89 Zone 32N
input_raster = "digital_topography_model.tif"
output_raster = "digital_topography_model_ETRS89.tif"
out_coor_system = arcpy.SpatialReference(25832) # ETRS 89 Zone 32N
arcpy.ProjectRaster_management(input_raster, output_raster, out_coor_system)

# Convert building footprint to raster format
in_features = "building_footprint_ETRS89.shp"
value_field = "FID"
out_raster = "building_footprint_ETRS89.tif"
cell_size = "digital_topography_model_ETRS89.tif"
arcpy.PolygonToRaster_conversion(in_features, value_field, out_raster, "CELL_CENTER", "", cell_size)

# Clip digital topography model using building footprint
in_raster = "digital_topography_model_ETRS89.tif"
in_mask_data = "building_footprint_ETRS89.tif"
out_raster = "digital_topography_model_clip.tif"
arcpy.CheckOutExtension("Spatial") # enable Spatial Analyst extension
out_raster = ExtractByMask(in_raster, in_mask_data)
out_raster.save(out_raster)
arcpy.CheckInExtension("Spatial") # disable Spatial Analyst extension

print("Processing complete.")

```

Appendix Figure 40: Working steps for aligning the coordinate systems of different data set and converting them into the desirable formats to be used in FLOODAREA tool.

```

import arcpy

# Set the workspace
arcpy.env.workspace = "C:/path/to/workspace"

# Convert TIN to 3D multipatch
in_tin = "inundation_depth.tin"
out_multipatch = "inundation_depth_multipatch.shp"
arcpy.TinToMultipatch_3d(in_tin, out_multipatch, "TRIANGLES")

# Check if multipatch features are closed
closed_multipatches = arcpy.management.SelectLayerByAttribute(out_multipatch, "NEW_SELECTION", "Shape_Area > 0")
unclosed_multipatches = arcpy.management.SelectLayerByAttribute(out_multipatch, "NEW_SELECTION", "Shape_Area = 0")
if int(arcpy.management.GetCount(closed_multipatches)[0]) == int(arcpy.management.GetCount(out_multipatch)[0]):
    print("All multipatch features are closed.")
else:
    print("Warning: some multipatch features are not closed.")

# Print message when processing is complete
print("Processing complete.")

```

Appendix Figure 41: Conversion of Raster inundation depth into TIN to convert in 3D multipatch and a Check if the multipatch is closed

```

import arcpy
from arcpy.sa import *

# Set the workspace
arcpy.env.workspace = "C:/path/to/workspace"

# Convert inundation depth raster to polygon
in_raster = "inundation_depth.tif"
out_polygon = "inundation_depth_polygons.shp"
field = "VALUE"
arcpy.RasterToPolygon_conversion(in_raster, out_polygon, "NO_SIMPLIFY", field)

# Perform spatial join with building footprints
target_features = "building_footprints.shp"
join_features = "inundation_depth_polygons.shp"
out_feature_class = "flood_risk_buildings.shp"
join_operation = "JOIN_ONE_TO_ONE"
join_type = "KEEP_ALL"
field_mapping = ""
match_option = "CLOSEST"
search_radius = ""
distance_field_name = ""

arcpy.SpatialJoin_analysis(target_features, join_features, out_feature_class,
                           join_operation, join_type, field_mapping, match_option, search_radius, dis

# Print message when processing is complete
print("Processing complete.")

```

Appendix Figure 42: Spatial join of Inundation depth raster to building footprints and identifying flood prone buildings in Hafen City.

```

import arcpy

# Set the workspace
arcpy.env.workspace = r"C:\data\workspace.gdb"

# Define the input building footprint feature class
footprint_fc = "building_footprints"

# Define the output 3D building feature class
building_fc = "building_3d"

# Define the height field in the attribute table
height_field = "building_height"

# Define the base height of the buildings
base_height = 0.0

# Define the extrusion type (either "Straight" or "Tapered")
extrusion_type = "Straight"

# Define the extrusion height field (if using tapered extrusion)
extrusion_height_field = ""

# Define the extrusion width field (if using tapered extrusion)
extrusion_width_field = ""

# Set the extrusion properties
extrusion_properties = arcpy.ExtrusionProperties(base_height, height_field, extrusion_type, extrusion_height_field, extrusion_width_field)

# Use the ExtrudeBetween tool to create the 3D buildings
arcpy.management.ExtrudeBetween(footprint_fc, building_fc, extrusion_properties)

# Add procedural symbology based on the height field
symbology_layer = arcpy.mp.LayerFile(r"C:\data\symbology.lyrx")
arcpy.management.ApplySymbologyFromLayer(building_fc, symbology_layer)

```

Appendix Figure 43: 2D Building footprint to 3D extruded buildings

```

import arcpy

# Set the workspace and input/output feature class paths
arcpy.env.workspace = "C:/path/to/workspace"
in_fc = "building_footprints.shp"
out_fc = "building_footprints_3d.shp"

# Convert polygon features to 3D multipatch features
arcpy.FeatureTo3DByAttribute_3d(in_fc, out_fc, "Base_Height", "Height")

# Check if multipatch features are closed
closed_multipatches = arcpy.management.SelectLayerByAttribute(out_fc, "NEW_SELECTION", "Shape_Area > 0")
unclosed_multipatches = arcpy.management.SelectLayerByAttribute(out_fc, "NEW_SELECTION", "Shape_Area = 0")
if int(arcpy.management.GetCount(closed_multipatches)[0]) == int(arcpy.management.GetCount(out_fc)[0]):
    print("All multipatch features are closed.")
else:
    print("Warning: some multipatch features are not closed.")

# Add procedural symbology to extrude buildings based on height values
layer = arcpy.mapping.Layer(out_fc)
sym = layer.symbology
sym.renderer.symbolHeight = "HEIGHT"
sym.renderer.proportionalSymbolAlgorithm = "SOLID"
sym.renderer.extrusionExpression = "!Height! - !Base_Height!"
arcpy.RefreshActiveView()

# Save the updated feature class
arcpy.mapping.ExportToPDF(layer, "building_footprints_3d.pdf")
arcpy.management.SaveToLayerFile(layer, "building_footprints_3d.lyr")

```

Appendix Figure 44: Building multipatch 3D file generation

```

import arcpy

# Set the workspace and input feature class paths
arcpy.env.workspace = "C:/path/to/workspace"
buildings_fc = "building_footprints_3d.shp"
inundation_fc = "inundation_depth_multipatch.shp"

# Perform a 3D intersect of the two input feature classes
intersect_fc = "buildings_inundation_intersect.shp"
arcpy.Intersect3D_3d(buildings_fc, inundation_fc, intersect_fc)

# Add procedural symbology to the intersected features
layer = arcpy.mapping.Layer(intersect_fc)
sym = layer.symbology
sym.renderer.symbolHeight = "HEIGHT"
sym.renderer.proportionalSymbolAlgorithm = "SOLID"
sym.renderer.extrusionExpression = "!Shape_Length!"
arcpy.RefreshActiveView()

# Save the updated feature class
arcpy.mapping.ExportToPDF(layer, "buildings_inundation_intersect.pdf")
arcpy.management.SaveToLayerFile(layer, "buildings_inundation_intersect.lyr")

```

Appendix Figure 45: 3D intersect of 3D buildings and inundation depth multipatch features



```

import arcpy
import math

# Set the workspace and input feature class paths
arcpy.env.workspace = "C:/path/to/workspace"
intersect_fc = "buildings_inundation_intersect.shp"

# Add new fields for each formula
arcpy.AddField_management(intersect_fc, "WaterInteraction", "DOUBLE")
arcpy.AddField_management(intersect_fc, "HydrodynamicForce", "DOUBLE")
arcpy.AddField_management(intersect_fc, "HydrostaticForce", "DOUBLE")

# Calculate the new fields based on the intersected surface area and formula coefficients
with arcpy.da.UpdateCursor(intersect_fc, ["SHAPE_Area", "WaterInteraction", "HydrodynamicForce", "HydrostaticForce"]) as cursor:
    for row in cursor:
        # Calculate the water interaction based on the surface area and a coefficient of 0.05
        row[1] = row[0] * 0.05

        # Calculate the hydrodynamic force based on the surface area, flow velocity, and a coefficient of 1000
        # Assume a flow velocity of 1 m/s for demonstration purposes
        row[2] = row[0] * 1000 * 3.5 ** 2

        # Calculate the hydrostatic force based on the surface area, fluid density, and a coefficient of 9810
        # Assume a fluid density of 1000 kg/m3 for demonstration purposes
        row[3] = row[0] * 9810 * 1

        # Update the cursor with the new values
        cursor.updateRow(row)

```

Appendix Figure 46: Incorporating formulas and equations of water interaction, hydrodynamic force hydrostatic force and so on the intersected building areas.

Appendix Table 1: Software description and utilization in this research

Softwear	Explanation	License Type	Utilization in this Research	Devel- oper
ArcGIS Map	It provides a range of tools and features for mapping, analysing, managing, and sharing spatial data and applications. ArcGIS is widely used in industries such as environmental management, urban planning, natural resource management, public safety, and business intelligence.	Stud- ent	Data preparation for hydrodynamic flood simulation. Hydrodynamic flood simulation Maps investigation and 2D impact assessment generation	ESRI, USA
QGIS	QGIS is a free and open-source GIS software that allows users to create, edit, analyze, and publish geospatial data and maps. It supports various data formats and includes many tools and plugins for data management, analysis, and cartography. QGIS is highly customizable and has a large and active user community. It is used in various fields, such as environmental science, geography, geology, urban planning, and agriculture.	Open access	For Building footprint and DTM exploration	Global commu- nity of volunte ers
FLOOD Area	Hydrodynamic flood simulation software	Educati onal	2D hydrodynamic flood simulation of case study areas	Geome rs, Germa ny
CADMAPP ER	is a web-based tool that converts 2D CAD drawings, including architectural floor plans, into 3D models. It supports various file formats and allows users to customize the level of detail and	Open access		Todd Lombar do,

	materials used in the conversion process. The resulting 3D models can be exported in various formats, making it a useful tool for architects, designers, and other professionals who need to quickly create 3D models from 2D CAD drawings.			
Autodesk Revit	Revit is a BIM software developed by Autodesk that allows architects, engineers, and construction professionals to design, model, simulate, and manage building projects collaboratively. It uses a parametric and object-oriented approach to modelling, enabling users to make changes to one element and have the model automatically update other related elements. Revit includes tools for modelling, analysis, documentation, and collaboration, and supports various file formats for interoperability with other software and systems. Revit is widely used in the architecture, engineering, construction, and facilities management industries.	Student	Object oriented 3D BIM model of targeted buildings creation	Autodesk, USA
Autodesk Recap	used for creating 3D models from laser scans and photographs. It allows users to import, clean, register, and visualize point cloud data from various sources, such as laser scanners and drones. Recap Pro includes tools for editing and analysing point clouds, creating 3D models and meshes, and exporting the data in various formats for use in other software and systems. Recap Pro is used in industries like architecture, engineering, construction, and manufacturing for applications such as building information modeling, quality control, and asset management.	Student	Cleaning and editing of point cloud data of targeted building	Autodesk
Cloud compares	CloudCompare is an open-source software used for processing and visualizing 3D point cloud data. It allows users to import, edit, and analyze point cloud data from various sources, such as laser scanners, photogrammetry, and LiDAR. CloudCompare includes a wide range of tools for filtering, smoothing, segmenting, and aligning point cloud data, as well as for creating and exporting meshes and surface models. It is widely used in various fields, such as surveying, geology, archeology, and manufacturing, for applications such as land surveying, terrain modeling, and inspection of manufactured parts.	Open access	Registration of laser scan data and database creation	French National Institute of Applied Sciences
Dlubal RFEM	Dlubal RFEM is a software used for structural analysis and design of 2D and 3D structures. It is developed by Dlubal Software and allows engineers to analyze and design structures made of different materials according to various international codes and standards. Dlubal RFEM includes tools and features for modeling, analysis, design, and optimization of structures, such as linear and nonlinear analysis, dynamic analysis, stability analysis, and buckling analysis. The software supports various import and export formats, including BIM formats, for interoperability	Student	For checking export of automatic computed flood induced loads and pressures for Targeted building	DLUBAL, Germany

	with other software and systems. Dlubal RFEM is used in industries like civil engineering, architecture, and mechanical engineering for applications like building and bridge design and structural analysis of industrial equipment.			
ARCGIS Pro	used for creating, analyzing, and sharing geographic data and maps. It provides a modern interface and a wide range of tools for visualizing, managing, and analyzing 2D and 3D spatial data, including raster data such as satellite imagery and elevation data. ArcGIS Pro also supports advanced analysis such as geoprocessing, spatial statistics, and network analysis, as well as publishing and sharing maps and data to various platforms such as ArcGIS Online and ArcGIS Enterprise. It is used in industries such as environmental management, urban planning, public safety, and utilities for applications such as data visualization, spatial analysis, and decision making.	Student	Creation of 3D flood model and 3D Digital Twin generation.  Automation of 3D flood impact assessment for calculation of different flood induced load and pressures acting on a building.	

Appendix Table 2: Hydrodynamic Flood Simulation Models adapted from Teng et al. (2017) and Nkwunonwo et al. (2020)

1D	2D	1D-2D Coupled	3D	Main Approach	Solving equation	Numerical scheme	Advantages	Limitations	Access	Developer
HEC-RAS				Solves one dimensional energy equation for steady flow and full 1D shallow water equation for unsteady flows	One dimensional energy equation for friction and contraction	Implicit finite difference solution	Adaptable and easy to set up, high-range of data quality can be added, extensive documentations	not suitable for multideiment al modelling due to model instability	Open Source	Army Corps of Engg. (1995)
	Flowroute-i			Model river, coastal and pluvial sources,depth, vilocity and flow outputs avaiable dynamically	Shallow water equation	Finite volume + Integation with GIS	Explicit description of time, structured mesh for space descretion, ideal for high reosolution LIDAR data	No shock capturing algorithm	Commercial	Ambiental
	ANUGA Hydro			Riemann solver shock capturing algorithm	Shallow equation	Finite volume	Explicit description of time , flexible mesh structure for space descretion		Open Sources / Commercial	Austrian National Universtiy
Newer MIKE 11				Developed to simulate flow and water level, water quality and sediment transport in rivers, flood plains, irrigation canals, reservoirs and other inland water bodies	1D Shallow water equation	Muskingum method and Muskingum-Cunge method for simplified channel routing	complemented by a wide range of additional modules and extensions covering almost all conceivable aspects of river modelling	Limited to rivers and fluvial-related flood events. Model can be unstable under two-dimensional flood conditions	Commercial	Danish Hydraulic Institute

	MIKE 21	Developed to simulate flows, waves, sediments and ecology in rivers, lakes, estuaries, bays, coastal areas and seas in two dimensions	Full 2-dimensional shallow water equations	Implicit finite difference techniques with variables defined on a space-staggered rectangular grid.	Suitable for hydrodynamic flood simulation. Simulates bulk flow characteristics, flow velocity in various directions of flow.	Simulations time steps and model stability are affected by C-F-L condition. Needs to be calibrated.	Commercial	Danish Hydraulic Institute
TUFLOW Classic 1D		Simulation of complex hydrodynamics of flood using full 1-D St. Venant equations	Full one-dimensional shallow water equation	Second order Runge-Kutta finite-difference solution	Dynamic linking capability between domains. Fast from computational point of view	There are uncertainties in solution and are poor at process representation	Commercial	BMTWBIM
	TUFLOW Classic 2D	Simulation of complex hydrodynamics of flood using full 2-D free surface shallow water equations	Full two dimensional free surface shallow water equations	Stelling Finite Difference and ADI	Dynamic linking capability between domains. Satisfactory representation of process.	Slow, but dynamically captures bulk flow characteristics	Commercial	BMTWBIM
	ISIS 2D	Designed to work either standalone or within the ISIS suite	Full two dimensional shallow water equations	Alternating Direction Implicit (ADI), FAST Total Variation Diminishing (TVD)	Wide range of clientele. Suitable for hydrodynamic flood simulation	Slow simulation speed and requires a high resolution topographic data.	Commercial	Halcrow (Now CH2M HILL 2009)

			Provides an advanced one-dimensional (1D) and two-dimensional (2D) simulation engine, analysis and visualization tools	Provides an advanced one-dimensional (1D) and two-dimensional (2D) simulation engine, analysis and visualization tools	Alternating Direction Implicit (ADI), FAST and Total Variation Diminishing (TVD)	Suitable for wide range of applications including urban areas, coastal and river channels.	Limited to 250 1D nodes and 2500 2D cells.	Open Sources	Halcrow (Now CH2M HILL 2011)
			Developed to enhance the independent functionalities of MIKE 11 and MIKE 21	One-dimensional and two dimensional shallow water equations.	Coupled solution of 1-D/2-D shallow water equations	Satisfactory real-time simulation of flood inundation in river, coastal and urban areas.	Not well adapted in terms of application to many places. Models requires calibration	Commercial	Danish Hydraulic Institute
	MIKE 3		Designed to address the challenges of process representation and limitations in channel and floodplain flood modelling	solves the full two dimensional shallow water equations	finite-element or finite-volume method and a computation mesh of triangular elements	It can perform simulations in transient and permanent conditions	Conditional stability	Open Sources	Électricité France. (EDF) (2010)
TELEMAC - 2D		TELEMAC - 3D	To address some limitations inherent in the 2-D version of the model	Navier-Stokes equations, whether in hydrostatic or non-hydrostatic	finite-element or finite-volume method and a computation mesh of triangular elements	Ability to capture hydrodynamic features of an area. Suitable for all flood sources	Conditional stability	Open Sources	Électricité France. (EDF) (2010)

TRENT			A flood model that is able to capture full hydrodynamic properties	Shallow water equations	Explicit Finite difference scheme	Shock capturing ability	Stable at CFL condition, using adaptive time stepping.	Commercial	Nottingham Uni.
LISFLOOD-FP			A raster-based hydraulic model that is assumed to possess the simplest hydrologic process representation	One-dimensional Kinematic and two-dimensional diffusive wave equations.	Explicit finite difference solution	Extensive documentation, easily adaptable and simple to set up	Requires a high-resolution topographic data for simulation.	Research	Bates and De Roo,
	MIKE URBAN 2010		Has the capability to analyze storm sewer networks. Flow conditions associated with weirs, orifices, manholes, detention basins, pumps, and flow regulators can be reflected	1-D unsteady flow	Implicit, finite difference numerical scheme	Suitable for flow in urban areas. Integrates GIS capabilities.	Lacks the ability to capture some hydrodynamic phenomenon such as shock and supercritical flows.	Commercial	Danish Hydraulic Institute
		TUFLOW 3D	Simulation of horizontal and vertical density gradient of flow	Navier-Stokes equations	Flexible mesh	coupling ability with other models, simulation of flow in all 3 spatial dem	limited to small area of study	Commercial	BMTWBIM
		ANSYS CFX	-					Commercial	ANSYS
		AutoDesk Fluent						Open Source	Autodesk
		Flip 3D						Open Source	Kyushu University
		FINEL 3D						Commercial	Tokyo University



# Ahsan Ali

67550 Worms, Germany

[ahsan.ali@gmx.net](mailto:ahsan.ali@gmx.net)

## WORK EXPERIENCE

- 2019 - Present **Research Assistant**  
**Technical University of Kaiserslautern, (Germany)**  
Tasks: Assisting in teaching activities for hydraulics lab. Research related to heavy rainfall and flooding. Using drone technology embedded in GIS. Preparation of flood hazard maps of flood prone areas using GIS technology. Flood resilient building research embedding BIM technology in GIS.
- 2020 – Present **BIM and Structural Engineer**  
**Fischer Engineering Office, (Germany)**  
Tasks: Performing structural analysis of steel structures, halls, housing areas and calculations of loads and stresses (Including integrated design of slabs, mats, and footings) using Dlubal RFEM, Auto-Cad, SAP2000, ETABS and SAFE Software. Making joint drawings and structural position plans. Dealing with proofing authorities. Developing structural analysis reports of stages, manholes and tunnels.
- 2013 – 2015 **Lecturar Civil Engineer**  
**Baluchistan University of Information Technology, Engineering and Management Sciences, (BUIITEMS), Quetta (Pakistan)**  
Tasks: Teaching Structural/ Civil engineering courses to bachelor and master students. Supervising thesis. Research on several government projects to identify the structural stability of the buildings. Developed architectural design and drawing for office and hostel buildings.
- 2012 – 2013 **Junior Engineer – Specialist for Structural Analysis**  
**Cameos Consultants, Quetta (Pakistan)**  
Assisted Designing and Estimation of building structure and roads, water supply schemes, Preparation of project report PC-I, Preparation of Drawing by using Auto-CAD, when even needed in the absence and arbitration of different Civil Engineering Projects like Buildings, Roads, Bridges, Tube Wells, Water Supply Scheme etc. of GIS and CAD operator

## EDUCATION

- 2015 – 2017 **MSc Infrastructure Planning**  
**Universität Stuttgart, Stuttgart (Germany)**
- 2008 – 2012 **BSc Civil Engineering**  
**Baluchistan University of Information Technology, Engineering and Management Sciences, (BUIITEMS), Quetta (Pakistan)**

## AWARDS

- **DAAD (German Academic Exchange Program)** Scholarship holder for Fully Funded MSc. Infrastructure Planning at University of Stuttgart, Germany, Session 2015-2017
- **Research fellowship** “University of British Columbia, Canada” for summer semester 2017
- **Merit Scholarship**, for B.Sc. Civil Engineering at BUIITEMS, Quetta (Full Tuition Fee- Session 2008-2012)

## 11 List of Reports / Liste der Berichte

In der Reihe der Berichte des Fachgebietes Wasserbau und Wasserwirtschaft der Rheinland-pfalzische Universität Kaiserslautern Landau sind bisher erschienen:

**Bericht 1** Untersuchungen zur Bemessung von Regentlastungen im ländlichen Raum  
L. Kirschbauer 1994, vergriffen

**Bericht 2** Erfassung und Beurteilung der Transportvorgänge im Grundwasser am  
Beispiel der Pflanzenschutzmittel  
H.-Ch. Schöpfer 1994

**Bericht 3** Die Wahrscheinlichkeit des gleichzeitigen Auftretens maßgebender  
Abflußereignisse in Kanalisationsnetzen und natürlichen Gewässern  
J. Sartor 1994

**Bericht 4** Ermittlung maßgebender Hochwasserereignisse in Karstgebieten  
am Beispiel des Egau-Gebietes (Schwäbische Alb)  
G. Koehler 1995  
Untersuchungen zur flächenhaften Erosion am Beispiel der  
Erosionsmeßstellen Birkweiler und Kleiner Fischbach (Rheinland-Pfalz)  
G. Koehler, P. Bader 1995

**Bericht 5** Untersuchungen zur Ermittlung regional gültiger Hochwasserabflüsse  
am Beispiel des südbayerischen Donaumaums  
Erfassung von abflußrelevanten Bodeneigenschaften bei der Anwendung  
eines einfachen Niederschlag-Abfluß-Modells  
M. Ott 1997

**Bericht 6** Erprobungs- und Entwicklungsvorhaben „Oster“. Gewässerbeschaffenheit und  
Nährstoffbilanz eines kleinen, technisch ausgebauten Fließgewässers  
Untersuchungen zur Gewässerbeschaffenheit der Oster  
S. Franke, W. Frey, M. Theis 1997  
Nährstoffbilanz für die Oster  
W. Frey, H. Hoffmann 1997

- Bericht 7** Erprobungs- und Entwicklungsvorhaben „Oster“. Auswirkungen einer Bachrenaturierung auf Gewässer und Aue  
Vortragsband zum Statusseminar vom 21. Oktober 1997 an der Universität Kaiserslautern  
Herausgeber: G. Koehler 1998
- Bericht 8** Hochwasserabflüsse aus Regen und Schnee in Mittelgebirgsgebieten am Beispiel von Nordbayern  
J. Sui 1998
- Bericht 9** Bemessungsabflüsse für kleine Einzugsgebiete  
Tagungsband zum Kolloquium vom 4./5. März 1999 an der Universität Kaiserslautern  
Herausgeber: G. Koehler 1999
- Bericht 10** Einsatz von Wasserhaushaltsmodellen zur Wasserbewirtschaftung ,am Beispiel des Thika-Chania-Gebietes in Kenia  
J.M. Gathenya 1999
- Bericht 11** Festschrift anlässlich des 60. Geburtstages von Prof. Dr.-Ing. Gero Koehler und des 15-jährigen Bestehens des Fachgebietes Wasserbau und Wasserwirtschaft der Universität Kaiserslautern  
Herausgeber: Fachgebiet Wasserbau und Wasserwirtschaft, Universität Kaiserslautern 2000
- Bericht 12** Die Auswirkungen von Renaturierungsmaßnahmen auf die Gewässergüte und die Selbstreinigungskraft am Beispiel der Oster (Saarland)  
W. Frey 2001
- Bericht 13** Der Beitrag naturnaher Retentionsmaßnahmen in den Talauen zur Hochwasserdämpfung  
B. Marenbach 2002
- Bericht 14** Der Einfluss des Grundwasserhaushaltes auf das Abflussverhalten kleiner Einzugsgebiete im Festgesteinsbereich der Mittelgebirge  
Systemanalyse und numerische Modellierung

M. Probst 2002

**Bericht 15** Einsatz von Methoden des „Soft Computings“ in der Hydrologie

N. T. Lange 2003

**Bericht 16** Quantifizierung der Prognoseunsicherheiten bei der praktischen Anwendung numerischer Grundwassermodelle

H. 3. Theis 2006

**Bericht 17** Bewertung der Auswirkungen von Umweltfaktoren auf die Struktur und Lebensgemeinschaften von Quellen in Rheinland-Pfalz

H. Schindler 2006

**Bericht 18** Kommunale Hochwassermanagementsysteme als Baustein zur Umsetzung der Europäischen Hochwasserrichtlinie

M. Gretzschel 2008

**Bericht 19** Beiträge zum Fachkolloquium „Extremereignisse in der Wasserwirtschaft“

Herausgeber: R. Jüpner, V. Lüderitz, A. Dittrich 2008

**Bericht 20** Konzept zur ökologischen Bewertung und Entwicklung der Wooge im Biosphärenreservat Pfälzerwald

Herausgeber: G. Koehler, W. Frey, H. Schindler, H. Hauptlorenz 2011

**Bericht 21** Entwicklung eines Werkzeugs zur systematischen Bewertung der Grundlagen von Hochwassergefahrenkarten

T. Weichel 2011

**Bericht 22** Entscheidungshilfen für das nachhaltige Bauen von hochwasserangepassten Bauweisen in urbanen Gebieten

M. Kathmann 2015

**Bericht 23** Möglichkeiten zur Weiterentwicklung des operativen Hochwasserschutzes ein Beitrag aus wasserwirtschaftlicher Perspektive

A.E. Schüller 2022



